In Profile:
Models of Ribosome Biogenesis Defects and Regulation of Protein Synthesis

In Profile:
Models of Ribosome Biogenesis Defects and Regulation of Protein Synthesis

En profil: modellen van defecten in ribosoom biogenese
en regulatie van eiwit synthese.
(met een samenvatting in het nederlands)

Proefschrift

ter verkrijging van de graad van doctor aan de Universiteit Utrecht op gezag van de rector magnificus, prof.dr. G.J. van der Zwaan, ingevolge het besluit van het college voor promoties in het openbaar te verdedigen op donderdag 5 december 2013 des middags te 12.45 uur

door
Paulus Bernardus Maria Essers
geboren op 18 maart 1983 te Maastricht

Promotor: Prof. dr. E. P.J.G. Cuppen

Co-promotor: Dr. A. W. MacInnes

Table of Contents

Introduction

1

This introduction consists of four parts, each giving the background needed to place the chapters of this thesis in their proper context. Part one will give a brief overview of ribosome biogenesis and translation. Part two will introduce the nucleostemin gene family and discuss its role in ribosome biogenesis and cell cycle regulation. Part three will give an overview of the discovery of pathways that influence an organisms' lifespan and their relationship with protein metabolism. Finally, Part four will introduce the Von Hippel-Lindau tumor suppressor and discuss its contribution to renal cell carcinoma pathogenesis.

Part 1: An Introduction to the Ribosome and Translation

Discovery of the ribosome

The development of the electron microscope in the first half of the 20th century allowed biologists to look more closely at the structure of the cell than ever before. Microscopy was combined with a technique named differential centrifugation, developed in the lab of Albert Claude at the Rockefeller Institute, in which cells are broken up and their components are separated according to their mass by a series of centrifugation steps. Together, these techniques allowed for the discovery of new organelles and their description. In 1955, George Palade described large molecules attached to the endoplasmic reticulum and determined their composition as ribonucleoprotein. He and his collaborators went on to discover their function as the site of protein production in the cell. In 1974, Albert Claude, George Palade and Christian de Duve received the Nobel Prize for discovering and describing many of the cells organelles and essentially creating the field of cell biology [1].

The ribosome

The eukaryotic ribosome is complex and abundant cellular machinery required for protein translation that consists of two subunits. The small subunit, 40S, contains one strand of ribosomal RNA (18S rRNA) and 33 ribosomal proteins (rps). The large subunit contains three strands of rRNA (25S, 5.8S and 5S) and 46 rps. In addition, over 200 non-ribosomal factors and 75 small nucleolar RNAs (snoRNAs) are involved in ribosome assembly. The ribosomal RNA constitutes about 80% of the RNA in the cell, with the remaining 20% divided between tRNAs (15%) and mRNAs (5%) [2].

Ribosome biogenesis

Ribosome biogenesis starts with the transcription by RNA polymerase II of a common rRNA precursor containing the 18S, 5.8S and 28S rRNA and the transcription of 5S rRNA (Fig 1). The nascent rRNA is modified by H/ACA and C/D small nucleolar ribonucleoprotein particles (snoRNPs). These are targeted by base pairing between snoRNAs and the pre-rRNA and mediate 2'-O-ribose methylation and pseudourydilation of nucleotides respectively. The modification sites are largely conserved between yeasts and humans [3]. A subset of small subunit rps and some non-ribosomal factors associate with the pre-rRNA to form an early pre-40S subunit. Upon cleavage of the pre-rRNA the pre-40S subunit is released and the remaining pre-rRNA associates with large subunit rps, non-ribosomal factors and the 5S rRNA, which is transcribed separately by RNA polymerase III, to form a pre-60S subunit. Both pre-subunits undergo a series of RNA cleavages in the nucleus before being exported to the cytoplasm. There, final modifications produce the mature 40S and 60S subunits. Ribosome biogenesis is extensively reviewed in ref [4].

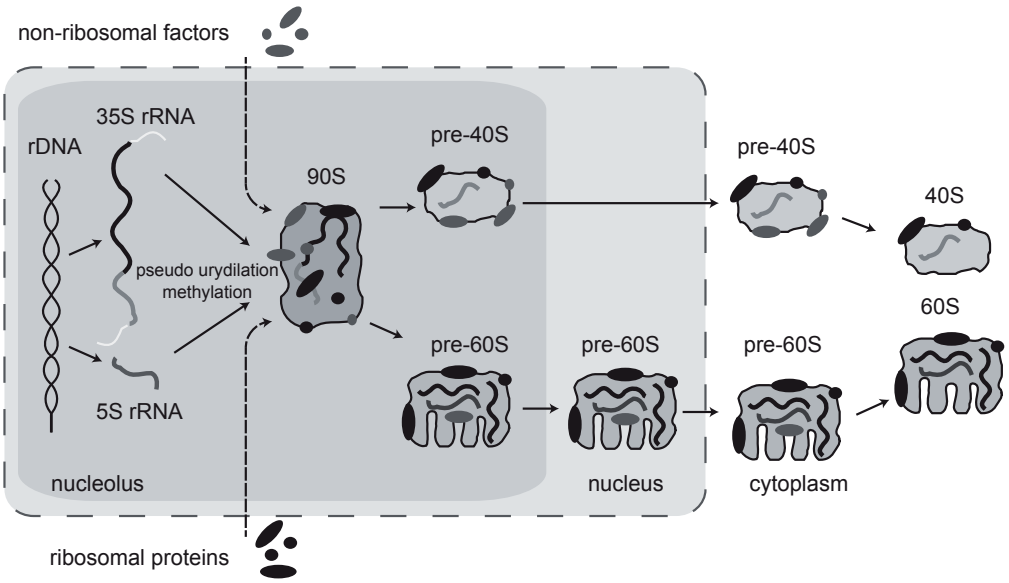

Figure 1: Simplified overview of ribosome biogenesis. In the nucleolus 18S, 5.8S and 28S are transcribed as a single strand, while 5S rRNA is transcribed separately. The external spacers are cleaved off and the pre rRNA is glucosylated and methylated by small nucleolar ribonucleoprotein particles. Together with ribosomal proteins and non-ribosomal factors the rRNA assembles into a 90S-pre-ribosome. rRNA cleavage results in release of a pre-40S subunit, containing the 18S rRNA, and a pre-60S subunit, containing 28S, 5.8S and 5S rRNA. The pre 40S subunit is directly exported into the cytoplasm, while the pre 60S undergoes modifications in the nucleus before it is exported. In the cytoplasm the non-ribosomal factors are lost, producing the mature 40S and 60S subunits. Adapted from [120].

Translation

In order to start translating mRNA into protein, both subunits need to assemble into an 80S ribosome, with the initiator methionyl-tRNA$_i$ (Met-tRNA$_i$) bound to the start codon of the mRNA. This initiation is the most highly regulated step in translation. Several modes of translation exist, including cap-dependent, IRES mediated translation and others in between [5].

The first step of cap-dependent translation initiation is the formation of the ternary complex, consisting of Met-tRNA$_i$, eukaryotic initiation factor 2 (eIF2) and GTP. eIF1, eIF1A, eIF3 and eIF5 then bind to the 40S subunit, allowing it to bind to the ternary complex, forming the pre-initiation complex. This complex is recruited to the 5' end of the mRNA, capped with 7-methyl-guanosine, by a range of proteins, including eIF3, poly(A)-binding protein (PABD), eIF4B and the eIF4F complex, composed of eIF4E, the cap-binding protein, eIF4a, an RNA helicase, and eIF4G [5]. The simultaneous interaction of eIF4E and PABP with eIF4G is believed to be responsible for circularizing the mRNA [6]. The pre-initiation complex scans the 5' untranslated region (UTR) until it recognizes the start codon, at which point eIF1 dissociates from the complex, triggering GTP to GDP cleavage by eIF2A and causing the pre-initiation complex to change to a closed conformation. In order to create the complete 80S initiation complex, eIF2A-GDP and eIF5 dissociate and are replaced by the 60S subunit. This step is mediated by eIF1A and eIF5B, which are subsequently released, making the ribosome ready to enter the elongation phase of protein synthesis [5].

During the elongation phase the nascent polypeptide is synthesized one amino acid at a time. The 40S and 60S subunits play distinct roles. The 40S subunit mediates correct base-pairing between the mRNA and the incoming tRNAs, determining the order of amino-acids; the 60S subunit

catalyses the formation of peptide bonds between the amino acid bound to the tRNA and the nascent polypeptide. Both subunits contain three binding sites with different functionalities. tRNA coupled to EF-1-GTP first binds to the A-site, followed by GTP hydrolysis, release of EF-1-GDP from the ribosome and the accommodation of the aminoacyl end of the tRNA in the peptidyl transferase centre (PTC) of the 60S subunit, where a peptide bond is formed. In order to incorporate the next amino acid, the ribosome must shift one position forward, a process facilitated by binding of GTPase EF-G. GTP hydrolysis and EF-G release results in the tRNA shifting from the A to the P site, freeing the A site for another round of elongation. In the process, the tRNA occupying the P-site is translocated to the E-site and will be released after the next round. For a review of elongation, see ref [7].

Translation ends when a stop codon is encountered. The A-site is occupied by a complex consisting of eukaryotic Release Factor 1 (eRF1), which is responsible for recognizing the stop codon, and eRF3-GTP. Upon GTP hydrolysis by eRF3, eRF1 induces the release of the now finished peptide. eRF1 stays bound to the ribosome, allowing binding of ABCE1, which results in dissociation of the 60S subunit. The mRNA and residual tRNA are then released from the 40S subunit by eIF3, eIF1, eIF1A and eIF3 subunit 3j. Thus, both ribosomal subunits are ready to begin another round of translation. For a more detailed description of translation termination, see ref [8].

Preferential translation of mRNA transcripts

Global regulation of translation mainly occurs by the modification of translation factors, but translation of specific mRNAs can also be regulated. The importance of such mechanisms is exemplified by the finding that the abundance of an mRNA poorly correlates with the abundance of the protein encoded [9]. Regulation of translation is mediated by regulatory sequences and structural characteristics of mRNAs and the binding of ribo-protein complexes to sequences in the 5' and 3' untranslated regions in the mRNA. Structural properties of mRNA include the presence of a 5' cap and polyA tail, which are present in the majority of mRNAs and both of which promote translation efficiency. Most other examples of translational regulation are inhibitory mechanisms, indicating that an mRNA is translationally active by default. The presence of secondary structures in the 5' UTR, such as hairpins and pseudoknots, can block initiation, unless they are part of an internal ribosome entry site (IRES, discussed below). Secondary structures can also inhibit translation by providing a recognition site for regulatory proteins, as can regulatory sequences. The binding of RNA-induced silencing complexes to miRNA binding sites in the 3'UTR is a widespread example of the latter type of regulation. Another form of regulation is the presence of an upstream open reading frame, which reduces translation efficiency from the real open reading frame [10].

The most widely known structural property of an mRNA that promotes translation is the presence of an internal ribosome entry site (IRES) [5], a secondary structure in the mRNA that allows ribosome binding near the start codon while many upstream start codons are bypassed. IRES elements were first discovered in viral mRNAs and were later shown to also be present in cellular mRNAs. At least three different classes of IRES exist, classified by their requirement (or lack thereof) of initiation factors. As a result of its inefficiency, IRES mediated translation is greatly increased by inhibition of cap-dependent translation, a strategy used by viruses as well as cells. In situations of cellular stress, activation of the mTOR pathway causes 4E-BP to sequester eIF4E, allowing translation of IRES containing mRNAs, many of which code for proteins involved in stress response. About 3% of cellular mRNA was shown to be translated in the absence of cap-dependent translation [11]. In contrast to viral IRES elements, cellular IRES elements do not share a common structural motif, but seem to be dependent upon short motifs and trans-acting factors for their function [12]

Structural variation in ribosomes results in preferential translation of certain transcripts

In addition to regulation by structural characteristics of mRNA, there is increasing evidence that not all ribosomes are created equal and that structural variation of ribosomes can result in the preferential translation of specific mRNAs. Such variations can include rRNA modifications, lack of one or more ribosomal proteins and binding of translation machinery associated (TMA) proteins, which stably bind a subset of ribosomes but are not required for global translation [13]. One striking example of such a mechanism is the requirement of rpL38 for the translation of various *hox* mRNAs, while being dispensable for global translation [14]. Expression patterns of rpL38 correspond to locations of *hox* gene expression, indicating that rpL38 is incorporated in the ribosome where translation of *hox* mRNA is needed. In the cellular slime mold, *Dicyostelium discoideum*, the expression of rpL11 and rpS9 are shown to be cell type specific during development, indicating that developmental regulation of ribosome composition is shared between kingdoms [15]. Another interesting example of specialized ribosomes can be found in *E. Coli* treated with the antibiotic kasugamycin, which binds to the small sub-unit and inhibits translation initiation. It was shown that leaderless mRNAs (lmRNAs) escape this inhibition, the reason being that they are translated by alternative 61S ribosomes, which lack 6 core small sub-unit rps and contain non stochiometric amounts of several other rps [16]. This may well mean that even the pool of 61S ribosomes contains ribosomes of varying composition. In conclusion, evidence against the general assumption that ribosomes always contain stochiometric amounts of rps is mounting, and many rps may have specific roles in translation, only being required for a subpopulation of mRNAs [17].

Polysome profiling

An experimental approach which is commonly used to study ribosome function and the efficiency of mRNA translation is polysome profiling. Sucrose gradients are used to separate free ribosomal subunits from translating ribosomes through velocity separation [18]. These are then visualized by displacing the sucrose gradient through a spectrophotometer and measuring the absorbance of the fraction at 254 nM, detecting RNA content (Fig 2). Since ribosomal subunits are the largest RNA structures in the cell, this technique separates ribosomes from cellular extracts [19]. mRNAs which are bound to multiple ribosomes, forming so-called polysomes, sediment as increasingly larger fractions as the number of bound ribosomes increases. This makes it possible to visualize the amount of ribosomes bound to mRNA and to isolate mRNAs based on their ribosome occupancy. A typical polysome profile shows, from beginning to end, the 40S subunit, the 60S subunit, the 80S monosome and polysomes of increasing magnitude.

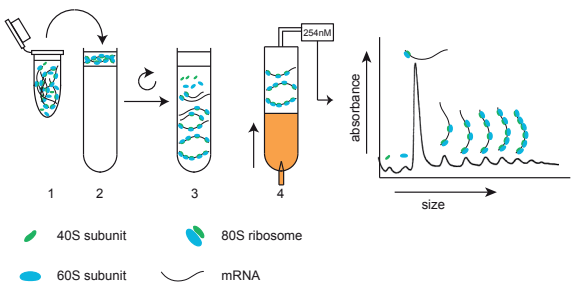

Figure 2: Polysome profiling. Samples are lysed and nuclei and mitochondria are pelleted by centrifugation (1). The remaining supernatant is loaded on top of a sucrose gradient (2). The gradient is centrifuged at high velocity (3), causing particles to settle in the gradient according to their size: heavy particles travel far, while light particles remain high in the gradient. The gradient is then displaced into a spectrophotometer, which determines absorption at 254nM, a measure for RNA content (4). This produces the polysome profile, which shows the abundance of particles according to their size.

Ribosome biogenesis defects cause human disease

An increasing body of evidence is linking mutations in genes involved in ribosome biogenesis to human disease. One example is Diamond-Blackfan anemia (DBA), a bone marrow failure disorder that is characterized by red cell aplasia, physical deformities and a predisposition to malignancies [20]. Genetic analysis has linked a number of haploinsufficient *rp* gene mutations, including *rpS7* [21], to DBA patients [22]. Haploinsufficiency of *rpS14* has also been associated with the bone marrow failure disorder myelodysplastic syndrome (MDS) [23]. Another example is dyskeratosis congenita (DC), a rare disease associated with nail dystrophy, oral leukoplakia, abnormal skin pigmentation, bone marrow failure, and also a predisposition to malignancies [24]. Mutations in several components of the H/ACA ribonucleoprotein (RNP) complex that is involved in rRNA pseudouridinylation and crucial for ribosome biogenesis are involved in the pathogenesis of DC [25]. While most DC mutations are linked to the dyskerin protein of the H/ACA complex, mutations in NOP10 are also linked to DC [26]. Shwachman-Diamond syndrome is another rare autosomal recessive multi-system disease, characterized by impaired hematopoiesis, leukemia predisposition and pancreatic dysfunction [27]. It is caused by mutations in the Shwachman-Bodian-Diamond syndrome gene, which has been shown to be critical for the late maturation of 60S rRNA particles by mediating the release of eIF6 [27, 28].

Part 2: The Role of nucleolar guanine nucleotide binding protein-like family members in ribosome biogenesis and cell cycle regulation

GTP-binding proteins or GTPases play a role in essential cellular processes, including intracellular signal transduction, mRNA translation and intracellular transport. Their activity is regulated by binding of GTP, which causes conformational changes and activates the protein. Subsequent hydrolysis of the GTP returns the protein to an inactive state [29, 30].
The family of YlqF Related GTPases is characterized by a central MMR_HSR1 GTPase domain showing a unique circular permutation of the known G motifs of the GTP binding proteins [30]. Three members of this family were identified that localize to the nucleolus: guanine like binding protein 2 (GNL2, or NGP-1), nucleostemin (NS or GNL3) and GNL3-LIKE (GNL3L) [30]. All three proteins shuttle back and forth between the nucleolus and the nucleoplasm [31]. The nucleolar retention time of GNL3L is short and primarily controlled by the basic coiled coil domain, while the nucleolar retention time of NS and GNL2 is long and requires the basic and the GTP-binding domains. All three contain a nucleoplasmic localization signal (NpLS), which prevents their accumulation in the nucleolus. The activity of the NpLS is determined by the GTP binding status, allowing for dynamic localization [31]. The two other most closely related, family members, GNL1 and hLsg1, are located in the cytoplasm [30].

Nucleostemin is required in the cell cycle

NS was first discovered for being highly expressed in stem cells and being rapidly downregulated upon differentiation. It was furthermore found to be upregulated in several cancer cell lines [32]. Conversely, NS was found to be highly upregulated in dedifferentiated newt muscle cells during limb regeneration [33]. It was therefore suggested that NS is involved in multipotency in stem cells and is required for proliferation of cancer cells and stem cells [32]. More recent data shows that NS is also expressed in normal proliferating cells. It was found to be expressed in malignant as well as normal kidney tissue [29]. Nucleostemin expression is also induced upon activation of T-lymphocytes using concavilin A [29] and upon stimulation of bone marrow stem cells with fibroblast growth factor 2 [30]. These findings suggest that NS is more probably required for

normal cell proliferation.
One of the mechanisms by which NS family members regulate the cell cycle is by regulating the activity of telomeric repeat factor 1 (TRF1). Both NS and GNL3L bind to TRF1, but their association with TRF1 has opposite outcomes: binding of NS results in degradation of TRF1 [34], while GNL3L stabilizes TRF1 and promotes its homodimerization and telomeric residence [35]. While the effects of NS and GNL3L binding on telomere maintenance are not resolved [35], the interaction between GNL3L and TRF1 plays an important role in mitosis. During mitosis, GNL3L levels rise, resulting in an increase in TRF1 levels. Both TRF1 and GNL3L are required for metaphase-to-anaphase transition, although the mechanism behind this, apart from being unrelated to the telomere, is unclear [35]. The interaction of NS with TRF1 was not found to play a role in the cell cycle [36].
Alongside with its initial discovery, NS was found to interact with and stabilize p53 [32], thus inhibiting cell cycle progression. This was later found to occur through association with and inhibition of MDM2 [37]. Interestingly, loss of NS has also been described to induce p53 activation. This occurs through the release of rpL5 and rpL11 from the nucleolus. These bind to MDM2 and cause p53 stabilization [38]. The release of free ribosomal proteins from the nucleolus and their association with MDM2 represents a more general pathway of nucleolar stress signaling, reviewed in ref [39].

Nucleostemin family members play a role in ribosome biogenesis

Apart from being involved in control of the cell cycle and sensing stress, which occur primarily in the nucleoplasm, NS was hypothesized to also have other functions more in line with its nucleolar localization. Mass spectrometry analysis of purified NS complexes from human cell lines indeed uncovered several proteins involved in ribosome biogenesis [40]. Further experiments revealed that loss of NS reduced the efficiency of rRNA processing, while overexpression increased processing efficiency [40]. Likewise, loss of the *C. elegans* NS homolog nst-1 was shown to result in a reduction of rRNA levels [41]. In *drosophila melanogaster,* loss of NS resulted in impaired large ribosomal subunit biogenesis [42]. GNL3L was also proposed to have a role in ribosome biogenesis. In fission yeast, heterologous expression of human GNL3L was able to rescue ribosome biogenesis defects caused by the deletion of *grn1,* a putative GTPase from the HSR1_MMR1 GTP-binding protein subfamily [43]. The exact function of NS and GNL3L in ribosome biogenesis is still unclear, while the involvement of GNL2 in ribosome biogenesis has not been studied at all.

Part 3: Biological Regulation of Lifespan

In 1977, Michael Klass showed that the roundworm *Caenorhabditis Elegans* lives longer and has fewer progeny when their caloric intake is reduced. Being an ectotherm, the worms also live longer at low than at high temperature [44]. These findings induced him to set up a forward genetic screen to identify genes that affect aging. He identified 8 lines which were long-lived, but upon closer inspection these harbored mutations that cause feeding defects. This led to the conclusion that the mechanism for longevity in these mutants was indirect caloric restriction and none of the genes found have any direct influence on aging [45].
Later, some of Klass' mutants were outcrossed and a line was discovered that had no trouble feeding but was still long lived. The *age-1* allele was found to be recessive and cause a 40%-65% increase in lifespan, depending on the temperature [46]. However, this mutant also showed a 75% reduction in fertility, causing the investigators to conclude that this was the reason for the longevity phenotype [46]. Years later they managed to cross out the fertility defect without losing the effect on lifespan [47].
In the meantime, Cynthia Kenyon had become interested in aging and prepared to do her own forward genetic screen. She decided to do her screen in worms with a background mutation causing constitutive dauer formation. Dauer is an alternative developmental stage a worm larva can go into when there is low food availability or high population density. In this state they can survive for a long time, much like a bacterial spore, until the environment becomes more favorable. Once the larva has developed past the second larval stage, it can no longer go into dauer. The *daf-2* mutation is only active at high temperature, so when adults are grown at high temperature they are easily followed throughout the course of their life because their progeny will go into dauer and not develop to maturity. In a stroke of luck, she found that the *daf-2* mutation itself dramatically increased the lifespan of the adult worms, making the whole screening process superfluous [48]. A more detailed historical account of the discovery of long-lived mutants can be found in ref [49].

The insulin pathway

The *daf-2* gene codes for the tyrosine kinase receptor for both insulin and Insulin Growth Factor 1 (IGF-1). Ligand binding results in autophosphorylation and subsequent activation of AGE-1, the C elegans homolog of PI3 Kinase (Fig 3A). This results in activation of 3-phosphoinositide dependent kinase (PDK), AKT1/AKT2, two functionally redundant *C. Elegans* AKT homologs, and SGK-1 [50]. Activated AKT1/AKT2 and SGK-1 phosphorylate the Forkhead transcription factor DAF-16 [50] and the Nrf-like xenobiotic response factor SKN-1 [51], which prevents them from entering the nucleus and initiating transcription. Additionally, insulin/IGF-1 Signaling (IIS) decreases the pool of available heat shock factor 1 (HSF-1) protein, by preventing dissociation of the DDL-1 HSF-1 Inhibitory Complex (DHIC). This occurs partially through AKT-1 signaling [52].
Abrogation of IIS by *daf-2* mutation results in activation of DAF-16 [48] and SKN-1 [51] mediated transcription and increases nuclear HSF-1 levels even in the absence of heat shock [52]. Interestingly, a subset of target genes requires transcriptional activity of both DAF-16 and SKN-1 [51] or both DAF-16 and HSF-1 [53]. Genetic epistasis analyses show that the lifespan extending effect of *daf-2* mutation is wholly dependent on DAF-16 [54] and HSF-1 [53] and partially dependent on SKN-1 signaling [51]. All these transcription factors activate pathways involved in response to a broad spectrum of stresses, including oxidative damage, heat shock and infection [55]. In addition, inhibition of Insulin/IGF-1 signaling induces high levels of autophagy [56]. Activation of all these pathways has a cumulative effect on lifespan.

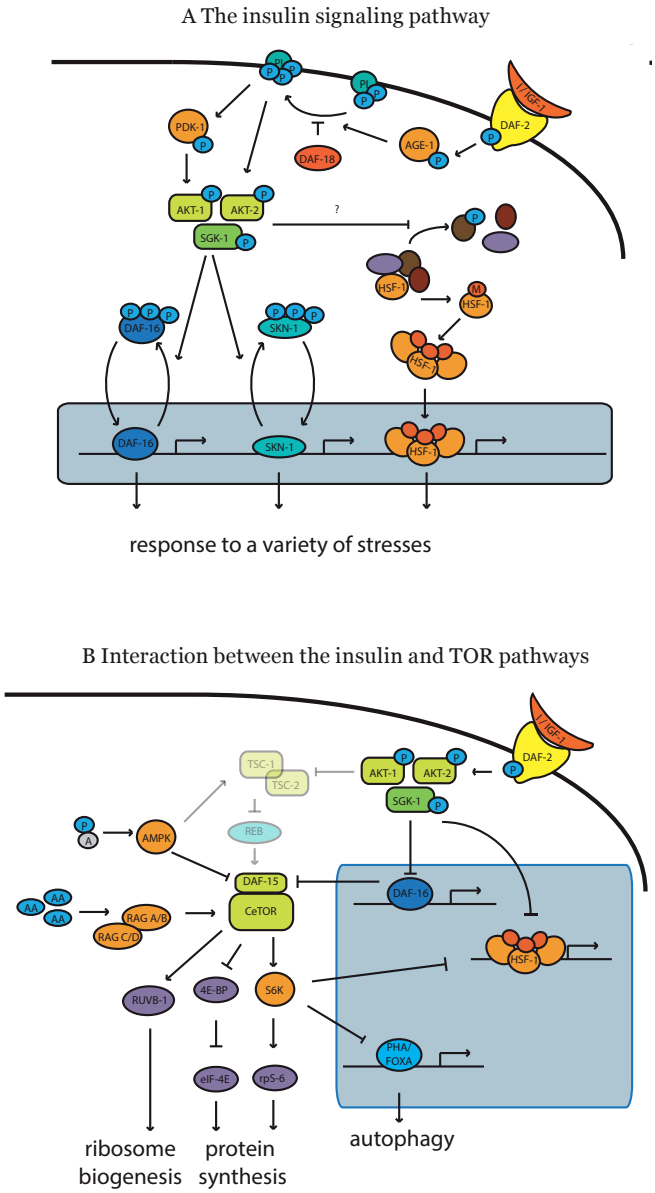

Figure 3: The insulin/insulin growth factor and TOR pathways of lifespan extension. (A) IIS regulates the localization of the transcription factors DAF-16, SKN-1 and HSF-1. (B) Interplay between the TOR and IIS signalling pathways. Transparent factors are absent in nematodes but play a role in other species. See text for detailed explanation. AA: amino acids, A: adenosine, P: phosphate.

The caloric restriction pathway of lifespan extension

The discovery that reducing caloric intake in rats results in an increased lifespan was already made in the late 1930's [57]. This effect has since been reproduced in a variety of animals [58], although a long running experiment in primates failed to show any increase in lifespan [59]. As

the IIS pathway functions in nutrient sensing, it would be expected that caloric restriction mediated lifespan extension occurs through IIS. This is partially the case. In worms, every-other-day feeding extends lifespan by inhibiting insulin/IGF-1 signaling [60]. In flies, long-lived IIS mutants respond to dietary restriction as though they were already somewhat diet restricted by their genotype, but the lifespan extension was not increased over the maximum increase achieved with dietary restriction alone [61]. However, lifespan extending effects of *eat-2* mutations, which cause difficulties in feeding and thus caloric restriction, are cumulative with those of *daf-2* mutations, suggesting they extend lifespan through separate pathways [62].

The TOR pathway

Next to the IIS pathway, the TOR kinase pathway is another major pathway for detection of nutrient levels. TOR is short for target of rapamycin, a compound first discovered as the product of the bacterium *Streptomyces hygroscopicus* from Easter Island, Rapa Nui [63]. TOR functions in two complexes, TOR Complex 1 (TORC1) and TORC2, which have different functions: TORC1 activates protein synthesis and induces cell growth, while TORC2 is involved in regulation of the cytoskeleton [64]. TORC1 consists of TOR, regulatory associated protein of TOR (raptor) and mLST8. TORC1 integrates a variety of signals, including nutrient, oxygen and growth factor availability and cellular energy status, to regulate cell growth [64].

Inhibiting the TOR pathway extends lifespan in species ranging from yeast to mice [65-69]. The TOR pathway has been identified as a key mediator of nutrient induced changes in life span in yeast [65], flies [66] and worms [70], as inhibition of the TOR pathway does not further extend the lifespan of dietary restricted animals. Unlike IIS mediated life span extension, TOR mediated life span extension does not depend on DAF-16 [66-68], suggesting that TOR either acts in parallel or downstream of IIS to extend lifespan. The finding that inhibition of TOR does not further increase the lifespan of *daf-2* mutants [68] suggests the latter.

The TOR and IIS pathways are connected in several ways (Fig 3B). In most species, AKT phosphorylates the TSC-1/TSC-2 complex, which releases its inhibition on the small GTPase Rheb, activating TORC1 [64]. *C. Elegans* lacks homologs for TSC-1/TSC-2. Instead, DAF-16 represses transcription of DAF-15, the C elegans homolog of raptor, inhibiting TOR activity [64]. Conversely, the TOR pathway feeds into IIS by regulation of HSF-1 through RPS6 kinase [71]. IIS is far from being the only pathway influencing TORC1 activity. High levels of AMP, indicating a depletion of ATP, triggers AMP dependent kinase (AMPK) activity, which phosphorylates and activates the TSC-1/TSC-2 complex and directly inhibits TORC1 activity by inhibitory phosphorylation of DAF-15/raptor. High levels of amino acids in the cell activate TOR through an unknown mechanism, which involves two small heteromeric GTPases, RagA/RagB and RagC/RagD [72]. TORC1 also responds to oxygen levels. Hypoxia allows stabilization of the transcription factor HIF1a (discussed below). The hypoxic response gene REDD1 inhibits TORC1 activity by a TSC2-dependent mechanism [73].

TORC1 activates a variety of pathways that influence lifespan. It increases translational activity by activating the small ribosomal subunit S6 kinase and deactivating 4E-BP, an inhibitor of eIF-4E [64], as well as inducing transcription of ribosomal protein genes [64]. TORC1 also controls ribosome biogenesis by determining the nucleolar localization of Box C/D snoRNPs through RUVB-1 [74]. Direct inhibition of ribosome biogenesis and translation was shown to be sufficient to extend lifespan, as inhibition of any of a large number of ribosomal protein genes, as well as S6K, eIF2 β / iftb-1 , eIF4E/ ife-2, and eIF4G/ ifg-1 all had this effect [70, 75-77]. In addition to these direct effects on translation, inhibition of TOR depends on transcription factors to induce longevity, notably PHA-4 (the only *C Elegans* FoxA transcription factor), which activates autophagy [74]. Autophagy is required for a reduction of TOR signaling to extend lifespan [74], as is the case

for DR [78] and IIS mediated life span extension [56], although autophagy alone is not enough to extend lifespan [56].

The mitochondrion as a site for life span determination

Another class of genes that influence lifespan is the components of the mitochondria. Loss of several of these respiratory chain components has been shown to reduce respiration rates and extend lifespan [79, 80]. Inhibiting mitochondrial complexes only in adult neurons was sufficient to increase lifespan in flies, indicating that this is a cell non-autonomous defect [80]. Only 13 of the proteins that make up the mitochondrion are actually encoded in the mitochondrial DNA, while over a thousand are encoded in the nuclear DNA. These mitochondrial genes require separate translation machinery, including mitochondrial ribosomal proteins (mrps) [81, 82]. Loss of several of these mrps was also shown to extend lifespan [83]. In worms it was shown that lifespan extension only occurs when the treatment takes place during larval development. Intriguingly, the increase in lifespan, and the reduction in ATP production persist even when the treatment is removed after the worms have reached adulthood [79, 83]. Starting treatment after the worms have reached adulthood lowers ATP production, but fails to increase lifespan in worms [79], although it is possible to increase lifespan this way in flies [80]. This argues against the idea that a reduction in oxidative stress is responsible for this phenotype [84]. The lifespan extension observed upon inhibition of mitochondrial components is cumulative with daf-2 mediated lifespan extension [79] and does not depend on daf-16 [79, 83].
In contrast, dietary restriction actually increases mitochondrial respiration, through preferential translation of nuclear encoded mitochondrial proteins [85]. It has been postulated that increasing respiration extends lifespan for one reason, and inhibiting respiration extends lifespan for another [86]. However, recent evidence suggests that both upregulation and downregulation of a subset of mitochondrial proteins causes an imbalance in mitochondrial components and elicits an unfolded mitochondrial protein response, which is responsible for lifespan extension [83].

Other processes affecting lifespan

Besides changes in IIS, TOR signaling and respiration, several other processes have been shown to influence lifespan. Overexpression of sirtuins, NAD^+-dependent protein de-acetylases, has also been shown to extend lifespan in various species, but the exact mechanisms behind this remain unclear [86]. In C. Elegans, sirt-2.1 activates DAF-16 directly by de-acetylation [87], indicating that sirt-2.1 acts in parallel to IIS to extend lifespan. Sirtuins have also been proposed as one of the mediators of caloric restriction induced longevity, but so far the experimental evidence has not been entirely consistent with this hypothesis [88].
Another influence on lifespan is reproductive capacity. In nature, it seems as if animals make a trade-off between reproduction and longevity. Strong IIS mutants show reduced fertility, but in weaker mutations the effect on lifespan is maintained without the reproduction phenotype, so a trade-off does not necessarily occur. Ablation of the germline (but not the whole gonad) does increase lifespan, in both worms [89] and flies [90], indicating that there is a connection between lifespan and reproduction [86].

In summary, the main pathways which influence lifespan are insulin/IGF-1 signaling, the TOR pathway and the mitochondrial unfolded protein response. These all induce a global shift from growth to tissue maintenance and stress resistance. It is an interesting challenge to find out exactly how these pathways overlap and how they differ and to use this information in the future to increase our own lifespans.

Part 4: The Von Hippel-Lindau Tumor Suppressor

The Von Hippel-Lindau disease (MIM193300) is an autosomal dominant disorder caused by mutations in the VHL gene [91]. Symptoms include vascular neoplasia, hemangioblastomas of the central nervous system and the retina, endocrine neoplasia of the adrenal gland (pheochromocytomas) and the development of benign as well as malignant tumors in many organ systems [92]. Of these tumors, clear cell Renal Cell Carcinoma (ccRCC) is the most common cause of disease related death and develops in about 70% of patients [92]. In addition to being the underlying cause of ccRCC in the inherited VHL syndrome, loss of function of the *vhl* gene, both by somatic mutation or epigenetic silencing, is also found in 40-70% of sporadic cases of ccRCC [93-95], indicating that VHL functions as a tumor suppressor. In this part of the introduction we will give an overview of the ways in which VHL is involved in tumor formation and what other mutations drive RCC development.

VHL regulates the hypoxic response

The best described function of pVHL is in oxygen sensing, as it is the substrate binding component of a SCF (Skp1-Cdc53/Cul-1-F-box protein) type E3 ubiquitin ligase containing, besides pVHL, Cullin-2, elongin B and C and Rbx-1. In this complex, pVHL binds the transcription factor hypoxia inducible factor 1α (HIF1α) under normoxic conditions, when its proline residues are hydroxylated by prolyl hydroxylase domain proteins, resulting in HIF1α ubiquitination and subsequent degradation. Under hypoxic conditions, hydroxylation cannot take place and HIF1α is no longer targeted by pVHL, resulting in its stabilization and the upregulation of its target genes, such as VEGF, VEGF-R, Epo and c-myb [96]. Mutation of pVHL similarly results in a failure to recognize HIF1α, inducing a continuous hypoxic response (Fig 4).

The upregulation of hypoxic response genes activates many processes that assist tumor growth, such as angiogenesis, metabolic adaptation, apoptosis resistance and metastasis [97]. Although degradation of HIFα is crucial for pVHL tumor suppression [98], it has been shown that HIFα activation alone is not sufficient to drive tumorigenesis. Cells overexpressing HIF1α were unable to form tumors after injection into nude mice [99]. A mouse model in which the proline sites in HIF1α were mutated so that it escapes degradation, showed a kidney histology which was very similar to that observed in patients with VHL disease, but no tumor formation was observed [100]. These results suggest that pVHL has other functions besides oxygen sensing which contribute to its role as a tumor suppressor protein.

HIFα independent mechanism of tumor formation

In a mechanism similar to HIF1α degradation, pVHL recognizes Rbp1, the large subunit of the RNA polymerase II, in manner that depends on hydroxylation of one of its proline residues. Binding of pVHL promotes the recruitment of Rbp1 to chromatin and targets it for ubiquitination. The result of this ubiquitination is not Rbp1 degradation, its effect on transcription has not been elucidated [101].

Besides its role in an E3 ligase, VHL functions as an adaptor protein that controls a variety of gene expression programs, as well as extracellular matrix and microtubule associated processes, by linking target proteins to sites of enzymatic activity (Fig 5) [102]. Of particular interest is the finding that loss of VHL results in constitutive activation of NF-κB transcription factors [103]. pVHL serves as an adaptor that promotes the phosphorylation of the Card9 C terminus by CK2, thereby enhancing its ability to activate NF-κB [103]. NF-κB induces transcription of genes which inhibit apoptosis, such as members of the BCL family, survivin and inhibitor of apoptosis 2 [104]. This is likely to be one of the underlying causes of the high resistance to apoptosis inducing

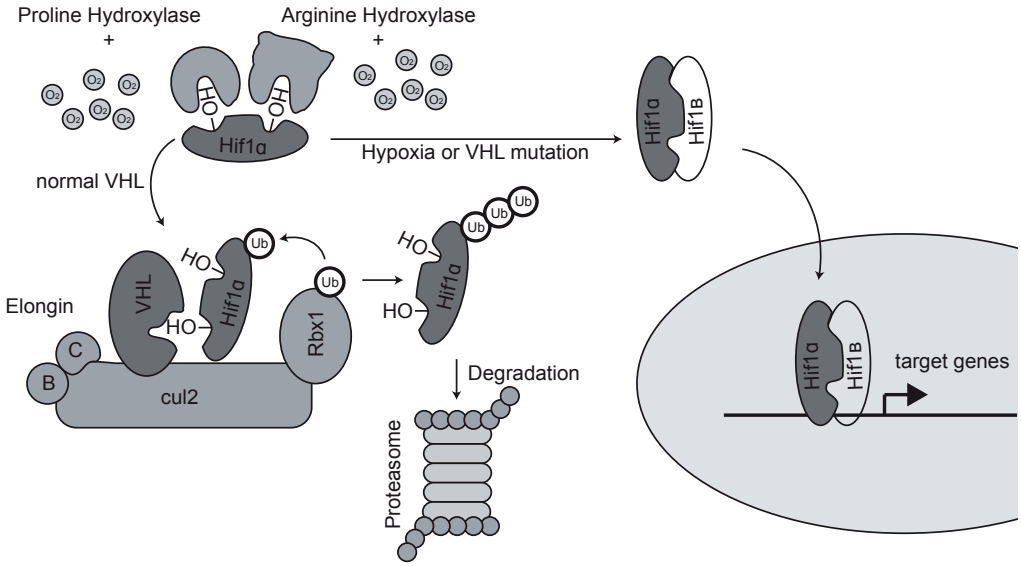

Figure 4: The oxygen sensing pathway. VHL is part of an SCF type E3 ubiquitin ligase responsible for targeting HIFα for degradation under normoxic conditions. In the absence of oxygen or functional VHL protein, HIFα accumulates, binds to HIFβ and activates transcription of hypoxia response elements. Adapted from [121].

therapies observed in ccRCC.

Another transcription related adaptor function of pVHL is its ability to bind to and inhibit atypical protein kinase C (aPKC), which in turn downregulates JunB [105]. Loss of pVHL promotes JunB activation, resulting in an overexpression of survival factors in neurons and reduced apoptosis in response to growth factor withdrawal. This is thought to be the underlying mechanism for the pheochromocytomas observed in VHL disease [105]. It remains unresolved whether this pathway also plays a role in tumor suppression by pVHL. Loss of vHL has also been shown to lead to overexpression of the p400 chromatin remodeling factor, resulting in increased levels of the cyclin-dependent kinase inhibitor and induction of an Rb-dependent pathway of senescence [106]. Senescence may be a mechanism to keep VHL-/- cells from proliferating, but may also constitute a selective pressure to overcome this growth arrest [103]. In RCC, p53 and pVHL are rarely found mutated simultaneously, suggesting an interaction between the two. In vitro studies did show that pVHL binds to p53 through recruiting it to a complex containing the p53 activating factors ATM and p300 [107], but the significance of this interaction has yet to be shown.

In addition to playing a role in regulating transcription factor activation, pVHL has also been shown to be required for the deposition of extracellular matrix and regulation of the microtubule cytoskeleton. Cells devoid of pVHL fail to form a collagen IV and fibronectin extracellular matrix, a defect which may aid in angiogenesis and tumor metastasis [108, 109]. pVHL also plays a key role in the maintenance of the structure of the primary cilium [110], which has been shown to regulate epithelial cell proliferation and inhibit cyst formation in the kidney [111]. However, for cells to lose the primary cilium, glycogen synthase kinase 3β (GSK3β) needs to be simultaneously inactivated, likely by activation of AKT [110].

This seems to be the general pattern. Despite its role in so many pathways linked to cancer, loss of VHL alone has not proven to be enough to induce tumor formation. In fact, cells lacking functional Vhl grew more slowly than cells retaining Vhl after injection into immunodeficient mice [99].

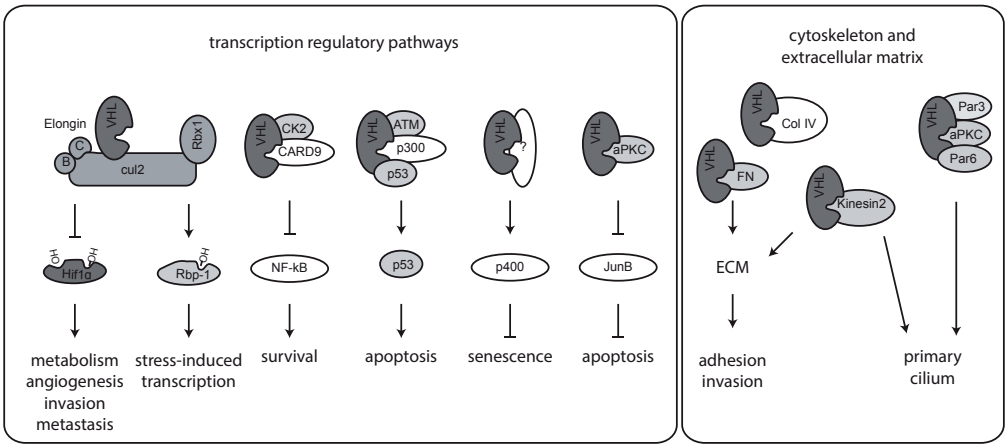

Figure 5: VHL functions as an adaptor protein in a variety of processes. See text for detailed explanation. Adapted from [102].

Despite much effort, few validated *in vivo* models exist for ccRCC. Neither mice heterozygous for Vhl [112] - not even after exposure to high doses of carcinogen [113] - nor mice which had a conditional knockout of *Vhl* in the renal proximal tubule [114] developed RCC, although the latter did develop renal cysts. Only a recently developed mouse model, in which *Vhl* and *p53* were simultaneously inactivated in the kidney, showed atypical cysts and neoplasms with characteristics similar to RCC [115]. These results indicate that a second mutation event is required for tumor formation to occur in VHL-/- cells.

Other mutations in RCC that drive tumor formation

Besides pVHL, mutation of several other well-known tumor suppressors and oncogenes has been reported to be associated with ccRCC. Taking all histologies combined, the COSMIC database [116] reports somatic point mutations in TP53 in 10% of cases, KRAS/HRAS/NRAS combined in < 1%, CDKN2A 10%, PTEN 3%, RB1 3%, STK11/LKB1 <1%, PIK3Ca <1%, EGFR 1%, BRAF <1%. Amplification of Myc and rare cases of EGFR amplification inRCC have been reported [117]. Taken together, these mutations can hardly account for all cases of RCC, suggesting that others have not been found.

A large scale systematic effort to find novel genes mutated in RCC, in which 3,544 protein-coding genes were screened via PCR- based exon resequencing in 101 cases of ccRCC, identified several new cancer genes in RCC [118, 119]. Interestingly, 4 out of 5 the genes most robustly associated with RCC encode proteins involved in histone methylation/demethylation. Truncating mutations were identified in KDM6A/UTX (a histone 3 lysine 27 (H3K27) demethylase), SETD2 (a H3K36 methyltransferase) and KDM5C/JARID1C (a H3K4 demethylase). MLL2, an H3K4 methyltransferase, was also found to be mutated at a significant rate. These findings suggest a role for deregulation of histone H3 methylation, a major determinant of chromatin state and transcription efficiency [118]. Even so, each of these genes was only mutated in 3% of RCCs [118], indicating that there remain more cancer genes to be found.

Despite the high occurrence of VHL mutations, RCC has proven to be a very heterogeneous disease, and it will take more work to fully delineate the pathways that lead to cancer development, pVHL-related as well as unrelated

Outline of this thesis

Ribosome biogenesis and translation are ubiquitous processes, whose misregulation can lead to disease but whose inhibition can have beneficial benefits. In this thesis, examples of both sides can be found

Although there has been much interest in nucleostemin from a stem cell and cancer biology perspective, not much is known about its role in ribosome biogenesis and even less about its family members *gnl2* and *gnl3l*. In chapter 2, we performed a systematic analysis of the role of *ns* gene family members in both ribosome biogenesis and p53 stabilization. We found that both *gnl2* and *ns*, but not *gnl3l*, play an important role in ribosome biogenesis, while loss of all three genes led to an upregulation of p53. In addition, our lab previously showed that nucleostemin and gnl2 play a role in neurogenesis. To investigate whether this is an effect of their function in ribosome biogenesis, we compared neural phenotypes between *gnl2* and *ns* and two unrelated ribosome biogenesis mutants in chapter 3 and discovered that these phenotypes are common to ribosome biogenesis mutants.

In chapter 4, we describe the results of a large proteomics screen in long lived *daf-2* mutants and show that a strong downregulation of ribosome biogenesis and translation takes place. This is most apparent in the reduced numbers of polysomes. We show a simultaneous reduction of proteasomal activity, indicating that these mutants have a very low protein turnover. In chapter 5 we asked the question if any RNAs are preferentially translated by the low level of polysomes in *daf-2* mutants. We performed sequencing of the RNA associated with monosomes and polysomes in *daf-2* mutants and found, aside from evidence of preferential translation, several non-coding RNAs which were involved in reducing translation capacity.

In chapter 6, we describe how treatment of fawn hooded hypertensive rats with the nitric oxide donor drug molsidomine *in utero* reduces ribosome biogenesis in the kidney at two days after birth. Although this reduced ribosome biogenesis is corrected by two weeks of age, the treatment persistently lowers blood pressure in later life.

As described, many interactions of VHL remain unknown. In chapter 7 we set out to investigate the link between p53 and vhl *in vivo*. Due to the absence of compounding mutations, the zebrafish model of pVHL loss currently remains the most reliable *in vivo* system with which to characterize the effects of mutations in this tumor suppressor. Contrary to previous *in vitro* reports, we found that loss of vhl increases p53 stability, even in the absence of DNA damage. We establish a mechanism for the stabilization of the p53 tumor suppressor upon pVHL loss and hypoxia through the apoptosis protein programmed cell death 5 (PDCD5).

Finally, in chapter 8 we will give a summarizing discussion of the work in this thesis and its implications.

References

1. Physiology or Medicine 1974 - Press Release. Nobelprize.org, 1974(Oktober).
2. Warner, J.R., The economics of ribosome biosynthesis in yeast. Trends Biochem Sci, 24(11): p. 437-40.
3. Samarsky, D.A. and M.J. Fournier, A comprehensive database for the small nucleolar RNAs from Saccharomyces cerevisiae. Nucleic Acids Res, 27(1): p. 161-4.
4. Kressler, D., E. Hurt, and J. Bassler, Driving ribosome assembly. Biochim Biophys Acta, 1803(6): p. 673-83.
5. Komar, A.A., B. Mazumder, and W.C. Merrick, A new framework for understanding IRES-mediated translation. Gene, 502(2): p. 75-86.
6. Wells, S.E., et al., Circularization of mRNA by eukaryotic translation initiation factors. Mol Cell, 2(1): p. 135-40.
7. Steitz, T.A., A structural understanding of the dynamic ribosome machine. Nat Rev Mol Cell Biol, 9(3): p. 242-53.
8. Jackson, R.J., C.U. Hellen, and T.V. Pestova, Termination and post-termination events in eukaryotic translation. Adv Protein Chem Struct Biol, 86: p. 45-93.
9. Maier, T., M. Guell, and L. Serrano, Correlation of mRNA and protein in complex biological samples. FEBS Lett, 583(24): p. 3966-73.
10. Gebauer, F. and M.W. Hentze, Molecular mechanisms of translational control. Nat Rev Mol Cell Biol, 5(10): p. 827-35.
11. Johannes, G., et al., Identification of eukaryotic mRNAs that are translated at reduced cap binding complex eIF4F concentrations using a cDNA microarray. Proc Natl Acad Sci U S A, 96(23): p. 13118-23.
12. Baird, S.D., et al., A search for structurally similar cellular internal ribosome entry sites. Nucleic Acids Res, 35(14): p. 4664-77.
13. Fleischer, T.C., et al., Systematic identification and functional screens of uncharacterized proteins associated with eukaryotic ribosomal complexes. Genes Dev, 20(10): p. 1294-307.
14. Kondrashov, N., et al., Ribosome-mediated specificity in Hox mRNA translation and vertebrate tissue patterning. Cell, 145(3): p. 383-97.
15. Agarwal, A.K., S.N. Parrish, and D.D. Blumberg, Ribosomal protein gene expression is cell type specific during development in Dictyostelium discoideum. Differentiation, 65(2): p. 73-88.
16. Kaberdina, A.C., et al., An unexpected type of ribosomes induced by kasugamycin: a look into ancestral times of protein synthesis? Mol Cell, 33(2): p. 227-36.
17. Gilbert, W.V., Functional specialization of ribosomes? Trends Biochem Sci, 36(3): p. 127-32.
18. Lecocq, R.E., et al., Quantitative evaluation of polysomes and ribosomes by density gradient centrifugation and electron microscopy. Anal Biochem, 43(1): p. 71-9.
19. Krokowski, D., et al., Characterization of hibernating ribosomes in mammalian cells. Cell Cycle, 10(16): p. 2691-702.
20. Willig, T.N., H. Gazda, and C.A. Sieff, Diamond-Blackfan anemia. Curr Opin Hematol, 7(2): p. 85-94.
21. Gazda, H.T., et al., Ribosomal protein L5 and L11 mutations are associated with cleft palate and abnormal thumbs in Diamond-Blackfan anemia patients. Am J Hum Genet, 83(6): p. 769-80.
22. Farrar, J.E. and N. Dahl, Untangling the phenotypic heterogeneity of Diamond Blackfan anemia. Semin Hematol, 48(2): p. 124-35.
23. Ebert, B.L., et al., Identification of RPS14 as a 5q- syndrome gene by RNA interference screen. Nature, 451(7176): p. 335-9.
24. Nishio, N. and S. Kojima, Recent progress in dyskeratosis congenita. Int J Hematol, 92(3): p. 419-24.
25. Nelson, N.D. and A.A. Bertuch, Dyskeratosis congenita as a disorder of telomere maintenance. Mutat Res, 2011.
26. Nelson, N.D. and A.A. Bertuch, Dyskeratosis congenita as a disorder of telomere maintenance. Mutat Res, 730(1-2): p. 43-51.
27. Burroughs, L., A. Woolfrey, and A. Shimamura, Shwachman-Diamond syndrome: a review of the clinical presentation, molecular pathogenesis, diagnosis, and treatment. Hematol Oncol Clin North Am, 23(2): p. 233-48.
28. Finch, A.J., et al., Uncoupling of GTP hydrolysis from eIF6 release on the ribosome causes Shwachman-Diamond syndrome. Genes Dev, 25(9): p. 917-29.
29. Fan, Y., et al., Nucleostemin mRNA is expressed in both normal and malignant renal tissues. Br J Cancer, 94(11): p. 1658-62.
30. Kafienah, W., et al., Nucleostemin is a marker of proliferating stromal stem cells in adult human bone marrow. Stem Cells, 24(4): p. 1113-20.
31. Meng, L., Q. Zhu, and R.Y. Tsai, Nucleolar trafficking of nucleostemin family proteins: common versus protein-specific mechanisms. Mol Cell Biol, 27(24): p. 8670-82.

32. Tsai, R.Y. and R.D. McKay, A nucleolar mechanism controlling cell proliferation in stem cells and cancer cells. Genes Dev, 16(23): p. 2991-3003.
33. Maki, N., et al., Rapid accumulation of nucleostemin in nucleolus during newt regeneration. Dev Dyn, 236(4): p. 941-50.
34. Zhu, Q., H. Yasumoto, and R.Y. Tsai, Nucleostemin delays cellular senescence and negatively regulates TRF1 protein stability. Mol Cell Biol, 26(24): p. 9279-90.
35. Zhu, Q., et al., GNL3L stabilizes the TRF1 complex and promotes mitotic transition. J Cell Biol, 185(5): p. 827-39.
36. Tsai, R.Y., Nucleolar modulation of TRF1: a dynamic way to regulate telomere and cell cycle by nucleostemin and GNL3L. Cell Cycle, 8(18): p. 2912-6.
37. Dai, M.S., X.X. Sun, and H. Lu, Aberrant expression of nucleostemin activates p53 and induces cell cycle arrest via inhibition of MDMMol Cell Biol, 28(13): p. 4365-76.
38. Dai, M.S. and H. Lu, Inhibition of MDM2-mediated p53 ubiquitination and degradation by ribosomal protein LJ Biol Chem, 279(43): p. 44475-82.
39. Zhou, X., et al., Scission of the p53-MDM2 Loop by Ribosomal Proteins. Genes Cancer, 3(3-4): p. 298-310.
40. Romanova, L., et al., Critical role of nucleostemin in pre-rRNA processing. J Biol Chem, 284(8): p. 4968-77.
41. Kudron, M.M. and V. Reinke, C. elegans nucleostemin is required for larval growth and germline stem cell division. PLoS Genet, 4(8): p. e1000181.
42. Rosby, R., et al., Knockdown of the Drosophila GTPase nucleostemin 1 impairs large ribosomal subunit biogenesis, cell growth, and midgut precursor cell maintenance. Mol Biol Cell, 20(20): p. 4424-34.
43. Du, X., et al., The homologous putative GTPases Grn1p from fission yeast and the human GNL3L are required for growth and play a role in processing of nucleolar pre-rRNA. Mol Biol Cell, 17(1): p. 460-74.
44. Klass, M.R., Aging in the nematode Caenorhabditis elegans: major biological and environmental factors influencing life span. Mech Ageing Dev, 6(6): p. 413-29.
45. Klass, M.R., A method for the isolation of longevity mutants in the nematode Caenorhabditis elegans and initial results. Mech Ageing Dev, 22(3-4): p. 279-86.
46. Friedman, D.B. and T.E. Johnson, A mutation in the age-1 gene in Caenorhabditis elegans lengthens life and reduces hermaphrodite fertility. Genetics, 118(1): p. 75-86.
47. Johnson, T.E., P.M. Tedesco, and G.J. Lithgow, Comparing mutants, selective breeding, and transgenics in the dissection of aging processes of Caenorhabditis elegans. Genetica, 91(1-3): p. 65-77.
48. Kenyon, C., et al., A C. elegans mutant that lives twice as long as wild type. Nature, 366(6454): p. 461-4.
49. Kenyon, C., The first long-lived mutants: discovery of the insulin/IGF-1 pathway for ageing. Philos Trans R Soc Lond B Biol Sci, 366(1561): p. 9-16.
50. Lant, B. and K.B. Storey, An overview of stress response and hypometabolic strategies in Caenorhabditis elegans: conserved and contrasting signals with the mammalian system. Int J Biol Sci, 6(1): p. 9-50.
51. Tullet, J.M., et al., Direct inhibition of the longevity-promoting factor SKN-1 by insulin-like signaling in C. elegans. Cell, 132(6): p. 1025-38.
52. Chiang, W.C., et al., HSF-1 regulators DDL-1/2 link insulin-like signaling to heat-shock responses and modulation of longevity. Cell, 148(1-2): p. 322-34.
53. Hsu, A.L., C.T. Murphy, and C. Kenyon, Regulation of aging and age-related disease by DAF-16 and heat-shock factor. Science, 300(5622): p. 1142-5.
54. Jasper, H., SKNy worms and long life. Cell, 132(6): p. 915-6.
55. Murphy, C.T., et al., Genes that act downstream of DAF-16 to influence the lifespan of Caenorhabditis elegans. Nature, 424(6946): p. 277-83.
56. Hansen, M., et al., A role for autophagy in the extension of lifespan by dietary restriction in C. elegans. PLoS Genet, 4(2): p. e24.
57. McCay, C.M., et al., The Journal of Nutrition. Volume 18 July--December, Pages 1--Retarded growth, life span, ultimate body size and age changes in the albino rat after feeding diets restricted in calories. Nutr Rev, 33(8): p. 241-3.
58. Masoro, E.J., Subfield history: caloric restriction, slowing aging, and extending life. Sci Aging Knowledge Environ, 2003(8): p. RE2.
59. Mattison, J.A., et al., Impact of caloric restriction on health and survival in rhesus monkeys from the NIA study. Nature, 489(7415): p. 318-21.
60. Honjoh, S., et al., Signalling through RHEB-1 mediates intermittent fasting-induced longevity in C. elegans. Nature, 457(7230): p. 726-30.
61. Clancy, D.J., et al., Dietary restriction in long-lived dwarf flies. Science, 296(5566): p. 319.

62. Lakowski, B. and S. Hekimi, The genetics of caloric restriction in Caenorhabditis elegans. Proc Natl Acad Sci U S A, 95(22): p. 13091-6.
63. Heitman, J., N.R. Movva, and M.N. Hall, Targets for cell cycle arrest by the immunosuppressant rapamycin in yeast. Science, 253(5022): p. 905-9.
64. Martin, D.E. and M.N. Hall, The expanding TOR signaling network. Curr Opin Cell Biol, 17(2): p. 158-66.
65. Kaeberlein, M., et al., Regulation of yeast replicative life span by TOR and Sch9 in response to nutrients. Science, 310(5751): p. 1193-6.
66. Kapahi, P., et al., Regulation of lifespan in Drosophila by modulation of genes in the TOR signaling pathway. Curr Biol, 14(10): p. 885-90.
67. Jia, K., D. Chen, and D.L. Riddle, The TOR pathway interacts with the insulin signaling pathway to regulate C. elegans larval development, metabolism and life span. Development, 131(16): p. 3897-906.
68. Vellai, T., et al., Genetics: influence of TOR kinase on lifespan in C. elegans. Nature, 426(6967): p. 620.
69. Harrison, D.E., et al., Rapamycin fed late in life extends lifespan in genetically heterogeneous mice. Nature, 460(7253): p. 392-5.
70. Hansen, M., et al., Lifespan extension by conditions that inhibit translation in Caenorhabditis elegans. Aging Cell, 6(1): p. 95-110.
71. Seo, K., et al., Heat shock factor 1 mediates the longevity conferred by inhibition of TOR and insulin/IGF-1 signaling pathways in C. elegans. Aging Cell, 2013.
72. Kim, E., et al., Regulation of TORC1 by Rag GTPases in nutrient response. Nat Cell Biol, 10(8): p. 935-45.
73. Brugarolas, J., et al., Regulation of mTOR function in response to hypoxia by REDD1 and the TSC1/TSC2 tumor suppressor complex. Genes Dev, 18(23): p. 2893-904.
74. Sheaffer, K.L., D.L. Updike, and S.E. Mango, The Target of Rapamycin pathway antagonizes pha-4/FoxA to control development and aging. Curr Biol, 18(18): p. 1355-64.
75. Henderson, S.T., M. Bonafe, and T.E. Johnson, daf-16 protects the nematode Caenorhabditis elegans during food deprivation. J Gerontol A Biol Sci Med Sci, 61(5): p. 444-60.
76. Pan, K.Z., et al., Inhibition of mRNA translation extends lifespan in Caenorhabditis elegans. Aging Cell, 6(1): p. 111-9.
77. Syntichaki, P., K. Troulinaki, and N. Tavernarakis, eIF4E function in somatic cells modulates ageing in Caenorhabditis elegans. Nature, 445(7130): p. 922-6.
78. Jia, K. and B. Levine, Autophagy is required for dietary restriction-mediated life span extension in C. elegans. Autophagy, 3(6): p. 597-9.
79. Dillin, A., et al., Rates of behavior and aging specified by mitochondrial function during development. Science, 298(5602): p. 2398-401.
80. Copeland, J.M., et al., Extension of Drosophila life span by RNAi of the mitochondrial respiratory chain. Curr Biol, 19(19): p. 1591-8.
81. Sharma, M.R., et al., Structure of the mammalian mitochondrial ribosome reveals an expanded functional role for its component proteins. Cell, 115(1): p. 97-108.
82. Anderson, S., et al., Sequence and organization of the human mitochondrial genome. Nature, 290(5806): p. 457-65.
83. Houtkooper, R.H., et al., Mitonuclear protein imbalance as a conserved longevity mechanism. Nature, 497(7450): p. 451-7.
84. Feng, J., F. Bussiere, and S. Hekimi, Mitochondrial electron transport is a key determinant of life span in Caenorhabditis elegans. Dev Cell, 1(5): p. 633-44.
85. Zid, B.M., et al., 4E-BP extends lifespan upon dietary restriction by enhancing mitochondrial activity in Drosophila. Cell, 139(1): p. 149-60.
86. Kenyon, C.J., The genetics of ageing. Nature, 464(7288): p. 504-12.
87. Berdichevsky, A., et al., C. elegans SIR-2.1 interacts with 14-3-3 proteins to activate DAF-16 and extend life span. Cell, 125(6): p. 1165-77.
88. Kaeberlein, M. and R.W. Powers, 3rd, Sir2 and calorie restriction in yeast: a skeptical perspective. Ageing Res Rev, 6(2): p. 128-40.
89. Hsin, H. and C. Kenyon, Signals from the reproductive system regulate the lifespan of C. elegans. Nature, 399(6734): p. 362-6.
90. Flatt, T., et al., Drosophila germ-line modulation of insulin signaling and lifespan. Proc Natl Acad Sci U S A, 105(17): p. 6368-73.
91. Latif, F., et al., Identification of the von Hippel-Lindau disease tumor suppressor gene. Science, 260(5112): p. 1317-20.
92. Lonser, R.R., et al., von Hippel-Lindau disease. Lancet, 361(9374): p. 2059-67.
93. Herman, J.G., et al., Silencing of the VHL tumor-suppressor gene by DNA methylation in renal carcinoma. Proc Natl Acad Sci U S A, 91(21): p. 9700-4.

94. Kim, W.Y. and W.G. Kaelin, Role of VHL gene mutation in human cancer. J Clin Oncol, 22(24): p. 4991-5004.
95. Banks, R.E., et al., Genetic and epigenetic analysis of von Hippel-Lindau (VHL) gene alterations and relationship with clinical variables in sporadic renal cancer. Cancer Res, 66(4): p. 2000-11.
96. Hsu, T., Complex cellular functions of the von Hippel-Lindau tumor suppressor gene: insights from model organisms. Oncogene, 31(18): p. 2247-57.
97. Semenza, G.L., Targeting HIF-1 for cancer therapy. Nat Rev Cancer, 3(10): p. 721-32.
98. Kondo, K., et al., Inhibition of HIF is necessary for tumor suppression by the von Hippel-Lindau protein. Cancer Cell, 1(3): p. 237-46.
99. Mack, F.A., et al., Loss of pVHL is sufficient to cause HIF dysregulation in primary cells but does not promote tumor growth. Cancer Cell, 3(1): p. 75-88.
100. Fu, L., et al., Generation of a mouse model of Von Hippel-Lindau kidney disease leading to renal cancers by expression of a constitutively active mutant of HIF1alpha. Cancer Res, 71(21): p. 6848-56.
101. Mikhaylova, O., et al., The von Hippel-Lindau tumor suppressor protein and Egl-9-Type proline hydroxylases regulate the large subunit of RNA polymerase II in response to oxidative stress. Mol Cell Biol, 28(8): p. 2701-17.
102. Frew, I.J. and W. Krek, pVHL: a multipurpose adaptor protein. Sci Signal, 1(24): p. pe30.
103. Yang, H., et al., pVHL acts as an adaptor to promote the inhibitory phosphorylation of the NF-kappaB agonist Card9 by CKMol Cell, 28(1): p. 15-27.
104. Morais, C., et al., The emerging role of nuclear factor kappa B in renal cell carcinoma. Int J Biochem Cell Biol, 43(11): p. 1537-49.
105. Lee, S., et al., Neuronal apoptosis linked to EglN3 prolyl hydroxylase and familial pheochromocytoma genes: developmental culling and cancer. Cancer Cell, 8(2): p. 155-67.
106. Young, A.P., et al., VHL loss actuates a HIF-independent senescence programme mediated by Rb and pNat Cell Biol, 10(3): p. 361-9.
107. Roe, J.S., et al., p53 stabilization and transactivation by a von Hippel-Lindau protein. Mol Cell, 22(3): p. 395-405.
108. Kurban, G., et al., Collagen matrix assembly is driven by the interaction of von Hippel-Lindau tumor suppressor protein with hydroxylated collagen IV alpha Oncogene, 27(7): p. 1004-12.
109. Ohh, M., et al., The von Hippel-Lindau tumor suppressor protein is required for proper assembly of an extracellular fibronectin matrix. Mol Cell, 1(7): p. 959-68.
110. Thoma, C.R., I.J. Frew, and W. Krek, The VHL tumor suppressor: riding tandem with GSK3beta in primary cilium maintenance. Cell Cycle, 6(15): p. 1809-13.
111. Eley, L., L.M. Yates, and J.A. Goodship, Cilia and disease. Curr Opin Genet Dev, 15(3): p. 308-14.
112. Haase, V.H., et al., Vascular tumors in livers with targeted inactivation of the von Hippel-Lindau tumor suppressor. Proc Natl Acad Sci U S A, 98(4): p. 1583-8.
113. Kleymenova, E., et al., Susceptibility to vascular neoplasms but no increased susceptibility to renal carcinogenesis in Vhl knockout mice. Carcinogenesis, 25(3): p. 309-15.
114. Rankin, E.B., J.E. Tomaszewski, and V.H. Haase, Renal cyst development in mice with conditional inactivation of the von Hippel-Lindau tumor suppressor. Cancer Res, 66(5): p. 2576-83.
115. Albers, J., et al., Combined mutation of Vhl and Trp53 causes renal cysts and tumours in mice. EMBO Mol Med, 5(6): p. 949-64.
116. http://www.sanger.ac.uk/genetics/CGP/cosmic/.
117. Jonasch, E., et al., State of the science: an update on renal cell carcinoma. Mol Cancer Res, 10(7): p. 859-80.
118. Dalgliesh, G.L., et al., Systematic sequencing of renal carcinoma reveals inactivation of histone modifying genes. Nature, 463(7279): p. 360-3.
119. van Haaften, G., et al., Somatic mutations of the histone H3K27 demethylase gene UTX in human cancer. Nat Genet, 41(5): p. 521-3.
120. http://www.uni-graz.at/en/imbmafwwpublications1/imbmafww-research.htm.
121. Cohen, H.T. and F.J. McGovern, Renal-cell carcinoma. N Engl J Med, 353(23): p. 2477-90.

2

A Comparative Study of Nucleostemin Family Members in Zebrafish Reveals Specific Roles in Ribosome Biogenesis

Paul B. Essers, Tamara C. Pereboom, Yvonne J. Goos, Judith Paridaen, Alyson W. MacInnes

Dev Biol, 2013, In Press

Abstract

Nucleostemin (NS) is an essential protein for the growth and viability of developmental stem cells. Its functions are multi-faceted, including important roles in ribosome biogenesis and in the p53-induced apoptosis pathway. While NS has been well studied, the functions of its family members GNL2 and GNL3-like (GNL3L) remain relatively obscure despite a high degree of sequence and domain homology. Here, we use zebrafish lines carrying mutations in the ns family to compare and contrast their functions in vertebrates. We find the loss of zebrafish ns or gnl2 has a major impact on 60S large ribosomal subunit formation and/or function due to cleavage impairments at distinct sites of pre-rRNA transcript. In both cases this leads to a reduction of total protein synthesis. In contrast, gnl3l loss shows relatively minor rRNA processing delays that ultimately have no appreciable effects on ribosome biogenesis or protein synthesis. However, the loss of gnl3l still results in p53 stabilization, apoptosis, and lethality similarly to ns and gnl2 loss. The depletion of p53 in all three of the mutants led to partial rescues of the morphological phenotypes and surprisingly, a rescue of the 60S subunit collapse in the ns mutants. We show that this rescue is due to an unexpected effect of p53 loss that even in wild type embryos results in an increase of 60S subunits. Our study presents an in-depth description of the mechanisms through which ns and gnl2 function in vertebrate ribosome biogenesis and shows that despite the high degree of sequence and domain homology, gnl3l has critical functions in development that are unrelated to the ribosome.

Introduction

Nucleostemin (NS or GNL3) is a protein critical for development via its function in the growth and maintenance of stem cells. The initial studies of NS showed that while its expression is very high in stem and cancer cells, this expression rapidly declined as cells proceeded towards terminal differentiation (Tsai and McKay, 2002). Conversely, ns (or Ns) expression has been shown to accumulate in de-differentiating cells of regenerating newt limbs and murine hepatocytes after severe liver injury, suggesting it plays an important role in tissue regeneration (Maki et al., 2007; Shugo et al., 2012). Recently it has also been shown that the self-renewal of stem cells requires functional Ns in murine blastocytes to facilitate a rapid transition through G1 phase of the cell cycle (Qu and Bishop, 2012). Yet despite the unquestionable importance of NS in development and stem cell maintenance, the exact functions of NS remain incompletely understood.

NS has two family members, GNL2 (or Ngp-1) and GNL3-like (GNL3L), that all contain a MMR_HSR1 domain described by five GTP-binding motifs arranged in a circularly permuted order (Meng et al., 2007). *GNL3L* is the vertebrate paralogue of *NS*, the two sharing the common *Grnlp* orthologue in yeast and the highest level of sequence similarity in vertebrates, while *GNL2* remains a single gene in both vertebrates and invertebrates. In all three proteins the binding of GTP to their common motifs controls the shuttling of the proteins from the nucleus to the nucleolus, the organelle where the majority of ribosome biogenesis takes place (Tsai and McKay, 2005). This observation led to a number of studies focusing on a potential function of NS in synthesis of the ribosome. Co-immunoprecipitation studies show that NS forms a complex with several ribosomal proteins and factors involved in ribosomal RNA (rRNA) processing, although NS is not itself part of the ribosome The knockdown of ns in *Drosophila melanogaster* results in failure of the nucleolus to release 60S ribosomal subunits (Romanova et al., 2009b, a; Rosby et al., 2009), and the knockdown of human NS in HeLa cells followed by pulse-chase experiments suggests this involves delayed processing of 32S to 28S rRNA (Romanova et al., 2009a). However, the precise role of NS and how it functions to process pre-rRNA into mature rRNA is still unknown, and a specific ribosomal function for GNL2 or GNL3L in vertebrates has not been reported to date.

NS also has an established role in the p53 tumor suppressor pathway. The initial functional analysis of NS revealed that its overexpression prevents cells from entering mitosis and induces apoptosis in a p53-dependent manner (Tsai and McKay, 2002). It was later reported that overexpression of NS is able to stabilize the p53 tumor suppressor protein by directly binding to MDM2 and dissociating p53 in a manner dependent on the nucleoplasmic mobilization of NS (Dai et al., 2008). Conversely, depletion of NS has been demonstrated to activate p53 by the nucleolar release of ribosomal proteins L11 and L5 that bind to MDM2, resulting in the dissociation of the p53/MDM2 complex and activation of p53 (Dai et al., 2008). GNL3L has also been reported to bind to and stabilize MDM2 *in vivo* while its depletion results in p53-dependent G2/M arrest, however unlike NS the interaction with MDM2 does not appear to be dependent on protein localization (Meng et al., 2011a).

Other lines of evidence also suggest that despite the homologies of the vertebrate NS family members that they have evolved to perform independent functions. For example, the expression of murine Gnl3l is lower in undifferentiated vs. differentiated neural stem cells is in stark contrast to Ns expression. (Yasumoto et al., 2007). Moreover, in adult murine tissues Gnl3l is found expressed in the cerebellum and forebrain, while the expression of Ns is limited to the testis (Ohmura et al., 2008). In the developing zebrafish embryo, early expression (1 day post

fertilization [dpf]) of *ns* is more restricted in the brain compared to *gnl2* and *gnl3l*, while only *gnl3l* shows strong expression in the tail (Paridaen et al., 2011a; Thisse, 2004). Protein interaction and cellular localization in mammalian studies also suggest divergent functions of human NS and GNL3L. NS binds not only to MDM2 and p53 but also ARF (alternate reading frame) and RSL1D1 (ribosomal L1 domain containing 1) (Dai et al., 2008; Ma and Pederson, 2007; Meng et al., 2006). GNL3L has also been shown to bind MDM2, as well as TERT (telomerase reverse transcriptase) and ERR (estrogen related receptor) protein (Fu and Collins, 2007; Meng et al., 2011a; Meng et al., 2006). Both NS and GNL3L bind to TRF1 and exert opposite effects, resulting in TRF1 degradation or stabilization, respectively (Meng et al., 2011b). In terms of localization, human NS is predominantly localized in the nucleolus while GNL3L is found mostly in the nucleoplasm and displays a shorter nucleolar retention time than does NS (Rao et al., 2006). No protein interaction studies or localization studies of GNL2 in any species have been done to date.

Our previous work demonstrated that the loss of ns or gnl2 protein in zebrafish results in incomplete retinal neurogenesis due to a failure of these cells to exit the cell cycle properly, consistent with previous *in vitro* and *in vivo* murine studies showing knockdown of Ns leads to G1-S phase arrest and reduced cell proliferation (Beekman et al., 2006b; Paridaen et al., 2011b; Tsai and McKay, 2002). Zebrafish ns and gnl2 proteins have some degree of overlapping functions. We showed that expressing *ns* mRNA in gnl2 mutants, and vice versa, was able to partially rescue the small head, small eye, and hindbrain ventricle inflation phenotypes that are characteristic of most ribosome biogenesis mutants in zebrafish embryos (Amsterdam et al., 1999; Paridaen et al., 2011b). Moreover, the loss of both ns and gnl2 revealed a synergy of these phenotypes that was more substantial than the loss of either protein alone. The ns and gnl2 mutants also revealed an increase in p53 stabilization, the expression of p53 target genes, and apoptosis; particularly in areas of robust proliferation such as the head and eye regions (Paridaen et al., 2011b). However, expressing a loss-of-function *p53* gene or depleting p53 with morpholinos in mutant embryos did not rescue the retina phenotype or the lethality to any significant degree (Paridaen et al., 2011b). This was in line with murine studies that showed no rescue effect of mutant *p53* expression on the lethal phenotype induced by the deletion of *Ns* (Beekman et al., 2006a). These data together suggested the relevance of p53-induced apoptosis upon ns or gnl2 loss is minor, and that other pathways contribute to the overall phenotypes. In our previous zebrafish study however, we did not examine the effects of ns or gnl2 loss on ribosome biogenesis.

As mentioned above, the deletion of *Ns* in mice is known to result in embryonic lethality at e.4 due to the failure of blastocysts to enter S-phase (Beekman et al., 2006a). However, the early lethality of these *Ns(-/-)* cells renders it challenging to perform experimental assays that require large numbers of cells, such as polysome profiling. In contrast, given the high fecundity and *ex utero* fertilization of zebrafish embryos we are able to collect unrestricted numbers of cells for assays that test how the loss of each ns family member affects various aspects of ribosome biogenesis despite the lethal phenotype. Given our previous results showing the overlapping functions of ns and gnl2, coupled to the high degree of homology of gnl3l with ns, we sought to determine in a vertebrate model if all three of the family members function similarly with respect to ribosome biogenesis and protein translation.

Materials and Methods

Zebrafish mutant lines

Zebrafish embryos were raised and staged as previously described (Westerfield, 1995) in accordance with all Dutch regulations and guidelines under DEC protocol #08.2011. The *gnl2*^{bw41c} mutation was recovered in a forward genetic screen, whereas the *ns*^{hu3259} mutation was generated in a reverse genetic screen using the TILLING method (Wienholds and Plasterk, 2004). The *gnl3l* mutant was uncovered in a viral insertion mutagenesis screen (Golling et al., 2002). Mutants were identified by their morphological phenotypes including reduced body size, smaller heads and eyes, and inflation of the hindbrain ventricle. The success of mutant identification was in all cases >95%, confirmed by PCR genotyping after selection using previously described sequences for *gnl2* and *ns* (Paridaen et al., 2011b) and 5'-agatctgttgacacaaatga-3' (*gnl3l* gene sequence) paired with the nLTR3 viral sequence 5'-ctgttccatctgttcctgac-3'. Wnt5a control primers are 5'-cagttctcacgtctgctacttgca-3' and 5'-acttccggcgtgttggagaattc-3'.

Morpholinos

Injections of embryos at the 1-2 cell stage with morpholinos against p53 (Gene Tools) have been previously described (Langheinrich et al., 2002). After bright field microscopy, the embryos were genotyped to confirm the identity of the mutants.

Northern Blots

Total RNA was isolated from embryos (5/sample) using Trizol (Invitrogen). RNA was run on a formaldehyde 1% agarose gel in MOPS buffer and DEPC-treated water for 4 hrs at 50V. The gel was soaked in 50mM NaOH for 15 min followed by 5 min in DEPC-treated water followed by 30 min in 10X SSC buffer. The RNA was transferred to a positively charged nylon membrane (GE Healthcare) overnight by capillary action and bound to the membrane by UV-crosslinking at 120 mJ. Blots were pre-hybridized for 1 hour at 65°C and subsequently hybridized with DNA probes overnight in ExpressHyb Hybridization Buffer (Clontech) at 65°C. Probes were made as previously described (Azuma et al., 2006) and labeled with 32P-αCTP (Perkin-Elmer) using a random primer DNA labeling system (Invitrogen). Following hybridization, blots were washed twice for 30 min with 0.1% SDS/0.2x SSC at 65°C. Blots were exposed to phospho-imaging screens (Molecular Dynamics) overnight and scanned using a Typhoon Scanner (GE Healthcare). Quantifications here and elsewhere are all tested for statistical significance using a Student's two-tailed t-test.

Polysome profiling

All steps of this protocol are performed at 4°C or on ice. Gradients of 17% to 50% sucrose (11ml) in gradient buffer (110mM KAc, 20mM MgAc and 10mM HEPES pH 7.6) were poured the evening before use. 25 embryos were lysed in 500µl polysome lysis buffer (gradient buffer containing 100mM KCl, 10mM MgCl, 0.1% NP-40, and freshly added 2mM DTT and 40U/ml RNAsin (Promega) using a Dounce tissue grinder (Wheaton). The samples were centrifuged at 1200g for 10 minutes to remove debris and loaded onto the sucrose gradients. The gradients were ultracentrifuged for 2 hours at 120565g in an SW41 Ti rotor (Beckman-Coulter, US). The gradients were displaced into a UA6 absorbance reader (Teledyne ISCO) using a syringe pump (Brandel, US) containing 60% sucrose. Absorbance was recorded at an OD of 254nm. Profiles were performed at least in triplicate, and then were scanned and peak heights were determined using Photoshop CS5 software.

^{35}S- incorporation assay

Per lane, 5 embryos were collected and washed in PBS. Embryos were dissociated by regularly pipetting them up and down in 0.25% trypsin for 10-20 minutes at 28°C. The dissociated cells were washed in PBS and incubated in DME medium without methionine or cysteine (Sigma Aldrich) at 28°C for 30 min. The medium was removed and the cells incubated in DME containing 20µCi of ^{35}S-labeled methionine and cysteine (Perkin Elmer) at 28°C for 30 min. The cells were washed twice in PBS, lysed and run on a 10% SDS/acrylamide gel as described [8]. The gel was fixed in 40% methanol/10% glacial acetic acid for 45 minutes, washed in water for 20 minutes and dried in a gel dryer (BioRad) for 2h at 80°C. The gels were then exposed to autoradiography film at room temperature.

Acridine orange staining

Live 1 dpf embryos were incubated in E3-embryo medium + 10µg/mL AO stain (Sigma) in the dark for 30 min. Embryos were washed twice with E3-medium and images were obtained using a Zeiss Axioplan Stereomicroscope (Oberkochen, Germany) equipped with a Leica (Wetzlar, Germany) digital camera using 10x magnifications. Quantifications were performed by averaging the results of blind counting by 4 individuals of the number of AO positive cells in the tail area beginning where the yolk extension meets the yolk and ending at the tail tip.

Western blots

Western blots were performed as described previously using 5 embryos per lane and a zebrafish-specific p53 antibody (MacInnes et al., 2008). The zebrafish-specific mdm2 antibody was purchased from Anaspec, Fremont CA (#55470), the actin antibody was purchased from Santa Cruz Biotech (sc-1616).

qPCR

Total RNA was isolated using Trizol (Invitrogen) and cDNA was made using iScript (BioRad). qPCR reactions were run using iQ SYBR Green Supermix (BioRad) on a myIQ iCycler (BioRad). The following primers were used: *gnl3l* fw: 5'- acgtgcagtcatgtccaaag-3', *gnl3l* rv: 5'-gatccttcttccctccatga-3', *p21* fw: 5'-tgtcaggaaaagcagcagaa-3', *p21* rv: 5'-ctggtgttttcgggatgttt-3', *puma* fw: 5'-tcccctccagcttaaggaat-3', *puma* rv: 5'-atcccagaatcgtgatgtcc-3', *ef1α* fw: 5'-gagtttgaggctggtatctccaag-3', *ef1α* rv: 5'- ctcagtggagtccatcttgttgac-3'.

Results

Loss of homologous NS family members results in embryonic lethality.

The evolutionary distance between zebrafish gnl2, ns and gnl3l and their homologs in other species is shown in Fig. 1A (the aforementioned genes are boxed in red). By Clustal Omega analysis (http://www.ebi.ac.uk/Tools/msa/clustalo/) of gene sequence homologies, zebrafish ns and gnl3l are the most closely related (36.5%), while gnl2 is more distant (26.9% homology to ns and 31.9% homology to gnl3l). The similarity of the protein domains and their locations in zebrafish gnl2, ns, and gnl3l are also very similar, shown in Fig. 1B, with the 5 GTP-binding domains represented in the middle of all three proteins. Given this high degree of sequence and domain homology between gnl3l and gnl2 or ns, we decided to include gnl3l mutants in our study. We decided to exclude the gnl1 and lsg1 genes that are only very distantly related to ns and whose protein products are localized in the cytosol (Reynaud et al., 2005). To generate mutant embryos of these proteins, we

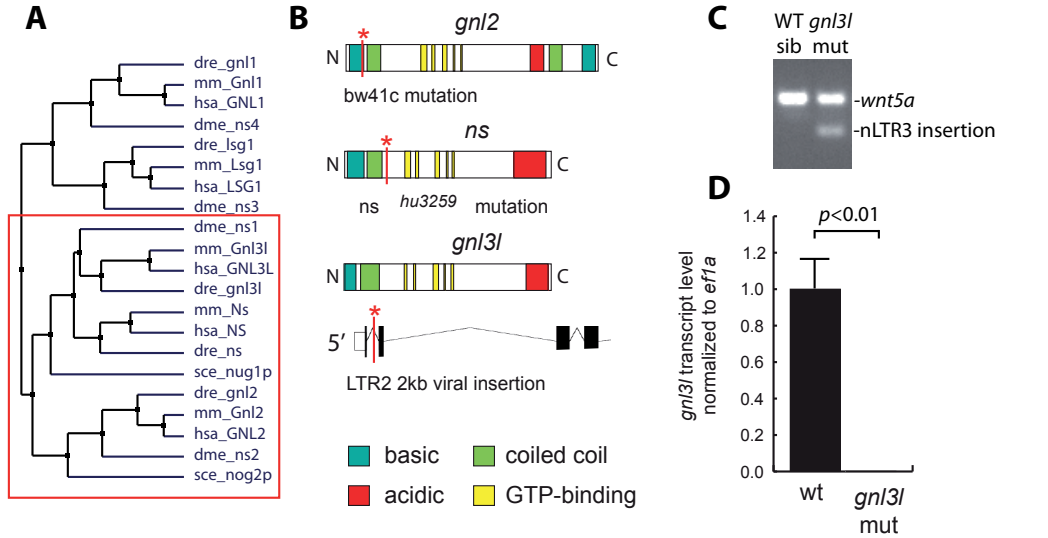

Fig. 1. Overview of the ns family in zebrafish. (A) Representation of the homology between the three family members, and their similarity to homologs in other species. The red box indicates the section of the family tree including ns, gnl2, and gnl3l. This tree was generated using the Blossum algorithm in Jalview (Waterhouse et al., 2009). (B) Graphical representation of the domains of gnl2, ns and gnl3l proteins and part of the gnl3l transcript, respectively showing the location (*) of stop mutations in the bw41c and hu3259 mutants and the location of the viral insert in the hi1437 (gnl3l) mutant used in this study. (C) PCR results using genotyping primers to identify the nLTR3 viral inserts in gnl3l mutants. The wnt5a primers are used as controls for the PCR. (D) qPCR analysis of the abundance of correctly spliced gnl3l transcript, using primers on both sides of the junction between Exon1 and 2, in wild type and hi1437 embryos. Expression levels were normalized to ef1α expression. p<0.01 by Student's two-tailed t-test.

identified ENU-induced point mutations in the ns gene (NM_001002297.1) and gnl2 gene (NM_213224.1) by TILING, both resulting in early stop codons (Fig. 1B)(Paridaen et al., 2011b). The gnl3l (NM_001002875.1) mutant was derived by a viral insertion into the first intron of gnl3l (Fig. 1B) (Amsterdam et al., 1999). Fig. 1C shows PCR analysis of a single gnl3l mutant compared to a wild type sibling using primers that bind the viral insert and the gnl3l gene (which would not be expected to amplify any sequence that does not carry the insert in the correct location) along with control primers that amplify the wnt5a gene. qPCR analysis using primers spanning the junction between the first two exons was used to verify that the viral insert in the gnl3l embryos resulted in an almost complete knockdown of the correctly spliced gnl3l transcript (Fig. 1D).

The loss of any ns family member is lethal.

Fig. 2 describes in detail the phenotypes of all three mutant embryos during the first 5 days of development. The mutant phenotypes are detectable by morphology at 1 dpf. On this day, mutant embryos appear smaller in head and body size, although these phenotypes are most easily discernable in the gnl2 and gnl3l mutants at this age compared to a subtler phenotype in the ns mutants as previously noted (Paridaen et al., 2011b). In addition, at 1 dpf both gnl2 and gnl3l mutants reveal a general apoptotic phenotype (mostly in the head region) including disorganized greying cells and a ragged surface of the skin that is not appreciable in the ns mutants until 2 dpf. Both gnl2 and ns mutants at 1 dpf also display an enlarged forebrain and hindbrain ventricle inflation that, along with the small head and eyes phenotype, are featured in several other ribosome biogenesis mutants (Amsterdam et al., 1999; Chakraborty et al., 2009). Almost all the mutant embryos begin to develop cardiac edemas by 3 dpf, fail to absorb the yolk or inflate the

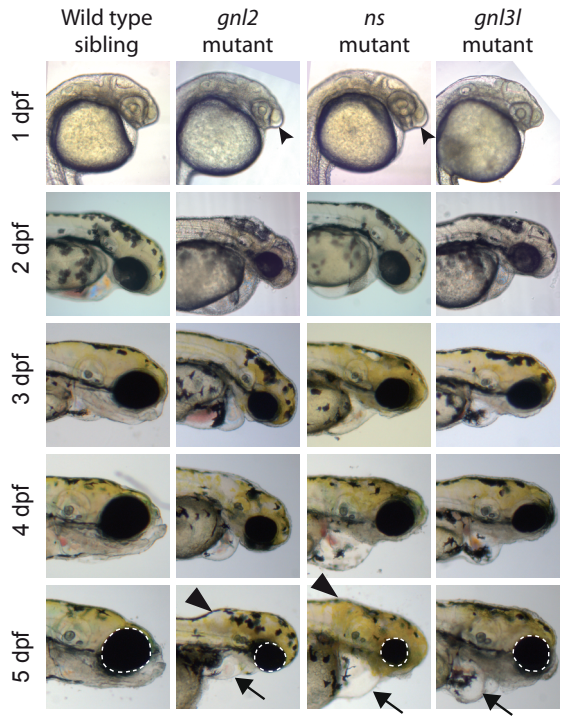

Fig. 2. Morphology of ns family member mutants. Bright-field microscopy showing the morphological phenotypes of the mutants compared to a wild type sibling of gnl2 (there was no appreciable difference between wild type siblings of ns, gnl2, or gnl3l, therefore only gnl2 wild type siblings are shown for space reasons). The enlargement of the forebrain at 1 dpf is depicted with forked arrowheads. The inflation of the hindbrain ventricle is depicted at 5 dpf with arrowheads, and the cardiac edemas depicted with arrows. The size of the eyes at 5 dpf is illustrated with the white dotted circles.

swim bladder, and are dead at the end of 5 dpf. By 5 dpf the phenotypes common in ribosome biogenesis mutants, including the small head and eyes, are particularly evident in the gnl2 and ns mutants, presumably due to a loss of protein synthesis that we show later in Fig. 4C.

Ns family members cleave specific rRNA sites.

To examine the effects that the mutation of each zebrafish ns family member has on the processing of rRNA in vertebrates, we performed northern blot analysis of total RNA isolated from each mutant compared to wild type siblings. Fig. 3A illustrates a basic schematic of rRNA processing in zebrafish embryos, derived from previous results (Azuma et al., 2006; Romanova et al., 2009b) and our own observations in this and other studies. In short, pre-rRNA is initially transcribed in a single transcript including the 18S rRNA, 5.8S rRNA, 28S rRNA, the externally transcribed sequence (ETS), and the two internally transcribed sequences (ITS1 and ITS2). This pre-rRNA then undergoes a series of cleavage steps in one of at least two pathways. In Pathway 1, the first nucleotides to be removed are the ETS sequences flanking each side of the transcript, followed by separation of the 18S strand from the 5.8S and 28S strand. In Pathway 2, the first cleavage step separates the 18S from the 5.8S and 28S strand, followed by removal of the ETS sequences. Using probes that bind the ETS, ITS1, ITS2, or 18S rRNA sequence (delineated in Fig. 3A) we were able to detect various impairments of rRNA processing in the mutant embryos compared to their wild type siblings (Fig. 3B). Ratios of band intensities in the mutant lines compared to those of the wild type siblings were determined to estimate the extent of the processing defects (Fig 3C). In all three mutants, there is an increase of a long rRNA containing the ETS probe sequence, along with a decrease of processing intermediate “d”, suggesting an overall retention of the full-length initial pre-rRNA transcript. Further processing of “d” to “f” is not affected in any of the mutants. The gnl2 mutant shows a large 2.34±0.15 fold increased retention of the processing intermediates “c”

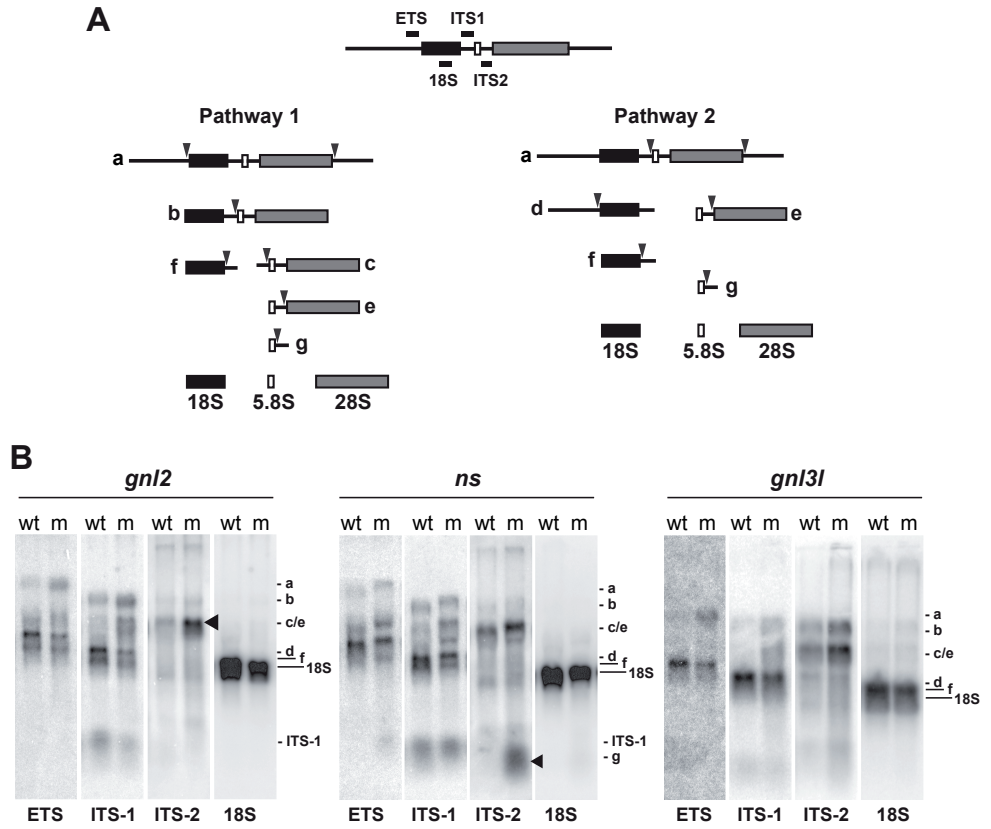

C

Relative band intensity compared to sibling

blot	step	gnl2	ns	gnl3l
ETS	a→d	0.64±0.27	0.308±0.095	0.3±0.18
ITS1	b→c/e	1.54±0.12	1.62±0.84	1.47±0.31
ITS1	d→f	0.990±0.013	0.993±0.079	0.97±0.15
ITS2	ce	2.34±0.15	1.37±0.37	1.332±0.083
18S	18S	0.831±0.013	0.95±0.11	0.85±0.11

Fig. 3. Specific rRNA processing defects are evident in ns and gnl2 mutants. (A) Simplified schematic of rRNA processing. The locations of the probes used and the processing intermediates visualized in (B) are indicated. (B) Northern blots showing reduced cleavage activity in various rRNA processing steps in gnl2, ns and gnl3l mutants at 2 dpf. The arrowheads indicate sites of major processing defects in the mutants. Results are representative of at least three independent experiments. (C) Relative band intensities were measured using ImageJ software and are represented relative to the wild type sibling for each mutant. $p<0.01$ by Student's two-tailed t-test.

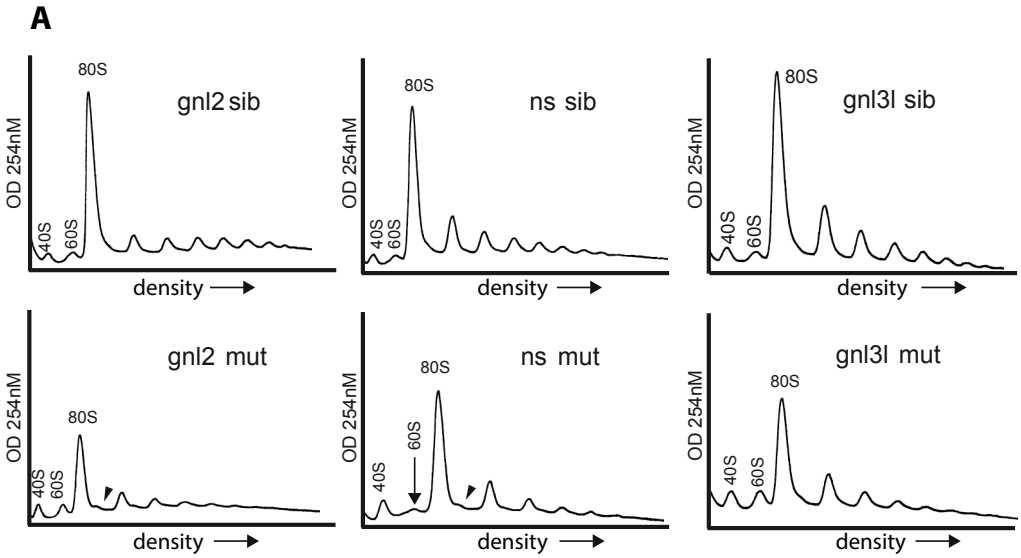

B

	Mutant 80S peak/ Wild type sib 80S peak			Mutant 60S peak/ Mutant 40S peak		
	ratio	STD	*p*-value	ratio	STD	*p*-value
gnl2	0.543	0.106	0.003	0.849	0.307	NS
ns	0.585	0.218	0.036	0.368	0.089	0.003
gnl3l	0.615	0.117	0.001	1.123	0.499	NS

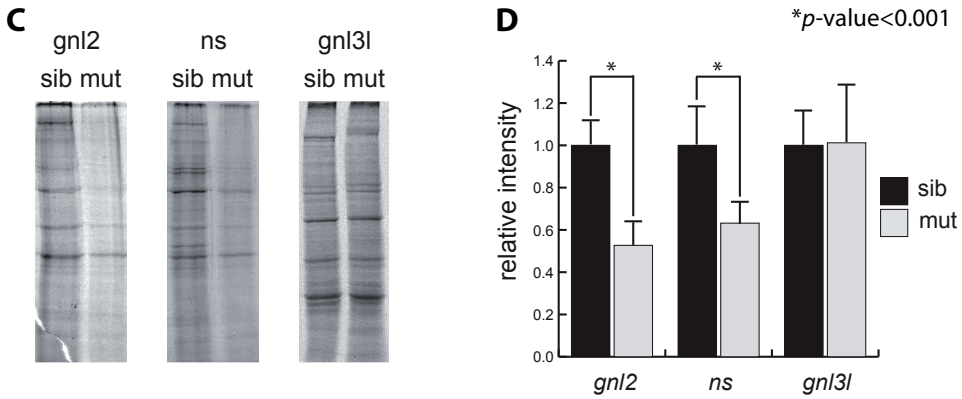

Fig. 4. Polysome profiles reveal different effects of the mutations on ribosome biogenesis. (A) Polysome profiles of gnl2, ns and gnl3l mutants at 2 dpf. Location of the small (40S) and large (60S) subunits, as well as the monosome (80S) and halfmers (arrowheads) are indicated. The arrow indicates the collapsed 60S peak in the ns mutants. Results are representative of at least three independent experiments (shown in Fig. S1). (B) Quantification of peak sizes including profiles in Fig S1. The ratios of the size of the mutant 80S peak to the wild type sibling 80S peak are shown on the left. The ratio of the mutant 60S peaks to the mutant 40S peaks are shown on the right. STD = standard deviation, NS = not significant. (C) Representative exposures of 35S-radiolabeled total protein synthesized in a 30-minute pulse in embryonic cells. (D) Quantifications of whole lane intensity in at least 3 samples (11 samples for gnl3l experiments). p<0.01 by Student's two-tailed t-test.

and "e", which ultimately lead to the mature 5.8S and 28S rRNAs that make up the 60S subunit. In the ns and gnl3l mutants, a similar defect is observed, but to a far lesser extent. The ns mutant shows retention of an additional intermediate, 5.8S rRNA associated with ITS2, labeled "g". Accumulation of this product is not detected in the other mutants. Given the importance of the 5.8S rRNA in forming the 60S subunit, these results suggest that the ns mutants will be especially impaired in their ability to form 60S subunits. The gnl3l mutant shows no specific cleavage defects that are not also detected in the other mutants. In all three mutants, a small decrease in the total amount of 18S RNA is observed. These data suggest that both gnl2 and ns have distinctly unique functions regarding the sites of pre-RNA that they cleave. Moreover, given that in both cases the strongest defects are observed in the processing of the 28S rRNA, it would be expected that mutations in gnl2 and ns affect both affect formation of the large 60S ribosomal subunit. In contrast, gnl3l appears to have no distinct function in processing rRNA.

Mutant embryos reveal different ribosome biogenesis and protein synthesis defects.

To determine the effect of these rRNA processing impairments on the formation of ribosomal subunits and mature ribosomes, we performed polysome profiling on the lysates of mutant embryos compared to their wild type siblings. Representative profiles are shown in Fig. 4A, an overview of all the profiles in this experiment is shown in Fig. S1. We observe that the loss of gnl2 and ns results in much more severe impacts on the ribosome profiles compared to the loss of gnl3l. A reduction of the 80S peak is seen in all three of the mutants, although the most significant reductions are observed in the gnl2 and ns mutants (Fig. 4A-B). Strikingly, an almost complete collapse of the 60S peak is seen in the ns mutants, which is not observed in the gnl2 or gnl3l mutants (Fig. 4A-B). Moreover, consistent with the results in Fig. 3 suggesting impairment of 60S subunits, we observe the presence of halfmers in both gnl2 and ns mutant profiles, which correspond to an increase of mRNAs that are only bound to the 40S small subunit (Pisarev et al., 2008). We do not detect a decrease of the 60S peak in the gnl2 mutant profiles, but the 80S peak is more strongly decreased than in the ns mutant profiles, suggesting that the 60S ribosomal subunits are present in normal amounts in the gnl2 mutants, albeit impaired in such a way as to prevent proper association with the 40S subunit. We showed previously that the loss of both *ns* and *gnl2* results in a synergistic worsening of the morphological phenotypes described in Fig. 2 (Paridaen et al., 2011b). Likewise, when we injected ns mutant embryos with morpholinos that block the translation of *gnl2* mRNA we observe a dramatic decrease of the 80S peak and polysome numbers in the profiles, reinforcing the notion that both proteins function distinctly in ribosome biogenesis (Fig. S2). The gnl3l mutant profiles are also consistent with the northern blot results in Fig. 3, in that there appears to be a minor reduction of the overall number of monosomes and polysomes, but no specific defects are visible. To confirm that alterations in the polysome profile are not a common result of embryonic lethal mutations, we performed polysome profiling on embryos with an unrelated lethal mutation in the cilia gene *lccr50*. As expected, loss of *lccr50* had no effect on polysome profiles (Fig. S1).

To determine how the observed defects in rRNA processing and 60S ribosomal subunit formation in the ns and gnl2 mutants affect protein synthesis compared to the gnl3l mutants, we labeled mutant embryonic cells with ^{35}S-methionine for 30 minutes and compared the total amount of protein produced to their wild type siblings. Both ns and gnl2 mutant cells show a significant reduction of the amount of total protein synthesized in the 30-minute pulse (Fig. 4C-D). Surprisingly, no difference was observed in the gnl3l mutant cells (Fig. 4C-D). These results for ns and gnl2 correspond as would be expected with the polysome profile results, and also suggest that despite the minor reduction of peak sizes in the profiles of the gnl3l mutants that this is not sufficient to impair protein synthesis.

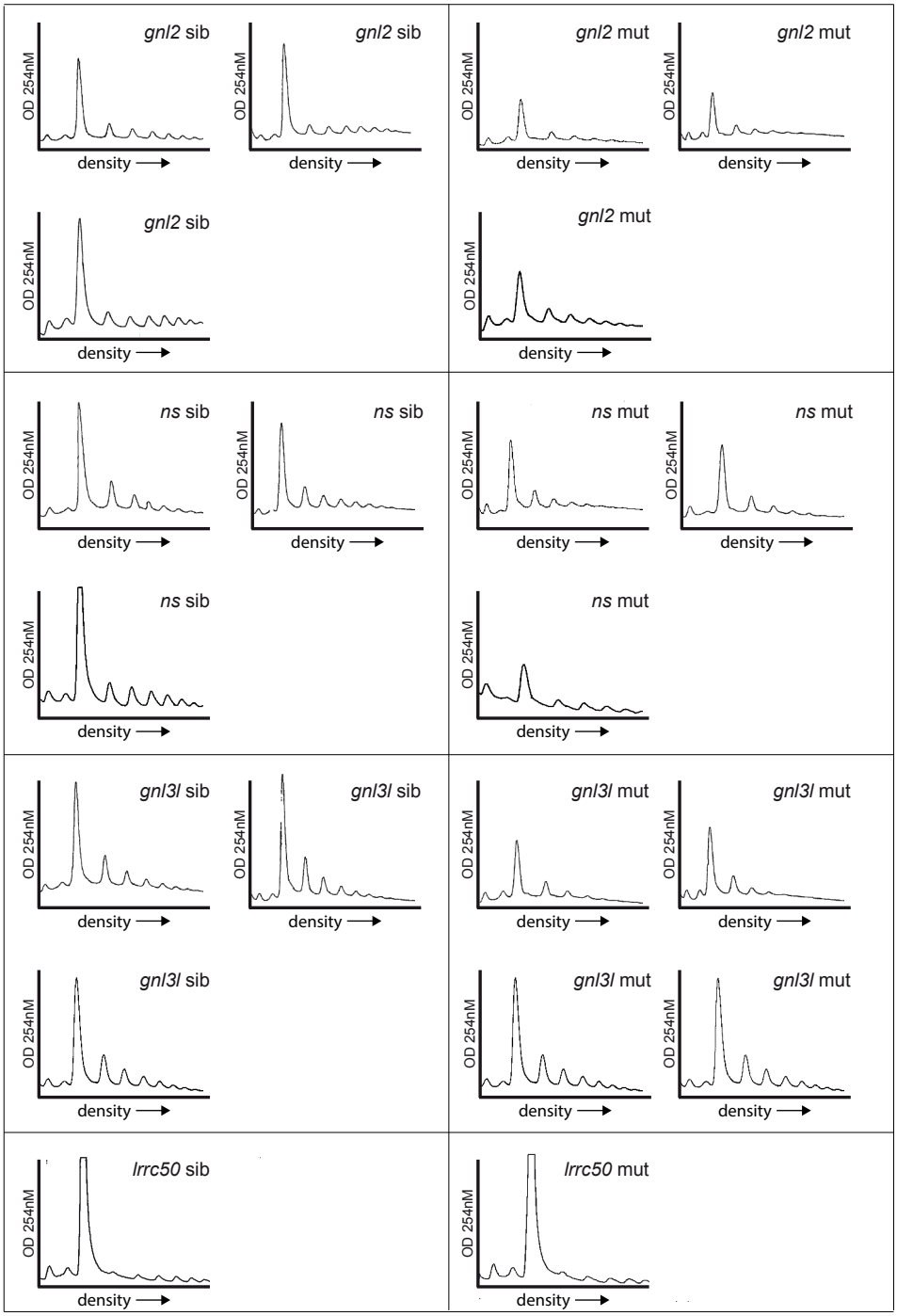

Fig. S1. Overview of polysome profiles. (A) All polysome profiles done in this study, of which representative profiles are shown in Fig. 3. (B) Polysome profiles of lrrc50 mutants at 5 dpf, as close to embryonic lethality as possible. No difference between siblings and mutants is observed (it is normal to see a reduction of the polysome peak sizes when the embryos reach 5 dpf compared to 2-3 dpf).

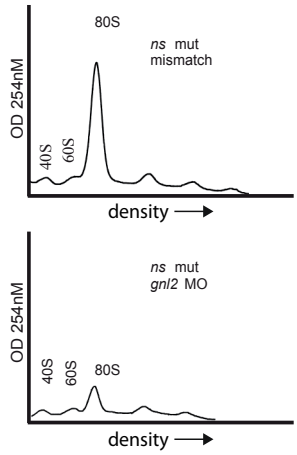

Fig. S2. gnl2 MOs exacerbate the ribosome biogenesis phenotype of *ns* mutants. Representative profiles of mutant ns embryos injected with the gnl2 MO.

Loss of all ns family members induces p53 stabilization and apoptosis.

In order to determine if the differences in ribosome formation and protein synthesis we observe in the gnl3l compared to ns and gnl2 mutants results in a corresponding reduction of p53 stabilization, we measured the level of apoptosis and p53 stabilization in all the mutants compared to their wild-type siblings. Despite the relatively unaffected levels of ribosome biogenesis and normal levels of protein synthesis in the gnl3l mutants, we found that apoptosis measured by acridine orange staining is in fact significantly increased in the gnl3l mutants to similar levels as we expected to observe in the gnl2 and ns mutants (Fig. 5A-B). Correspondingly, western blot analysis reveals all three of the mutant lines stabilize p53 to a similar degree (Fig. 5C). p53 stabilization in all three mutant lines additionally leads to transcription of the p53 target genes *p21* and *puma*, associated with the induction of senescence and apoptosis respectively (Fig 5D).

A major negative regulator of the p53 tumor suppressor is the MDM2 protein, which in normal cells keeps p53 at low expression levels via constitutive ubiquitination and degradation (Momand et al., 1992). Since NS and GNL3L have both been shown in human cell lines to have roles destabilizing or stabilizing MDM2, respectively (Meng et al., 2011a; Meng et al., 2008), we determined what the effects were of the loss of zebrafish gnl2, ns, and gnl3l on the stability of mdm2. Fig. 5E shows western blot analysis with a zebrafish-specific mdm2 antibody indicating that the loss of none of the ns family member proteins in this model results in any appreciable difference in the levels of endogenous mdm2.

Loss of p53 partially rescues mutant phenotypes.

Morpholinos (MO) designed to deplete zebrafish embryos of p53 have been previously described (Langheinrich et al., 2002). The injection of mutant embryos with the p53 MO results in a partial rescue of the morphological phenotypes, including the small head and eyes phenotypes (Fig. 6A). Specifically in the ns and gnl2 mutants a rescue effect is observed in the inflation of the hindbrain ventricle and enlarged forebrain, while in the gnl3l mutants a smoothing of the ragged skin phenotype is seen (Fig. 6A). We then profiled the mutant embryos injected with the p53 MO. We first injected mutant embryos with missense MOs and found that all the profiles looked identical to those presented in Fig. 4A (data not shown). When we injected the p53 MO into the mutant embryos we observed an increase of the peak sizes in all the mutants (Fig. 6B). This is particularly striking in the ns mutants, where the collapse of the 60S subunit appears to be completely restored and the monosomal as well as the polysomal peaks are substantially higher. This increase of peak sizes in the mutants is likely due to the effect of the p53 MO in general to increase the amount 60S subunits, since in all our wild type sibling control injections we also observed an increase of 60S and 80S peak sizes (Fig. 6B). This is shown in detail in Fig. 6C where we compared the 40S and 60S peaks of wild type sibling embryos injected with the missense MO compared to

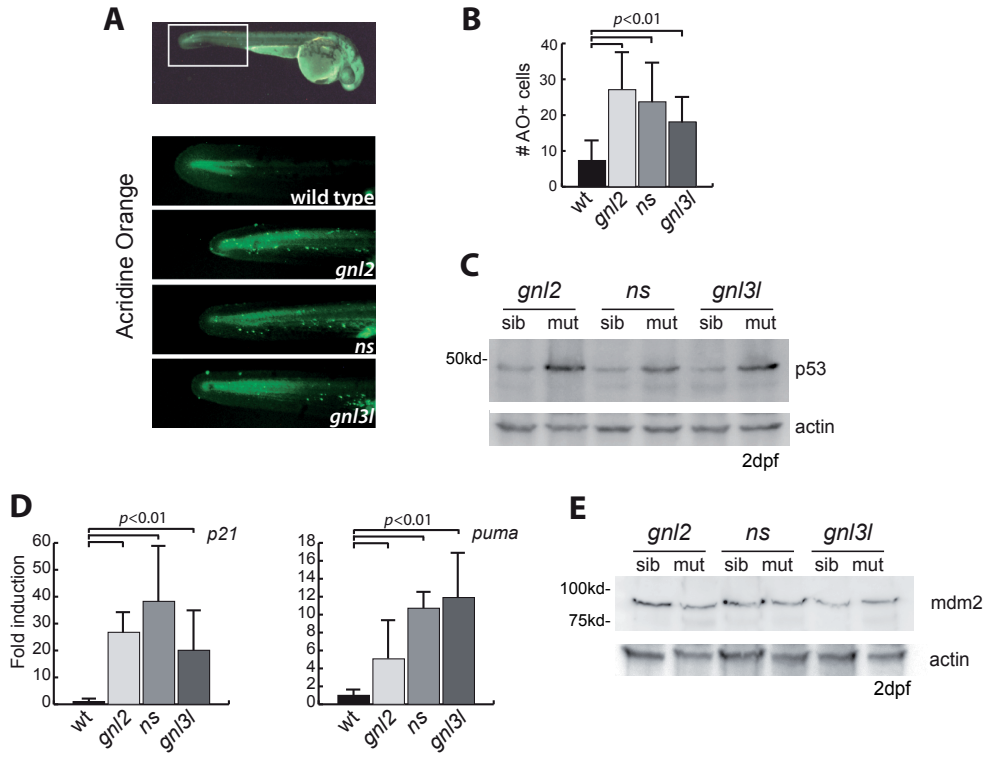

Fig. 5. p53 induced apoptosis in ns family mutants. (A) Representative fluorescent microscopy images showing acridine orange staining at 1 dpf. The top box illustrates with the white box the portion of the tail used for quantification of acridine orange positive cells. (B) Quantifications of the number of acridine orange positive cells. At least 7 animals were blindly scored for these quantifications. p<0.01 by Student's two-tailed t-test. (C) Western blot analysis of p53 stabilization in all three mutant lines at 2 dpf. (D) qPCR analysis of p21 and puma transcript levels at 2dpf, normalized to ef1α expression. p<0.01 by Student's two-tailed t-test. (E) Western blot analysis of zebrafish mdm2 levels in mutants and wild type siblings at 2 dpf.

the p53 MO. The size ratio of the 60S peak to the 40S peak in the missense MO injected embryos compared to the p53 MO is quantified in Fig. 6D, indicating that the p53 MO clearly has an unexpected effect of increasing the number of 60S ribosomal subunits.

Discussion

This work provides a detailed analysis of how the NS family members function in vertebrate ribosome biogenesis and protein synthesis, the most important finding being that gnl3l does not function as expected in these contexts at all. This result was surprising, given the high sequence and protein domain homology of gnl3l to the ns and gnl2 proteins, both with critical functions in ribosome biogenesis and protein production that we describe in depth in this work. Since the loss of gnl3l in zebrafish is equally lethal as the loss of ns or gnl2, it is clear that gnl3l has functions unrelated to ribosome biogenesis that are nonetheless critical for development.

Our results suggest that in the ns mutants, the failure of the 5.8S rRNA sequence (an integral component of the large 60S ribosomal subunit) to be cleaved from the ITS2 sequence may be the

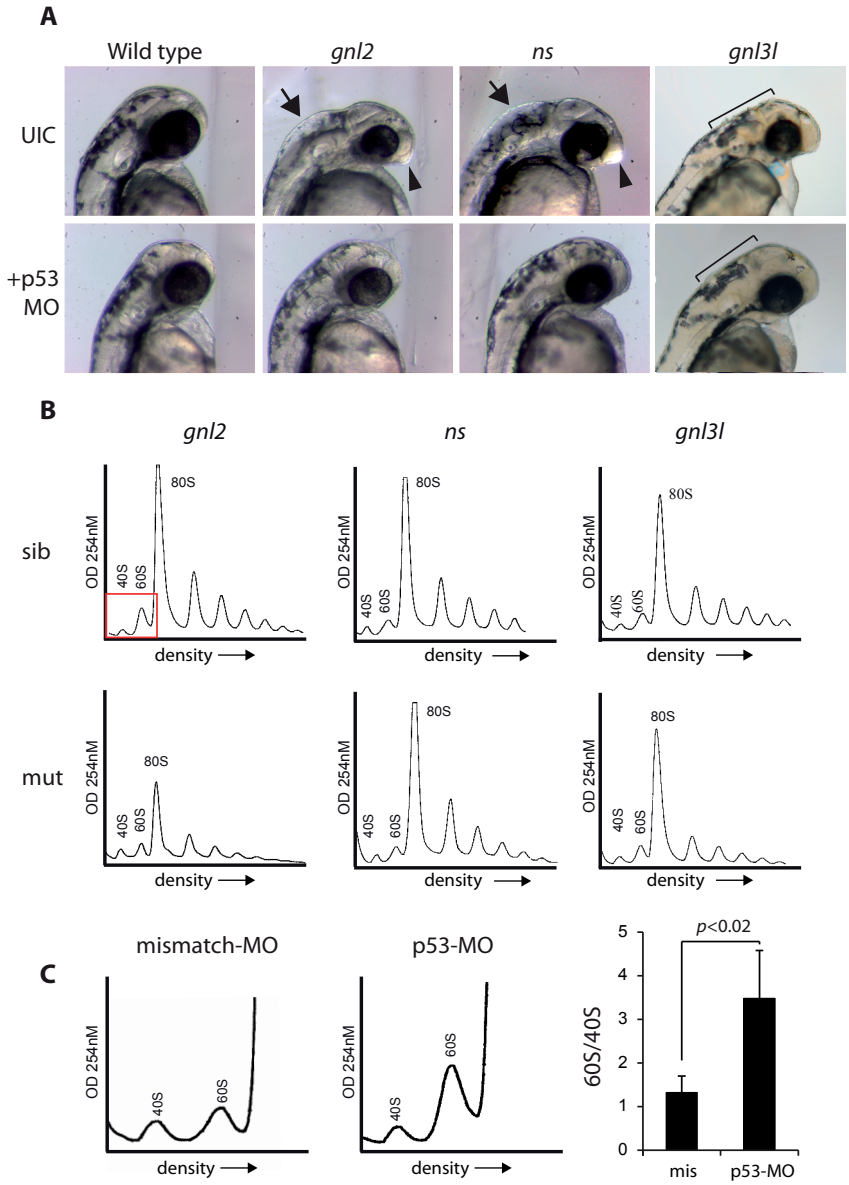

Fig 6. Loss of p53 partially rescues mutant phenotypes. (A) Bright field microscopy of p53 MO injections at 2 dpf. UIC = uninjected control embryos. Arrows depict inflation of the hindbrain ventricle, arrowheads depict enlargement of the forebrain. The ragged skin phenotype in gnl3l mutants and the rescue are depicted with the black bars. (B) Representative profiles of mutant embryos injected with the p53 MO. (C) Magnified representation of polysome profiles showing an increase in 60S peak size in p53 MO compared to missense MO injected embryos. (D) Quantification of the ratio of 60S to 40S peak size in missense vs. p53 MO injected embryos.

cause of the unique collapse of the 60S subunit we observe in the polysome profiles of Fig. 4A. Interestingly, pre-5.8S rRNA in *S. cerevisiae* has been shown to co-precipitate with Lsg1, a more distant family member of NS (see Fig. 1A), suggesting a conserved function of 5.8S rRNA processing between the two proteins. As mentioned in the introduction, NS is able to shuttle from the nucleoplasm to the nucleolus depending on the binding of GTP (Tsai and McKay, 2005). It seems likely then that NS is functioning to shuttle other nuclear proteins into the nucleolus that are required for pre-RNA processing. One potential protein that could fit this role is the NOP2 protein, which has been previously shown by a large-scale quantitative tandem mass spectrometry analysis of cell fractions to complex with NS (Havugimana et al., 2012). NOP2 is also known to localize to both the nucleus and nucleoplasm, and the loss of NOP2 has been demonstrated to cause pre-RNA processing defects including impaired maturation of the 5.8S rRNA and collapse of the 60S ribosomal subunit (de Beus et al., 1994; Hong et al., 1997). Interestingly, the expression of NOP2 in cells also increases in states of high growth and decreases in stationary phases, similar to the expression of NS (de Beus et al., 1994; Tsai and McKay, 2002). Taken together, these studies and our data suggest that a major role of NS is to shuttle rRNA processing proteins, such as NOP2 (although other proteins are likely involved), into the nucleolus from the nucleus during pre-differentiated states of high cell growth requiring robust levels of ribosome biogenesis in order to function in the processing of 5.8S rRNA that will ultimately assemble the large 60S ribosomal subunit. While a complete description of the interactions between NS and NOP2 are presently beyond the scope of this manuscript, we hope this analysis will provide a cogent platform for future studies of NS function.

Given the marked rRNA processing delays revealed in the gnl2 mutants, we were surprised to see very little difference in the total numbers of 40S and 60S subunits on the profiles. However, it is clear that despite this insignificant reduction, the loss of gnl2 has a major effect on the ability of the 60S subunit to bind the 40S subunit, accounting for the decrease of the 80S monosome peak, the appearance of halmers, and the subsequent reduction of total protein synthesis. While at this point we may only speculate upon the nature of this impairment, possibly gnl2 has a second role in the export of the 60S subunit to the cytoplasm in a manner reminiscent of another function of Lsg1 besides 5.8S rRNA maturation. Studies in *S. cerevisiae* and more recently in *Drosophila* have shown that the GTPase domain of Lsg1 is required for release of the nuclear export signal (NES)-bearing protein Nmd3 from cytoplasmic 60S subunits, and that mutations reducing GTPase activity of Lsg1 result in the nucleolar retention of 60S subunits (Hartl et al., 2013; Kallstrom et al., 2003). Therefore while the loss of gnl2 may slow the production of 60S subunits due to rRNA impairments as we show in Fig. 3B, a potential retention and accumulation of immature 60S subunits in the nucleolus may represent the unchanged 60S peak size we see in Fig. 4A, and also explain the decrease of the 80S monosomal peak.

Previous reports have suggested that the mechanism for p53 stabilization upon the depletion of NS in mammalian cells involves the nucleolar release of ribosomal proteins RPL5 and RPL11 and the subsequent binding of these proteins with MDM2, the negative regulator of p53 (Dai et al., 2008). Recently it was revealed that impaired ribosome biogenesis in fact results in a complex containing RPL5, RPL11, and 5S rRNA being redirected to HDM2 (human MDM2) instead of nascent 60S subunits, suggesting this may also be occurring in the ns mutants (Donati et al., 2013) Our results regarding the collapse of the 60S ribosomal subunit, where RPL5 and RPL11 normally reside, upon the loss of ns in zebrafish are consistent with this mechanism. However, our data suggest that this is not what is occurring with the loss of gnl2 or gnl3l3, neither of which results in a decrease of 60S subunits (suggesting RPL5 and RPL11 are maintained in the subunit).

Attempts to perform co-immunoprecipitation assays with RPL11 or RPL5 and MDM2 antibodies with lysates from zebrafish embryos were not successful, we are therefore unable to state for certain that the loss of any ns family member in zebrafish embryos results in the endogenous interaction between these proteins. The mechanism of p53 stabilization in the gnl3l mutants is even more mysterious, given how there is no ribosome biogenesis or protein production phenotype upon its loss. While there are reports that the reduction of GNL3L in human cell lines destabilizes MDM2 and leads to p53 stabilization (Meng et al., 2011a), our results indicate that the levels of endogenous mdm2 in zebrafish remain unchanged upon the loss of gnl3l. Other studies have shown a function of human GNL3L in the transition of metaphase-to-anaphase through the stabilization of the telomere-capping protein TRF1 (part of the chromosome-protective shelterin complex), and demonstrate that GNL3L overexpression leads to shortening of the telomeres (Fu and Collins, 2007). In may be then that a reduction of GNL3L destabilizes TRF1 and results in improper telomere lengthening. Such lengthening has been shown in *S. cerevisae* to activate the checkpoint protein Rad53, the homolog of human CHK2, and cause cell cycle arrest (Viscardi et al., 2003). Since CHK2 in vertebrate cells is a well-known upstream mediator of the p53 pathway (Chehab et al., 2000), future studies on p53 stabilization from the loss of GNL3L may be more appropriately focused on the role of GNL3L in the protection of telomere ends rather than a role in ribosome biogenesis.

The remarkable rescue effect of the p53 MO on the peak sizes of the ns polysomes profiles was unexpected, however it is clear that the loss of p53 has a general effect on increasing the number of 60S subunits. This may be relevant in the context of studies demonstrating that the RPL5/RPL11/5S rRNA complex has an important role in stabilizing p53 through inhibition of HDM2 (Donati et al., 2013). Here the authors propose that in a model of hyperactivated ribosome biogenesis (such as embryonic development) excessive amounts of the RPL5/RPL11/5S rRNA complex may instead inhibit HDM2 rather than being incorporated into 60S subunits. Presumably in such a case p53 is used as a checkpoint to prevent uncontrolled levels of translation. Thus in the absence of p53, cells containing unusually high numbers of 60S subunits would not undergo apoptosis per usual. While the physiological relevance of this observation is not clear (p53 MO injected embryos have no obvious phenotypes unless challenged with DNA damage (Langheinrich et al., 2002)) this is nonetheless a very interesting observation that is certainly worthy of future study.

The increasing importance of NS is underscored by the large amount of attention it has been receiving lately in the fields of stem cells, cancer cells, and tissue regeneration. The potential clinical relevance of NS is demonstrated by the recent observation that inhibiting NS in cancer cells results in cell cycle arrest regardless of the status of the p53 tumor suppressor (Liu et al., 2010). We show in this report that despite their large degree of sequence and domain homology, the NS family members in vertebrates function in unexpectedly different roles. These results will hopefully increasing understanding about the specific cellular functions of each NS family member in a way that is useful to those in the fields of stem cells, cancer, and tissue regeneration. Moreover, we envision this work will be beneficial for the current efforts underway to target NS in cancer cells, as well as for future work that may include the targeting GNL2 and GNL3L.

References

1. Amsterdam, A., Burgess, S., Golling, G., Chen, W., Sun, Z., Townsend, K., Farrington, S., Haldi, M., Hopkins, N., 1999. A large-scale insertional mutagenesis screen in zebrafish. Genes & development 13, 2713-2724.
2. Azuma, M., Toyama, R., Laver, E., Dawid, I.B., 2006. Perturbation of rRNA synthesis in the bap28 mutation leads to apoptosis mediated by p53 in the zebrafish central nervous system. J Biol Chem 281, 13309-13316.
3. Beekman, C., Nichane, M., De Clercq, S., Maetens, M., Floss, T., Wurst, W., Bellefroid, E., Marine, J.C., 2006a. Evolutionarily conserved role of nucleostemin: controlling proliferation of stem/progenitor cells during early vertebrate development. Mol Cell Biol 26, 9291-9301.
4. Beekman, C., Nichane, M., De Clercq, S., Maetens, M., Floss, T., Wurst, W., Bellefroid, E., Marine, J.C., 2006b. Evolutionarily conserved role of nucleostemin: controlling proliferation of stem/progenitor cells during early vertebrate development. Mol Cell Biol 26, 9291-9301.
5. Chakraborty, A., Uechi, T., Higa, S., Torihara, H., Kenmochi, N., 2009. Loss of ribosomal protein L11 affects zebrafish embryonic development through a p53-dependent apoptotic response. PloS one 4, e4152.
6. Chehab, N.H., Malikzay, A., Appel, M., Halazonetis, T.D., 2000. Chk2/hCds1 functions as a DNA damage checkpoint in G(1) by stabilizing p53. Genes & development 14, 278-288.
7. Dai, M.S., Sun, X.X., Lu, H., 2008. Aberrant expression of nucleostemin activates p53 and induces cell cycle arrest via inhibition of MDM2. Mol Cell Biol 28, 4365-4376.
8. de Beus, E., Brockenbrough, J.S., Hong, B., Aris, J.P., 1994. Yeast NOP2 encodes an essential nucleolar protein with homology to a human proliferation marker. The Journal of cell biology 127, 1799-1813.
9. Donati, G., Peddigari, S., Mercer, C.A., Thomas, G., 2013. 5S Ribosomal RNA Is an Essential Component of a Nascent Ribosomal Precursor Complex that Regulates the Hdm2-p53 Checkpoint. Cell reports 4, 87-98.
10. Fu, D., Collins, K., 2007. Purification of human telomerase complexes identifies factors involved in telomerase biogenesis and telomere length regulation. Molecular cell 28, 773-785.
11. Golling, G., Amsterdam, A., Sun, Z., Antonelli, M., Maldonado, E., Chen, W., Burgess, S., Haldi, M., Artzt, K., Farrington, S., Lin, S.Y., Nissen, R.M., Hopkins, N., 2002. Insertional mutagenesis in zebrafish rapidly identifies genes essential for early vertebrate development. Nat Genet 31, 135-140.
12. Hartl, T.A., Ni, J., Cao, J., Suyama, K.L., Patchett, S., Bussiere, C., Gui, D.Y., Tang, S., Kaplan, D.D., Fish, M., Johnson, A.W., Scott, M.P., 2013. Regulation of ribosome biogenesis by nucleostemin 3 promotes local and systemic growth in Drosophila. Genetics 194, 101-115.
13. Havugimana, P.C., Hart, G.T., Nepusz, T., Yang, H., Turinsky, A.L., Li, Z., Wang, P.I., Boutz, D.R., Fong, V., Phanse, S., Babu, M., Craig, S.A., Hu, P., Wan, C., Vlasblom, J., Dar, V.U., Bezginov, A., Clark, G.W., Wu, G.C., Wodak, S.J., Tillier, E.R., Paccanaro, A., Marcotte, E.M., Emili, A., 2012. A census of human soluble protein complexes. Cell 150, 1068-1081.
14. Hong, B., Brockenbrough, J.S., Wu, P., Aris, J.P., 1997. Nop2p is required for pre-rRNA processing and 60S ribosome subunit synthesis in yeast. Mol Cell Biol 17, 378-388.
15. Kallstrom, G., Hedges, J., Johnson, A., 2003. The putative GTPases Nog1p and Lsg1p are required for 60S ribosomal subunit biogenesis and are localized to the nucleus and cytoplasm, respectively. Mol Cell Biol 23, 4344-4355.
16. Langheinrich, U., Hennen, E., Stott, G., Vacun, G., 2002. Zebrafish as a model organism for the identification and characterization of drugs and genes affecting p53 signaling. Current biology : CB 12, 2023-2028.
17. Liu, R., Zhang, Z., Xu, Y., 2010. Downregulation of nucleostemin causes G1 cell cycle arrest via a p53-independent pathway in prostate cancer PC-3 cells. Urologia internationalis 85, 221-227.
18. Ma, H., Pederson, T., 2007. Depletion of the nucleolar protein nucleostemin causes G1 cell cycle arrest via the p53 pathway. Molecular biology of the cell 18, 2630-2635.
19. MacInnes, A.W., Amsterdam, A., Whittaker, C.A., Hopkins, N., Lees, J.A., 2008. Loss of p53 synthesis in zebrafish tumors with ribosomal protein gene mutations. Proc Natl Acad Sci U S A 105, 10408-10413.
20. Maki, N., Takechi, K., Sano, S., Tarui, H., Sasai, Y., Agata, K., 2007. Rapid accumulation of nucleostemin in nucleolus during newt regeneration. Developmental dynamics : an official publication of the American Association of Anatomists 236, 941-950.
21. Meng, L., Hsu, J.K., Tsai, R.Y., 2011a. GNL3L depletion destabilizes MDM2 and induces p53-dependent G2/M arrest. Oncogene 30, 1716-1726.
22. Meng, L., Hsu, J.K., Zhu, Q., Lin, T., Tsai, R.Y., 2011b. Nucleostemin inhibits TRF1 dimerization and shortens its dynamic association with the telomere. Journal of cell science 124, 3706-3714.

23. Meng, L., Lin, T., Tsai, R.Y., 2008. Nucleoplasmic mobilization of nucleostemin stabilizes MDM2 and promotes G2-M progression and cell survival. Journal of cell science 121, 4037-4046.
24. Meng, L., Yasumoto, H., Tsai, R.Y., 2006. Multiple controls regulate nucleostemin partitioning between nucleolus and nucleoplasm. Journal of cell science 119, 5124-5136.
25. Meng, L., Zhu, Q., Tsai, R.Y., 2007. Nucleolar trafficking of nucleostemin family proteins: common versus protein-specific mechanisms. Mol Cell Biol 27, 8670-8682.
26. Momand, J., Zambetti, G.P., Olson, D.C., George, D., Levine, A.J., 1992. The mdm-2 oncogene product forms a complex with the p53 protein and inhibits p53-mediated transactivation. Cell 69, 1237-1245.
27. Ohmura, M., Naka, K., Hoshii, T., Muraguchi, T., Shugo, H., Tamase, A., Uema, N., Ooshio, T., Arai, F., Takubo, K., Nagamatsu, G., Hamaguchi, I., Takagi, M., Ishihara, M., Sakurada, K., Miyaji, H., Suda, T., Hirao, A., 2008. Identification of stem cells during prepubertal spermatogenesis via monitoring of nucleostemin promoter activity. Stem Cells 26, 3237-3246.
28. Paridaen, J.T., Janson, E., Utami, K.H., Pereboom, T.C., Essers, P.B., van Rooijen, C., Zivkovic, D., Macinnes, A.W., 2011a. The nucleolar GTP-binding proteins Gnl2 and nucleostemin are required for retinal neurogenesis in developing zebrafish. Dev Biol 355, 286-301.
29. Paridaen, J.T., Janson, E., Utami, K.H., Pereboom, T.C., Essers, P.B., van Rooijen, C., Zivkovic, D., Macinnes, A.W., 2011b. The nucleolar GTP-binding proteins Gnl2 and nucleostemin are required for retinal neurogenesis in developing zebrafish. Developmental biology 355, 286-301.
30. Pisarev, A.V., Kolupaeva, V.G., Yusupov, M.M., Hellen, C.U., Pestova, T.V., 2008. Ribosomal position and contacts of mRNA in eukaryotic translation initiation complexes. The EMBO journal 27, 1609-1621.
31. Qu, J., Bishop, J.M., 2012. Nucleostemin maintains self-renewal of embryonic stem cells and promotes reprogramming of somatic cells to pluripotency. The Journal of cell biology 197, 731-745.
32. Rao, M.R., Kumari, G., Balasundaram, D., Sankaranarayanan, R., Mahalingam, S., 2006. A novel lysine-rich domain and GTP binding motifs regulate the nucleolar retention of human guanine nucleotide binding protein, GNL3L. Journal of molecular biology 364, 637-654.
33. Reynaud, E.G., Andrade, M.A., Bonneau, F., Ly, T.B., Knop, M., Scheffzek, K., Pepperkok, R., 2005. Human Lsg1 defines a family of essential GTPases that correlates with the evolution of compartmentalization. BMC biology 3, 21.
34. Romanova, L., Grand, A., Zhang, L., Rayner, S., Katoku-Kikyo, N., Kellner, S., Kikyo, N., 2009a. Critical role of nucleostemin in pre-rRNA processing. J Biol Chem 284, 4968-4977.
35. Romanova, L., Grand, A., Zhang, L., Rayner, S., Katoku-Kikyo, N., Kellner, S., Kikyo, N., 2009b. Critical role of nucleostemin in pre-rRNA processing. J Biol Chem 284, 4968-4977.
36. Rosby, R., Cui, Z., Rogers, E., deLivron, M.A., Robinson, V.L., DiMario, P.J., 2009. Knockdown of the Drosophila GTPase nucleostemin 1 impairs large ribosomal subunit biogenesis, cell growth, and midgut precursor cell maintenance. Molecular biology of the cell 20, 4424-4434.
37. Shugo, H., Ooshio, T., Naito, M., Naka, K., Hoshii, T., Tadokoro, Y., Muraguchi, T., Tamase, A., Uema, N., Yamashita, T., Nakamoto, Y., Suda, T., Kaneko, S., Hirao, A., 2012. Nucleostemin in injury-induced liver regeneration. Stem cells and development 21, 3044-3054.
38. Thisse, B., Thisse, C, 2004. Fast Release Clones: A High Throughput Expression Analysis, ZFIN Direct Data Submission, http://zfin.org.
39. Tsai, R.Y., McKay, R.D., 2002. A nucleolar mechanism controlling cell proliferation in stem cells and cancer cells. Genes & development 16, 2991-3003.
40. Tsai, R.Y., McKay, R.D., 2005. A multistep, GTP-driven mechanism controlling the dynamic cycling of nucleostemin. The Journal of cell biology 168, 179-184.
41. Viscardi, V., Baroni, E., Romano, M., Lucchini, G., Longhese, M.P., 2003. Sudden telomere lengthening triggers a Rad53-dependent checkpoint in Saccharomyces cerevisiae. Molecular biology of the cell 14, 3126-3143.
42. Waterhouse, A.M., Procter, J.B., Martin, D.M., Clamp, M., Barton, G.J., 2009. Jalview Version 2--a multiple sequence alignment editor and analysis workbench. Bioinformatics 25, 1189-1191.
43. Westerfield, M., 1995. The zebrafish book: a guide for the laboratory use of zebrafish (Brachydanio rerio). University of Oregon Press, Eugene, OR.
44. Wienholds, E., Plasterk, R.H., 2004. Target-selected gene inactivation in zebrafish. Methods in cell biology 77, 69-90.
45. Yasumoto, H., Meng, L., Lin, T., Zhu, Q., Tsai, R.Y., 2007. GNL3L inhibits activity of estrogen-related receptor gamma by competing for coactivator binding. Journal of cell science 120, 2532-2543.

3

Nucleostemin Loss Reveals the Role of Ribosome Numbers in Cell Fate Decision-making

Paul B. Essers, Tamara C. Pereboom, Judith T. Paridaen, Alyson W. MacInnes

Abstract

Nucleostemin (NS) is from a small family of multifunctional nucleolar GTPases that play a key role in maintaining the pluripotent capacity of stem cells and oncogenic activity of tumor cells. NS functions both in the biogenesis of ribosomes and in the p53 tumor suppressor-signaling pathway, yet the relative contribution of these roles in vertebrate development and cell fate decision-making are still largely unknown. Here we show that widespread precocious neuronal differentiation occurs in the developing brains of zebrafish embryos carrying homozygous mutations in *ns* or its family member *gnl2*. Moreover, we observe this pattern of neuronal differentiation in embryonic lines carrying two other unrelated ribosome biogenesis mutations, and demonstrate that these effects are independent of p53 activation. Our results suggest that the critical role NS family members play in the maintenance of stem cells is to keep ribosomes at a sufficiently high number so as to allow continuation of a pluripotent state, and that failure to reach this number results in cells defaulting to a decision to terminally differentiate. These results could have important implications for devising cancer strategies that seek to limit the numbers and capacities of tumor-initiating or cancer stem cells.

Introduction

Nucleostemin (NS) has been of great interest lately in the field of stem cell and cancer research due to its increased expression in highly proliferative cells, including most tumor cells, that rapidly diminishes as differentiation progresses [1]. The high expression of NS in neural stem cells suggests it plays an important role in neurogenesis [2], and the elevated expression of NS or its family member GNL3-like (GNL3L) has been shown to be required for the pluripotent maintenance and radioresistance of tumor-initiating cells [3]. Murine embryos carrying homozygous deletions of *Ns* are arrested at the blastocyst stage due to a block in cell proliferation [4,5], and the accumulation of NS is observed in dedifferentiating cells of regenerating newt limbs [6]. Thus in many species there is clearly an early and conserved role of NS and its family members in maintaining cells in a highly proliferative state.

NS and its family member GNL2 have functions in ribosome biogenesis [ref other chapter]. These proteins are GTPases that shuttle from the nucleus to the nucleolus depending on their GTP binding state, although their main localization is in the nucleolus where the majority of ribosome biogenesis takes place [7]. In HeLa cells, knockdown of *NS* impairs ribosome biogenesis while its overexpression facilitates pre-rRNA processing [8]. Deletion of *GNL2* in yeast has also been shown to affect rRNA processing [9]. In addition to this function in ribosome biogenesis, overexpression of NS is also able to stabilize the p53 tumor suppressor protein by directly binding to MDM2 and dissociating p53 [10]. Conversely, depletion of NS has been demonstrated to activate p53 by the release of ribosomal proteins L11 and L5 which bind to the negative regulator of p53, MDM2, resulting in the dissociation of the p53/MDM2 complex and the stabilization and activation of p53 [11]. p53 then induces cell cycle arrest which, depending on the level and duration of activation, is followed by activation of apoptosis pathways [12]. Homozygous mutations of *ns* or *gnl2* in zebrafish embryos also results in widespread p53-induced apoptosis, however introduction of a p53 loss-of-function background does not rescue the lethal phenotype of these mutants or in the mouse model of Ns loss [5,13].

One of the most important molecular pathways in differentiation is the Notch pathway, which is involved in the binary decision-making of developmental processes including neurogenesis and hematopoiesis. It functions mainly through the process of lateral inhibition, whereby cells committed to differentiation prevent neighboring cells from undergoing a similar fate. In zebrafish neuronal differentiation, the proneural genes *ascaete-scute homolog 1a* (*zash1a*) and *neurogenin1* (*neurog1*) induce expression of the membrane bound Notch ligand DeltaA. Upon binding of members of the Delta/Serrate/Jagged family to the Notch receptor, the intracellular domain (N^{icd}) of the receptor is cleaved by the γ-secretase complex and translocates to the nucleus, where it forms different complexes to either activate or repress the transcription of target genes [14]. A major family of up-regulated target genes by Notch signaling is the *Hes* transcription factors, the expression of which inhibits *zash1a* and *ngn1* and promotes a non-neuronal fate. Because *Hes1* (*her4* in zebrafish), also represses its own transcription, an oscillatory loop is created, which results in early cells initially alternating between *zash1a*/*neurog1* and *hes1* expression, keeping them in a progenitor state until the decision to differentiate is made [15]. Several models demonstrate that inhibition of the Notch pathway impairs this binary-decision making, resulting in an overall expansion of neurogenesis as neighboring cells both decide to proceed down the differentiation pathway instead of one maintaining its progenitor status [16].

Some recent findings suggest a link between ribosome biogenesis and Notch signaling. In *Drosophila*, it has been shown that loss of the dyskerin ortholog *mfl*, known to be important for rRNA processing, affects wing patterning and cell differentiation in a manner reminiscent of reduced Notch signaling [17]. Another study demonstrated that overexpression of the 28S rRNA-

interacting neural-specific splicing receptor (SRp38) inhibits neurogenesis in *Xenopus* in a manner requiring active Notch signaling [18]. Depletion of SRp38 also led to dysregulation of neurogenesis that was synergized with inactivation of Delta receptors [18]. However, the mechanisms by which ribosome biogenesis link to Notch signaling are still not well defined.
Here, we show that inactivation of *gnl2* and *ns* induces ectopic expression of the pro-neural genes *zash1a* and *ngn1*, *deltaA* ligands, and terminal neuronal differentiation markers in a manner that phenocopies the neuronal expansion observed upon a reduction of Notch signaling. We go on to show that mutations in other genes required for ribosome biogenesis (both linked to human bone marrow failure disorders) *rpS7* and *nop10* [19,20] exhibit the same expansion of terminally differentiated neural cells. This phenomenon is independent of p53 activation, as a loss-of function p53 background or knockdown of p53 does not affect the pattern of neurogenesis in these mutant embryos. Finally, we demonstrate that Notch-activated cells with higher levels of *her4* contain a significantly increased number of ribosomes compared to *her4* negative cells, consistent with the notion that translation capacity and ribosome numbers decrease as cells proceed down the differentiation pathway. Our results suggest that there exists a minimum threshold of ribosome numbers in order for the receiving cell of the lateral inhibition process to proceed down a non-differentiated pathway, most likely reflecting the translation capacity requirement of continued proliferation. Taken together, these results suggest that the role of NS and its family members in stem cell maintenance is to sustain the high numbers of ribosomes required for the translation capacity necessary to support a continued proliferative state.

Materials and Methods

Zebrafish embryos and fish maintenance

Zebrafish were raised and embryos obtained through natural spawning as previously described [21] in accordance with all Dutch regulations and guidelines. The *gnl2*^{bw41c} and *ns* mutant were previously described [13]. The hi1034b (*rpS7*) and hi2578 (*nop10*) lines were a generous gift from the lab of Dr. Nancy Hopkins. *p53*$^{M214K/M214K}$ fish were previously described [22] as was the *her4::gfp* transgenic line [23].

In Situ Hybridizations

In situ hybridizations were performed as previously described [24]. The zash1a, neurog1 and deltaA1 probes were a generous gift from Dr. Dana Zivkovic. Microscopy was done with a Leico Axxioplan microscope at 10x magnification.

Immunohistochemistry

Embryos were fixed overnight in 4% paraformaldehyde at 4°C and rinsed in PBT. They were then bleached in 30% H_20_2 in 5x SSC/5% formamide, rinsed in PBT and ddH_2O and then permeabilized in ice-cold acetone. After a rinse in ddH_2O and PBT, embryos were incubated in blocking buffer (5% FCS, 1% BSA, 1% DMSO, 1% Triton X-100, 0.2% saponin [Sigma] in PBS) for 2 hours and then incubated in mouse α-HuC/D (Molecular Probes, A-21271, 1:200) in blocking buffer for 4 nights at 4°C. They were then rinsed in PBT containing 0.2% saponin and incubated in goat α-mouse IgG-HRP (Cell Signaling #7076X, 1:250) in blocking buffer overnight at 4°C, washed in PBT containing 2% saponin and developed using SigmaFast DAB (Sigma Aldrich). Photographs were taken using a Leico Axxioplan microscope at 10x magnification.

Cell culture

K562 cells were cultured in RPMI1640 supplemented with 10% fetal calf serum and 1% penicillin/streptomycin. For differentiation experiments, cells were cultured in 40nM Phorbol 12-myristate 13-acetate [25] for 48 hours.

Western Blots

Western blots were performed as previously described [26]. Goat anti-Gnl2 (sc-55690) was obtained from Santa Cruz Biotechnology (Santa Cruz, California).

FACS analysis

Embryos were collected at 2 dpf and rinsed in wash buffer PBS/30% FCS/10% ddH_2O. They were then incubated in dissociation buffer (wash buffer containing dispase I [Sigma] 2.5%, Trypsin 0.125%, DNase (Promega) 5U/mL) at 30°C in a shaker for 30 minutes and vigorously pulled through a 23G needle several times during this incubation. The dissociated cells were filtered through a 35µm nylon mesh cell strainer cap (Falcon) and flushed with PBS/10%ddH_2O to obtain a single cell suspension. Propidium iodide (Sigma, 1µg/ml) was added before analysis. Sorting of the *her4* positive cells was done using a FACS Diva (BD). After sorting, cells were collected in wash buffer, spun down and snap frozen in liquid nitrogen.

Results

Cellular differentiation results in diminished expression of Gnl2 in vertebrates.

The diminished expression of NS as cells proceed down the differentiation pathway has been well established, however the fate of GNL2 expression has been unexplored. To confirm that GNL2 is similarly reduced upon cellular differentiation, we measured its expression in the human myelogenous leukemia cell line K562. This cell line differentiates into megakaryocytes upon exposure to the chemical phorbol myristate acetate (PMA) [25,27], also observed in Fig. 1A. Measurement of *GNL2* transcripts (Fig. 1B) and protein levels (Fig 1C) reveals a strong downregulation of both *Gnl2* mRNA and GNL2 protein upon K562 cell exposure to PMA, indicating that like its family member NS, GNL2 is functioning predominantly in undifferentiated cells.

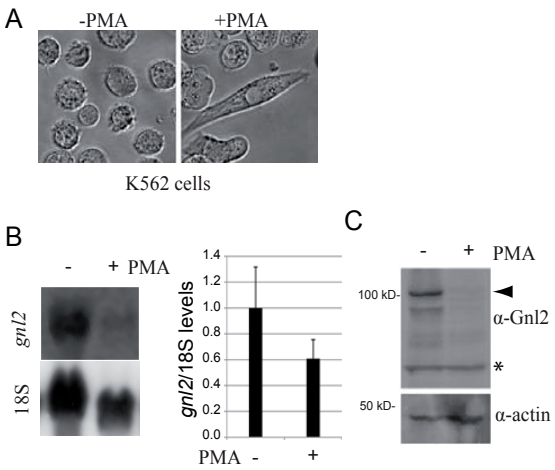

Figure 1. gnl2 mRNA and protein levels decrease upon K562 cell differentiation. (A) Bright field microscopy of K562 cells exposed to 40nM of PMA or control medium for 48 hours. **(B)** Northern blot showing reduced *gnl2* expression after exposure to PMA, with quantification (normalized to 18S levels, n=4). **(C)** Western blot showing reduced Gnl2 levels after exposure to PMA. Asterix indicates a non-specific band.

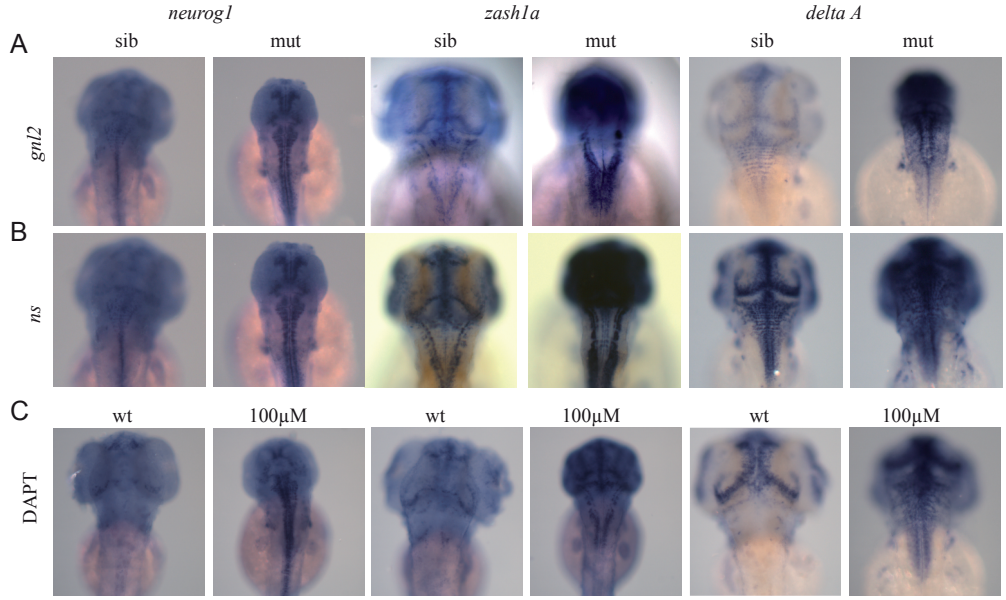

Figure 2. Proneural genes and deltaA are upregulated in gnl2 and ns mutants. (A,B) Dorsal view of Wholemount In Situ Hybridization (WISH) for zash1a, ngn1 and deltaA in the gnl2 mutant (A) and ns mutant (B) at 36hpf. Upregulation of all three genes can be observed in both mutants. (C) DAPT treated embryos were used as a positive control. Stainings of mutants and siblings were performed in the same tube.

Ns and gnl2 mutations result in precocious neuronal gene expression

A zebrafish mutagenesis screen for genes with a role in neural differentiation uncovered *gnl2* as important in maintaining normal levels of *zash1a* [28]. This mutant line carries an early stop codon resulting in expression of a truncated protein and lethality by 3 days post fertilization (dpf). We also screened a library of mutagenized zebrafish sperm by Targeting Induced Local Lesions in Genomes (TILLING) to generate a similar line with mutations in *ns* [13], also lethal by 5 dpf. On these mutant lines at 36 hours post fertilization (hpf) we performed *in situ* hybridizations (ISH) to measure the proneural gene transcripts *zash1a*, *neurog1* and one of their downstream targets, the Notch ligand *deltaA* (Fig. 2A,B). Wild type embryos treated with DAPT, known to result in neurogenesis expansion through inhibition of the Notch pathway, were used as positive controls [29] (Fig. 2C). These results reveal a considerable expansion of *deltaA*, *zash1a*, and *neurog1* expression in *gnl2* and *ns* mutants similar to the DAPT-treated embryos, indicating that the number of cells differentiating into neurons increases upon loss of Ns or Gnl2.

Terminal neuronal differentiation increases with ns and gnl2 mutations

To determine the ultimate fate of the cells in Fig. 2 overexpressing the neuronal genes, we immuno-stained *gnl2* and *ns* mutant embryos at 48 hpf for HuC/D, a known marker of terminal neuronal differentiation [30] (Fig. 3A-C). The staining of the DAPT-treated embryos (Fig. 3C) is similar to that observed in embryos with *gnl2* and *ns* mutations, indicating that the precocious increase of neural gene expression seen in Fig. 2 leads to an increase in the number of terminally differentiated neurons.

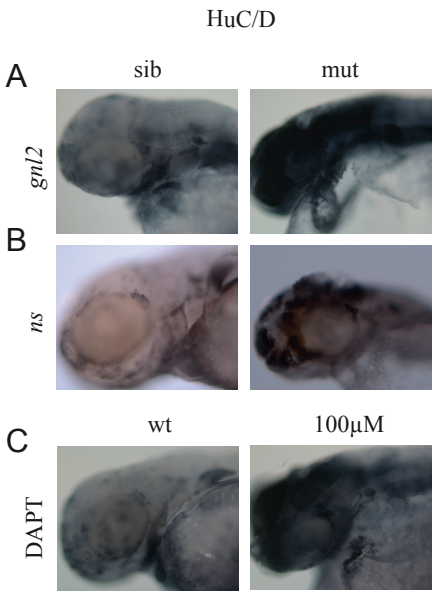

Figure 3. Increased terminal neuronal differentiation in *gnl2* and *ns* mutants. **(A,B)** Lateral view of immunohistochemical staining with αHuC/D in the *gnl2* (A) and *ns* (B) mutants. **(C)** DAPT treated embryos were used as a positive control. Stainings of mutants and siblings were performed in the same tube.

Other ribosome biogenesis mutants also show precocious neurogenesis

To establish whether the increase of neuronal gene expression and terminally differentiated neurons observed in the *gnl2* and *ns* mutants are unique to this family of GTPases or if in fact these are general phenotypes that result from ribosome biogenesis impairments, we repeated our neurogenesis measurements in two other mutant lines. These include lines with mutations in ribosomal protein (RP) gene S7, and the *nop10* gene that is required for proper pseudouridinylation of rRNA [31]. Fig. 4 reveals that like the *ns* and *gnl2* mutants, *rpS7* (Fig. 4A) and *nop10* mutants (Fig. 4B) also show precocious expansion of neural genes *ngn1, zash1a,* and *deltaA*. Moreover, these two mutants also reveal an increase in the number of cells that have undergone terminal neuronal differentiation as shown by HuC/D staining (Fig. 4C). In order to determine if this expansion of neurogenesis in these mutants is linked to the activation of the p53 tumor suppressor we crossed the *nop10* mutant onto a previously described *p53* mutant background [22] and measured the levels of *zash1a* transcripts. Additionally we performed the same experiments in *gnl2* and *ns* embryos injected with a morpholino (MO) that prevents the translation of p53 protein [32]. Despite the known activation of p53 by the loss of *ns, gnl2,* and *nop10* [13,26], this activation plays no role in the expansion of neurogenesis, as seen by the unchanged increase of *zash1a* expression in the *nop10, ns,* and *gnl2* mutants upon the loss of p53 (Fig. 4D). These results indicate that the roles of ribosome biogenesis impairments in cell fate decision-making are independent of any effects the mutations have on p53-induced apoptosis.

Differentiation is linked to ribosome numbers

Her4 is a known target gene of the Notch pathway that becomes upregulated in the Notch signal-receiving cell, the cell that maintains its progenitor status after a neighboring cell has committed to terminal differentiation. To confirm that the expansion of neuronal gene expression in ribosome biogenesis mutants results in a concomitant decrease in expression of *her4*, we crossed the *gnl2, rpS7,* and *nop10* mutants onto a transgenic background that drives green fluorescent protein (gfp) expression from the *her4* promoter. These crosses resulted in mutant embryos with a marked reduction of gfp expression (Fig. 5A), confirming a loss of cells that maintain progenitor status as their neighboring cells differentiate. In order to measure the total number of ribosomes in cells that maintain their progenitor status versus those that proceed down the differentiation pathway, we FACS sorted wild type *her4*$^{+}$ and *her4*$^{-}$ cells from transgenic embryos and examined the polysome profiles from an equal number of starting cells. Fig. 5B illustrates that *her4*$^{+}$ cells contain approximately twice as many ribosomes as *her4*$^{-}$ cells, as indicated by the size of the 80S

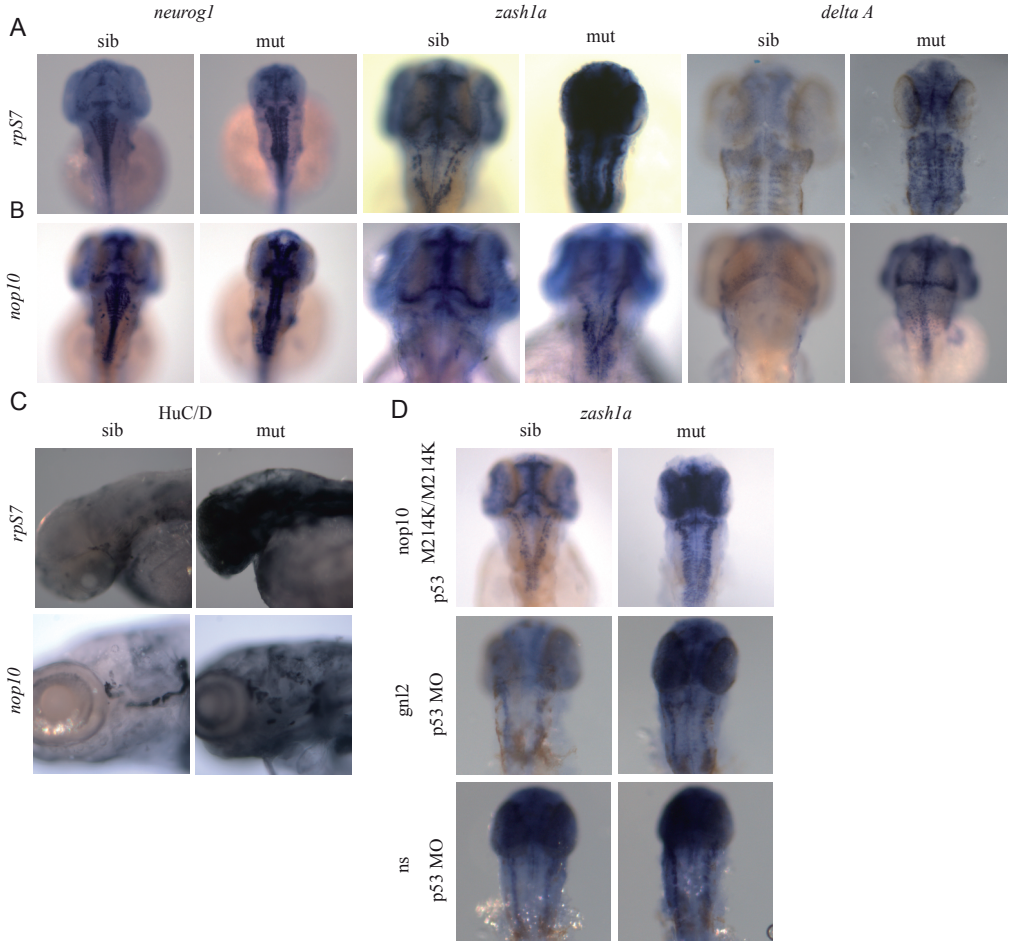

Figure 4. Increased neurogenesis is a phenotype common to ribosome biogenesis mutants and independent of p53 activation. (**A,B**) Dorsal view of *rpS7* (A) and *nop10* (B) embryos stained by WISH for *ngn-1, zash1a* and *deltaA* at 36hpf. Upregulation of these genes can be observed in both ribosome biogenesis mutants. **(C)** Lateral view of zebrafish embryos stained with anti-HuC/D antibody at 2dpf for *rpS7* and 4dpf for *nop10* showing increased neuronal differentiation in these mutants (**D**) Dorsal view of *nop10/p53*$^{M214K/M214}$ and *p53* morpholino injected *gnl2* and *ns* mutants and siblings stained by WISH for *zash1a* at 36hpf. Mutation or knockdown of p53 did not prevent proneural gene upregulation observed in the mutants. Stainings of mutants and siblings were performed in the same tube.

peak. The number of ribosomes and overall translation activity is also observed to diminish substantially in K562 cells induced to differentiate with PMA (Fig. 5C). Taken together, these results suggest that the total number of ribosomes in a given cell plays an important role in its decision to maintain its progenitor status or to proceed down the differentiation pathway.

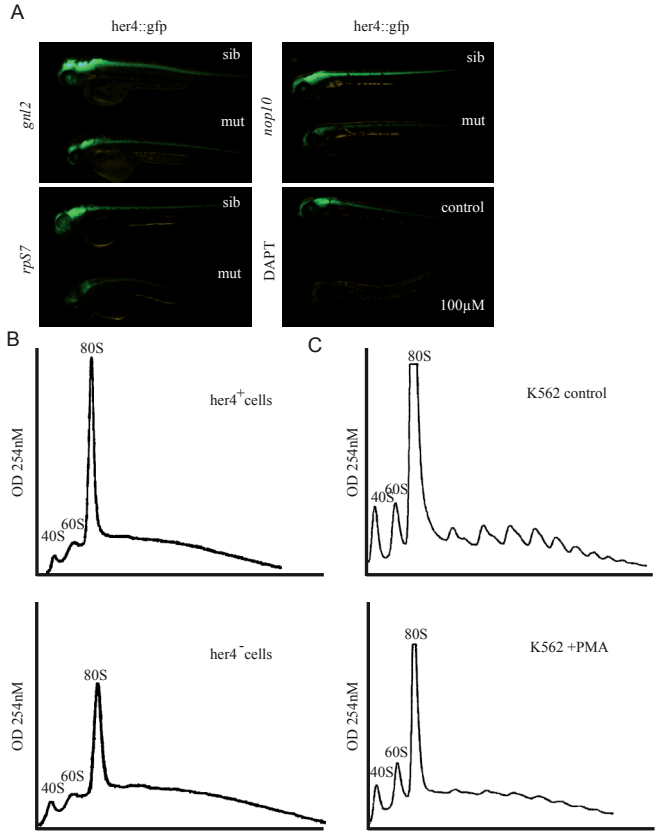

Figure 5. Cells that have not undergone differentiation have higher numbers of ribosomes than differentiated cells. (**A**) Reduced expression of *her4::gfp* in ribosome biogenesis mutants and DAPT treated embryos at 2dpf. **(B)** Polysome profiles of *her4*$^{+}$ and *her4*$^{-}$ cells, which were isolated and FACS sorted from embryos expressing *her4::gfp* at 2 dpf, show a downregulation of ribosome number. 5.75x10^{6} cells were used per sample. (**C**) Polysome profiles of K562 cells treated with PMA show a reduction of monosome and polysome numbers compared to control (DMSO). 366μg of protein was used per sample.

Discussion

The previous identification of *gnl2* in a screen for mutant zebrafish with increased expression of pro-neural genes was intensely curious. We demonstrate here that GNL2, like NS, is downregulated upon differentiation in human cells. Both *gnl2* and *ns* mutants in zebrafish show the same precocious expansion of pro-neural genes as well as terminally differentiated neurons, as did two other unrelated mutants involved in different aspects of ribosome biogenesis. The question therefore remained, why a mutation involved in ribosome biogenesis would result in a phenotype that expanded neurogenesis and the number of terminally differentiated neurons similarly to what one finds when inhibiting the Notch pathway, one of the most critical pathways in cell fate decision-making.

Many mutations in ribosome biogenesis genes can activate p53 signaling [5,13,33] and p53 signaling can influence cell differentiation decisions, either promoting or inhibiting differentiation [34,35]. Therefore, we determined whether activation of p53 is responsible for the neurogenic expansion observed in our ribosome biogenesis mutants. However, our data indicates that in fact, this precocious neurogenesis expansion is independent of the activation of p53, and suggests instead that the widespread neural differentiation observed in ribosome biogenesis mutants is due to other mechanisms.

We propose that one of these mechanisms lies in the total number of ribosomes in a given cell. There is already some evidence that proteins involved in ribosome biogenesis are involved in

neural stem cell maintenance [1,2,13,28,36]. In addition, a strong dependence of Notch activity on translational capacity has been reported in studies in *Drosophila* wing development [17,37]. In line with this is the recent finding that NS is needed for maintenance of embryonic stem cells, because it ensures rapid cell transit through the G1 phase of cell division [38]. Our finding that Notch-activated cells have 2-fold higher numbers of ribosome components supports the notion that a minimum threshold of translational capacity is necessary to maintain a proliferative state. These data suggest that the role that NS and GNL2 play in neural stem cells is increasing the rate of ribosome biogenesis and ultimately of total ribosome numbers, ensuring that some cells have the translational capacity required to maintain their status as proliferative progenitor cells.

Acknowledgements

We would like thank Stefan van der Elst for assistance with the FACS.

References

1. Tsai RY, McKay RD (2002) A nucleolar mechanism controlling cell proliferation in stem cells and cancer cells. Genes Dev 16: 2991-3003.
2. Cai J, Cheng A, Luo Y, Lu C, Mattson MP, et al. (2004) Membrane properties of rat embryonic multipotent neural stem cells. J Neurochem 88: 212-226.
3. Okamoto N, Yasukawa M, Nguyen C, Kasim V, Maida Y, et al. (2011) Maintenance of tumor initiating cells of defined genetic composition by nucleostemin. Proc Natl Acad Sci U S A 108: 20388-20393.
4. Beekman C, Nichane M, De Clercq S, Maetens M, Floss T, et al. (2006) Evolutionarily conserved role of nucleostemin: controlling proliferation of stem/progenitor cells during early vertebrate development. Mol Cell Biol 26: 9291-9301.
5. Zhu Q, Yasumoto H, Tsai RY (2006) Nucleostemin delays cellular senescence and negatively regulates TRF1 protein stability. Mol Cell Biol 26: 9279-9290.
6. Maki N, Takechi K, Sano S, Tarui H, Sasai Y, et al. (2007) Rapid accumulation of nucleostemin in nucleolus during newt regeneration. Dev Dyn 236: 941-950.
7. Meng L, Zhu Q, Tsai RY (2007) Nucleolar trafficking of nucleostemin family proteins: common versus protein-specific mechanisms. Mol Cell Biol 27: 8670-8682.
8. Romanova L, Grand A, Zhang L, Rayner S, Katoku-Kikyo N, et al. (2009) Critical role of nucleostemin in pre-rRNA processing. J Biol Chem 284: 4968-4977.
9. Du X, Rao MR, Chen XQ, Wu W, Mahalingam S, et al. (2006) The homologous putative GTPases Grn1p from fission yeast and the human GNL3L are required for growth and play a role in processing of nucleolar pre-rRNA. Mol Biol Cell 17: 460-474.
10. Dai MS, Sun XX, Lu H (2008) Aberrant expression of nucleostemin activates p53 and induces cell cycle arrest via inhibition of MDMMol Cell Biol 28: 4365-4376.
11. Lohrum MA, Ludwig RL, Kubbutat MH, Hanlon M, Vousden KH (2003) Regulation of HDM2 activity by the ribosomal protein LCancer Cell 3: 577-587.
12. Asai T, Liu Y, Bae N, Nimer SD (2011) The p53 tumor suppressor protein regulates hematopoietic stem cell fate. J Cell Physiol 226: 2215-2221.
13. Paridaen JT, Janson E, Utami KH, Pereboom TC, Essers PB, et al. (2011) The nucleolar GTP-binding proteins Gnl2 and nucleostemin are required for retinal neurogenesis in developing zebrafish. Dev Biol 355: 286-301.
14. Fiuza UM, Arias AM (2007) Cell and molecular biology of Notch. J Endocrinol 194: 459-474.
15. Kageyama R, Ohtsuka T, Shimojo H, Imayoshi I (2008) Dynamic Notch signaling in neural progenitor cells and a revised view of lateral inhibition. Nat Neurosci 11: 1247-1251.
16. Geling A, Steiner H, Willem M, Bally-Cuif L, Haass C (2002) A gamma-secretase inhibitor blocks Notch signaling in vivo and causes a severe neurogenic phenotype in zebrafish. EMBO Rep 3: 688-694.
17. Tortoriello G, de Celis JF, Furia M (2010) Linking pseudouridine synthases to growth, development and cell competition. FEBS J 277: 3249-3263.
18. Liu KJ, Harland RM (2005) Inhibition of neurogenesis by SRp38, a neuroD-regulated RNA-binding protein. Development 132: 1511-1523.
19. Gazda HT, Sheen MR, Vlachos A, Choesmel V, Oâ€™Donohue MF, et al. (2008) Ribosomal protein L5 and L11 mutations are associated with cleft palate and abnormal thumbs in Diamond-Blackfan anemia patients. Am J Hum Genet 83: 769-780.
20. Nelson ND, Bertuch AA (2011) Dyskeratosis congenita as a disorder of telomere maintenance. Mutat Res.
21. Westerfield M (2000) The zebrafish book. A guide for the laboratory use of zebrafish (Danio Rerio). University of Oregon Press, Eugene 4th edition.
22. Berghmans S, Murphey RD, Wienholds E, Neuberg D, Kutok JL, et al. (2005) tp53 mutant zebrafish develop malignant peripheral nerve sheath tumors. Proc Natl Acad Sci U S A 102: 407-412.
23. Yeo SY, Kim M, Kim HS, Huh TL, Chitnis AB (2007) Fluorescent protein expression driven by her4 regulatory elements reveals the spatiotemporal pattern of Notch signaling in the nervous system of zebrafish embryos. Dev Biol 301: 555-567.
24. Diks SH, Bink RJ, van de Water S, Joore J, van Rooijen C, et al. (2006) The novel gene asb11: a regulator of the size of the neural progenitor compartment. J Cell Biol 174: 581-592.
25. Bellodi C, Kopmar N, Ruggero D (2010) Deregulation of oncogene-induced senescence and p53 translational control in X-linked dyskeratosis congenita. EMBO J 29: 1865-1876.
26. Pereboom TC, van Weele LJ, Bondt A, Macinnes AW (2011) A zebrafish model of dyskeratosis congenita reveals hematopoetic stem cell formation failure due to ribosomal protein-mediated p53 stabilization. Blood.
27. Sutherland JA, Turner AR, Mannoni P, McGann LE, Turc JM (1986) Differentiation of K562 leukemia cells along erythroid, macrophage, and megakaryocyte lineages. J Biol Response Mod 5: 250-262.

28. Paridaen JT, Janson E, Utami KH, Pereboom TC, Essers PB, et al. The nucleolar GTP-binding proteins Gnl2 and nucleostemin are required for retinal neurogenesis in developing zebrafish. Dev Biol 355: 286-301.
29. Dovey HF, John V, Anderson JP, Chen LZ, de Saint Andrieu P, et al. (2001) Functional gamma-secretase inhibitors reduce beta-amyloid peptide levels in brain. J Neurochem 76: 173-181.
30. Wakamatsu Y, Weston JA (1997) Sequential expression and role of Hu RNA-binding proteins during neurogenesis. Development 124: 3449-3460.
31. Henras A, Henry Y, Bousquet-Antonelli C, Noaillac-Depeyre J, Gelugne JP, et al. (1998) Nhp2p and Nop10p are essential for the function of H/ACA snoRNPs. EMBO J 17: 7078-7090.
32. Langheinrich U, Hennen E, Stott G, Vacun G (2002) Zebrafish as a model organism for the identification and characterization of drugs and genes affecting p53 signaling. Curr Biol 12: 2023-2028.
33. Dai MS, Zeng SX, Jin Y, Sun XX, David L, et al. (2004) Ribosomal protein L23 activates p53 by inhibiting MDM2 function in response to ribosomal perturbation but not to translation inhibition. Mol Cell Biol 24: 7654-7668.
34. Almog N, Rotter V (1997) Involvement of p53 in cell differentiation and development. Biochim Biophys Acta 1333: F1-27.
35. Molchadsky A, Shats I, Goldfinger N, Pevsner-Fischer M, Olson M, et al. (2008) p53 plays a role in mesenchymal differentiation programs, in a cell fate dependent manner. PLoS One 3: e3707.
36. Ueno M, Nakayama H, Kajikawa S, Katayama K, Suzuki K, et al. (2002) Expression of ribosomal protein L4 (rpL4) during neurogenesis and 5-azacytidine (5AzC)-induced apoptotic process in the rat. Histol Histopathol 17: 789-798.
37. Tortoriello G, de Celis JF, Furia M Linking pseudouridine synthases to growth, development and cell competition. FEBS J 277: 3249-3263.
38. Qu J, Bishop JM (2012) Nucleostemin maintains self-renewal of embryonic stem cells and promotes reprogramming of somatic cells to pluripotency. J Cell Biol 197: 731-745.

4

Insulin/IGF-1-mediated longevity is marked by reduced protein metabolism

Gerdine J Stout*, Edwin C A Stigter*, Paul B Essers*, Klaas W Mulder, Annemieke Kolkman, Dorien S Snijders, Niels J F van den Broek, Marco C Betist, Hendrik C Korswagen, Alyson W MacInnes & Arjan B Brenkman

*These authors contributed equally to this work.

Mol Syst Biol. 2013 Jul 2;9:679.

Abstract

Mutations in the daf-2 gene of the conserved Insulin/Insulin-like Growth Factor (IGF-1) pathway double the lifespan of the nematode Caenorhabditis elegans. This phenotype is completely suppressed by deletion of Forkhead transcription factor daf-16. To uncover regulatory mechanisms coordinating this extension of life, we employed a quantitative proteomics strategy with daf-2 mutants in comparison with N2 and daf-16; daf-2 double mutants. This revealed a remarkable longevity-specific decrease in proteins involved in mRNA processing and transport, the translational machinery, and protein metabolism. Correspondingly, the daf-2 mutants display lower amounts of mRNA and 20S proteasome activity, despite maintaining total protein levels equal to that observed in wild types. Polyribosome profiling in the daf-2 and daf-16;daf-2 double mutants confirmed a daf-16-dependent reduction in overall translation, a phenotype reminiscent of Dietary Restriction-mediated longevity, which was independent of germline activity. RNA interference (RNAi)-mediated knockdown of proteins identified by our approach resulted in modified C. elegans lifespan confirming the importance of these processes in Insulin/IGF-1-mediated longevity. Together, the results demonstrate a role for the metabolism of proteins in the Insulin/IGF-1-mediated extension of life.

Introduction

The ageing of eukaryotes is subject to environmental and genetic control with conserved features across species, suggesting the presence of common lifespan-regulating mechanisms (Kenyon, 2010). In the nematode C. elegans, mutation of the daf-2 gene encoding for the Insulin/Insulin-like Growth Factor (IGF-1) receptor extends C. elegans lifespan two- to three-fold (Kenyon, 2010). The Insulin/IGF-1 pathway is highly conserved and regulates lifespan in organisms ranging from invertebrates to mammals (Kenyon, 2010). Insulin/IGF-1-mediated longevity signalling in C. elegans acts exclusively during adulthood, when development has completed (Dillin et al, 2002). Interestingly, genetic epistasis analysis has revealed that Insulin/IGF-1-mediated lifespan extension is completely suppressed upon knockdown of a number of transcription factors, including the Forkhead transcription factor DAF-16 (Kenyon et al, 1993), the heat-shock factor HSF-1 (Hsu et al, 2003), and partially by the Nrf-like xenobiotic response factor SKN-1(Tullet et al, 2008).

Microarray analysis has revealed numerous DAF-16 target genes, including a distinct enrichment of genes involved in stress response (McElwee et al, 2003; Murphy et al, 2003). These findings are in accordance with the observation that many lifespan-extending mutations concomitantly increase the resistance to stress, including oxidative stress (Wolff and Dillin, 2006). In addition to enhanced stress resistance, Insulin/IGF-1-mediated lifespan extension has been reported to reprogram the ER stress response and to depend on autophagy, the cellular process of self-digestion and recycling (Melendez et al, 2003; Hansen et al, 2008; Henis-Korenblit et al, 2010). Thus, the increased protection of organisms against toxic environmental stress compounded by the activation of autophagy is indispensable to Insulin/IGF-1-mediated longevity.

To date, the biological processes underlying Insulin/IGF-1-mediated longevity remain studied predominantly at the gene level. However, organismal phenotypes are far more dependent on protein function. An initial quantitative proteomics study of Insulin/IGF-1 pathway confirmed the role of stress-protective pathways (Dong et al, 2007) during longevity signalling. Additionally, it uncovered several compensatory pathways involved in longevity, underscoring the potential of this approach to identify novel longevity pathways (Dong et al, 2007). However, this analysis was restricted to a subset of the nematode proteome, involving mainly cytoplasmic and non-membrane bound proteins (Dong et al, 2007). In this study, a more stringent and non-biased proteomics approach of the whole nematode using TMT proteomics was employed (Dayon et al, 2008). This recently developed quantification method was used to identify novel processes and pathways involved in Insulin/IGF-1-mediated longevity. The obtained results confirmed the previously reported alteration of several proteins in daf-2(e1370) nematodes (Dong et al, 2007), including an increased representation of stress-resistance enzymes and a decrease in chaperone proteins. However, our results go on to reveal a severe and previously overlooked reduction in ribosomal proteins and concomitant translational activity. In addition, reduced expression of proteins involved in mRNA processing, translation, and the ubiquitin-proteasome system (UPS) was observed. Functional assays confirmed reduced mRNA levels and 20S proteasomal activity while at the same time total protein content of the mutants compared with wild-type nematodes remained unchanged. Moreover, the importance of these processes for lifespan extension is demonstrated using RNA interference (RNAi)-mediated knockdown of identified candidates.

All together, we propose a model for Insulin/IGF-1-mediated longevity that, in addition to an enhanced stress response, relies on protein metabolism coupled to the reduction in de novo protein synthesis and a shift from the UPS of degradation to recycling of proteins via autophagy.

Results

Quantitative proteomics of Insulin/IGF-1-mediated longevity

To uncover novel Insulin/IGF-1 lifespan regulators at the protein level, we performed mass spectrometry (MS)-based quantitative proteomics using TMT technology (Dayon et al, 2008). TMT involves post-lysis peptide labelling with chemically engineered unique mass tags that appear after peptide fragmentation by MS/MS. These tags allow for accurate protein quantification and when mixed, enable the simultaneous evaluation of protein changes in multiple conditions within a single experiment.

Whole nematode lysates of the long-lived daf-2(e1370) Insulin/IGF-1 receptor mutant were compared with wild-type (N2) and daf-16(mu86); daf-2(e1370) double mutants (Figure 1A) as the daf-2-dependent longevity phenotype is fully suppressed by the daf-16 mutation (Kenyon et al, 1993). As daf-2(e1370) is a temperature-sensitive mutant, nematodes were age synchronized at the permissive temperature and allowed to grow to larval stage L4. These nematodes were then

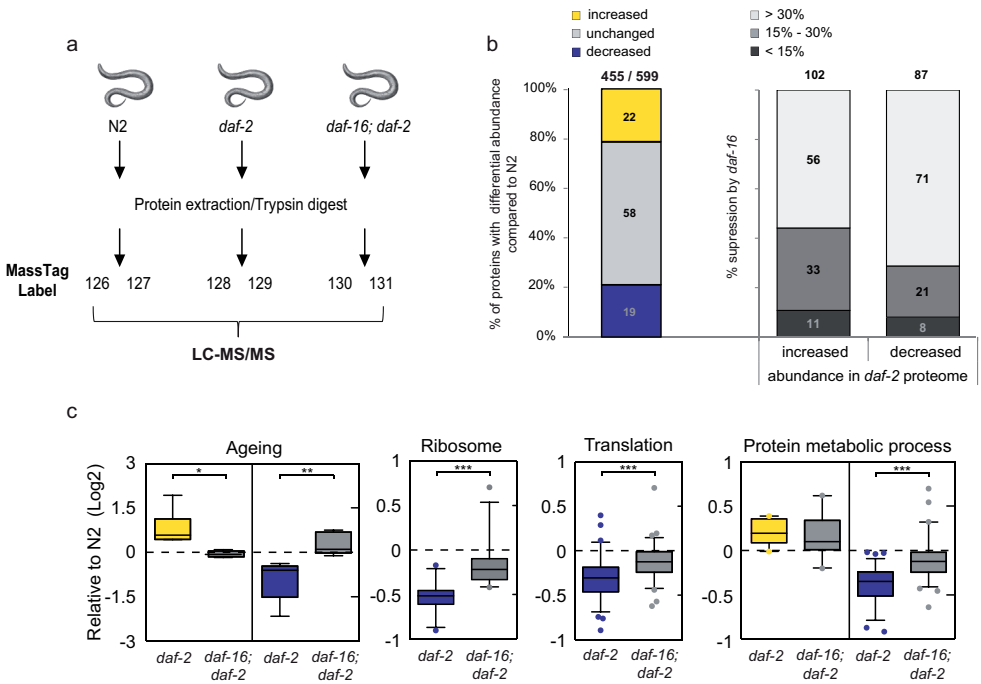

Figure 1: Quantitative proteomics reveals daf-16-mediated reduction in protein metabolism in long-lived daf-2(e1370) mutants. (A) Schematic overview of experimental set-up. Protein extracts were generated from three sample sets as biological replicates, harvested at day 1 of adulthood. Proteins were trypsin digested and labelled with unique mass tags. Labelled peptides were combined, fractionated by strong cation exchange chromatography to reduce sample complexity and subsequently analysed by LC-MS/MS. Data from 66 fractions were merged and analysed using Proteome Discoverer software. (B) Percentage of proteins with differential abundance (>1.3 fold change) in daf-2(e1370) mutants compared with N2 (left bar), and their expression dependency on daf-16 (right bars) for proteins with increased and decreased abundance to N2, respectively. The number of quantified proteins out of total amount of identified proteins is indicated on top of the bars. (C) Boxplots show expression analysis for GO-enriched processes in daf-2(e1370) and daf-16(mu86); daf-2(e1370) mutants relative to N2 (Log2). Asterisks indicate statistical significance (*P<0.01, **P<0.001, ***P<0.0001) as determined by paired t-test analysis.

switched to the non-permissive temperature (25°C) and harvested at the first day of adulthood when Insulin/IGF-1-dependent lifespan signalling is effective (Dillin et al, 2002). Of note, absence of oocytes and eggs was verified by Nomarsky microscopy, to avoid confounding of our observations by a developmental or reproductive phenotype previously reported in the daf-2(e1370) mutants (Gems et al, 1998).

Total protein extracts from whole nematodes were prepared for each strain in duplicate (6-plex TMT), digested into peptides, and labelled with unique mass tags. Samples were then combined, fractionated to reduce sample complexity, and subjected to LC-MS/MS (Figure 1A). LC-MS/MS analysis resulted in the identification of 599 proteins of which 455 could be quantified (Figure 1B, false discovery rate (FDR)<5%, Supplementary Figure S1 for representative MS/MS spectrum). Reproducibility of the independent biological replicates for each strain was significant (Supplementary Figure S2, rgreater than or equal to0.996) and proteins were recovered from all major C. elegans tissues including nuclear, cytoplasmic, and membrane-bound pools (Supplementary Figure S3).

Major changes were found in the proteome of the daf-2(e1370) mutants compared with either N2 (r=0.834) or daf-16(mu86); daf-2(e1370) double mutant nematodes (r=0.738, Figure 1B, Supplementary Figure S2). However, little difference was observed between the N2 and daf-16(mu86); daf-2(e1370) proteomes (r=0.952, Supplementary Figure S2), in agreement with the observation that daf-2-dependent longevity phenotype is completely suppressed by the absence of functional daf-16 gene expression (Kenyon, 2010).

The abundance of ~40% (cutoff>1.3 fold change) of all identified proteins was found to be altered in daf-2(e1370) mutants (Figure 1B; Supplementary Figure S4). In the daf-2(e1370) proteome, 22% of the quantified proteins showed increased abundance, whereas 19% were found decreased as compared with N2. Remarkably, about 90% of all changes depended at least 15–30% on the presence of daf-16 (Figure 1B), confirming that daf-16 is indeed a major downstream effector of daf-2 signalling for the observed proteomic changes.

Protein translation, proteasomal activity, and mRNA processing are novel pathways downregulated in Insulin/IGF-1 longevity signalling

Over Representation Analysis (ORA) (Backes et al, 2007) was used to identify the biological pathways involved in Insulin/IGF-1-mediated longevity. This revealed overrepresentation of stress protective pathways (e.g., thioredoxins and glutathione S-transferases) as well as metabolic pathways (e.g., phosphoenol pyruvate carboxykinases) (Supplementary Figure S5; Supplementary Table I) and confirmed previous studies illustrating the importance of these pathways in Insulin/IGF-1-mediated longevity (Murphy et al, 2003). As expected, ORA of proteins with decreased abundance in daf-2(e1370) proteome identified pathways with Gene Ontology (GO) classification terms 'ageing' (GO: 0007568) and 'determination of adult lifespan' (GO: 0008340). Growth and developmental processes were also found among the most significantly overrepresented GO categories (Figure 1C; Supplementary Figure S5; Supplementary Table II). Analysis using a cutoff-independent statistical method, Gene Set Enrichment Analysis (GSEA), confirmed these observations (Supplementary Table III). Our results are consistent with previous reports (Kenyon, 2010) and despite considerable technological differences, significant concordance was observed between our data set and published microarray (Murphy et al, 2003) and proteomics data sets (Dong et al, 2007) performed on the Insulin/IGF-1 signalling pathway (Supplementary Figure S6). Remarkably, significantly enriched and overrepresented GO terms (GSEA and ORA, respectively) that had not previously been associated with Insulin/IGF-1-mediated longevity were identified. A dramatic decrease was observed in proteins belonging to GO terms 'structural constituent of ribosome' (GO: 0003735) and 'ribosome' (GO: 0005840) (Figure 1C; Suppl. Tables II and III)

Accension	Gene name	NCBI/KOG description	Fold change 6-plex	% DAF-16 suppression
RNA processing				
C44E4.4	C44E4.4	RNA-binding protein La	–1.92	67.8
Y39A1C.3	cey-4	Predicted RNA-binding protein involved in translation or RNA processing	–1.47	41.8
C07H6.5	cgh-1	ATP-dependent RNA helicase (germline/P granule)	–1.64	71
T01C3.7	fib-1	ScNop1p (U3 SnoRN3P)—Fibrillating and related nucleolar RNA-binding proteins	–1.34	28.2
Y65B4BR.5a	Y65B4BR.5	Transcription factor containing NAC and TS-N domains	–1.49	56.7
ZK381.4	pgl-1	Predicted RNA-binding protein that contains a number of C-terminal RGG box motifs	–1.28	13
mRNA processing				
Y106G6H.2b	pab-1	Polyadenylate-binding protein (RRM superfamily)	–1.49	45.8
M28.5	phi-9	60S ribosomal protein 15.5kD/SNU13 involved in splicing	–1.41	45
R09B3.3	R09B3.3	mRNA cleavage and polyadenylation factor I complex, subunit RNA15	–2.39	101.9
W08E3.1	snr-2	U1 snRNP component	–1.53	49.5
F56D12.5a	vig-1	Predicted RNA-binding protein (RISC complex—regulation of translation)	–1.48	47
Translation				
F28H1.3	aars-2	Alanyl-tRNA synthetase	–1.43	48
F54H12.6	eef-1B.1	Elongation factor 1 beta/delta chain	–1.33	33.7
Y41E3.10a	eef-1B.2	Elongation factor 1 beta/delta chain	–1.33	33.8
F17C11.9b	eef-1G	Translation elongation factor EF-1 gamma Glutathione S-transferase	–1.36	39
T23D8.4	eif-3.C	Translation initiation factor 3, subunit c (eIF-3c)	–1.57	2
C47B2.5	eif-6	Translation initiation factor 6 (eIF-6)	–2.01	n.a.
F57B9.6	inf-1	Translation initiation factor 4a	–1.21	n.a.
Ribosome				
K07C5.4	K07C5.4	Ribosome biogenesis protein—Nop56p/Sik1p	–1.43	28.9
C53D5.6 i	mb-3	Karyopherin (importin) beta 3 nuclear import of ribosomes	–1.30	27.6
M28.5	phi-9	60S rp15.5kD/SNU13	–1.41	88
F13B10.2c	rpl-3	60S rpL3	–1.33	16.2
B0041.4	rpl-4	60S ribosomal protein RPL1/RPL2/RL4L4	–1.53	20.8
Y48G8AL.8a	rpl-17	60S rpL22	–1.70	30.8
C09D4.5	rpl-19	60S rpL19	–1.45	12.5
E04A4.8	rpl-20	60S rpL18A	–1.44	4.7
C27A2.2a	rpl-22	60S rpL22	–1.44	9.3
C03D6.8	rpl-24.2	60S rpL30 isologue	–1.87	39.9
F52B5.6	rpl-25.2	60s rpL23	–1.52	45.8
F28C6.7a	rpl-26	60S rpL26	–1.37	38.7
R11D1.8	rpl-28	60S rpL28	–1.53	36.9
W09C5.6a	rpl-31	60S rpL31	–1.42	15.5
C42C1.14	rpl-34	60s rpL34	–1.35	13.8
ZK652.4	rpl-35	60S rpL35	–1.52	25.5
F37C12.4	rpl-36	60S rpL36	–1.40	18.3
C54C6.1	rpl-37	60S rpL37	–1.38	17.5
Y48B6A.2	rpl-43	60S rpL37	–1.68	51.9
C37A2.7	rpl-P2	60S rp	–1.37	n.a.
Y71A12B.1	rps-6	40S rpS6	–1.43	24.3
F42C5.8	rps-8	40S rpS8	–1.43	19.2
T07A9.11	rps-24	40S ribosomal subunit S24	–1.36	28.3
F39B2.6	rps-26	40S rpS26	–1.48	15.6

Accension	Gene name	NCBI/KOG description	Fold change 6-plex	% DAF-16 suppression
Protein folding				
C47E8.5	daf-21	Molecular chaperone (HSP90 family)	–1.31	35.1
F26D10.3	hsp-1	Molecular chaperones HSP70/HSC70 HSP70 superfamily	–1.36	31.2
C37H5.8	hsp-6	Molecular chaperones mortalin/ PBP74/GRP75/HSP70 superfamily	–1.51	38.5
Protein breakdown				
Y67D8C.5	eel-1	E3 ubiquitin-protein ligase/putative upstream regulatory element binding protein	–1.34	26.4
Y110A7A.14	pas-3	20S proteasome, regulatory subunit alpha type PSMA4/PRE9	–2.01	n.a.
C36B1.4	pas-4	20S proteasome, regulatory subunit alpha type PSMA7/PRE6	–1.32	26.2
F25H2.9	pas-5	20S proteasome, regulatory subunit alpha type PSMA5/PRE	–1.15	32.5
CD4.6	pas-6	20S proteasome, regulatory subunit alpha type PSMA1/PRE5	–1.81	56.1
K05C4.1	pbs-5	20S proteasome, regulatory subunit beta type PSMB5/PSMB8/PRE2	–1.46	38.4
Other				
C06G3.5b	C06G3.5	Adenine deaminase/adenosine deaminase	–3.17	313.9
C24F3.2	C24F3.2	Dual specificity phosphatase	–6.71	n.a.
ZK863.6	dpy-30	Histone H3 (Lys4) methyltransferase complex, subunit CPS25/DPY-30	–1.35	n.a.
D2096.8	nap-1	Nucleosome assembly protein NAP-1	–1.52	44.3
C50B6.2	nasp-2	Cell cycle-regulated histone H1-binding protein	–3.50	n.a.
K04D7.1	rack-1	G protein beta subunit-like protein	–1.37	n.a.
ZK742.1a	xpo-1	Nuclear transport receptor CRM1/MSN5 (importin beta superfamily)	–2.01	n.a.

Table 1: Identified proteins related to protein metabolism that, compared with N2, display reduced abundance in the daf-2(e1370) proteome, and are suppressed by daf-16.Table 1 - Identified proteins related to protein metabolism that, compared with N2, display reduced abundance in the daf-2(e1370) proteome, and are suppressed by daf-16.

In addition to this reduction in numerous proteins composing the small and large C. elegans ribosomal subunits, several translation initiation and elongation factors with decreased abundance were identified (Table I). These observations suggest that the protein translation machinery is significantly reduced in the daf-2 proteome. Further analysis of proteins with decreased abundance identified the GO terms 'translation' (GO: 0006412), 'protein metabolism' (GO: 0019538) and 'proteasome core complex' (GO: 0005839) as significantly overrepresented in a daf-16-dependent manner (Figure 1C; Table I; Supplementary Tables I and III), pointing towards a general reduction in de novo protein production and protein turnover in the long-lived daf-2(e1370) mutant.

An additional independent quantitative proteomics experiment was conducted, comparing N2 with daf-2(e1370) (duplex). The results showed considerable overlap in the results and confirmed our observations (Supplementary Figure S7). Finally, western blot analysis confirmed the quantitative proteomics results for several identified proteins (Supplementary Figure S8). Thus, these findings suggest that Insulin/IGF-1-mediated longevity is associated with altered protein homeostasis.

Active mRNA translation is diminished in Insulin/IGF-1 mutants

Depletion of specific ribosomal and translation initiation factors has been shown to extend longevity in a range of organisms, including C. elegans (Hansen et al, 2007; Kapahi et al, 2010; McCormick et al, 2011). However, reduced protein translation is thought to facilitate Dietary Restriction (DR, defined as reduction in food intake without malnutrition) mediated lifespan extension (Stanfel et al, 2009; Kapahi et al, 2010), but not Insulin/IGF-1-dependent longevity (Hansen et al, 2007). Both longevity pathways genetically interact with signalling by the Target of Rapamycin (TOR) protein complex, which activates several cellular processes, including protein translation (Stanfel et al, 2009). Although loss of let-363, the C. elegans mTOR orthologue, extends lifespan and genetically interacts with daf-2 (Vellai et al, 2003), it was proposed to mediate C. elegans Insulin/IGF-1 longevity through upregulation of autophagy rather than reducing protein translation (Melendez et al, 2003; Hansen et al, 2007, 2008). This, together with the results from ORA and GSEA, prompted us to directly measure protein translation activity in Insulin/IGF-1 mutants.

Actively translated mRNA molecules contain multiple ribosomes (polysomes), whereas translationally inactive mRNA is retained in messenger ribonucleoprotein (mRNP) particles. Polysomes can be quantified after generation of an absorbance profile for rRNA, separated by sucrose gradient velocity sedimentation (Pereboom et al, 2011). A profound decrease in the 60S peaks, corresponding to the large ribosomal subunit, as well as a dramatic reduction in polysomal peaks was observed in daf-2(e1370) mutants compared with wild-type nematodes (Figure 2A). These findings are consistent with decreased levels of several ribosomal proteins and suggest that the daf-2(e1370) mutation drives a decrease in active polysomal protein translation. This decrease is almost completely suppressed by the daf-16 mutation, illustrating the specific control the Insulin/IGF-1 pathway is able to wield on polysomal mRNA translation (Figure 2A and B) during lifespan extension.

Insulin/IGF-1 pathway mutants exhibit altered protein metabolism

In addition to a reduced abundance of proteins directly involved in translation, several mRNA processing factors and elements associated with translation initiation were found decreased in the daf-2(e1370) proteome (Table I). PAB-1 tightly binds poly(A) tails of mRNA (Sonenberg and Hinnebusch, 2009) and is a key component of the translation initiation complex (Squirrell et al, 2006). Interestingly, PAB-1 is present in the cellular mRNA storage bodies (Noble et al, 2008) and involved in mRNA transport as well as release of mRNAs from sites of transcription (Dunn et al, 2005). Moreover, CGH-1, a putative DEAD box RNA helicase, and CEY-4 (Parker and Sheth, 2007; Updike and Strome, 2010) displayed a daf-16-dependent reduction in abundance in the daf-2(e1370) proteome (Table I). A similar observation was made for Sm-protein SNR-2, the C. elegans U1 subunit orthologue of the spliceosome. Based on these observations, we hypothesized that the global decrease in protein translation is accompanied by a reduction in total mRNA levels. Indeed, using equal numbers of nematodes, the daf-2(e1370) mutant yielded significantly less mRNA compared with N2, and this phenotype was partially suppressed in the daf-16(mu86); daf-2(e1370) double mutant (Figure 2C; Supplementary Figure S11). Although the daf-2 (e1370) mutant has a 5% smaller body size (McCulloch and Gems, 2003) compared with N2 nematodes at the chosen time point for our experiment, it is unlikely that this small difference in body size can account for the 48% reduction in mRNA levels observed in the daf-2(e1370).

Interestingly, despite reduced mRNA levels and polysomal translation, total protein levels per nematode were unchanged in daf-2(e1370) mutants (Figure 2D). We reasoned that reduced protein translation evokes less protein misfolding, ER stress, and reduced protease activity

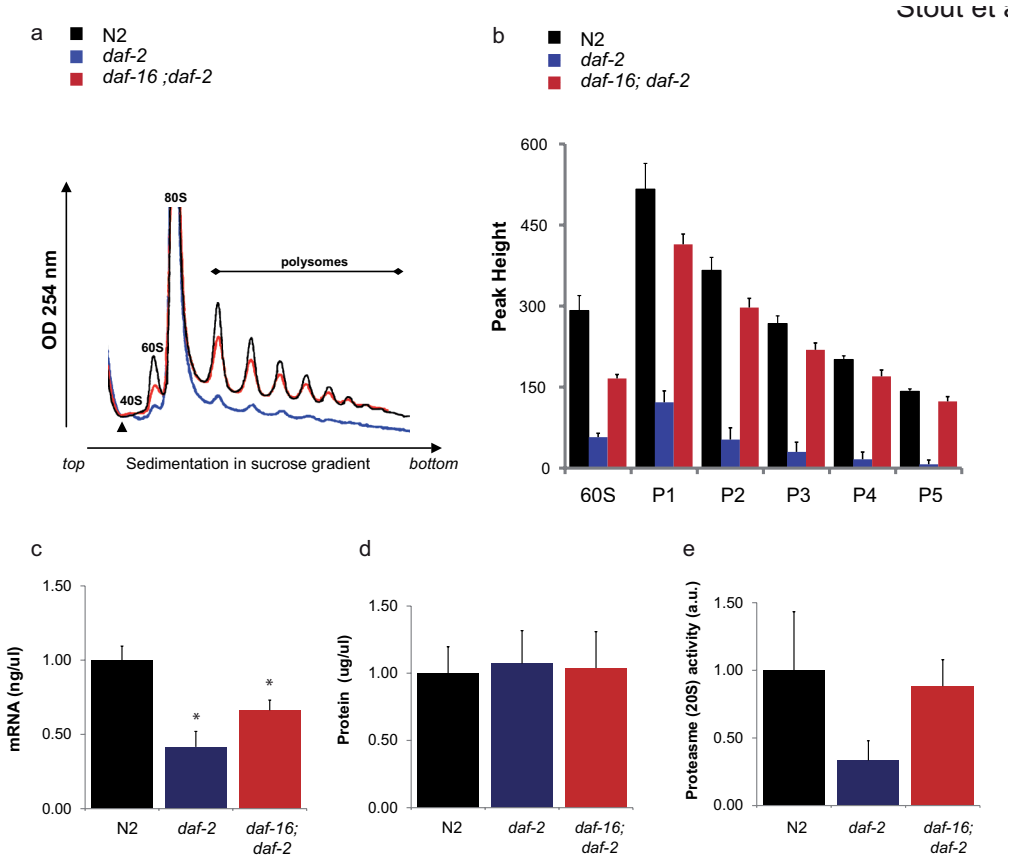

Figure 2: Functional assays confirm daf-2-dependent reduction in protein metabolism. (A) Representative traces of polyribosome profiles obtained from N2 (black), daf-2(e1370) (blue), and daf-16(mu86); daf-2(e1370) (red) nematodes harvested at day 1 of adulthood (identical conditions as described for the proteomics experiments). (B) Quantification of the peak (P) heights in the obtained polyribosome profiles using the starting point before the 40S peak (marked by an arrowhead, Figure 2A) as the zero value in at least four independent experiments. Values represent mean±s.e.m. All measured peaks are significantly lower in daf-2(e1370) compared with N2 ($P<0.0002$) and this response is dependent on daf-16 ($P<0.00003$) as tested by Student's t-test. a.u., arbitrary units. (C) The daf-2(e1370) mutant contained significantly less mRNA than N2. mRNA yield (ng/µl) was determined from 1500 nematodes of each strain in triplicate, using poly(A)+ trapping. (D) Total protein levels are similar in all three strains. Protein extracts from 1500 synchronized young adults were determined by spectrophotometric analysis. (E) The daf-2(e1370) has lower 20S proteasomal core complex activity. 20S proteasomal activity was measured in triplicate on 1500 synchronized day 1 adults for each strain using fluorescence analysis. Statistical significant differences represent means±s.e.m. as calculated with Student's t-test (*$P<0.05$).

coupled to the constitutive recycling of intrinsic proteins by autophagy. In line with this hypothesis, ORA of proteins with decreased abundance in the daf-2(e1370) proteome revealed a significant overrepresentation of proteins involved in protein degradation ('proteasome core complex' (GO: 0005839), Table I; Supplementary Table II). Furthermore, decreased abundance of proteins involved in protein folding (e.g., chaperone DAF-21) and breakdown (E3-ligase, EEL-1 as well as 20S proteasomal subunits (PAS-3, 4, 6, 7, and PBS-5) was observed. This suggests that the daf-2(e1370) mutant may display reduced protein degradation activity, pointing to a global

protein metabolic phenotype during Insulin/IGF-1-mediated longevity. To investigate this hypothesis, the activity of a main protein degradation pathway, the 20S proteasome (Finley, 2009) was determined. Indeed, reduced activity of this complex was observed in daf-2(e1370) mutants, and this response seemed to depend on daf-16 (Figure 2E). These observations link Insulin/IGF-1-mediated longevity to reduction of proteasomal activity.
Altogether, biological validation of our proteomics results suggests that Insulin/IGF-1-mediated longevity signalling is strongly associated with a global alteration of protein metabolism, in particular downregulation of mRNA processing, protein translation, and protein breakdown activity.

Reduced protein metabolism regulates longevity

To determine whether the identified processes have an important role in longevity assurance, lifespan assays with RNAi on the identified candidates involved in protein metabolism were performed. siRNA-mediated targeting of snr-2 and pab-1 significantly extended median lifespan of wild-type nematodes with 10–30%, indeed suggesting that mRNA transport and processing contribute to C. elegans longevity (Supplementary Table IV). It has previously been reported that RNAi-mediated knockdown of several translation initiation and elongation factors, as well as multiple components of the small and large ribosomal subunit, extend C. elegans lifespan (Henderson et al, 2006; Hansen et al, 2007; Reis-Rodrigues et al, 2012). Interestingly, many of these proteins showed a decreased abundance in the daf-2(e1370) proteome (Table I). Lifespan was also significantly extended with 10–20% when rpl-17 and rpl-28 expression is abrogated (Supplementary Table IV).
Knockdown of two identified proteasome subunits significantly decreased lifespan compared with control (Supplementary Table IV) with 10 and 30% for pas-3 and pbs-5, respectively, suggesting that reduced proteasomal activity may induce toxicity. These findings are in agreement to a previous report that showed decreased lifespan of nematodes with knockdown of proteosomal subunits (Ghazi et al, 2007). Finally, abrogation of aars-2, a predicted class II aminoacyl-tRNA synthetase that catalyses the attachment of alanine to its cognate tRNA, significantly extended longevity of N2 nematodes by ~10% (Figure 3A; Supplementary Table IV). Together, these findings indicate that downregulation of many proteins involved in mRNA processing, protein translation, and protein breakdown significantly modify C. elegans lifespan.
Next, we determined whether the extended longevity was mediated by transcription factor daf-16/FOXO. Indeed, knockdown of all tested RNAi constructs failed to extend lifespan of the daf-16(mu86) mutants (Supplementary Table V). It was also discovered that the long lifespan of daf-2(e1370) could not be further extended by knockdown of rpl-17 and rpl-28. These observations suggest that the daf-16-dependent longevity pathway activity in daf-2(e1370) mutants overlaps with the longevity signalling induced by knockdown of the rpl-17 and rpl-28 ribosomal proteins.
The strong daf-2(e1370) mutant has previously been described to show reduced fecundity at 25°C, independently from its effects on longevity (Gems et al, 1998). Nematodes for the proteomics experiments were harvested as young adults, before presence of progeny (oocytes and eggs) production. Nevertheless, we found a number of proteins significantly downregulated in the daf-2(e1370) mutant for which the expression is either localized or enriched to the germline, including PGL-1, CGH-1,
PAB-1, CAR-1, and CEY-4 (Table I). Several of these proteins were found to mediate lifespan upon RNAi knockdown (Supplementary Table IV). These findings suggest that at least part of the longevity phenotype of the daf-2(e1370) is mediated by reduced germline activity. We therefore performed brood size experiments to determine whether the reduced protein metabolism phenotype is an epi-phenomenon of the reduced fecundity. The reduced fecundity phenotype of

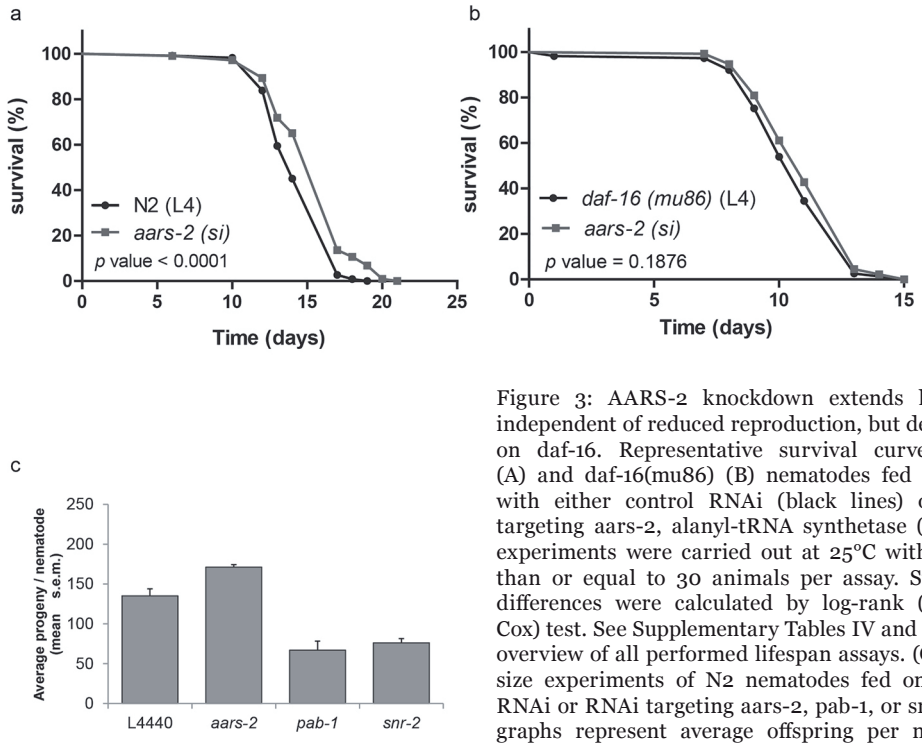

Figure 3: AARS-2 knockdown extends longevity independent of reduced reproduction, but dependent on daf-16. Representative survival curve of N2 (A) and daf-16(mu86) (B) nematodes fed from L4 with either control RNAi (black lines) or RNAi targeting aars-2, alanyl-tRNA synthetase (red). All experiments were carried out at 25°C with greater than or equal to 30 animals per assay. Statistical differences were calculated by log-rank (Mantel–Cox) test. See Supplementary Tables IV and V for the overview of all performed lifespan assays. (C) Brood size experiments of N2 nematodes fed on control RNAi or RNAi targeting aars-2, pab-1, or snr-2. Bar graphs represent average offspring per nematode and greater than or equal to 14 per condition. See Supplementary Table VI for more detail.

the daf-2(e1370) mutant was partially dependent on daf-16 as shown by the significant recovery of brood size in the daf-16(mu86); daf-2(e1370) double mutant (Supplementary Figure S9; Supplementary Table VI). Knockdown of both SNR-2 and PAB-1 expression significantly reduced fecundity in the N2 (Figure 3C), in agreement with the strong expression of both proteins in the germline. In contrast, fecundity was unaffected upon siRNA-mediated knockdown of aars-2 which is predominantly expressed in the nematode intestine and hypodermis. As RNAi-mediated knockdown of aars-2 extends longevity (Supplementary Table IV), this result suggests that longevity and reproduction can be uncoupled at the level of protein metabolism regulation.

Next, polyribosome analysis was performed in the daf-2(e1370) mutant propagated at 15 and 20°C when a longevity phenotype is observed either in the absence (15°C) or with a small (20°C) reproductive effect (Gems et al, 1998); (Kenyon et al, 1993). A reduction in active protein translation was found (Supplementary Figure S10), although the magnitude of the reduction tracks with the severity of the reproductive phenotype.
These observations do not fully exclude the possibility that the germline is involved in mediating the observed daf-16-dependent protein metabolism phenotype. To investigate this possibility, polyribosome profiling experiments were performed in germline-ablated nematodes. To this end, daf-2(e1370) and N2 nematodes were fed siRNA against GLP-1, a germline-specific GLP-/Notch receptor (Arantes-Oliveira et al, 2002). Interestingly, polyribosome profiles of N2 nematodes did not markedly differ upon abrogation of GLP-1 (Figure 4A), a condition that has been reported to induce lifespan extension (Arantes-Oliveira et al, 2002). Despite the fact that global protein translation of the daf-2(e1370) mutant was strongly reduced compared with N2 nematodes

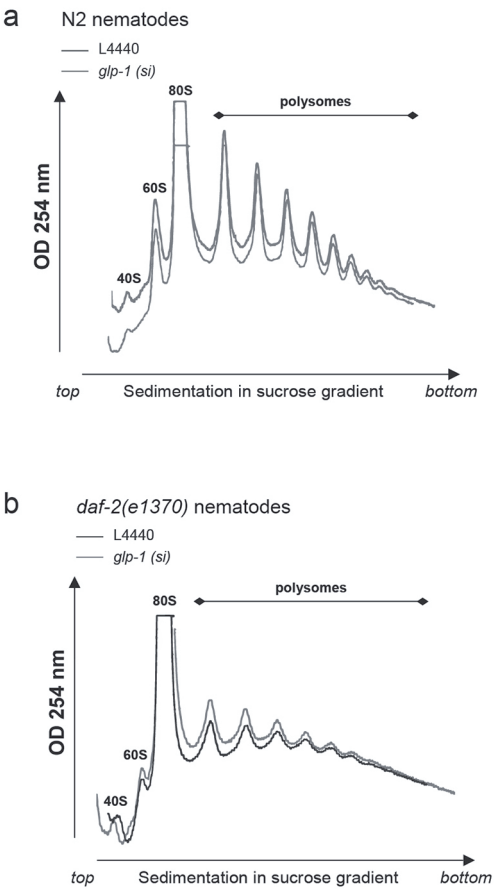

Figure 4: Germline ablation does not affect active protein translation. Representative traces of polyribosome profiles obtained from (A) N2 nematodes and (B) daf-2(e1370) mutants fed on control (black line) or glp-1 siRNA (green line). Nematodes were synchronized, cultured on glp-1 siRNA from L1 stage, switched to 25°C from L4 and harvested at day 1 of adulthood. Observed minor differences in profiles reflect experimental variation.

(Figures 2A and 4), polyribosome profiles of germline ablated and control daf-2(e1370) mutants did not markedly differ (Figure 4B). Together, these findings indicate that the observed global changes in protein translation in Insulin/IGF-1 signalling are unlikely to result from reduced reproduction or germline activity.

In summary, these observations provide evidence of a causal role for altered protein metabolism in Insulin/IGF-1-mediated longevity, and additionally suggest that protein metabolism, rather than protein translation alone, governs Insulin/IGF-1-mediated longevity assurance.

4

Discussion

Insulin/IGF-1-mediated longevity is associated with altered protein metabolism

The performed unbiased quantitative proteomics study of Insulin/IGF-1 signalling pathway mutants revealed that Insulin/IGF-1-mediated longevity is strongly associated with a global reduction in protein metabolism at the levels of mRNA processing, protein translation, and protein breakdown (Figures 1 and 2; Table I; Supplementary Figure S5; Supplementary Tables I–III). Moreover, reduced expression of multiple proteins (through RNAi) involved in these processes extended C. elegans lifespan in a daf-16-dependent manner (Figure 3; Supplementary Tables IV and V), indicating that these proteins contribute to Insulin/IGF-1-mediated longevity.

An initial proteomics study on the C. elegans Insulin/IGF-1 pathway revealed comparable results to our study (Supplementary Figure S6), however, failed to identify the massive reduction in ribosomal proteins reported here (Dong et al, 2007). The experiment described by Dong et al was restricted to a subset of the nematode proteome, involving mainly cytoplasmic and non-membrane bound proteins (S-100 fraction), thereby likely missing the ribosomal protein fraction bound to the ER or localized in the nucleolus.

A role for protein translation in Insulin/IGF-1-mediated lifespan regulation has not been demonstrated to date. This is underscored by the fact that de novo incorporation of labelled

methionine in daf-2(e1370) and wild-type nematodes did not differ, thus arguing against a role for decreased protein translation in Insulin/IGF-1-mediated longevity (Hansen et al, 2007). However, as recognized by Hansen et al, a possible contribution from protein degradation to their phenotype could not be ruled out due to the absence of a kinetic analysis. As a result, the authors reported a balance between protein synthesis and breakdown rather than active protein translation alone (Hansen et al, 2007). The observations from direct assays as reported here (Figure 2), e.g. lower abundance of core 20S proteasome subunits and decreased proteasomal activity, concomitant with strongly decreased protein translation in daf-2(e1370) mutants, resolves this apparent paradox, particularly since equal total protein levels were observed in all tested strains. Thus, the daf-2(e1370)-mediated longevity phenotype involves both reduced protein translation and proteasomal degradation.

We propose that reduced protein translation in the Insulin/IGF-1 pathway leads to less protein misfolding, protein aggregation, and subsequent ER stress. We envisage that, in turn, the demand for proteasomal breakdown is reduced resulting in high fidelity protein homeostasis. In support of this hypothesis, daf-2(e1370) mutants indeed show lower 20S activity (Figure 2E) and moreover, two recent quantitative proteomics analysis of insoluble proteins that gradually accumulate during normal ageing revealed an age-related decline in protein homeostasis (David et al, 2010; Reis-Rodrigues et al, 2012). It has additionally been established that increased ER stress and protein aggregation strongly reduce longevity, processes which depend on Insulin/IGF-1 signalling (Henis-Korenblit et al, 2010; Taylor and Dillin, 2011; Reis-Rodrigues et al, 2012). Therefore, we propose that preservation of total protein levels in daf-2(e1370) mutants, despite reduction in total mRNA and translational activity, is due to the previously established increase in autophagy activity (Melendez et al, 2003; Hansen et al, 2008) coupled to our novel results demonstrating abatement of protein degradation.

Reproduction and Insulin/IGF-1-mediated longevity

The daf-2(e1370) proteome also disclosed an altered abundance of several proteins involved in reproduction (Supplementary Figure S5; Table I; Supplementary Tables II and III), including proteins like CGH-1, PGL-1, CAR-1, PAB-1, and SNR-2, which all show expression specific to or enriched in the germline (Squirrell et al, 2006; Parker and Sheth, 2007; Buchan and Parker, 2009; Sonenberg and Hinnebusch, 2009; Updike and Strome, 2010). This observation is in line with the delayed reproduction and reduced fertility phenotype displayed by the daf-2(e1370) mutant at the non-permissive conditions used in our proteomics study, in addition to its longevity phenotype (Gems et al, 1998). Interestingly, RNAi-mediated knockdown of several of these proteins enhanced longevity (Supplementary Tables IV and V). These results therefore suggest that the longevity phenotype of daf-2(e1370) mutants at the non-permissive temperature can be at least partially explained by reduced germline function, as germline ablation extends C. elegans lifespan (Arantes-Oliveira et al, 2002). This notion raises the question as to whether the reduced protein metabolism phenotype could be a mere epi-phenomenon of the reduced fecundity reported for the daf-2(e1370) mutant (Gems et al, 1998; Supplementary Figure 9). However, several lines of evidence indicate that the observed longevity effects mediated by reduced protein metabolism activity are distinct from effects on the germline. First, abrogation of ribosomal proteins did not further extend the lifespan of daf-2(e1370) mutants (Supplementary Table V), consistent with previous work from the Kenyon laboratory (Hansen et al, 2007), whereas germline ablation does extend the lifespan of daf-2(e1370) nematodes (Arantes-Oliveira et al, 2002). Second, knockdown of the predominantly somatically expressed aars-2 extended the longevity in the absence of a reproduction phenotype (Figure 3; Supplementary Tables IV and VI). Finally, while germline ablation extends longevity (Arantes-Oliveira et al, 2002), this occurs independently of changes in

global protein translation (Figure 4).
Altogether, these findings argue that the protein metabolism phenotype identified in Insulin/IGF-1 signalling stems predominantly from somatic tissue. Interestingly, this is consistent with the observation that the germline is not required for lifespan extension of the eukaryotic soma-specific IFE-2 isoform of mRNA translation initiation factor 4E (Syntichaki et al, 2007). Of note, germline signalling has been genetically linked to a putative translation elongation factor (Ghazi et al, 2009) and it therefore remains possible that germline ablation-mediated longevity signals through specific changes in protein metabolism that occur below the detection limits of our polysome profiling assay.

Regulation of reduced protein metabolism in Insulin/IGF-1-mediated longevity

The concordance between our results and previous microarray studies (McElwee et al, 2003; Murphy et al, 2003) suggests good correlation between gene and protein expression of relevant genes (Supplementary Figure S6). Of note, a conspicuous absence of correlation with respect to regulation of protein translation genes was noticed, particularly regarding ribosomal proteins even when specifically queried (McElwee et al, 2003). Our data indicated that the reduced abundance of ribosome proteins was at least partially dependent on daf-16 (Supplementary Tables II and III), but ribosomal protein genes have not been identified as direct DAF-16 targets (Oh et al, 2006). These findings suggest longevity to be regulated at the post-transcriptional/translational level rather than exclusive regulation of gene expression. TOR signalling, which was recently identified to relay its effect on longevity through SKN-1/Nrf and DAF-16/FOXO, is an attractive candidate pathway to mediate such regulation given its conserved role in protein translation control and longevity regulation across species, including C. elegans (Kapahi et al, 2010; McCormick et al, 2011; Robida-Stubbs et al, 2012). This hypothesis is supported by the observation that lifespan of daf-2(e1370) mutants is not further extended by knockdown of the C. elegans TOR orthologue, let-363, suggesting overlapping signalling pathways (Vellai et al, 2003).
TOR mediates protein homeostasis via regulation of mRNA translation initiation, as well as ribosome biogenesis. Interestingly, several proteins involved in translation initiation (e.g., EIF-3.C, EIF-6, PAB-1, and INF-1), as well as ribosomal biogenesis have been identified as significantly reduced in the daf-2(e1370) proteome (Table I; Supplementary Tables II and III). Therefore, reduced TOR signalling could explain the observed reduced protein translation in daf-2(e1370) nematodes, although several reported observations are inconsistent with such a model. For instance, in higher organisms TOR and Insulin/IGF-1 signalling are linked through the tuberous sclerosis proteins TSC1/2, thereby regulating processes like protein synthesis for cell growth. However, no orthologues of these proteins have thus far been identified in C. elegans and reduced Insulin/IGF-1 signalling in C. elegans does not change cell size (Finch and Ruvkun, 2001). Moreover, let-363 RNAi decreased 35S-Methionine incorporation in N2 nematodes in line with reduced protein translation, whereas the daf-2(e1370) mutant did not (Hansen et al, 2007), suggesting that alternative or additional mechanisms are involved. In contrast to TSC1/2, the GTPase RHEB-1 is conserved in C. elegans and bridges the GTPase activating protein (GAP) activity of the TSC1/2 complex to TOR activity in multiple organisms (Aspuria and Tamanoi, 2004). Although a role for RHEB-1 in protein translation has not been demonstrated directly in C. elegans, RHEB-1 has been shown to mediate longevity induced by intermitted fasting (IF) in a daf-16-dependent manner. Interestingly, this supports the concept of molecular coupling between the IF-induced longevity and the Insulin/IGF-like signalling pathway (Honjoh et al, 2009).

A translation initiation factor (Syntichaki et al, 2007) and several ribosomal proteins have recently been described to extend longevity in a daf-16-independent manner (Hansen et al, 2007).

In contrast, other proteins involved in protein synthesis have recently been shown to mediate longevity through daf-16 signalling (Henderson et al, 2006; Hansen et al, 2007; Tohyama et al, 2008). The latter is in agreement with our observations revealing that the expression, translation, and function of all tested proteins involved in protein metabolism mediate longevity in a daf-16-dependent manner (Figure 1B; Table I; Supplementary Table V). This apparent paradox may be explained by several recent observations, which indicate that daf-16 signalling is complex. For instance, the extent of DAF-16 knockdown may be important, since most downregulated proteins involved in Insulin/IGF-1 protein metabolism are only partially suppressed by daf-16 (Table I). Moreover, knockdown of translation elongation initiation factors eIF-4G and eiF2b extends longevity in a daf-16-dependent manner when expression is suppressed in adulthood, and independent of daf-16 when suppressed during development (Henderson et al, 2006), suggesting that the timing of daf-16 suppression is important. Lastly, additional proteins or modifications could be involved in regulating the daf-16 dependency. Indeed, although let-363 knockdown was shown to mediate longevity in a daf-16-independent manner (Vellai et al, 2003), closer inspection of the TOR complexes TORC1 and TORC2 recently revealed that reduced TORC1 activity extends longevity in a daf-16-dependent manner (Robida-Stubbs et al, 2012). Future biochemical and genetic analysis will be required to characterize how Insulin/IGF-1 signalling is coupled to protein metabolism in C. elegans.

Protein translation as a common longevity assurance mechanism

Insulin/IGF-1- and DR-mediated longevity have long been considered as distinct processes (Lakowski and Hekimi, 1998; Houthoofd et al, 2003; Min et al, 2008), however, others have recently suggested that Insulin/IGF-1- and DR-mediated longevity may share mechanistic features (Clancy et al, 2002; Greer et al, 2007; Narasimhan et al, 2009; Kenyon, 2010). The work presented here is in strong support of the latter model, and moreover extends this parallel between Insulin/IGF-1- and DR-mediated longevity since DR-mediated longevity was recently shown to also depend on decreased protein translation in D. melanogaster (Zid et al, 2009) and S. cerevisiae (Kapahi et al, 2010; McCormick et al, 2011). In fact, reduced expression of proteins involved in translation has been shown to extend longevity in a range of animals, including S. cerevisiae (both chronological and replicative models), D. melanogaster, and C. elegans (McCormick et al, 2011). Moreover, knockdown of the mTOR-responsive S6K and rapamycin administration (both known to inhibit protein translation) extended longevity in mice (Harrison et al, 2009; Selman et al, 2009). Also as previously mentioned, longevity mediated by germline signalling was genetically linked to a putative translation elongation factor (Ghazi et al, 2009). Together with our findings, we propose that protein homeostasis provides a common denominator in longevity assurance. In support of this hypothesis, a genome-wide linkage analysis performed on a cohort of human individuals with exceptional longevity identified a locus on chromosome 4 that exerts substantial influence on the ability to achieve exceptional old age (Puca et al, 2001). Interestingly, the human orthologue of RPL34 directly flanks this locus. Our proteomics study reveals that abundance of rpL34 is decreased in daf-2(e1370) mutants (Table I; Supplementary Table II), while abrogation of rpl-34 was found to contribute to C. elegans longevity (Hansen et al, 2007). It is therefore attractive to speculate that human longevity assurance may also be orchestrated through the fundamental regulation of protein translation.

Concluding remarks

This study demonstrates that Insulin/IGF-1-mediated longevity assurance is directly linked to decreased protein translation, which draws a parallel to DR-mediated longevity and suggests that these longevity mechanisms share mechanistic features. Additionally, reduced mRNA processing and protein degradation is shown to contribute to an overall decreased protein metabolism phenotype and Insulin/IGF-1-mediated longevity. These findings support a role for decreased protein translation in Insulin/IGF-1-mediated longevity and potentially as a common longevity assurance mechanism.

Materials and methods

Nematode growing and conditions

Strains

All strains were maintained expanded as described previously (Brenner, 1974). N2, daf-2(e1370), daf-16(mu86), and daf-16(mu86):daf-2(e1370) were obtained from the Caenorhabditis Genetics Center (CGC). Nematodes were propagated on 150 mm NGM OP50 plates at 15–20°C.

RNAi clone analysis

All RNAi containing bacteria (HT115) clones, except for the daf-2 and cgh-1 siRNA which were kind gifts of Dr D Gems (University College, London, UK) and Dr TK Blackwell (Harvard Medical School, Boston, USA) respectively, were purified from Ahringer's or Vidal libraries (Kamath et al, 2003; Rual et al, 2004). The identity of all RNAi clones was verified by sequencing. Clones were grown overnight at 37°C in LB containing 100 µg/ml ampicillin before seeding.

Germline ablation

Synchronized L1 nematodes were plated on vector control or glp-1 RNAi-containing HT115 bacteria plates, incubated at 15°C until the worms reached L4 stage, then temperature shifted to 25°C for 16–20 h, harvested and subsequently snap frozen for polysome profiling. Ablation of the germline of adult nematodes was confirmed by Nomarsky microscopy before the nematodes were harvested.

Lifespan analysis

Lifespan analysis was performed as described previously (Hansen et al, 2005) and conducted at 25°C. In brief, strains were synchronized by hypochlorite treatment and isolated eggs were grown on 150 mm NGM OP50 plates at 20°C until late L3/early L4 stage. Of note, the development of obtained synchronized N2, daf-16(mu86);daf-2(e1370), and daf-16(mu86) eggs/larvae was delayed by placing them 16–20 h at 15°C to compensate for the slight delayed development of the daf-2(e1370) nematodes (Hirsh et al, 1976; Gems et al, 1998). In all, 10–12 nematodes in L4 or young adult (YA) stage were picked and passed onto 10–12 35 mm NGM plates inoculated with the gene-specific RNAi bacteria (HT115) of interest, pre-cultured as described above. After picking, the nematodes were switched to 25°C for lifespan evaluation. The pre-fertile period of adulthood was chosen as T=0 for lifespan analysis. Strains were grown at optimal growth conditions (20°C) for at least two generations before lifespan analysis was started. The NGM plates used for lifespan were supplemented with 100 µg/ml ampicillin, 40 µM IPTG, and 200 µg/ml 2′fluoro-5′deoxyuridine (FUDR) (all obtained from Sigma, St Louis, MO, USA) to induce siRNA expression

and to restrict progeny development during the lifespan assay, respectively. Nematodes were counted daily until all nematodes were deceased. An animal was scored dead responded to (mechanical) probing/stimulation. Blind scoring was followed for all experiments. Censoring in the lifespan analysis included animals that ruptured, bagged (i.e., exhibited internal progeny hatching), or crawled off the plates. Statistical significance was calculated using the log-rank (Mantel-Cox) method.

Brood size experiments

Brood size experiments were performed essentially as described previously (Gems et al, 1998). Synchronized eggs were incubated at 15°C until worm reach L4 stage, than placed on fresh plates individually and temperature shifted to 25°C. For the RNAi experiments, nematodes in L4 stage were placed NGM RNAi-containing HT115 bacteria plates, which targeted indicated RNAi constructs. The nematodes were transferred to fresh plates twice a day, and the average number of progeny was scored in a blind manner. Statistical significance was calculated using Student's t-test with Welch correction.

Quantitative proteomics

Peptide generation

Nematodes of all three strains were age synchronized as described. In brief, eggs were collected after hypochlorite treatment and propagated until L4 larval stage at 20°C, except for N2 and daf-2(e1370); daf-16(mu86) which were placed for 16–20 h at 15°C to compensate for the reported delayed growth phenotype of daf-2(e1370) as described (Hirsh et al, 1976; Gems et al, 1998). At early L4 larval stage, all three strains were shifted to 25°C for 16–20 h. After visual confirmation of absence of the oocytes, eggs, and progeny by Nomarsky microscopy the nematodes were harvested.

Nematode pellets (about 12 000 day 1 adults per biological replicate) were homogenized and the proteins were extracted in protein extraction buffer (8 M Urea, HALT protease and HALT phosphatase inhibitors (Thermo) with a BulletBlender, using 0.5 mm Zirconium Oxide beads (NextAdvance) for 3 min. After 10 min on ice, extracts were centrifuged and protein concentrations were determined using Nanodrop (Thermo) technology at OD280. Equal amounts of protein (100 µg) were reduced by Tris(2-carboxyethyl)-phosphine hydrochloride for 1 h at 55°C, alkylated by iodoacetamide for 30 min at RT in dark conditions, diluted and digested o/n with trypsin (Thermo). Next, peptides mixtures were labelled with TMT labelling 6-plex kit (Thermo) according to manufacturer's instructions, merged in equal quantities and dried in a vacuum centrifuge.

Liquid chromatography and MS analysis

Complexity of peptide mixture was reduced by Strong Cation Exchange (SCX) chromatography on an Accela HPLC system (Thermo) coupled to a 2996 Photodiode Array Detector (Waters) using a PolySulfethyl A SCX column (100 mm × 2.1 mm i.d., 5 µm, 300 Å, PolyLC, Columbia, MD) over a 25-min linear gradient from 0 to40% B at a constant flow rate of 200 µl/min (Buffer A=5 mM KH2PO4, 30% acetonitrile and 0.05% formic acid, Buffer B=Buffer A supplemented with 350 mM KCl). A total of 33 fractions were collected off-line every minute. The collected samples were dried in a vacuum centrifuge and dissolved in 20 µl 5% FA. Next, samples were subjected to nano-flow LC (Eksigent) using a C18 reverse phase trap column (Phenomenex; column dimensions 2 cm × 100 µm, packed in-house) and subsequently separated on C18 analytical columns (Reprosil-Pur C18-AQ 5µm; column dimensions, 20 cm × 50 µm; packed in-house) using a linear gradient from 0

to 40% B (Buffer A=0.1 M acetic acid; Buffer B=95% (v/v) acetonitrile with 0.1 M acetic acid) in 60 min and at a constant flow rate of 150 nl/min. Column eluate was analysed directly in a coupled LTQ-Orbitrap-XL mass spectrometer (Thermo Fisher Scientific) operating in positive mode, using internal Lock mass calibration. For optimal identification and quantification, samples were run in both CID and HCD fragmentation mode.

Data analysis and quantification

All 66 data sets (33 fractions analysed in CID and HCD mode) from 6-plex experiment were merged, processed, and quantified using Proteome Discoverer (Thermo) software and subjected to database searches (Mascot, version 2.3.01, Matrixscience) against a C. elegans database (Wormprep 2.12: www.wormbase.org). For the database search, up to two missed trypsin cleavages were allowed with a 10-p.p.m. precursor mass tolerance and 0.8 Da for the fragment ion. Cysteine carbamidomethylation was set as a fixed modification and oxidation of Methionine and TMT labelling on Lysine and NH2 terminus was set as variable modifications. Assembly of individual peptides into proteins follows 5% FDR as peptide confidence threshold and require at least one unique peptide. The vast majority of peptides were identified multiple times in sequential SCX fractions. Relative protein quantification was performed using Proteome Discoverer software (version 1.2.0.208) according to manufacturer's instructions on either the two or six reporter ion intensities per peptide. Redundant peptides, peptides lacking >2 mass tag values or ratios were all excluded.

The MS data used for this publication have been submitted Peptide Atlas (http://www.peptideatlas.org/PASS/PAS00192) and assigned the identifier (PASS00192).

Bioinformatics analysis

Over/under-representation analysis (ORA) and GSEA were performed using web-based tool GeneTrail (Backes et al, 2007). Significance (cutoff $P<0.05$) was determined by a hypergeometric distribution test using all C. elegans genes as background with a 5% FDR multiple testing correction. Genes with a 1.3-fold change in daf-2(e1370) mutants relative to wild type were included in the analysis. The results of the ORA were subsequently confirmed by GSEA, a method that is independent of any fold change cutoff. We refer to Supplementary Tables I–III for full overview of ORA and GSEA results.

Polyribosome profiling

Gradients of 17–50% sucrose (11 ml) in gradient buffer (110 mM KAc, 20 mM MgAc2 and 10 mM HEPES pH 7.6) were prepared on the day before use in thin-walled, 13.2 ml, polyallomer 14 × 89 mm centrifuge tubes (Beckman-Coulter, USA). Nematodes were lysed in 500 µl polysome lysis buffer (gradient buffer containing 100 mM KCl, 10 mM MgCl2, 0.1% NP-40, 2 mM DTT and 40 U/ml RNasin; Promega, Leiden, Netherlands) using a dounce homogenizer. The samples were centrifuged at 1200 g for 10 min to remove debris and the supernatant was subjected to protein content analysis by Bradford reagent (Biorad). In all, 610 µg of total protein for each sample was loaded atop the sucrose gradients. The gradients were ultra-centrifuged for 2 h at 40 000 r.p.m. in a SW41Ti rotor (Beckman-Coulter, USA). The gradients were displaced into a UA6 absorbance reader (Teledyne ISCO, USA) using a syringe pump (Brandel, USA) containing 60% sucrose. Absorbance was recorded at an OD of 254 nm. All steps of this assay were performed at 4°C or on ice and all chemicals came from Sigma-Aldrich (St Louis, MO, USA) unless stated otherwise.

Western blotting

Proteins were extracted from nematode pellets and the protein concentration was measured, as described before. In all, 40–200 µg of protein was separated on SDS–PAGE and transferred onto polyvinylidene difluoride membrane (PVDF) membrane (Immobilon; Millipore, Billerica, MA). Western blot analysis was performed in duplicate under standard conditions (1/500 in 2.5% milk/2.5% BSA) using the indicated antibodies. For quantification of protein levels, membranes were probed with HRP-conjugated secondary antibodies (1/10 000 in 2.5% milk/2.5% BSA). Immunocomplexes were detected using enhanced chemiluminescence (ECL-Plus GE Healthcare) and ImageQuant™ LAS 4000 bimolecular imager with provided software according to the manufacturer (GE Healthcare Europe, Diegem, Belgium).

Antibodies

Polyclonal antibodies raised against proteasome 20 α-subunits (ab22674), ribosomal protein L22 (sc-98857) and L28 (sc14151) and Lasu1/Ureb1 (A300-486A) were purchased from Abcam (3) (Cambridge, UK), Santa Cruz Biotechnology (2) (Santa Cruz, CA, USA), and Bethyl Laboratories (1) (Montgomery, TX, USA), respectively. Rabbit polyclonal antibody recognizing actin (20–33) was obtained from Sigma-Aldrich.

mRNA extraction

mRNA was extracted from 1500 young adults for each strain using Dynabeads mRNA DIRECT Mini Kit (610.11, Invitrogen, Oslo, Norway) according to manufacturer's instructions in triplicate. mRNA yield was determined using Nanodrop (Thermo) technology at OD260. Student's t-test with Welch correction was used to test the null hypothesis.

20S Proteasome activity assay

Nematode pellets (1500 day 1 adults) were homogenized and the proteins were extracted under native conditions in NP-40 extraction buffer (1% Nonidet P-40; 50 mM Tris–HCl, pH 8; 150 mM NaCl; 0.1% SDS; 0.5% SDS). After 10 min on ice, extracts were centrifuged and the protein concentrations were determined using Nanodrop technology at OD280. 20S proteasome activity was determined in triplicate using the 20S proteasome activity Assay Kit according to manufacturer's instructions (Chemicon International, Inc.). The assay is based on detection of the fluorophore 7-Amino-4-methylcoumarin (AMC) after proteasomal cleavage from the labelled substrate LLVY-AMC. After 2 h of incubation at 37°C, the free AMC fluorescence, a measure for proteasomal activity, was quantified using fluorometer equipped with 380/450 nm filter sets. Statistical significance was calculated with Student's t-test with Welch correction.

Acknowledgements

The Gems and Blackwell laboratories are acknowledged for providing daf-2 and cgh-1 siRNA bacteria strains, respectively. Members of the Brenkman laboratory are acknowledged for stimulating discussions. GJS, AK, and ECAS were financed by grants from the Netherlands Metabolomics Centre which is part of the Netherlands Genomics Initiative/Netherlands Organisation for Scientific Research.

References

1. Arantes-Oliveira N, Apfeld J, Dillin A, Kenyon C (2002) Regulation of life-span by germ-line stem cells in Caenorhabditis elegans. Science 295: 502-505
2. Aspuria PJ, Tamanoi F (2004) The Rheb family of GTP-binding proteins. Cell Signal 16: 1105-1112
3. Backes C, Keller A, Kuentzer J, Kneissl B, Comtesse N, Elnakady YA, Muller R, Meese E, Lenhof HP (2007) GeneTrail--advanced gene set enrichment analysis. Nucleic Acids Res 35: W186-W192
4. Brenner S (1974) The genetics of Caenorhabditis elegans. Genetics 77: 71-94
5. Buchan JR, Parker R (2009) Eukaryotic stress granules: the ins and outs of translation. Mol Cell 36: 932-941
6. Clancy DJ, Gems D, Hafen E, Leevers SJ, Partridge L (2002) Dietary restriction in long-lived dwarf flies. Science 296: 319
7. David DC, Ollikainen N, Trinidad JC, Cary MP, Burlingame AL, Kenyon C (2010) Widespread protein aggregation as an inherent part of aging in C. elegans. PLoS Biol 8: e1000450
8. Dayon L, Hainard A, Licker V, Turck N, Kuhn K, Hochstrasser DF, Burkhard PR, Sanchez JC (2008) Relative quantification of proteins in human cerebrospinal fluids by MS/MS using 6-plex isobaric tags. Anal Chem 80: 2921-2931
9. Dillin A, Crawford DK, Kenyon C (2002) Timing requirements for insulin/IGF-1 signaling in C. elegans. Science 298: 830-834
10. Dong MQ, Venable JD, Au N, Xu T, Park SK, Cociorva D, Johnson JR, Dillin A, Yates JR 3rd (2007) Quantitative mass spectrometry identifies insulin signaling targets in C. elegans. Science 317: 660-663
11. Dunn EF, Hammell CM, Hodge CA, Cole CN (2005) Yeast poly(A)-binding protein, Pab1, and PAN, a poly(A) nuclease complex recruited by Pab1, connect mRNA biogenesis to export. Genes Dev 19: 90-103
12. Finch CE, Ruvkun G (2001) The genetics of aging. Annu Rev Genomics Hum Genet 2: 435-462
13. Finley D (2009) Recognition and processing of ubiquitin-protein conjugates by the proteasome. Annu Rev Biochem 78: 477-513
14. Gems D, Sutton AJ, Sundermeyer ML, Albert PS, King KV, Edgley ML, Larsen PL, Riddle DL (1998) Two pleiotropic classes of daf-2 mutation affect larval arrest, adult behavior, reproduction and longevity in Caenorhabditis elegans. Genetics 150: 129-155
15. Ghazi A, Henis-Korenblit S, Kenyon C (2007) Regulation of Caenorhabditis elegans lifespan by a proteasomal E3 ligase complex. PNAS 104: 5947-5952
16. Ghazi A, Henis-Korenblit S, Kenyon C (2009) A transcription elongation factor that links signals from the reproductive system to lifespan extension in Caenorhabditis elegans. PLoS Genet 5: e1000639
17. Greer EL, Dowlatshahi D, Banko MR, Villen J, Hoang K, Blanchard D, Gygi SP, Brunet A (2007) An AMPK-FOXO pathway mediates longevity induced by a novel method of dietary restriction in C. elegans. Curr Biol 17: 1646-1656
18. Hansen M, Chandra A, Mitic LL, Onken B, Driscoll M, Kenyon C (2008) A role for autophagy in the extension of lifespan by dietary restriction in C. elegans. PLoS Genet 4: e24
19. Hansen M, Hsu AL, Dillin A, Kenyon C (2005) New genes tied to endocrine, metabolic, and dietary regulation of lifespan from a Caenorhabditis elegans genomic RNAi screen. PLoS Genet 1: 119-128
20. Hansen M, Taubert S, Crawford D, Libina N, Lee SJ, Kenyon C (2007) Lifespan extension by conditions that inhibit translation in Caenorhabditis elegans. Aging Cell 6: 95-110
21. Harrison DE, Strong R, Sharp ZD, Nelson JF, Astle CM, Flurkey K, Nadon NL, Wilkinson JE, Frenkel K, Carter CS, Pahor M, Javors MA, Fernandez E, Miller RA (2009) Rapamycin fed late in life extends lifespan in genetically heterogeneous mice. Nature 460: 392-395
22. Henderson ST, Bonafe M, Johnson TE (2006) daf-16 protects the nematode Caenorhabditis elegans during food deprivation. J Gerontol A Biol Sci Med Sci 61: 444-460
23. Henis-Korenblit S, Zhang P, Hansen M, McCormick M, Lee SJ, Cary M, Kenyon C (2010) Insulin/IGF-1 signaling mutants reprogram ER stress response regulators to promote longevity. PNAS 107: 9730-9735
24. Hirsh D, Oppenheim D, Klass M (1976) Development of the reproductive system of Caenorhabditis elegans. Dev Biol 49: 200-219
25. Honjoh S, Yamamoto T, Uno M, Nishida E (2009) Signalling through RHEB-1 mediates intermittent fasting-induced longevity in C. elegans. Nature 457: 726-730
26. Houthoofd K, Braeckman BP, Johnson TE, Vanfleteren JR (2003) Life extension via dietary restriction is independent of the Ins/IGF-1 signalling pathway in Caenorhabditis elegans. Exp Gerontol 38: 947-954
27. Hsu AL, Murphy CT, Kenyon C (2003) Regulation of aging and age-related disease by DAF-16 and heat-shock factor. Science 300: 1142-1145

28. Kamath RS, Fraser AG, Dong Y, Poulin G, Durbin R, Gotta M, Kanapin A, Le Bot N, Moreno S, Sohrmann M, Welchman DP, Zipperlen P, Ahringer J (2003) Systematic functional analysis of the Caenorhabditis elegans genome using RNAi. Nature 421: 231-237
29. Kapahi P, Chen D, Rogers AN, Katewa SD, Li PW, Thomas EL, Kockel L (2010) With TOR, less is more: a key role for the conserved nutrient-sensing TOR pathway in aging. Cell Metab 11: 453-465
30. Kenyon C, Chang J, Gensch E, Rudner A, Tabtiang R (1993) A C. elegans mutant that lives twice as long as wild type. Nature 366: 461-464
31. Kenyon CJ (2010) The genetics of ageing. Nature 464: 504-512
32. Lakowski B, Hekimi S (1998) The genetics of caloric restriction in Caenorhabditis elegans. PNAS 95: 13091-13096
33. McCormick MA, Tsai SY, Kennedy BK (2011) TOR and ageing: a complex pathway for a complex process. Philos Trans R Soc Lond B Biol Sci 366: 17-27
34. McCulloch D, Gems D (2003) Body size, insulin/IGF signaling and aging in the nematode Caenorhabditis elegans. Exp Gerontol 38: 129-136
35. McElwee J, Bubb K, Thomas JH (2003) Transcriptional outputs of the Caenorhabditis elegans forkhead protein DAF-16. Aging cell 2: 111-121
36. Melendez A, Talloczy Z, Seaman M, Eskelinen EL, Hall DH, Levine B (2003) Autophagy genes are essential for dauer development and life-span extension in C. elegans. Science 301: 1387-1391
37. Min KJ, Yamamoto R, Buch S, Pankratz M, Tatar M (2008) Drosophila lifespan control by dietary restriction independent of insulin-like signaling. Aging Cell 7: 199-206
38. Murphy CT, McCarroll SA, Bargmann CI, Fraser A, Kamath RS, Ahringer J, Li H, Kenyon C (2003) Genes that act downstream of DAF-16 to influence the lifespan of Caenorhabditis elegans. Nature 424: 277-283
39. Narasimhan SD, Yen K, Tissenbaum HA (2009) Converging pathways in lifespan regulation. Curr Biol 19: R657-R666
40. Noble SL, Allen BL, Goh LK, Nordick K, Evans TC (2008) Maternal mRNAs are regulated by diverse P body-related mRNP granules during early Caenorhabditis elegans development. J Cell Biol 182: 559-572
41. Oh SW, Mukhopadhyay A, Dixit BL, Raha T, Green MR, Tissenbaum HA (2006) Identification of direct DAF-16 targets controlling longevity, metabolism and diapause by chromatin immunoprecipitation. Nat Genet 38: 251-257
42. Parker R, Sheth U (2007) P bodies and the control of mRNA translation and degradation. Mol Cell 25: 635-646
43. Pereboom TC, van Weele LJ, Bondt A, MacInnes AW (2011) A zebrafish model of dyskeratosis congenita reveals hematopoietic stem cell formation failure resulting from ribosomal protein-mediated p53 stabilization. Blood 118: 5458-5465
44. Puca AA, Daly MJ, Brewster SJ, Matise TC, Barrett J, Shea-Drinkwater M, Kang S, Joyce E, Nicoli J, Benson E, Kunkel LM, Perls T (2001) A genome-wide scan for linkage to human exceptional longevity identifies a locus on chromosome 4. PNAS 98: 10505-10508
45. Reis-Rodrigues P, Czerwieniec G, Peters TW, Evani US, Alavez S, Gaman EA, Vantipalli M, Mooney SD, Gibson BW, Lithgow GJ, Hughes RE (2012) Proteomic analysis of age-dependent changes in protein solubility identifies genes that modulate lifespan. Aging Cell 11: 120-127
46. Robida-Stubbs S, Glover-Cutter K, Lamming DW, Mizunuma M, Narasimhan SD, Neumann-Haefelin E, Sabatini DM, Blackwell TK (2012) TOR signaling and rapamycin influence longevity by regulating SKN-1/Nrf and DAF-16/FoxO. Cell Metab 15: 713-724
47. Rual JF, Ceron J, Koreth J, Hao T, Nicot AS, Hirozane-Kishikawa T, Vandenhaute J, Orkin SH, Hill DE, van den Heuvel S, Vidal M (2004) Toward improving Caenorhabditis elegans phenome mapping with an ORFeome-based RNAi library. Genome Res 14: 2162-2168
48. Selman C, Tullet JM, Wieser D, Irvine E, Lingard SJ, Choudhury AI, Claret M, Al-Qassab H, Carmignac D, Ramadani F, Woods A, Robinson IC, Schuster E, Batterham RL, Kozma SC, Thomas G, Carling D, Okkenhaug K, Thornton JM, Partridge L et al (2009) Ribosomal protein S6 kinase 1 signaling regulates mammalian life span. Science 326: 140-144
49. Sonenberg N, Hinnebusch AG (2009) Regulation of translation initiation in eukaryotes: mechanisms and biological targets. Cell 136: 731-745
50. Squirrell JM, Eggers ZT, Luedke N, Saari B, Grimson A, Lyons GE, Anderson P, White JG (2006) CAR-1, a protein that localizes with the mRNA decapping component DCAP-1, is required for cytokinesis and ER organization in Caenorhabditis elegans embryos. Mol Biol Cell 17: 336-344
51. Stanfel MN, Shamieh LS, Kaeberlein M, Kennedy BK (2009) The TOR pathway comes of age. Biochim Biophys Acta 1790: 1067-1074
52. Syntichaki P, Troulinaki K, Tavernarakis N (2007) eIF4E function in somatic cells modulates ageing in Caenorhabditis elegans. Nature 445: 922-926

53. Taylor RC, Dillin A (2011) Aging as an event of proteostasis collapse. Cold Spring Harb Perspect Biol 3: pii: a004440
54. Tohyama D, Yamaguchi A, Yamashita T (2008) Inhibition of a eukaryotic initiation factor (eIF2Bdelta/F11A3.2) during adulthood extends lifespan in Caenorhabditis elegans. FASEB J 22: 4327-4337
55. Tullet JM, Hertweck M, An JH, Baker J, Hwang JY, Liu S, Oliveira RP, Baumeister R, Blackwell TK (2008) Direct inhibition of the longevity-promoting factor SKN-1 by insulin-like signaling in C. elegans. Cell 132: 1025-1038
56. Updike D, Strome S (2010) P granule assembly and function in Caenorhabditis elegans germ cells. J Androl 31: 53-60
57. Vellai T, Takacs-Vellai K, Zhang Y, Kovacs AL, Orosz L, Muller F (2003) Genetics: influence of TOR kinase on lifespan in C. elegans. Nature 426: 620
58. Wolff S, Dillin A (2006) The trifecta of aging in Caenorhabditis elegans. Exp Gerontol 41: 894903
59. Zid BM, Rogers AN, Katewa SD, Vargas MA, Kolipinski MC, Lu TA, Benzer S, Kapahi P (2009) 4E-BP extends lifespan upon dietary restriction by enhancing mitochondrial activity in Drosophila. Cell 139: 149-160

5

Sequence analysis of monosome and polysome associated RNAs in the long-lived daf-2 mutant reveals a ncRNA required for lifespan extension

Paul B Essers, Rob Jelier, Yvonne J Goos, Britt Mossink, Marjon Viester, Arjan B Brenkman, Alyson W MacInnes

Manucript in preparation

Abstract

Our recent discovery that translation is heavily downregulated in the *C.elegans daf-2* insulin/insulin-like growth factor pathway mutant suggests that this pathway of lifespan extension has more in common with the dietary restriction pathway of lifespan extension than previously thought. Despite a global decrease in translation, a subset of mRNAs was shown to be translated with higher efficiency in dietary restricted flies. To investigate if such a mechanism also exists in *daf-2* mutants, we sequenced RNA from monosomes, which are translationally largely inactive, and polysomes, which have high translation efficiency. We found that many RNAs are differentially associated with either the monosome or the polysome. In the *daf-2* mutant, RNAs associated with processes known to be activated in lifespan extension (aging and respiration) are more enriched in the polysome. Likewise, RNAs associated with processes that are known to be downregulated (genitalia development and cell cycle progression) are less enriched in polysomal fractions compared to wild type nematodes. In addition to mRNAs we found many ncRNAs to be associated with either the monosome or the polysome or both. Transcribed telomere sequence 1 (*tts-1*) is such a ncRNA which is associated with both monosomes and polysomes in *daf-2* mutants. We show that *tts-1* inhibits translation efficiency and that it is partially required for *daf-2* mediated lifespan extension, making this to our knowledge the first polysomal-associated ncRNA to be associated with lifespan extension.

Introduction

Rather than being a gradual physical decline, aging in eukaryotes is regulated by environmental and genetic factors which are shared among species, suggesting common mechanisms to control lifespan. In the nematode *C.elegans*, deletion of a single gene, the Insulin/Insulin Growth Factor Receptor homolog *daf-2*, can increase lifespan two- to threefold [1]. The Insulin/IGF-1 pathway is highly conserved and regulates lifespan in organisms ranging from invertebrates to mammals [2]. Interestingly, genetic epistasis analysis has revealed that Insulin/IGF-1 mediated lifespan extension is completely dependent on the function of a number of transcription factors, including the Forkhead transcription factor DAF-16 [1], the heat-shock factor HSF-1 [3], and partially on the Nrf-like xenobiotic response factor SKN-1 [4]. All these transcription factors activate pathways involved in response to a broad spectrum of stresses, including oxidative damage, heat shock and infection [5,6]. In addition, inhibition of Insulin/IGF-1 signaling induces high levels of autophagy, without which lifespan extension cannot occur [7].

A large scale proteomics study in the *daf-2* mutant recently revealed a large reduction in the levels of many components of the protein synthesis machinery and the proteasome, which was largely dependent on DAF-16 signaling [8]. In contrast to previous reports [9], *daf-2* mutants showed a strong decrease of translational activity, similar to that observed in the *eat-2* mutant, a genetic model for dietary restriction (DR) [9]. These findings indicated that *daf-2* and DR mediated lifespan extension have more in common than previously believed. In addition to leading to a global decrease of translation, it was previously shown that DR results in the preferential translation of certain mRNAs [10], a phenomenon that has been shown to occur most often in situations of stress [11].

In order to determine if preferential loading of mRNAs onto polysomes occurs in *daf-2* mutants, we used polysome profiling to separate the poorly translated monosomal and the highly translated polysomal fraction. We isolated RNA from these fractions and performed RNA sequence analysis. Surprisingly, many of the RNAs associated with ribosomes and showing the strongest expression difference between the N2 and *daf-2* strains were non-coding RNAs which had never before been ascribed a ribosomal function.

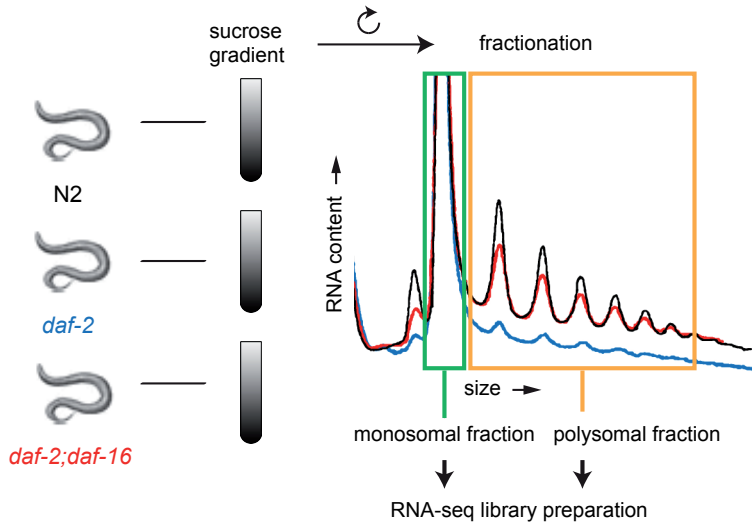

Figure 1: Overview of the experimental procedure. N2, daf-2 and daf-2;daf-16 nematodes were collected and lysed for polysome profiling. Monosomal and polysomal fractions were collected and the polysomal fractions were pooled. RNA was isolated and processed for next generation sequencing.

Results and Discussion

Deep sequence analysis of ribosome associated transcripts

To identify subsets of differentially translated RNAs, polysome profiling of N2 (wild type), *daf-2* (e1370) and *daf-2;daf-16* (e1370;mu86) young adult nematodes was performed [8] and the monosomal and polysomal fractions were collected. RNA isolated from these fractions was used for RNA-sequencing (Fig 1). Using a false discovery rate of less than 5%, many transcripts were found to be differentially associated with the ribosome between *daf-2* and N2 and between *daf-2* and *daf-2;daf-16* nematodes, in the monosomal as well as the polysomal fraction (Fig 2A-B). A far smaller number of transcripts was differentially associated with the ribosome between the N2 and *daf-2;daf-16*, indicating that most differential regulation of transcript association in the *daf-2* mutant in both fractions is dependent on DAF-16 signaling (Fig2A-B).

More transcripts are differentially associated with the monosomal fraction and 77% (47 out 61) of transcripts differentially associated in the polysomal fractions are also differentially associated in the monosomal fractions (Fig 2C). As expected, there is a large overlap of genes differentially associated between the *daf-2* vs N2 and the *daf-2* vs *daf-2;daf-16* analysis (Fig 2D). A larger number of genes is differentially expressed between *daf-2* and *daf-2;daf-16* than between *daf-2* and N2 (Fig 2D). This is possibly explained by low level activation of DAF-16 in the N2 line, exemplified by the finding that *daf-16* mutants have shorter lifespans than N2 wildtype nematodes (8247153).

Many RNAs are preferentially associated with either the monosome or the polysome

To determine whether there is a post-transcriptional mechanism that targets mRNA to either the monosome or the polysome, we compared RNA levels between fractions for each nematode line (Fig 3A). Surprisingly, there is poor correlation between the transcript levels in the monosome and the polysome, suggesting the existence of a selection mechanism that determines which monosomal transcripts are loaded with additional ribosomes.

mRNAs in the polysomal fraction represent mRNAs in active translation, while the current dogma suggests that transcripts in the monosome are more inactive (13998950). In line with this, we found tRNAs to be highly abundant in the polysomal, but not the monosomal fractions (Fig 3B).

In dietary restricted *Drosophila melanogaster*, it was shown that transcripts with short 5' UTRs are preferentially located in the polysomal fraction [10]. We compared the 5'UTR lengths of the transcripts preferentially located in monosomal and polysomal fractions, but found no difference (Fig 3C). This is most likely due to the mechanism of trans-splicing, unique to nematodes, in which 5'UTRs are trimmed of and replaced by one of two possible leader sequences [12]. This occurs in about 70% of transcripts [12], making the possibility that 5' UTRs play a role in determining ribosome occupancy in nematodes unlikely. Whether these RNAs have any other structural characteristics in common or share a sequence motif remains unclear.

To investigate whether transcripts overexpressed in the polysomal fractions have any functional commonalities, we looked for overrepresentation of gene ontology (GO) terms associated with the transcripts significantly overexpressed in either fraction. This type of analysis represents the transcripts that are preferentially translated rather than transcripts that are abundant in the polysome simply because they are transcribed at high levels and are abundant in the cytoplasm. In Fig 3D it can be seen that both N2 and *daf-2* polysomal fractions are highly enriched in transcripts associated with larval development, growth and metabolism. Compared to N2, d*af-2* polysomal fractions are enriched in transcripts associated with aging, cuticle development, glucose and fatty acid homeostasis, respiration and DNA packaging. Enrichment in the *daf-2* polysome is reduced for genes involved in genitalia development, representing the reduced

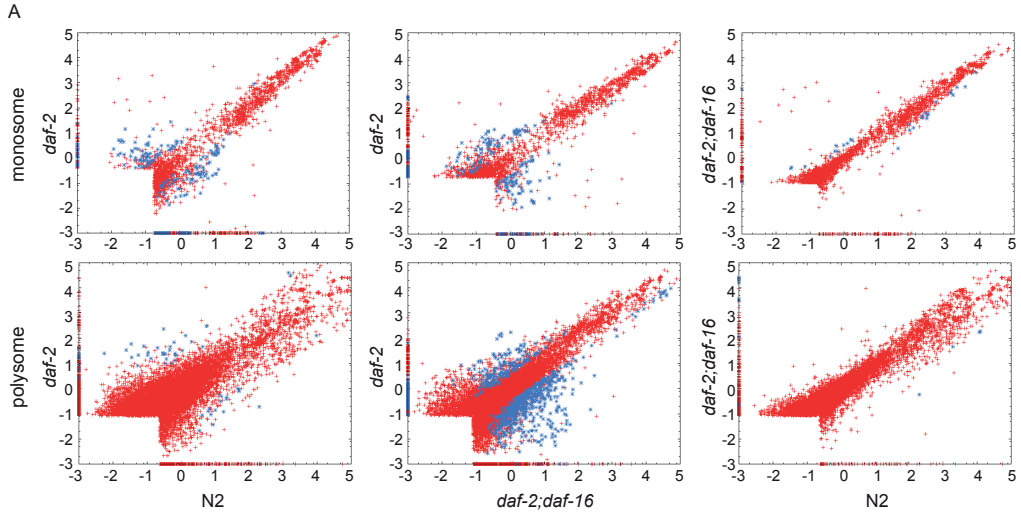

B

comparison:	upregulated mono	upregulated poly	downregulated mono	downregulated poly
daf-2 vs N2	119(122)	39(42)	178(181)	17(19)
daf-2 vs daf-2;daf-16	128(142)	530(556)	371(374)	282(287)
daf-2;daf-16 vs N2	10(11)	0(10)	1(19)	1(5)

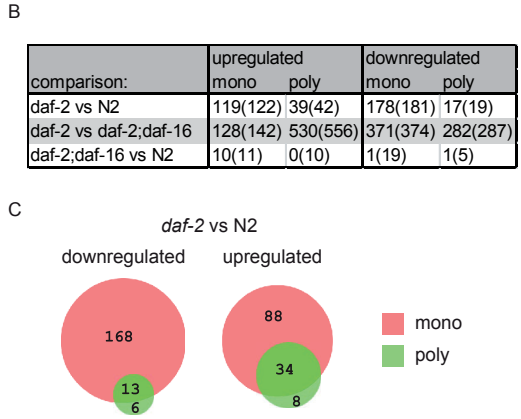

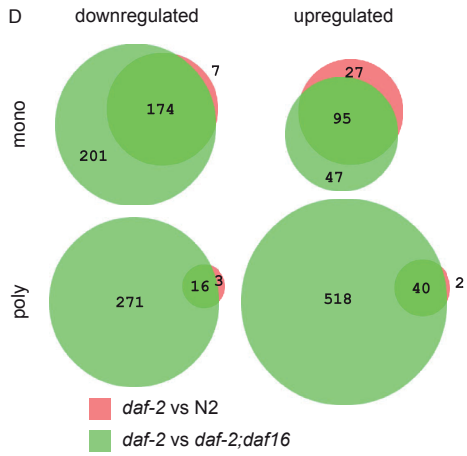

Figure 2: Differential expression between N2, *daf-2* and *daf-2;daf-16* nematodes. (A) Scatterplots showing the levels of transcripts that were associated with the monosome and polysome in the three lines tested. Transcripts found to be significantly differentially associated (FDR adjusted p<0.05) between the respective lines are represented as blue asterisks, other transcripts as red crosses. (B) Numbers of coding transcripts and total transcripts (between parentheses) differentially associated between each line. (C) Venn diagram showing the overlap between transcripts differentially associated in the monosome and polysome. (D) Venn diagrams showing the overlap between the *daf-2* vs. N2 and the *daf-2* vs. *daf-2;daf-16* analyses. Scatterplots were generated using GNUplot (www.gnuplot.info), Venn diagrams were created using BioVenn [21].

fecundity observed in these mutants. Transcripts involved in tRNA aminoacetylation and the cell cycle are enriched in N2, but not in *daf-2* mutant polysomes. tRNA aminoacetylation is a key process in protein synthesis, so this finding is in line with reduced levels of ribosomal proteins and elongation factors found in previous studies (23820781). The loss of cell cycle transcripts likely reflects the reduction in oocyte development rate observed in these mutants [13], as there is no somatic cell division in adult *C.elegans* [14].

Interestingly, in the monosomal fractions, only transcripts involved in sensory perception are

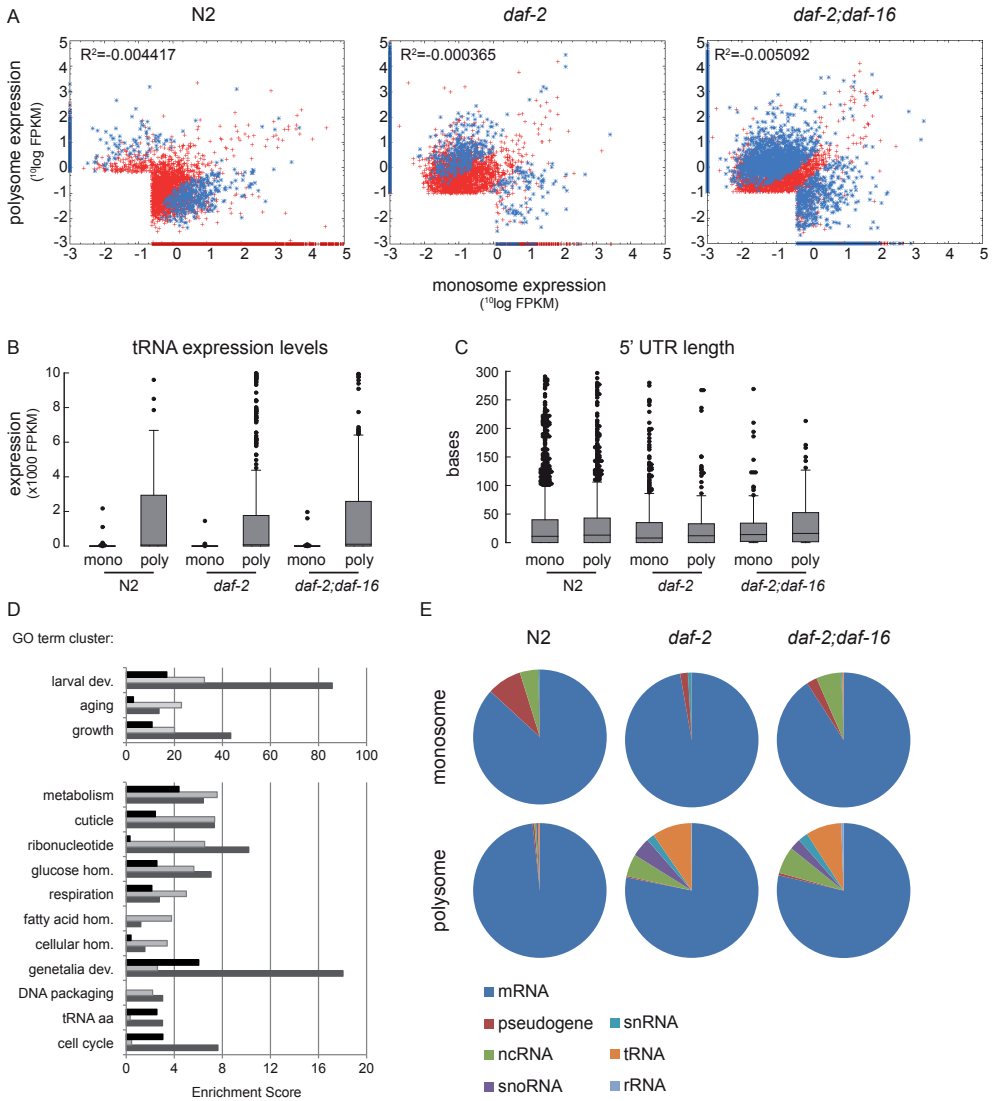

Figure 3: Differential expression between the monosome and polysome in N2, *daf-2* and *daf-2;daf-16*. (A) Scatterplots showing the levels of transcripts that were differentially associated with the monosome compared to the polysome in the three lines tested. Transcripts found to be significantly differentially associated (FDR adjusted p<0.05) between the respective lines are represented as blue asterisks, other transcripts as red crosses. (B) Boxplot of the expression levels of all tRNAs tested for in the monosomal and polysomal fractions. (C) Boxplot showing the occurrence of 5'UTR lengths in all fractions. (D) GO term analysis of transcripts differentially associated with the polysome in each cell line. GO terms were clustered using DAVID [22] and were manually named. (E) pie charts representing the biotypes of RNAs that were differentially regulated between the monosomal and polysomal fraction in each line. Scatterplots and boxplots were generated using GNUplot (www.gnuplot.info), pie charts were generated in excel software.

enriched in the N2, while no enrichment is observed in the *daf-2* mutant at all (data not shown), indicating that the mRNAs in the monosomal fraction represent a cross section of the genome and that specific functional groups of transcripts are loaded with more ribosomes for high efficiency translation.

Many ncRNAs are associated with monosomes and polysomes

Analysis of transcript expression levels in the monosomal and polysomal fractions revealed that, aside from mRNAs, high numbers of non-coding RNAs (ncRNAs) are associated with ribosomes, including long ncRNAs, small nuclear RNAs (snRNAs), small nucleolar RNAs (snoRNAs) and pseudogenes. Many of these were preferentially localized in either the monosome or the polysome (Fig 3E). In N2 and *daf-2;daf-16* mutants pseudogenes associate with the monosome but not the polysome, most likely reflecting their inability to be translated. The presence of snRNA and snoRNAs in the ribosomal fractions is puzzling. for example the highest differentially expressed RNA on monosomes of the *daf-2* mutants is the U2 snRNA which is normally associated with the spliceosome RNP complex. RNAs previously thought to be only involved in ribosome biogenesis may remain associated with the ribosome after maturation and possibly play a role in translation or mRNA recognition. One possibility is that the mono- and/or polysomal fractions contain non-ribosomal RNP complexes. However, we do not believe this is the case since we do not find any of the other spliceosome snRNAs (U1, U3-12) in the fractions.

tts-1 *associates with ribosomes in the* daf-2 *mutant line*

A number of ncRNAs were differentially expressed between the N2, *daf-2* and *daf-2;daf-16* nematode lines, in either or both of the monosomal or polysomal fraction (Table 1). Little is known about these ncRNAs. Telomeric transcribed sequence 1 (*tts-1*) is a long ncRNA that was previously found highly upregulated in the *daf-2* mutant polysomes in a DAF-16 dependent manner [24]. This ncRNA was also previously found to be highly expressed in nematodes in dauer, an arrested developmental stage nematodes enter at the second molt in response to environmental stress [24], as well as in nematodes exposed to nitric oxide, which results in lifespan extension [25]. To confirm that *tts-1* is present in the ribosome, qPCR was performed on RNA from monosomal and polysomal fractions collected in a new experiment, as well as RNA from total nematode lysates

			daf-2 vs N2		*daf-2* vs *daf-2;daf-16*	
gene	Biotype	direction	^{2}log(FC)	FDR	^{2}log(FC)	FDR
Monosome:						
Y47H9A.2	snRNA	up	100	0.016677	-	-
tts-1	ncRNA	up	5.39	0.036946	100	0.017696
ZC412.t2	tRNA	up	2.57	0.045896	2.33	0.010582
K03E6.8	ncRNA	down	-100	0.035552	-100	0.038324
W03C9.11	ncRNA	down	-100	0.03821	-	-
Y45F10B.16	snlRNA	down	-100	0.040934	-100	0.006108
Polysome:						
tts-1	ncRNA	up	8.03	0.012821	7.29	2.74E-12
M163.13	snRNA	up	4.79	0.023874	2.94	0.011628
T06C12.16	snoRNA	up	4.26	0.023359	-	-
R09E10.16	ncRNA	down	-8.83	0.014142	-	-
R04D3.13	ncRNA	down	-6.27	0.045014	-	-

Table 1: Overview of ncRNAs differentially expressed between *daf-2* and N2 and the corresponding values for *daf-2* vs *daf-2;daf-16*.

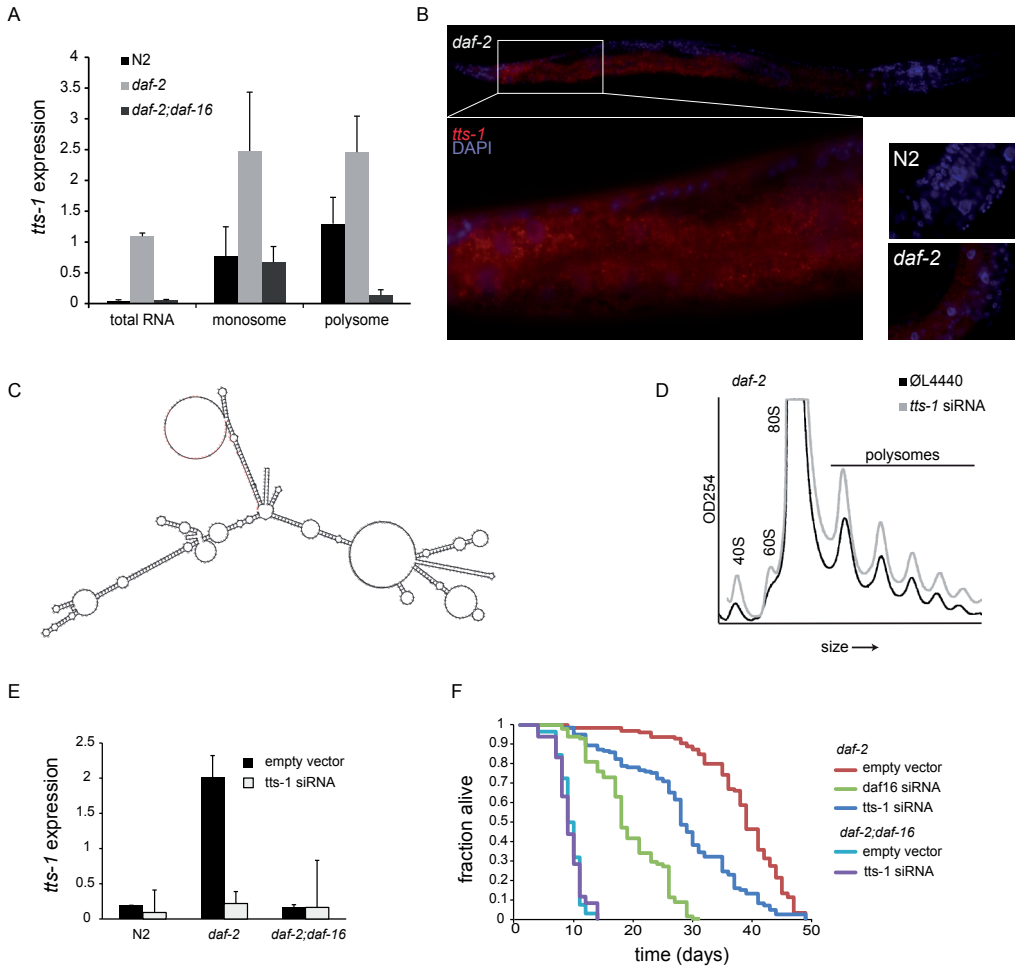

Figure 4: *tts-1* is an intestinal ncRNA that associates with the ribosome and decreases translation efficiency. (A) qPRC analysis of *tts-1* levels in total, monosomal and polysomal RNA in each worm line. (B) Fluorescent In Situ Hybridization of *tts-1* in an adult nematode. Inset: *tts-1* is not detected in N2 nematodes, showing the specificity of the probe used. (C) predicted secondary structure of *tts-1* generated using RNAfold [23]. The long stretch of uridines at the 3' end is indicated in red. (D) polysome profiles of *daf-2* mutants grown on bacteria producing *tts-1* siRNA or empty L4440 vector. (E) Survival curves for *daf-2* and *daf-2;daf-16* nematodes grown on bacteria producing *tts-1* siRNA, *daf-16* siRNA or empty vector.

(Fig 4A). The high expression level in the ribosome compared to total cell lysate suggests that *tts-1* is preferentially localized in the ribosome. We performed fluorescent in situ hybridization to determine which cell types express *tts-1* (Fig 4B) and found high expression in the gut, an organ which has been associated with lifespan extension in *C elegans* [15].

tts-1 has two isoforms, 711bp or 659bp in length, and contains a long stretch of uridines at its 3' end (Fig 4C). To investigate whether *tts*-1 inhibits polysome formation, *daf-2* nematodes were fed bacteria producing *tts-1* siRNA. We measured polysome levels in these nematodes and found that

polysome levels were increased, although not restored to wildtype levels (Fig 4D). In addition, the levels of 40S and 60S ribosomal subunits were also increased. The siRNA effectivity was validated using qPCR (Fig 4E).
To determine whether *tts-1* is required for *daf-2* mediated lifespan extension, *daf-2* nematodes were grown on *tts-1* siRNA producing bacteria and their lifespans were measured. *tts-1* siRNA reduced the lifespan of *daf-2* mutants, indicating that this ncRNA is required for lifespan extension (Fig 4F).

Conclusion

Our previous findings that translation is greatly decreased in *daf-2* mutants suggested that the insulin/Insulin like growth factor and dietary restriction pathways of lifespan extension are more similar than previously thought [8]. In *Drosophila*, dietary restriction leads to increased translation efficiency of specific mRNAs. We set out to identify such preferentially translated mRNAs in *C.elegans daf-2* mutants.
Many transcripts were found to be specifically present in the monosome or the polysome, even in the wild type situation. When polysomes were first discovered, it was already reported that they were the site of translation and that monosomes are translationally less active [16], a finding which is confirmed here by the abundance of tRNAs in polysomes compared to monosomes. This indicates that transcripts enriched in the polysome are preferentially translated. Note that comparing transcript levels in polysomes to those in monosomes makes the analysis independent of the overall transcript abundance.
GO term analysis of the transcripts that were preferentially translated in each nematode line, revealed that *daf*-2 mutants have an altered preference for certain RNAs to translate. Transcripts associated with processes known to play a role in *daf-2* mediated lifespan extension were translated with increased (aging, cuticle, respiration) or decreased (genitalia development, tRNA aminoacetylation, cell cycle) efficiency compared to wildtype. In most, but not all cases, this altered preference was DAF-16 dependent.
The underlying mechanism of the preferential translation observed here has yet to be determined. Undoubtedly, inhibition of translation by miRNAs and mRNA structure are involved, but there is also evidence that structural variation in the ribosome itself plays a role in mRNA recognition and translation efficiency [17]. Such structural variation has been described to include variations of ribosomal protein in the ribosome, the binding of translation machinery associated proteins, and variations in ribosomal RNA, which is present in multiples copies in the DNA. In this study, we find a large number of ncRNAs associated with the ribosome. Further investigation is required to determine whether some of these can be added to the list of factors that influence translation efficiency of specific mRNAs.
One of these ncRNAs associated with the ribosome is transcribed telomere sequence 1 (*tts-1*). We show that *tts-1* is expressed in the gut and that knocking down *tts-1* levels partially restores polysome levels in the *daf-2* mutant. Knockdown of *tts-1* also represses the lifespan extension phenotype of the *daf-2* mutant, making this, to our knowledge, the first ncRNA to be shown to be required for lifespan extension. It would be interesting to determine through what mechanism *tts-1* influences translation efficiency and if this effect is global or is one of the underlying mechanisms for the altered preferential translation observed in the *daf-2* mutant. One intriguing possibility refers to the recent work by Guttman et al [18] demonstrating that lncRNAs are associated with polysomes that do not synthesize protein. It may be that in order to conserve energy during nutrient depletion or insulin signaling reductions the cell expresses *tts-1* in order to hold mature ribosomes in a non-protein synthesis state until nutrients become available or

insulin signaling returns to normal. Such a mechanism would be logical considering the huge amount of cellular energy required in the biogenesis of nascent ribosomes, and the fact that in such states of nutrient depletion or insulin signaling reduction the amount of expendable energy is extremely low.

Methods

Nematode growing and conditions

Strains. All strains were maintained expanded as described previously (Brenner, 1974/ Kenyon/ Dillin). N2, CB1370 daf-2(e1370), CF1038 daf-16(mu86) and CF1515 daf-16(mu86):daf-2(e1370) were obtained from the Caenorhabditis Genetics Center (CGC, MN, US). Nematodes were maintained on 150mmNG OP50 plates at 15°C.
RNA interference. A vector containing the first intron of tts-1 was synthesized by Eurofins (Breda, The Netherlands) and cloned into an empty L4440 vector (Addgene, Cambridge MA, US). This vector was transformed into HT115 E. Coli. Positive clones were selected by Sanger sequencing and grown overnight at 37°C in LB with 50 µg/ml ampicillin before seeding.
Synchronization. For experiments, nematodes were synchronized by bleeching and allowed to hatch overnight in M9 buffer [14]. The L1 arrested larvae were plated onto 150mmNG OP50 plates or plates inoculated with tts-1 specific RNAi bacteria and grown at 15ºC until they reached L4, at which point they were shifted to 25ºC overnight.
Lifespan analysis. Lifespan analysis was performed as previously described [8].

Polysome profiling and RNA sequence analysis

Polysome profiles were performed as described [8]. Fractions were collected using a Foxy Jr Fraction Collector (Teledyne ISCO). Monosomal and polysomal fractions from two experiments were pooled and RNA was extracted using TRIzol LS (Invitrogen). For each condition, two libraries were constructed from RNA isolated in two separate experiments using the SOLiD® Total RNA-Seq Kit (Life Technologies) and analysed on the SOLiD platform. Differential expression analysis was performed using Cufflinks software [19].

qPCR analysis

Total RNA was isolated using TRIzol (Invitrogen) and cDNA was made using iScript (BioRad). qPCR reactions were run using iQ SYBR Green Supermix (BioRad) on a myIQ iCycler (BioRad). The following primers were used: *tts-1* fw 5'-ccgacacgtttcagacacac-3', *tts-1* rv 5'-ggttttacccattgactcaacc-3'. *pmp-3* was used as a housekeeping gene [20]: *pmp-3* fw 5'-tccttgatgaatccacgtca-3', *pmp-3* rv 5'-accgatgaccaattgacaca-3' .

Single molecule fluorescent in situ hybridization

A set of 11 short probes targeting *tts-1* was designed with the Stellaris RNA FISH probe designer, using the highest level of masking (BioSearch Technologies, Novato CA, US). FISH was performed according to the manufacturers' protocol with the following modifications: nematodes were hybridized in a 1250µM probe solution overnight at 37ºC, washed once for 8 hours, once overnight and finally for 1 hour in the presence of DAPI before imaging on a DM6000 microscope (Leica Microsystems, Wetzlar, Germany). Images were processed using ImageJ V1.46r.

References

1. Kenyon C, Chang J, Gensch E, Rudner A, Tabtiang R (1993) A C. elegans mutant that lives twice as long as wild type. Nature 366: 461-464.
2. Kenyon CJ (2010) The genetics of ageing. Nature 464: 504-512.
3. Hsu AL, Murphy CT, Kenyon C (2003) Regulation of aging and age-related disease by DAF-16 and heat-shock factor. Science 300: 1142-1145.
4. Tullet JM, Hertweck M, An JH, Baker J, Hwang JY, et al. (2008) Direct inhibition of the longevity-promoting factor SKN-1 by insulin-like signaling in C. elegans. Cell 132: 1025-1038.
5. Murphy CT, McCarroll SA, Bargmann CI, Fraser A, Kamath RS, et al. (2003) Genes that act downstream of DAF-16 to influence the lifespan of Caenorhabditis elegans. Nature 424: 277-283.
6. An JH, Blackwell TK (2003) SKN-1 links C. elegans mesendodermal specification to a conserved oxidative stress response. Genes Dev 17: 1882-1893.
7. Hansen M, Chandra A, Mitic LL, Onken B, Driscoll M, et al. (2008) A role for autophagy in the extension of lifespan by dietary restriction in C. elegans. PLoS Genet 4: e24.
8. Stout GJ, Stigter EC, Essers PB, Mulder KW, Kolkman A, et al. (2013) Insulin/IGF-1-mediated longevity is marked by reduced protein metabolism. Mol Syst Biol 9: 679.
9. Hansen M, Taubert S, Crawford D, Libina N, Lee SJ, et al. (2007) Lifespan extension by conditions that inhibit translation in Caenorhabditis elegans. Aging Cell 6: 95-110.
10. Zid BM, Rogers AN, Katewa SD, Vargas MA, Kolipinski MC, et al. (2009) 4E-BP extends lifespan upon dietary restriction by enhancing mitochondrial activity in Drosophila. Cell 139: 149-160.
11. Sonberg N (2001) Translational Control of Gene Expression. Cold Spring Harbor: Cold Spring Harbor Laboratory Press.
12. Blumenthal T (2012) Trans-splicing and operons in C. elegans. WormBook: 1-11.
13. Van Voorhies WA, Ward S (1999) Genetic and environmental conditions that increase longevity in Caenorhabditis elegans decrease metabolic rate. Proc Natl Acad Sci U S A 96: 11399-11403.
14. Community TCeR (2005) Wormbook.
15. Rera M, Azizi MJ, Walker DW (2013) Organ-specific mediation of lifespan extension: more than a gut feeling? Ageing Res Rev 12: 436-444.
16. Warner JR, Knopf PM, Rich A (1963) A multiple ribosomal structure in protein synthesis. Proc Natl Acad Sci U S A 49: 122-129.
17. Gilbert WV (2011) Functional specialization of ribosomes? Trends Biochem Sci 36: 127-132.
18. Guttman M, Russell P, Ingolia NT, Weissman JS, Lander ES (2013) Ribosome Profiling Provides Evidence that Large Noncoding RNAs Do Not Encode Proteins. Cell 154: 240-251.
19. Trapnell C, Williams BA, Pertea G, Mortazavi A, Kwan G, et al. (2010) Transcript assembly and quantification by RNA-Seq reveals unannotated transcripts and isoform switching during cell differentiation. Nat Biotechnol 28: 511-515.
20. Zhang Y, Chen D, Smith MA, Zhang B, Pan X (2012) Selection of reliable reference genes in Caenorhabditis elegans for analysis of nanotoxicity. PLoS One 7: e31849.
21. Hulsen T, de Vlieg J, Alkema W (2008) BioVenn - a web application for the comparison and visualization of biological lists using area-proportional Venn diagrams. BMC Genomics 9: 488.
22. Huang da W, Sherman BT, Lempicki RA (2009) Systematic and integrative analysis of large gene lists using DAVID bioinformatics resources. Nat Protoc 4: 44-57.
23. Sukosd Z, Knudsen B, Vaerum M, Kjems J, Andersen ES (2011) Multithreaded comparative RNA secondary structure prediction using stochastic context-free grammars. BMC Bioinformatics 12: 103.
24. Jones SJ, Riddle DL, Pouzyrev AT, Velculescu VE, Hillier L, et al. (2001) Changes in gene expression associated with developmental arrest and longevity in Caenorhabditis elegans. Genome Res 11(8):1346-52.
25. Gusarov I, Gautier L, Smolentseva O, Shamovsky I, Eremina S, et al. (2013) Bacterial nitric oxide extends the lifespan of C. elegans. Cell 14;152(4):818-30.

Perinatal Exogenous Nitric Oxide in Fawnhooded Hypertensive Rats Reduces Renal Ribosomal Biogenesis in Early Life

Sebastiaan Wesseling*, Paul B. Essers*, Maarten P. Koeners , Tamara C. Pereboom, Branko Braam, Ernst E. van Faassen, Alyson W MacInnes and Jaap A. Joles

*These authors contributed equally to this work.

Front Genet. 2011;2:52.

Abstract

Nitric oxide (NO) is known to depress ribosome biogenesis in vitro. In this study we analyzed the influence of exogenous NO on ribosome biogenesis in vivo using a proven antihypertensive model of perinatal NO administration in genetically hypertensive rats. Fawn-hooded hypertensive rat (FHH) dams were supplied with the NO-donor molsidomine in drinking water from 2 weeks before to 4 weeks after birth, and the kidneys were subsequently collected from 2 day, 2 week, and 9 to 10-month-old adult offspring. Although the NO-donor increased maternal NO metabolite excretion, the NO status of juvenile renal (and liver) tissue was unchanged as assayed by EPR spectroscopy of NO trapped with iron-dithiocarbamate complexes. Nevertheless, microarray analysis revealed marked differential up-regulation of renal ribosomal protein genes at 2 days and down-regulation at 2 weeks and in adult males. Such differential regulation of renal ribosomal protein genes was not observed in females. These changes were confirmed in males at 2 weeks by expression analysis of renal ribosomal protein L36a and by polysome profiling, which also revealed a down-regulation of ribosomes in females at that age. However, renal polysome profiles returned to normal in adults after early exposure to molsidomine. No direct effects of molsidomine were observed on cellular proliferation in kidneys at any age, and the changes induced by molsidomine in renal polysome profiles at 2 weeks were absent in the livers of the same rats. Our results suggest that the previously found prolonged antihypertensive effects of perinatal NO administration may be due to epigenetically programmed alterations in renal ribosome biogenesis during a critical fetal period of renal development, and provide a salient example of a drug-induced reduction of ribosome biogenesis that is accompanied by a beneficial long-term health effect in both males and females.

Introduction

Plasticity of organogenesis provides an opportunity for interventions in a specific window of early development that may have long-term beneficial or detrimental effects on adult health and disease (McMillen and Robinson, 2005). One critical regulation of such plasticity is protein synthesis. Upstream factors affecting protein synthesis include tight regulations at multiple stages of ribosome biogenesis. For example, it is well known that epigenetic silencing of ribosomal DNA (rDNA) regularly occurs, even in proliferating cells (McStay and Grummt, 2008; Sanij and Hannan, 2009). One exogenous factor that has been shown to affect rDNA and ribosome biogenesis is nitric oxide (NO). Exposure of cells to high levels of NO, using either NO-donors, or inducing expression of inducible NO synthase (iNOS), results in inhibition of the 80S ribosomal complex (Kim et al., 1998) and enhanced rRNA cleavage resulting in a reduction of both 60S and 80S ribosomal particles (Cai et al., 2000).

Hypertension is associated with decreased NO availability (Wilcox, 2005). The fawn-hooded hypertensive rat (FHH) is a genetic model of hypertension susceptible to progressive renal injury. In FHH hypertension is aggravated and the development of renal injury is accelerated when NOS is chronically inhibited, revealing partial NO dependency of the adult FHH phenotype (Van Dokkum et al., 1998). Renal transplantation under different conditions has shown that blood pressure regulation is intricately linked to the kidney (Smallegange et al., 2004; Crowley et al., 2005), and we hypothesized that this is also the case in the perinatal phase (Koeners et al., 2008a). Recently, we observed that perinatal supplementation of FHH dams with molsidomine, an NO-releasing prodrug (Feelisch, 1998; Singh et al., 1999), persistently lowered the blood pressure and attenuated the development of renal injury in male and female FHH (Koeners et al., 2008b).

Long-term regulation of blood pressure is determined by the relationship between renal perfusion pressure and NaCl excretion, and this relationship is facilitated by renal NO availability (Cowley, 2008; Garvin et al., 2011). Thus our interest is directed at mechanisms in the kidney that link availability of NO in early development to regulation blood pressure in adult life. Conceivably temporal changes in the regulation of renal protein synthesis via ribosomal control of gene translation could constitute such a link (Kasinath et al., 2006). For instance, compensatory renal hypertrophy involves a global increase in polysome profiles within less than 1 day after uninephrectomy (Chen et al., 2005). Based on the known effects of high levels of NO on the ribosomal elements in cultured cells, we hypothesized that ribosome biogenesis in vivo in the neonatal FHH kidney may also be regulated by NO availability. This perinatal regulation of ribosome biogenesis may then affect kidney organogenesis in a manner that impacts the long-term regulation of blood pressure and renal integrity.

Here we demonstrate that the perinatal administration of NO results in a dramatic biphasic change of ribosomal protein gene expression in FHH rats at 2 days and 2 weeks of age. This results in decreased post-translational levels of certain ribosomal proteins, and a remarkable reduction of assembled ribosome structures at the 2-week point. Intriguingly, we did not find an increase in renal NO content at 2 weeks in the offspring of NO-donor-treated rats. Our results suggest that the increased availability of NO in gestation epigenetically alters renal ribosome biogenesis during a critical period of renal development. In conjunction with previously published findings, we conclude that this effect by NO may alter renal organogenesis in a manner that alleviates the hypertension phenotype normally experienced by FHH rats.

Materials and Methods

Animal Experiment

Fawn-hooded hypertensive rat were from our own colony, derived from the original colony at Erasmus University Rotterdam (FHH/EUR) maintained by Dr. A. Provoost. FHH dams were supplied with molsidomine (Sigma-Aldrich, Zwijndrecht, Netherlands) in drinking water (120 mg/L) 2 weeks before to 4 weeks after birth. Control FHH mothers and their offspring received regular tap water. All offspring from 4 weeks of age received regular tap water and regular chow (Special Diets Services, Witham, Essex, England). Offspring were sacrificed at 2 days, 2 weeks, 36 weeks (males), and 42 weeks (females). The adult ages were chosen when renal injury in males and females was similar. Kidneys were isolated and snap-frozen (for microarray analysis), kept on ice (for Western blotting and polysome profiling), or fixed in formaldehyde (for immunohistochemistry). Note that although functional and morphological data from the adult rats have been published previously (Koeners et al., 2008b), all microarray data and all data pertaining to renal ribosomal proteins in adult kidneys is novel. Directly after weaning of the pups, the dams were placed in metabolic cages without food but with access to water with 2% glucose and 24-h urine was collected on antibiotic/antimycotic solution (Sigma-Aldrich) to prevent degradation of NO metabolites. NO metabolites were determined as described (Bongartz et al., 2010). Sentinel animals were housed under the same conditions and regularly monitored for infections by nematodes, pathogenic bacteria, and antibodies for rodent viral pathogens (International Council for Laboratory Animal Science, Nijmegen, Netherlands). The Utrecht University Board for studies in experimental animals approved the protocol.

Microarray

For an overview and extensive explanation of microarray data processing, please see Appendix. In short, a piece of snap-frozen kidney was put in 1 mL TRIzol (Invitrogen, Breda, Netherlands) containing 100–150 mg 1 mm glass beads (BioSpec Products, Bartlesville, OK, USA) and immediately homogenized in 30 s using a mini-beadbeater (BioSpec). The total RNA was isolated according to the manufacturer's instructions. Total RNA was purified using NucleoSpin RNA II kit (Macherey-Nagel, Düren, Germany). Samples were then put on Illumina BeadChips (RatRef-12) by ServiceXS1 (Leiden, Netherlands). Kidneys from 2 days, 2 weeks, and adult FHH of both genders were used (at least n = 5/group). All samples were randomly placed on different arrays in order to minimize variation between BeadChips and between arrays.

After calculating the average intensity per probe, all arrays were Log2-transformed and Quantile normalized. The arrays were grouped and the average intensity was calculated. The significance of the differences in intensity between the groups was calculated using Cyber t-test. This final data containing normalized data, average intensity per group and statistical significance between groups were used in data evaluation. The data are submitted as MIAME-complaint to GEO2 under accession number GSE27725.

The number of genes differentially expressed in the molsidomine samples were counted per age in each gender. These were then compared in order to elucidate whether there were genes persistently affected by molsidomine. The 40 genes that were most differentially regulated (20 up and 20 down) by molsidomine were collected at each age for each gender.

All genes encoding for ribosomal proteins were collected. The differentially expressed genes encoding for ribosomal proteins were compared at each age. In order to determine whether the effect of molsidomine on ribosomal genes was stronger than on general gene expression profiles, the ratio of differentially regulated ribosomal genes to the whole ribosomal gene population was

compared to the ratio of total differentially expressed genes with whole microarray data in a size test.

Western Blot Analysis

Fresh kidney samples were lysed on ice in lysis buffer (50 mM Tris–HCl pH 7.5, 150 mM NaCl, 2 mM EDTA, 1% Triton X-100; all from Sigma-Aldrich) plus protease inhibitors (Santa Cruz Biotech, #29130) and subjected to centrifugation at 14K rpm at 4°C for 10 min. Protein content in the supernatants was quantified using Biorad Protein Assay. 6× Laemmli loading buffer was added to 50 µg samples which were then boiled for 5 min and loaded on a 10% SDS/PAGE gel. Transfers to PVDF membranes (Millipore, #IPVH00010) were done overnight at 15 V at 4°C, blocked in 5% milk/TBST solution for 1 h at RT, and subjected to blotting with αL36a (Abnova, #H00006173-M02) or α-actin (Santa Cruz Biotech, #1616) at dilutions of 1:200 in blocking buffer overnight at 4°C. Either α-mouse (L36a) or α-rabbit (actin) HRP-conjugated secondary antibodies (GE Healthcare, #NXA931 and NA934) were used at a dilution of 1:5000 in TBST for 20 min at RT. Blots were washed 3× in TBST for 10 min at RT. Detection was done with the ECL Advance Western Blot Detection Kit (GE Healthcare, #RPN2135). Quantifications were performed using a GS-800 densitometer (Biorad, Veenendaal, Netherlands) and Quantity One software (Biorad).

Polysome Profiling

The kidneys from FHH pups from control dams or dams treated with molsidomine were collected at age 2 days and 2 weeks, maintained fresh on ice, and processed for polysome profiling on the same day. For polysome profiling of adult tissue frozen kidney tissue was used. Comparisons were only performed between treated and control rats of both genders at each age. Livers from 2-week-old pups were used to determine tissue-specificity. All steps of this protocol were performed at 4°C or on ice. Gradients of 17–50% sucrose (11 ml) in gradient buffer (110 mM KAc, 20 mM MgAc2, and 10 mM HEPES pH 7.6) were prepared on the day prior to use. Kidneys were lysed in 500 µl polysome lysis buffer (gradient buffer containing 100 mM KCl, 10 mM MgCl2, 0.1% NP-40, 2 mM DTT, and 40 U/ml RNasin; Promega, Leiden, Netherlands) using a dounce homogenizer. The samples were centrifuged at 1200 g for 10 min to remove debris and loaded onto sucrose gradients. The gradients were ultracentrifuged for 2 h at 40,000 rpm in an SW41Ti rotor (Beckman-Coulter, USA). The gradients were displaced into a UA6 absorbance reader (Teledyne ISCO, USA) using a syringe pump (Brandel, USA) containing 60% sucrose. Absorbance was recorded at an OD of 254 nm. All chemicals came from Sigma-Aldrich unless stated otherwise.

Tissue NO Content

Endogenous NO levels in kidney and liver tissues of FHH pups were assayed at 2 weeks by NO trapping with iron-dithiocarbamate (Fe-DETC) complexes, as previously described (Koeners et al., 2007; Van Faassen et al., 2008). Briefly, the yields of paramagnetic NO-Fe(II)-DETC complexes (mononitrosyl-iron complexes, MNIC) in tissues was quantified with EPR spectroscopy of intact frozen tissue sections at 77K. The tissues were reduced at room temperature with dithionite (50 mM for 15 min) to remove the overlapping EPR signal from paramagnetic Cu(II)-DETC complexes as commonly found in biological materials.

Immunohistochemistry

Kidneys were fixed overnight at room temperature in 4% formaldehyde. The tissue was embedded in paraffin and 4 µm sections were made on silanized glass slides. The slides were baked at 58°C overnight, deparaffinated, and rehydrated. Endogenous peroxidase was blocked using citric acid. For antigen retrieval, the sections were boiled for 20 min in citrate buffer (pH 6) and allowed to

cool slowly. The sections were then blocked in 1% BSA (w/v) in PBS and incubated with rabbit-anti-pH3 (Santa Cruz Biotech, #1791) overnight at 4°C. The sections were then incubated in anti-rabbit Powervision PO (Immunologic, #DPVR110 HRP) for 30 min at RT and developed using DAB. Finally the sections were counterstained in hematoxylin, dehydrated, and enclosed in pertex. The quantification was performed as follows: At 20× magnification random fields were chosen, taking care not to include the edges of the tissue. The number of positive cells was counted in three fields of two sections per kidney. The average of these six counts was used for analysis.

Statistics

For statistics in microarray, please refer to the methodology. For other measurements the values are expressed as means ± SEM. Data were compared with unpaired t-test, one-way ANOVA, and two-way ANOVA where appropriate followed by post hoc test Student-Newman–Keuls. $P < 0.05$ is considered significant.

Results

Biometrical Data

Biometrical data of FHH offspring and the number of rats studied are collected in Table 1. Note that adult kidney weight and tail-cuff blood pressure data, which were published previously (Koeners et al., 2008b), are included in the table for the sake of convenience. Molsidomine treatment decreased the kidney weight relative to body weight in 2-day-old females ($P < 0.05$) but not at older ages. However, in both male and female 2-week-old FHH rats relative kidney weight was unchanged. The kidneys of adult males exposed to perinatal molsidomine weighed less than controls, probably in association with reduced injury (Koeners et al., 2008b). Perinatal molsidomine decreased systolic blood pressure in adult FHH offspring (Koeners et al., 2008b). NO metabolites were determined in a 24-h collection of urine from FHH dams to substantiate the direct effects of molsidomine in their pups. Indeed, maternal urine NOx was increased by molsidomine (n = 4) vs. controls (n = 4) from 1.6 ± 0.1 to 2.6 ± 0.2 µmol/(100 g BW)/d ($P < 0.01$).

Table 1 Biometrical data of control FHH and FHH during molsidomine (2 days and 2 weeks) or after perinatal molsidomine (adult).

	Males		**Females**	
	Controls	Molsidomine	Controls	Molsidomine
2 DAYS				
nr of pups/ nr of litters	12/7	12/7	12/6	19/10
RKW/BW (mg/g)	4.9±0.1	4.8±0.1	5.3±0.1	4.9±0.1#
2 WEEKS				
nr of pups/ nr of litters	15/8	17/10	13/8	18/10
RKW/BW (mg/g)	5.2±0.1	5.3±0.1	5.3±0.1	5.5±0.1
ADULT				
nr of pups/ nr of litters	23/10	13/4	24/10	16/5
RKW/BW (mg/g)	3.8±0.1	3.4±0.03#	4.4±0.1	4.3±0.1
Systolic blood pressure (mmHg)	158±3	139±4#	145±5	118±5#

#P<0.05 vs. controls of same gender. Biometrical data in adults published previously (Koeners et al., 2008b) are included for the sake of convenience.

Tissue NO Content

Although the NO-donor increased maternal NO metabolite excretion, the NO status of 2-week-old renal (and liver) tissue was unchanged as assayed by EPR spectroscopy of NO trapped with iron-dithiocarbamate complexes (Table 2). Unfortunately, the NO trapping procedure is not possible in 2-day-old pups.

Table 2 Nitric oxide yields (pmol MNIC/mg tissue) determined by EPR in kidneys and liver in 2-week-old control FHH and 2-week-old FHH offspring of dams treated with molsidomine.

	Males		**Females**	
	Controls	Molsidomine	Controls	Molsidomine
2WEEKS				
nr of pups/nr of litters	4/2	7/4	4/2	8/4
NO yield in kidney (left and right)	0.49±0.03	0.53±0.01	0.50±0.04	0.49±0.02
NO yield in liver	1.30±0.08	1.39±0.04	1.35±0.08	1.32±0.04

MNIC: mononitrosyl-ironcomplexes.

Microarray

Perinatal treatment with molsidomine significantly affected transcription of hundreds of genes at 2 days and at older ages (see Figure A1 in Appendix). The data also clearly shows that the transcriptional effect of molsidomine differs between ages. Few genes remained differentially expressed at all ages and those that did displayed bidirectional expression between ages.

The 40 most differentially expressed genes (20 induced and 20 reduced) were nearly all different between males and females at the same age. Several genes encoding for ribosomal proteins were present in the top 20 genes in males at all ages, however were less present in the top 20 of females (see Tables A1 in Appendix).

The present study is focused on the changes in ribosomal protein gene expression. Remarkably, these ribosomal protein genes in males were differentially induced by molsidomine at 2 days, then differentially reduced by molsidomine at both 2 weeks and in adults (see Figures 1 and 2; the collection of genes are shown in Table A2 in Appendix). These changes in ribosomal protein gene expression were significant at all ages ($P < 0.05$) and this effect was specific for ribosomal genes only in males (vs. all genes in the microarray; $P < 0.001$).

Protein Expression of L36a

In order to determine if the changes in ribosomal protein gene expression suggested by the microarray analysis could be verified at the protein level, we analyzed the expression of ribosomal protein L36a at 2 days and 2 weeks. Table A2 in Appendix shows that genes coding for the ribosomal protein L36a are subject to some of the most significant up-regulation at 2 days and down-regulation at 2 weeks (and in adults) in molsidomine-treated FHH males. Note that more than one ribosomal protein L36a gene from different chromosomes is listed on Table 2. Western blot analysis of kidney samples of FHH rats demonstrated that ribosomal protein L36a protein tends to be down-regulated by molsidomine in 2 week males (Figure 3). Quantification of three independent experiments verified that this change in ribosomal protein L36a protein expression occurred only in molsidomine-treated males at 2 weeks (Figure 3). These results suggest that despite the increase in ribosomal protein gene expression seen in 2-day-old molsidomine-treated FHH males, this increases does not manifest as an increase in ribosomal protein levels (see also Figure 4). In contrast, the western blot results suggest that the decrease in ribosomal protein gene expression at 2 weeks in molsidomine-treated rats indeed does affect L36a proteins levels, as also supported by the profiles of Figure 4.

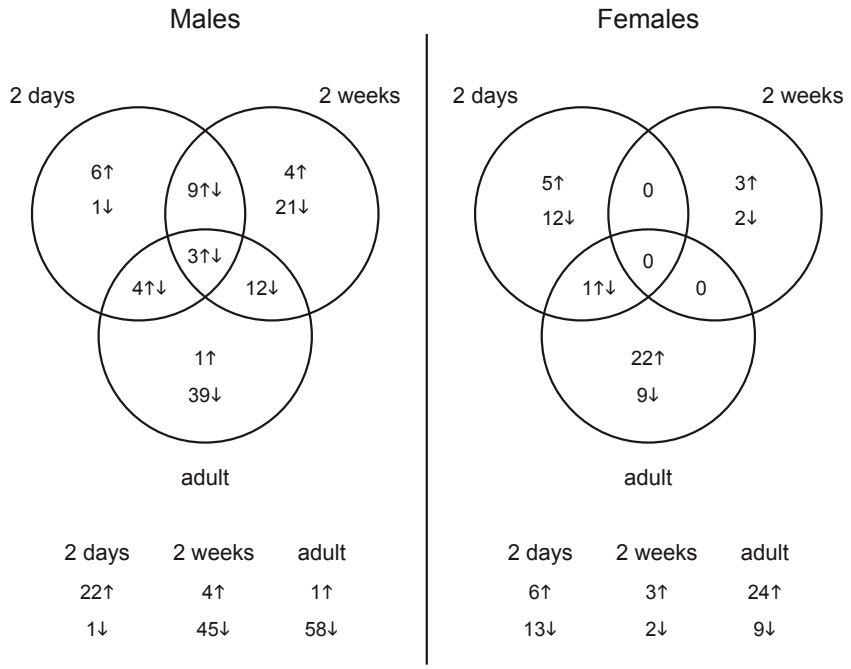

Figure 1. Number of ribosomal protein genes that are differentially expressed by molsidomine at each age per gender. The distribution of these genes between ages per gender is shown in the Venn diagram. Below the diagram is noted the total number of ribosomal protein genes that are significantly differentially expressed in molsidomine vs. control FHH rats at each age.

Ribosomal Evaluation

Polysome profiling was performed on kidneys and the effects on the peaks representing the small ribosomal subunit (40S), large ribosomal subunit (60S), and monosome (80S) were determined (Figure 4). Two days after birth and in adults, molsidomine had no effect on polysome profiles, but 2 weeks after birth all peaks were significantly reduced by molsidomine in both males and females ($P < 0.01$). This effect may be specific to the kidney, as no effect of molsidomine was observed in males at 2 weeks of age in liver polysome profiles (Figure 5). Northern blotting was performed on total RNA from 2 week FHH kidneys in order to determine rates of rRNA processing (Figure A2 in Appendix). However, no differences were observed in processing using probes binding to either the external transcribed spacer (ETS) or the internal transcribed spacer 1 (ITS1).

Immunohistochemistry

In order to determine if molsidomine resulted in a mitotic index change, we subjected kidneys from FHH rats to staining with a phospho-specific histone-3 (pH3) antibody (Figure 6). We saw no difference in the number of pH3-positive cells on molsidomine-treated FHH rat kidney slices compared to controls. As expected the number of pH3-positive cells decreased as the age of the rats increased. No pH3-positive cells were observed in adults (data not shown).

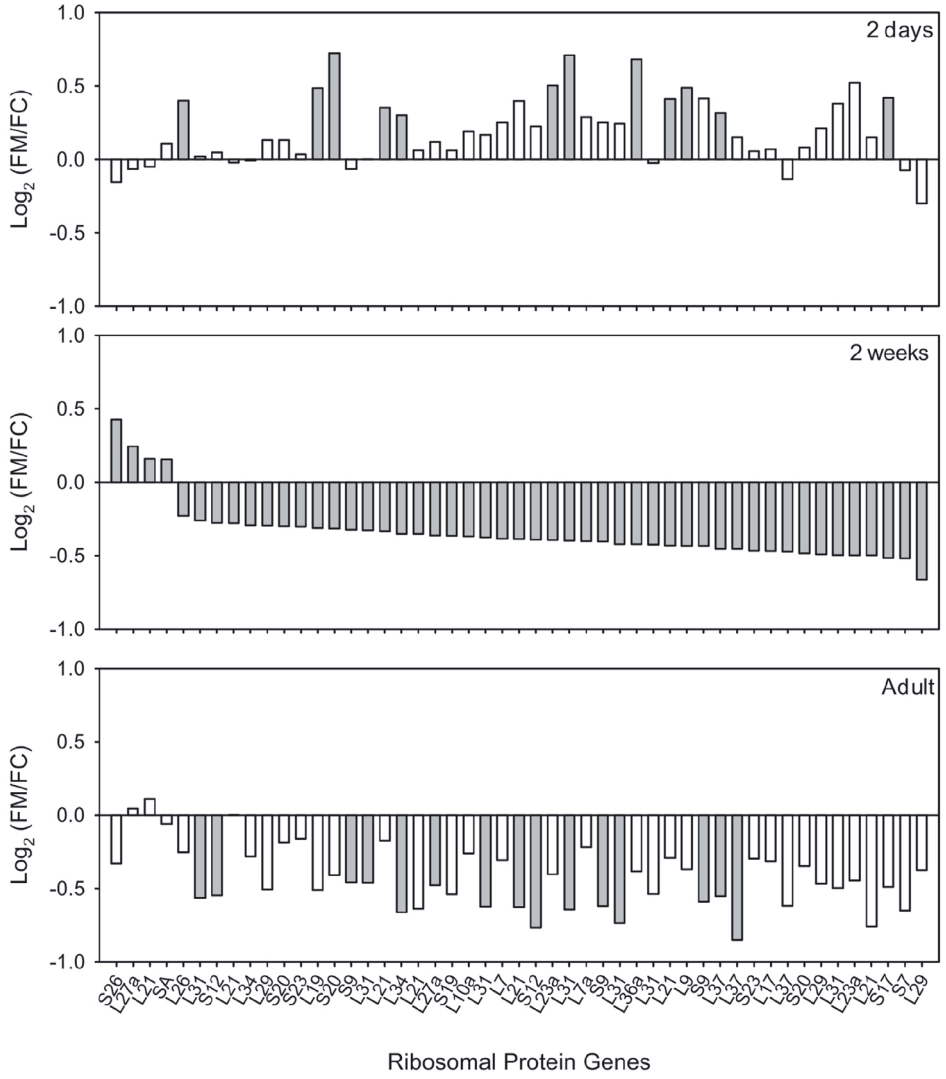

Figure 2. Ribosomal protein genes in kidneys of FHH males differentially expressed by molsidomine at 2 weeks and whether these genes were also regulated at other ages. All genes that are significantly differentially expressed by molsidomine at 2 weeks are ranked (middle panel). Some of these genes were also regulated at 2 days (upper panel) and in adults (lower panel). The ratio of the genes is expressed as Log2(FM/FC), where FM and FC are the normalized intensities of gene expression in the molsidomine and control groups, respectively. Significant differential expression is indicated by a closed bar, non-significant differential expression by an open bar.

Discussion

Nitric oxide donors are known to inhibit proliferation of mesangial and other glomerular cells in vitro (Rupprecht et al., 2000). Little is known about the effects of NO-donors on early growth and nephrogenesis. Recently we observed that administration of NO-donors during early development ameliorates the long-term phenotype in the FHH rat model of progressive hypertension-linked

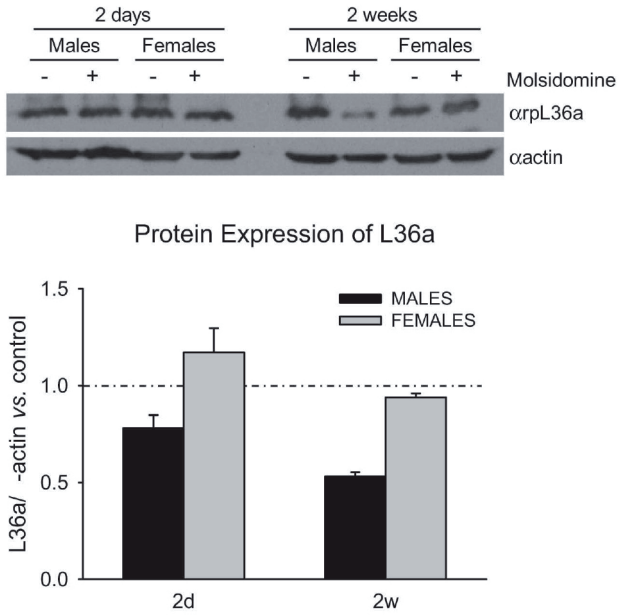

Figure 3. Western Blot on ribosomal protein L36a. Western blot analysis was performed on kidneys lysates from 2 day and 2 week control and molsidomine FHH rats of both genders using an antibody against ribosomal protein L36a (upper panel). The measured band intensity of ribosomal protein L36a was normalized by α-actin of the same sample (ribosomal protein L36a/actin). The molsidomine effect on ribosomal protein L36a/actin is expressed relative to the age- and gender matched control, shown in graph by the dotted line (lower panel). The reduction in 2 week molsidomine males is borderline significant ($p = 0.1$). All 3 replicates are biological.

renal injury (Koeners et al., 2008b). Assuming that the direct effects of the NO-donor in early development were related to an as of yet undefined aspect of renal development, the present study focused on a global analysis of ribosomal proteins as a key step in the post-transcriptional regulation of protein synthesis.

The prominent presence of ribosomal protein genes, especially in FHH males, on the lists of the most differentially expressed genes as a result of perinatal NO administration led us to examine how these changes in gene expression affected the protein levels of an individual ribosomal protein as well as the structures of mature, assembled ribosomes. Interestingly, when we measured the protein level of one of the most significantly differentially expressed gene in FHH males, ribosomal protein L36a, we found that only at 2 weeks of age did the change in gene expression correlate with a change in protein expression. This is in contrast to the ribosomal protein L36a protein levels at 2 days, which show no increase despite a substantial increase in ribosomal protein L36a gene expression at that age in males. This discrepancy may be due to the ribosome biogenesis machinery being saturated at 2 days of age and unable to incorporate higher levels of ribosomal proteins. The tight regulation of this biogenesis may likely be degrading excess ribosomal proteins at the protein level or blocking translation of ribosomal proteins at the mRNA level, although at present our data cannot distinguish between these two possibilities. No change in ribosomal protein L36a protein expression was observed in FHH females at 2 weeks of age, but this is not surprising given that no significant gene expression change of ribosomal protein L36a is seen in these animals. However, given the following data, it is likely that there is a reduction of one or more key ribosomal proteins at the protein level in FHH females at 2 weeks. Conceivably by the time the FHH rat has reached adulthood the kidney cells have adjusted the half-lives and/or degradation rates of certain ribosomal proteins in order to reach the normal number of mature ribosome structures.

The most significant finding of this study was that at 2 weeks after birth, i.e., at the end of nephrogenesis (Marquez et al., 2002), perinatal NO administration resulted in a global reduction of ribosome structures in both male and female FHH rats. All of the peaks representing major ribosome structures were found to be substantially decreased in molsidomine-treated FHH rats

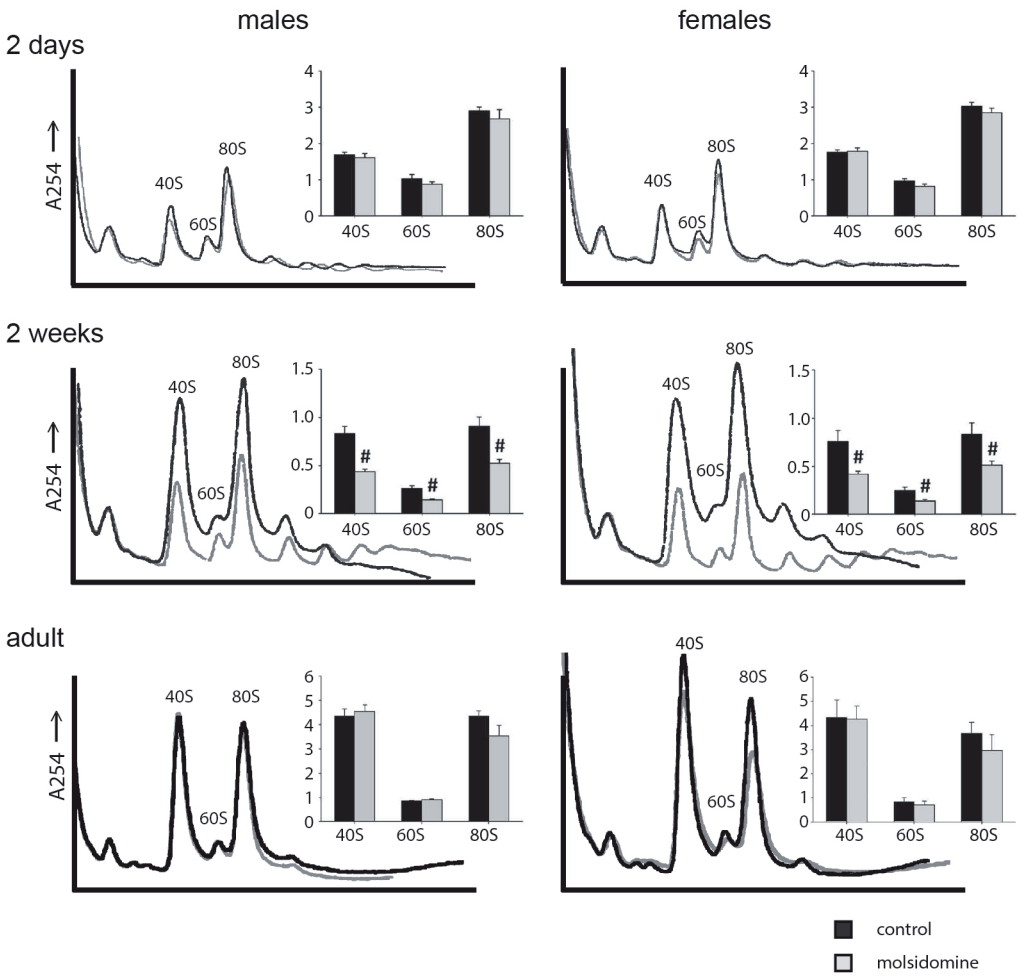

Figure 4. Polysome profiles of kidneys. Kidneys from control 2 day old (males n = 5, females n = 6), 2 week old (n = 8 in both genders), and adult (n = 4 in both genders) and molsidomine-treated 2 day old (males n = 4, females n = 6), 2 week old (n = 9 in both genders) and adult (n = 5 in both genders) FHH rats were profiled to measure the total number of assembled ribosome structures. The peaks of 40S, 60S, and 80S were normalized against the left-most peak and the results shown in the corresponding histograms. #P < 0.01 vs. untreated of the same peak.

at 2 weeks of age. This global reduction in NO-treated females at 2 weeks was surprising because only two ribosomal protein genes, coding for ribosomal protein L16 and ribosomal protein L21, were significantly reduced. Ribosomal protein L16 gene expression was not reduced by molsidomine in FHH males at 2 weeks, but strikingly 6 out of the 45 genes that were significantly reduced coded for ribosomal protein L21. This suggests that ribosomal protein L21 may be a key ribosomal protein in the biogenesis of the 60S large subunit and may also play an unappreciated role in the biogenesis of the 40S subunit. Additionally, ribosomal protein L21 appears to be important in the development of craniofacial organs (Xie et al., 2009) and a missense mutation in L21 leads to hereditary hypotrichosis simplex in humans (Zhou et al., 2011). Our findings suggest that ribosomal protein L21 may have an as yet unrecognized role in the development of blood pressure control mechanisms of the kidney.

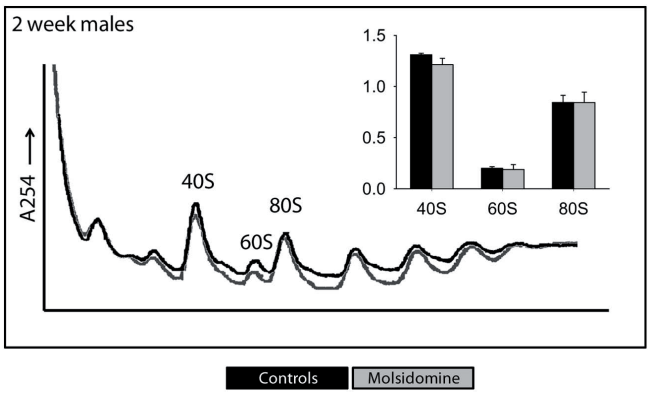

Figure 5. Polysome profiles of livers. Livers from 2-week-old FHH males were profiled to measure the total number of assembled ribosome structures. The peaks of 40S, 60S, and 80S were normalized against the left-most peak and the results shown in the corresponding histograms. Black and gray lines are from the control and molsidomine groups, respectively.

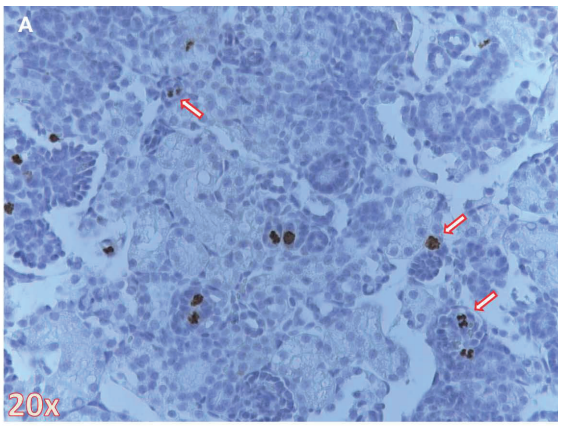

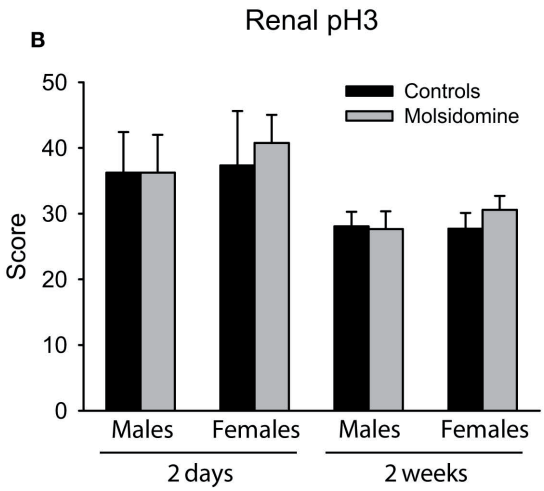

Figure 6. Phospho-histone H3 (pH3) immunohistochemistry. Histology was performed on the kidneys from 2 day, 2 week and adult control and molsidomine FHH rats of both genders for pH3. An example of positive staining for pH3 in 2 day female molsidomine-treated FHH rat is shown in (A). Several arrows indicate cells in mitosis staining positive for pH3. The number of positive cells at 2 days and 2 weeks is shown in (B). Note that data in adults is not shown as all stained sections were completely negative for pH3.

To our knowledge, this is the one of the most striking examples of a drug-induced decrease in ribosome biogenesis in an animal model to date that is not accompanied by deleterious effects. For example, rapamycin, a powerful inhibitor of the mTOR pathway that directly regulates ribosome biogenesis, when injected into rats had only a slight effect on polysome profiles of liver tissue (Reiter et al., 2004). However, doses of rapamycin as low as 1 ng/mL have been shown to negatively affect cell function and contribute to cell death, for instance in rodent islet cells (Bell et al., 2003; Tanemura et al., 2009). Moreover, many vertebrate and invertebrate models of deficiency of a single ribosomal protein due to gene deletion, knockdown, or missense mutations often show severe phenotypes (Caldarola et al., 2009), and models of biallelic loss of every ribosomal protein gene (with the one exception of ribosomal protein L22; Anderson et al., 2007) results in lethality. In contrast, our data suggest that a decrease of ribosome biogenesis during a critical period of nephrogenesis results in permanent physiologic changes to the kidney, which in turn ameliorate the hypertension phenotype late in life. Interestingly, the effects of exogenous NO on ribosomal biogenesis did not affect the liver, underlining the crucial role of NO in the developing cardiovascular system (Bustamante et al., 1996). An obvious change linked to a decrease in ribosome biogenesis would be a reduction in proliferation. However, immunohistochemistry did not reveal a change in proliferation. Note that although SIN-1, the active metabolite of molsidomine, can generate peroxynitrite in vitro, it appears to function solely as a NO-donor at in vivo oxygen concentrations (Singh et al., 1999). Indeed, recently we supplemented molsidomine to rescue cardiac function in rats with cardiorenal failure and found no increase in 3-nitrotyrosine in heart, kidney, or liver (Bongartz et al., 2010).

The mechanism of action of NO administered perinatally to FHH rats on ribosomal protein gene expression and the subsequent reduction of ribosome structures remains unclear. Indeed, direct measurement of whole kidney NO content at 2 weeks failed to show any effect of maternal NO-donor treatment, suggesting that the decrease in ribosome biogenesis at 2 weeks is programmed by an earlier event. Possibly maternal molsidomine intake results in increased placental transfer of NO adducts and increased fetal renal NO content. Alternatively, indirect effects on the placental circulation could play a role. Indeed, although previous studies (Cai et al., 2000) suggest a link between NO, rRNA synthesis and proliferation, we were unable to establish any differences in pre-rRNA levels in our model that would support direct effects of exogenous NO on rRNA production (Figure A2 in Appendix). This suggests that the effect of NO at 2 weeks more likely lies within epigenetically programmed transcriptional changes of ribosomal protein genes, as demonstrated by the microarray results. Note that in a previous study we did find an increase in offspring kidney NO content when spontaneously hypertensive rat (SHR) dams were treated with citrulline (Koeners et al., 2007). Subsequently siblings of these SHR had a lower blood pressure than control SHR. The results of the present study suggest that mechanisms underlying the antihypertensive effects of perinatal administration of the NO-donor molsidomine in rats with genetic hypertension could be quite different.

It has been previously established that perinatal NO administration alleviates the hypertension phenotype in FHH rats (Koeners et al., 2008b). The present study suggests a potential mechanism underlying this phenotype alleviation. At this stage we have no direct proof that the remarkable ribosomal changes we observe provide the causal mechanism for the beneficial effects of maternal NO on the blood pressure and renal function of the offspring. However, our data demonstrate a novel possibility that long-term amelioration of hypertension by NO in gestation may induce epigenetic changes that affect the postnatal transcription of ribosomal protein genes and a reduction of ribosome structures during a critical period of nephrogenesis.

Acknowledgments

Expert assistance: Paula P. Martens (UMC Utrecht), Jeroen Korving, and Harry Begthel (Hubrecht Institute). This study was financially supported by the Dutch Kidney Foundation (NSN C06.2168) and Royal Netherlands Academy of Arts and Sciences (KNAW).

References

1. Anderson, S. J., Lauritsen, J. P., Hartman, M. G., Foushee, A. M., Lefebvre, J. M., Shinton, S. A., Gerhardt, B., Hardy, R. R., Oravecz, T., and Wiest, D. L. (2007). Ablation of ribosomal protein L22 selectively impairs alphabeta T cell development by activation of a p53-dependent checkpoint. Immunity 26, 759–772.
2. Bell, E., Cao, X., Moibi, J. A., Greene, S. R., Young, R., Trucco, M., Gao, Z., Matschinsky, F. M., Deng, S., Markman, J. F., Naji, A., and Wolf, B. A. (2003). Rapamycin has a deleterious effect on MIN-6 cells and rat and human islets. Diabetes 52, 2731–2739.
3. Bongartz, L. G., Braam, B., Verhaar, M. C., Cramer, M. J., Goldschmeding, R., Gaillard, C. A., Steendijk, P., Doevendans, P. A., and Joles, J. A. (2010). The nitric oxide donor molsidomine rescues cardiac function in rats with chronic kidney disease and cardiac dysfunction. Am. J. Physiol. Heart Circ. Physiol. 299, H2037–H2045.
4. Bustamante, S. A., Pang, Y., Romero, S., Pierce, M. R., Voelker, C. A., Thompson, J. H., Sandoval, M., Liu, X., and Miller, M. J. (1996). Inducible nitric oxide synthase and the regulation of central vessel caliber in the fetal rat. Circulation 94, 1948–1953.
5. Cai, C. Q., Guo, H., Schroeder, R. A., Punzalan, C., and Kuo, P. C. (2000). Nitric oxide-dependent ribosomal RNA cleavage is associated with inhibition of ribosomal peptidyl transferase activity in ANA-1 murine macrophages. J. Immunol. 165, 3978–3984.
6. Caldarola, S., De Stefano, M. C., Amaldi, F., and Loreni, F. (2009). Synthesis and function of ribosomal proteins – fading models and new perspectives. FEBS J. 276, 3199–3210.
7. Chen, J. K., Chen, J., Neilson, E. G., and Harris, R. C. (2005). Role of mammalian target of rapamycin signaling in compensatory renal hypertrophy. J. Am. Soc. Nephrol. 16, 1384–1391.
8. Cowley, A. W. Jr. (2008). Renal medullary oxidative stress, pressure-natriuresis, and hypertension. Hypertension 52, 777–786.
9. Crowley, S. D., Gurley, S. B., Oliverio, M. I., Pazmino, A. K., Griffiths, R., Flannery, P. J., Spurney, R. F., Kim, H. S., Smithies, O., Le, T. H., and Coffman, T. M. (2005). Distinct roles for the kidney and systemic tissues in blood pressure regulation by the renin-angiotensin system. J. Clin. Invest. 115, 1092–1099.
10. Feelisch, M. (1998). The use of nitric oxide donors in pharmacological studies. Naunyn Schmiedebergs Arch. Pharmacol. 358, 113–122.
11. Garvin, J. L., Herrera, M., and Ortiz, P. A. (2011). Regulation of renal NaCl transport by nitric oxide, endothelin, and ATP: clinical implications. Annu. Rev. Physiol. 73, 359–376.
12. Kasinath, B. S., Mariappan, M. M., Sataranatarajan, K., Lee, M. J., and Feliers, D. (2006). mRNA translation: unexplored territory in renal science. J. Am. Soc. Nephrol. 17, 3281–3292.
13. Kim, Y. M., Son, K., Hong, S. J., Green, A., Chen, J. J., Tzeng, E., Hierholzer, C., and Billiar, T. R. (1998). Inhibition of protein synthesis by nitric oxide correlates with cytostatic activity: nitric oxide induces phosphorylation of initiation factor eIF-2 alpha. Mol. Med. 4, 179–190.
14. Koeners, M. P., Braam, B., and Joles, J. A. (2008a). Blood pressure follows the kidney: perinatal influences on hereditary hypertension. Organogenesis 4, 153–157.
15. Koeners, M. P., Braam, B., Van Der Giezen, D. M., Goldschmeding, R., and Joles, J. A. (2008b). A perinatal nitric oxide donor increases renal vascular resistance and ameliorates hypertension and glomerular injury in adult fawn-hooded hypertensive rats. Am. J. Physiol. Regul. Integr. Comp. Physiol. 294, R1847–R1855.
16. Koeners, M. P., Van Faassen, E. E., Wesseling, S., De Sain-Van Der Velden, M., Koomans, H. A., Braam, B., and Joles, J. A. (2007). Maternal supplementation with citrulline increases renal nitric oxide in young spontaneously hypertensive rats and has long-term antihypertensive effects. Hypertension 50, 1077–1084.
17. Marquez, M. G., Cabrera, I., Serrano, D. J., and Sterin-Speziale, N. (2002). Cell proliferation and morphometric changes in the rat kidney during postnatal development. Anat. Embryol. 205, 431–440.
18. McMillen, I. C., and Robinson, J. S. (2005). Developmental origins of the metabolic syndrome: prediction, plasticity, and programming. Physiol. Rev. 85, 571–633.

19. McStay, B., and Grummt, I. (2008). The epigenetics of rRNA genes: from molecular to chromosome biology. Annu. Rev. Cell Dev. Biol. 24, 131–157.
20. Reiter, A. K., Anthony, T. G., Anthony, J. C., Jefferson, L. S., and Kimball, S. R. (2004). The mTOR signaling pathway mediates control of ribosomal protein mRNA translation in rat liver. Int. J. Biochem. Cell Biol. 36, 2169–2179.
21. Rupprecht, H. D., Akagi, Y., Keil, A., and Hofer, G. (2000). Nitric oxide inhibits growth of glomerular mesangial cells: role of the transcription factor EGR-1. Kidney Int. 57, 70–82.
22. Sanij, E., and Hannan, R. D. (2009). The role of UBF in regulating the structure and dynamics of transcriptionally active rDNA chromatin. Epigenetics 4, 374–382.
23. Singh, R. J., Hogg, N., Joseph, J., Konorev, E., and Kalyanaraman, B. (1999). The peroxynitrite generator, SIN-1, becomes a nitric oxide donor in the presence of electron acceptors. Arch. Biochem. Biophys. 361, 331–339.
24. Smallegange, C., Hale, T. M., Bushfield, T. L., and Adams, M. A. (2004). Persistent lowering of pressure by transplanting kidneys from adult spontaneously hypertensive rats treated with brief antihypertensive therapy. Hypertension 44, 89–94.
25. Tanemura, M., Saga, A., Kawamoto, K., Machida, T., Deguchi, T., Nishida, T., Sawa, Y., Doki, Y., Mori, M., and Ito, T. (2009). Rapamycin induces autophagy in islets: relevance in islet transplantation. Transplant. Proc. 41, 334–338.
26. Van Dokkum, R. P., Jacob, H. J., and Provoost, A. P. (1998). Genetic differences define severity of renal damage after L-NAME-induced hypertension in rats. J. Am. Soc. Nephrol. 9, 363–371.
27. Van Faassen, E. E., Koeners, M. P., Joles, J. A., and Vanin, A. F. (2008). Detection of basal NO production in rat tissues using iron-dithiocarbamate complexes. Nitric Oxide 18, 279–286.
28. Wilcox, C. S. (2005). Oxidative stress and nitric oxide deficiency in the kidney: a critical link to hypertension? Am. J. Physiol. Regul. Integr. Comp. Physiol. 289, R913–R935.
29. Xie, M., Kobayashi, I., Kiyoshima, T., Nagata, K., Ookuma, Y., Fujiwara, H., and Sakai, H. (2009). In situ expression of ribosomal protein L21 in developing tooth germ of the mouse lower first molar. J. Mol. Histol. 40, 361–367.
30. Zhou, C., Zang, D., Jin, Y., Wu, H., Liu, Z., Du, J., and Zhang, J. (2011). Mutation in ribosomal protein L21 underlies hereditary hypotrichosis simplex. Hum. Mutat. 32, 710–714.

7

The Von Hippel Lindau tumor suppressor regulates Programmed Cell Death 5-mediated degradation of Mdm2

Paul B. Essers, Timothy A. Klasson, Tamara C. Pereboom, Dorus A. Mans, Karsten Boldt, Rachel H. Giles, Alyson W. MacInnes

Manuscript in preparation

Abstract

Functional loss of the von Hippel-Lindau tumor suppressor protein (pVHL), part of an E3 ubiquitin ligase complex, initiates most inherited and sporadic clear cell renal cell carcinomas (ccRCC). Genetic inactivation of the *TP53* gene in ccRCC is rare, suggesting that an alternate mechanism alleviates the selective pressure for *TP53* mutations in ccRCC. Here we use a zebrafish model to describe the functional consequences of pVHL loss on the p53/Mdm2 pathway. We show that p53 is stabilized in the absence of pVHL and becomes hyperstabilized upon DNA damage, which we propose is due to a novel interaction revealed between human pVHL and a negative regulator of Mdm2, the programmed cell death 5 (PDCD5) protein. PDCD5 is normally localized at the plasma membrane and in the cytoplasm, however upon hypoxia or loss of pVHL PDCD5 relocalizes to the nucleus, an event that is coupled to the degradation of Mdm2. However, despite the hyperstabilization and normal transcriptional activity of p53, we find that zebrafish *vhl-/-* cells are still as highly resistant to DNA damage-induced cell cycle arrest and apoptosis as human ccRCC cells. We suggest this is due to the large increase in expression of *birc5a*, the zebrafish homologue of survivin. Taken together, our study describes a new mechanism for p53 stabilization through PDCD5 upon pVHL loss, a finding which provides new clinical potential for the treatment of pathobiological disorders linked to hypoxic stress.

Introduction

Biallelic inactivation of the von Hippel-Lindau tumor suppressor protein (pVHL) causes the majority of inherited and sporadic kidney cancers, in particular of the clear cell renal cell carcinoma (ccRCC) subtype. Recent deep genomic sequencing efforts on sporadic ccRCCs from unrelated individuals have demonstrated that loss of function of the *VHL* gene by somatic mutation is the primary and sole driver of ccRCC until metastasis in the general population [1]. RCC is the seventh most common malignancy, responsible for 3% of all adult cancers [2] and metastasized RCC is associated with a poor prognosis in large part because of the resistance of these tumors to chemo- and radiotherapy [3].

pVHL is best known for its role in oxygen sensing, where it performs a critical function in an E3-ubiquitin ligase complex. In this complex, pVHL targets the transcription factors hypoxia inducible factor 1α and 2α (HIF1α/HIF2α) for degradation under normoxic conditions. Under hypoxic conditions, HIFα is no longer ubiquitinated by pVHL, resulting in its stabilization and the upregulation of target genes such as *VEGF, EPO* and *c-MYB* [4]. Mutations in pVHL may consequently result in a failure to recognize HIFα subunits, inducing a constitutive hypoxic response. The excessive blood vessel formation and metabolic switch to glycolysis as a result of this response can clearly assist tumorigenesis [5], but several studies have concluded that HIFα regulation alone is not sufficient to drive tumorigenesis [6-8].

The p53 tumor suppressor, normally kept at low levels by association with the E3-ubiquitin ligase MDM2, performs a critical role in the DNA damage response pathway [9]. In response to stress, p53 stabilizes and translocates as a tetramer to the nucleus to upregulate the expression of genes involved in cell cycle arrest and/or apoptosis [10]. The stabilization of p53 has been widely reported as a result of low oxygen levels [11], and there is evidence to suggest this is coupled to the hypoxia-mediated degradation of MDM2 [12]. However despite a number of hypotheses proposed [13], current understanding has not yet resolved the precise mechanisms of p53 stabilization and MDM2 degradation are in response to hypoxia.

Programmed cell death 5 (PDCD5) is a protein that functions in the apoptotic pathway to enhance caspase-3 activity through Bax translocation from the cytosol to the mitochondrial membrane resulting in cytochrome c release [14]. PDCD5 also rapidly translocates to the nucleus in an early response to DNA damage, where in addition to its effects on Bax localization has been shown to play a role in p53-induced apoptosis through the co-activation of Tip60 (a protein required for an acetylation event on p53 that leads to the transcription of apoptosis-related genes), the stabilization of p53, and the degradation of Mdm2 [15-17]. The expression of PDCD5 is found substantially reduced in several tumor types, including (but not limited to) breast tumors, gastric tumors, lung tumors, and ccRCCs compared to corresponding normal tissues [18-21]. In fact, immunohistological studies have concluded that the extent of PDCD5 expression loss is a major indicator of the tumor grade, stage, and prognosis in ccRCC patient samples [22]. However, despite the potential significance of PDCD5 expression in characterizing ccRCC, no studies of PDCD5 in relation to pVHL have been reported to date.

Little is also known about the relationship between p53 and pVHL. The mutation of both *TP53* and *VHL* in ccRCC is an extremely rare event, although it has been demonstrated in engineered mice that the loss of both genes can cause dysregulation of cellular proliferation and result in the formation of cysts and neoplastic lesions in kidneys as well as tumors in genital tract organs [23,24]. In line with the fact that most tumor cells maintaining wild type *TP53* have devised alternate mechanisms to impair p53 function, it has been reported that pVHL is able to directly bind to p53 *in vitro* and that this binding is required for p53 stabilization and induction of target gene expression [25]. However, there is significant evidence to suggest that the p53 pathway may

not be playing any role in the impaired DNA damage response that is the hallmark of ccRCC. Many other inhibitors of apoptosis are expressed during hypoxia, including the *IAP-2* and *survivin* genes [26], which are well known to inhibit caspase activation [27]. In a study using ccRCC cells devoid of functional pVHL, it was demonstrated that the observed caspase inhibition was largely due to the increased expression of antiapoptotic NFκB-target genes c-*FLIP*, *survivin*, *c-IAP-1*, and *cIAP-2* [28].

Here we investigate the functional consequences of pVHL loss on the p53/Mdm2 pathway using a previously described *in vivo* zebrafish model [29]. We provide evidence that, contrary to the previously reported *in vitro* study, the loss of pVHL results in stabilization of p53 and hyperstabilization of p53 when pVHL loss is accompanied by DNA-damage, yet this still does not initiate apoptosis. Additionally we show that Mdm2 degradation is regulated by the disruption of a pVHL-PDCD5 interaction either by hypoxia or pVHL loss resulting in the release of PDCD5 into the nucleus. Taken together, our results suggest a novel mechanism for p53 stabilization in response to hypoxia or pVHL loss that involves the degradation of Mdm2 by PDCD5

Methods

Zebrafish strains

Zebrafish were maintained as described [30]. Animal experiments were conducted in accordance with the Dutch guidelines for the care and use of laboratory animals, with the approval of the Animal Experimentation Committee (Dier Experimenten Commissie [DEC]) of the Royal Netherlands Academy of Arts and Sciences (Koninklijke Nederlandse Akademie van Wetenschappen [KNAW] (Protocol # 08.2001) The *vhl*^{hu2117} was described previously [31]. Where indicated, embryos were exposed to 25 Gy of ionizing radiation and used for analysis after 4 to 6 hours.

Cell culture

RCC10 and RCCp30d10 cells [32] were grown in RPMI medium 1640 supplemented with glutamax (Life Technologies, Carlsbad, CA, USA), 10% fetal calf serum (FCS), penicillin and streptomycin (Pen/Strep). mIMCD3 cells (CRL-2123, ATCC) were cultured in DMEM/Ham's F12 (1:1) supplemented with glutamax (Life Technologies), 10% FCS and Pen/Strep. For UV irradiation, culture medium was removed from cells and cells were irradiated in a Stratagene UV Stratalinker 2400 (Stratagene, La Jolla, CA, USA) using 1.5mJ/cm^2. Following UV irradiation, fresh medium was added to the cells..

Western Blotting

Western blots were performed using 5 embryos or, when cells were used, 30 µg of protein per lane as described [33]. The following antibodies were used: zebrafish specific anti-p53 [34], anti-p53 FL-393 (SC-6243, Santa Cruz Biotechnology, Santa Cruz, CA, USA), anti-MDM2 (SC-812, Santa Cruz Biotechnology), anti-p21 (EA10, AbCam, Cambridge, UK), anti-PDCD5 (1:500; SAB3500258, Sigma-Aldrich, St Louis, MO, USA), anti-β-actin (1:500; A5441. Sigma-Aldrich), donkey α-rabbit IgG (1:5000; NA934V, GE Healthcare, Chalfont St Giles, UK) and sheep α-mouse IgG (1:5000; NXA931, GE Healthcare). Visualization was performed with a Molecular Imager ChemiDoc XRS+ system (BioRad, Hercules, CA, USA) as per the manufacturer's instructions. Protein band quantification was done using Image J v1.44.

Strep/FLAG Tandem Affinity Purification (SF-TAP) and Mass Spectrometry (MS)

HEK293T were transfected using polyethyleneimine [35] for 48 hours with N-terminally Strep/FLAG tagged pVHL30, before being lysed in 30 mM Tris-HCl (pH 7.4), 150 mM NaCl, 0.5% Nonidet-P40, protease inhibitor cocktail (Roche, Basel, Switzerland) and phosphatase inhibitor cocktail 2 and 3 (Sigma-Aldrich) for 20 minutes at 4°C. The Streptavidin- and FLAG-based purification steps were performed as previously described [36]. 5% of final eluates were separated by SDS-PAGE and silver stained. Remaining samples were protein-precipitated with chloroform and methanol and stored at -80°C. Further processing of protein precipitates, MS analysis and peptide identification was carried out as reported previously [37]. Proteins identified in control SF-TAP experiments, were manually removed from the analysis.

qPCR analysis

Total RNA was isolated using Trizol (Invitrogen) and cDNA was made using iScript (BioRad). qPCR reactions were run using iQ SYBR Green Supermix (BioRad) on a myIQ iCycler (BioRad). The following primers were used: *p21* fw: 5'-tgtcaggaaaagcagcagaa-3', *p21* rv: 5'-ctggtgttttcgggatgttt-3', *bax* fw: 5'-gcaagttcaactggggaaga-3', *bax* rv: 5'-gtcaggaaccctggttgaaa-3', *puma* fw: 5'-tcccctccagcttaaggaat-3', *puma* rv: 5'-atcccagaatcgtgatgtcc-3', *birc2* fw: 5'-ccagtcccatttcatctcgt-3', *birc2* rv: 5'-agtgtcaaggcgttcctgtt-3', *birc5a* fw: 5'-ttgaagacgcagtgaagctc-3', *birc5a* rv: 5'-aaaaggaccacagccaaatg-3', *cflar* fw: 5'-ggatcacagaagccccagta-3', *cflar* rv: 5'-ggcattggaacacttcctgt-3', *p53* fw: 5'-ttaagtgatgtggtgcctgcct-3', *p53* rv: 5'-agcttctttccctgtttgggct-3', *Vhl* fw: 5'-ctcagccctacccgatcttac-3', *Vhl* rv 5'-acattgagggatggcacaaac-3', *Rpl27* fw: 5'-ggtgccatcgtcaatgttctt-3', *Rpl27* rv: 5'-cgccctcctttcctttctgc-3'. Three biological replicates and at least two technical replicates were performed for each measurement.

Immunohistochemistry and Acridine orange staining

Zebrafish embryos were grown in 200 μM of 1-phenyl 2-thiourea (PTU) from 28 hpf onwards. For pH3 staining, embryos were irradiated and fixed overnight in 4% paraformaldehyde [38] [38]. Embryos were then dehydrated by successive incubation in 25%, 50%, 75% and 100% methanol. The next day, embryos were rehydrated, washed in PBS with 0.1% Tween (PBST) four times and digested with 10μg/ml of proteinase K at RT for 20 min. Then, embryos were washed in PBST and refixed in 4% PFA for 20 min, washed in PBST five times and blocked in blocking buffer (PBST containing 10% lamb serum, 1% DMSO en 0.1% Tween-20) for at least 2 hours and incubated in rabbit α-pH3 antibody (1:200; Upstate Biotechnology, Lake Placid, USA) in blocking buffer overnight at 4°C. The embryos were washed extensively in PBST and incubated in Alexa-594 donkey α-rabbit IgG (1:200; Invitrogen) at 4°C overnight, washed extensively in PBST and mounted in 70% glycerol. For acridine orange staining, embryos were irradiated and soaked in 10μg/ml acridine orange (AO) (Sigma Aldrich) for 30 minutes, washed six times in E3 embryo water [30] and sedated with MS-222. Photos were obtained using a Leica MZ FLIII microscope and cells were counted using Image J v1.44. Embryos were genotyped afterwards using Sanger sequencing, as previously described [29]

siRNA treatments

Cells were seeded onto coverslips sterilized with 70% ethanol. mIMCD3 cells were transfected using the Lipofectamine RNAiMAX reagent (Invitrogen) according to the manufacturer's instructions. Mouse *Vhlh* siRNA pool (M-040755) and control siRNA pool (D–001206–13) were purchased from Dharmacon.

Immunocytochemistry

Coverslips with cells were rinsed with PBS and fixed with 4% PFA for 15 min at RT followed by permeabilization with 1% BSA plus 0.1% Triton X-100 in PBS. Cells were then subjected to immunofluorescence staining with anti-PDCD5 (1:500; SAB3500258, Sigma-Aldrich, St Louis, MO, USA) for 3 h at RT. Secondary antibody Alexa Fluor-488 anti-rabbit (1:500; Invitrogen) was incubated at RT for 2 h. Nuclei were counterstained with DAPI (1:5,000) and mounted on slides using Fluoromount G (Southern Biotech). Cells were examined using a Zeiss LSM700 confocal microscope and photographed using Zeiss Zen black edition software.

Caspase assays

Per sample, 3 zebrafish embryos were lysed in 100 µl western blot lysis buffer [33] without protease inhibitors for 30 minutes, in an opaque 96-well plate (Greiner Bio-One, Alphen a/d Rijn, The Netherlands). Subsequently, lysates were incubated with an equal volume of Caspase-Glo 3/7 assay or Caspase-Glo 2 reagent (Promega, Madison, WI, USA). For cells, 20.000 cells per well were seeded in 96-well plates and allowed to grow overnight. Medium was aspirated and the cells were lysed directly in the Caspase-Glo 3/7 or Caspase-Glo 2 reagent. Lysates were then transferred to an opaque 96-well plate. Luminescence, resulting from caspase activity was measured using a Berthold Centro XS^3 LB960 microplate reader (Berthold Technologies, Bad Wildbad, Germany).

Results

p53 is hyperstabilized in vhl zebrafish mutants upon DNA damage

To investigate whether VHL is required for p53 stabilization *in vivo*, we exposed 5 days post-fertilization (dpf) wild type and *vhl*$^{-/-}$ embryos to 25 Gy of ionizing radiation and performed western blotting with a zebrafish-specific p53 antibody [34]. Our results show that p53 becomes hyperstabilized in *vhl*$^{-/-}$ embryos upon irradiation compared to wild type embryos (Fig 1a,b). Moreover, an increase of p53 stabilization was observed in the *vhl*$^{-/-}$ embryos even in the absence of irradiation compared to wild type control embryos. *p53* transcript levels were equal between wild type and mutant embryos after irradiation, indicating that the increase of p53 protein is not due to increased *p53* transcription but increased p53 stabilization (Fig 1c). This *in vivo* data suggests that, in contrast to the previous finding that overexpressed pVHL is able to regulate p53 expression *in vitro* [25], in a physiological context an additional layer of regulation of endogenous p53 stability upon *VHL* loss must exist.

To determine whether loss of *vhl* affected transcription of p53 target genes, we measured transcript levels of the p53 target genes *p21*, *bax* and *puma* by qPCR. No significant differences were observed in the expression of these genes upon *vhl* loss (Fig 1d), indicating that functional *vhl* is not required for the transcriptional activity of p53. The transcription of p53 target genes does not increase further upon p53 hyperstabilization, which may reflect saturation of p53 binding sites on the promoters of target genes after DNA damage. To ensure that these observations are not specific to zebrafish vhl and p53, we analyzed p53 and p21 protein expression in isogenic VHL-null clear-cell RCC cells (RCC10) and RCC10 cells in which wild type pVHL has been stably reconstituted at near-endogenous levels, (RCCp30d10 cells [32]) were irradiated with 1.5mJ/cm^2 UV radiation. Western blotting showed that p53 was stabilized to normal levels (Fig 2a) and was capable of inducing p21 expression (Fig2b).

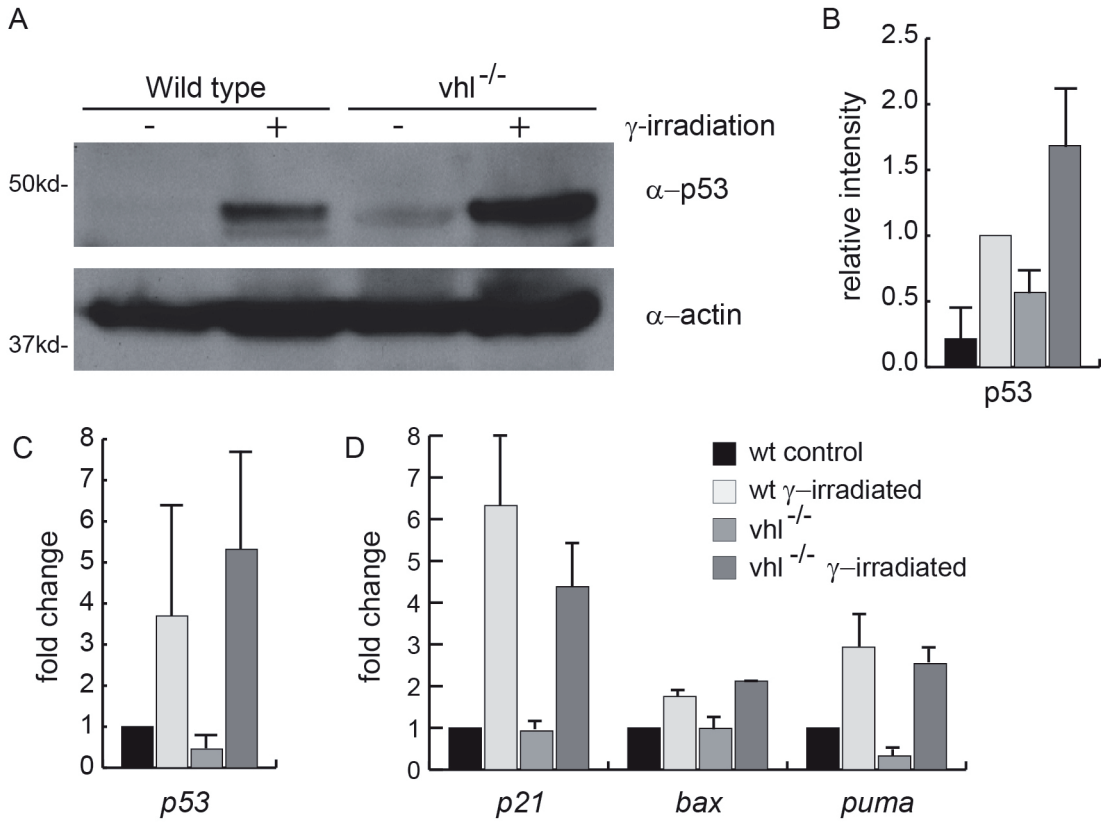

Figure 1. Loss of vhl stabilizes p53. A, western blot analysis of p53 levels in wild type and vhl-/- embryos at 5dpf, 6 hours after γ-irradiation. B, measurements of western blot band intensity, showing the results for 3 independent experiments. C and D, qPCR analysis of p53 transcript levels (C) and p53 target gene expression (D) in wild type and vhl-/- embryos at 5dpf, 6 hours after γ-irradiation.

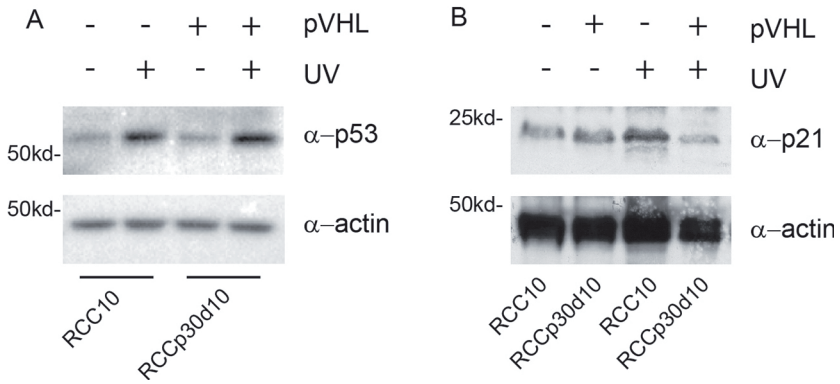

Figure 2. RCC cell lines are able to stabilize p53. A and B, Western blot analysis of p53 (A) and p21 (B) levels in RCC10 cells, devoid of functional *VHL*, and RCCP30d10 cells, which do express *VHL*. Where indicated, cells were exposed to UV irradiation to induce DNA damage.

Loss of vhl or hypoxia results in nuclear relocalization of PDCD5 and subsequent MDM2 degradation

To gain insight into the regulation of p53 by pVHL on protein level, we performed tandem-affinity purifications of TAP-tagged pVHL in HEK293 cells, followed by mass spectrometry in duplicate. We were able to identify established binding partners of pVHL, for example components of the E3 ubiquitin ligase complex (cullin-2, elongin B, elongin C and Rbx1) [39-41], von Hippel-Lindau binding protein [42] and collagens [43] (Table 1 and Fig S1). We did not observe an interaction between pVHL and p53, but we did identify a robust interaction in several independent experiments between pVHL and programmed cell death protein 5 (PDCD5), an important positive regulator of apoptosis [44]. Western blot analysis in 5 dpf zebrafish embryos and RCC lysates indicated that vhl does not target PDCD5 for degradation, as PDCD5 protein levels remain constant in the absence of vhl/pVHL (Fig S2a). Immunocytochemical analysis revealed that PDCD5 localizes to the membrane in RCCP30d10 cells and this membranous staining is lost in the RCC10 cells that are devoid of pVHL (Fig 3a). Cells were scored for membranous and cytosolic staining patterns to quantify this effect (Fig 3b). To verify that pVHL determines PDCD5 localization directly, and is not the result of clonal drift, we used siRNA to knock down *Vhlh* in mIMCD3 mouse inner collecting duct cells. Immunocytochemical analysis in these cells shows that PDCD5 localizes to the cell membrane and is absent from the nucleus in cells transfected with a control siRNA (Fig 3c). In cells transfected with the siRNA against vhl, PDCD5 is largely absent from the cell membrane and accumulates in the nucleus (Fig 3c). In order to ascertain if this PDCD5 relocalization to the nucleus is due to the stabilization of HIF in the absence of pVHL, we repeated the immunocytochemistry experiments with cells exposed to hypoxia (1% O_2) compared to normoxia (21% O_2). We recapitulated the same shift of PDCD5 to the nucleus of hypoxic cells, indicating that the relocalization of PDCD5 is regulated by HIF (Fig 3d). Staining of these cells with HIF antibodies illustrates the expected increase of HIF expression (Figure S2b). qPCR was used to confirm that knockdown of *Vhlh* was effective (Fig 3e). We then used western blot analysis to determine how this relocalization of PDCD5 upon pVHL loss affects Mdm2 expression. The transfection of mlMCD3 cells with siRNAs against Vhl, but not control siRNAs, resulted in a substantial reduction (56±2%) of Mdm2 protein (Fig 3f). Consistent with these results, we found that Mdm2 protein

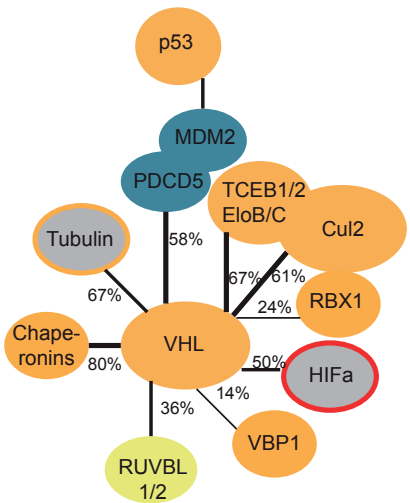

Figure S1. Schematic representation of protein-protein interaction data revealed from mass spectrometry of pVHL 4 independent TAP pull-down assays. Previously identified direct interactions are provided as orange nodes, previously identified and possibly indirect interactions are shown as grey nodes, and nodes with a red outline indicate proteins whose stability/ turnover is regulated by pVHL. This study focuses on the novel finding that pVHL binds PDCD5 thereby regulating MDM2 (blue nodes). An additional novel and robust finding is that VHL interacts with the RVBL1/2 complex (yellow node). Percentages on the edges between nodes represents the peptide coverage, which is often used as a surrogate for binding confidence.

Entrez Gene ID	Entrez Gene Symbol	VHL SeqCov	VHL Peptide Count
10576	CCT2	0.85	49
22948	CCT5	0.82	45
10574	CCT7	0.82	44
10575	CCT4	0.81	46
6950	TCP1	0.81	40
10694	CCT8	0.8	49
7203	CCT3	0.8	53
3303	HSPA1A	0.68	35
3304	HSPA1B	0.68	35
203068	TUBB	0.67	22
10383	TUBB4B	0.67	4
10382	TUBB4A	0.66	3
6921	TCEB1	0.66	7
3312	HSPA8	0.65	40
908	CCT6A	0.65	37
6923	TCEB2	0.65	12
3301	DNAJA1	0.64	21
8453	CUL2	0.61	47
347733	TUBB2B	0.6	5
7846	TUBA1A	0.6	23
9141	PDCD5	0.58	7
84790	TUBA1C	0.55	3
292	SLC25A5	0.51	18
293	SLC25A6	0.47	6
9349	RPL23	0.43	5
7428	VHL	0.43	13
84833	USMG5	0.43	2
10294	DNAJA2	0.4	13
7311	UBA52	0.38	5
10856	RUVBL2	0.37	14
9131	AIFM1	0.37	18
51060	TXNDC12	0.37	18
5250	SLC25A3	0.37	12
8607	RUVBL1	0.36	14
84617	TUBB6	0.36	5
4697	NDUFA4	0.36	3
6169	RPL38	0.36	2
9093	DNAJA3	0.36	17
6748	SSR4	0.36	5
1915	EEF1A1	0.35	14
8985	PLOD3	0.35	21

Table 1. Binding partners of VHL identified in our TAP - mass spectrometry experiment

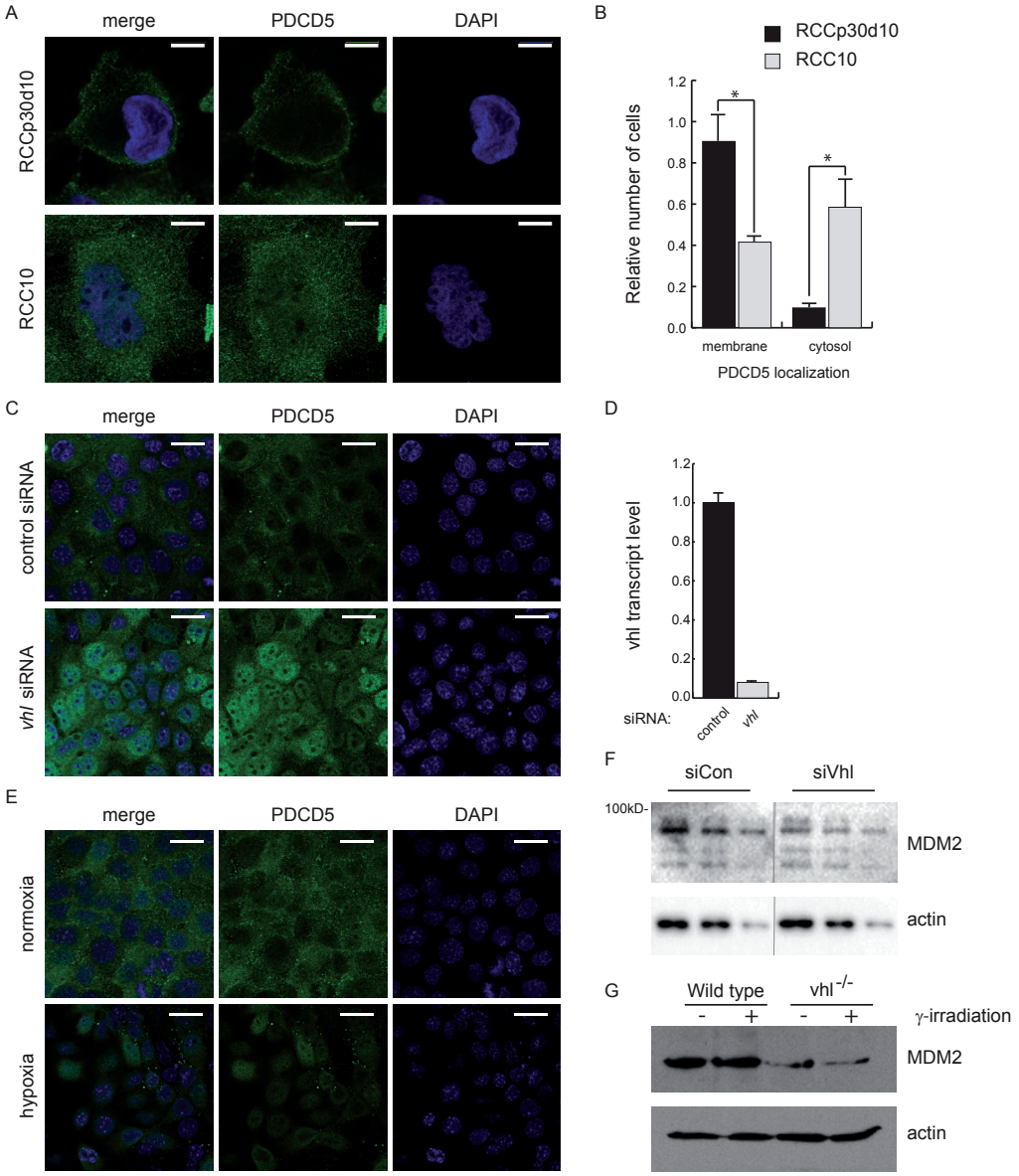

Figure 3. Loss of VHL causes PDCD5 to be released from the cell membrane and translocated into the nucleus. A, Immunocytochemical stain for PDCD5 protein (green) and nuclei (blue) in RCC cells, showing membranous staining in RCCp30d10 but not RCC10 cells. Scale bar = 10μm. B, manual quantification of the proportion of cells with membranous and cytoplasmic PDCD5 localization. C, Immunocytochemical analysis of PDCD5 (green) and nuclei (blue) in IMCD3 cells treated with siRNA agains *VHL,* showing PDCD5 nuclear translocation in the absence of *VHL*. Scale bar = 20μm. D, qPCR confirming the knockdown of *VHL* transcripts in the experiment described in C, normalized to Rpl27 expression. E, Immunocytochemical analysis of PDCD5 (green) and nuclei (blue) in IMCD3 cells cultured under hypoxic conditions. Scale bar = 20μm. F, western blot analysis of Mdm2 levels in IMCD3 cells treated with siRNA against *VHL*. A line indicates where several lanes were removed from the blot. G, Western blot analysis of mdm2 levels in wild type and *vhl*$^{-/-}$ embryos.. * $p < 0.01$.

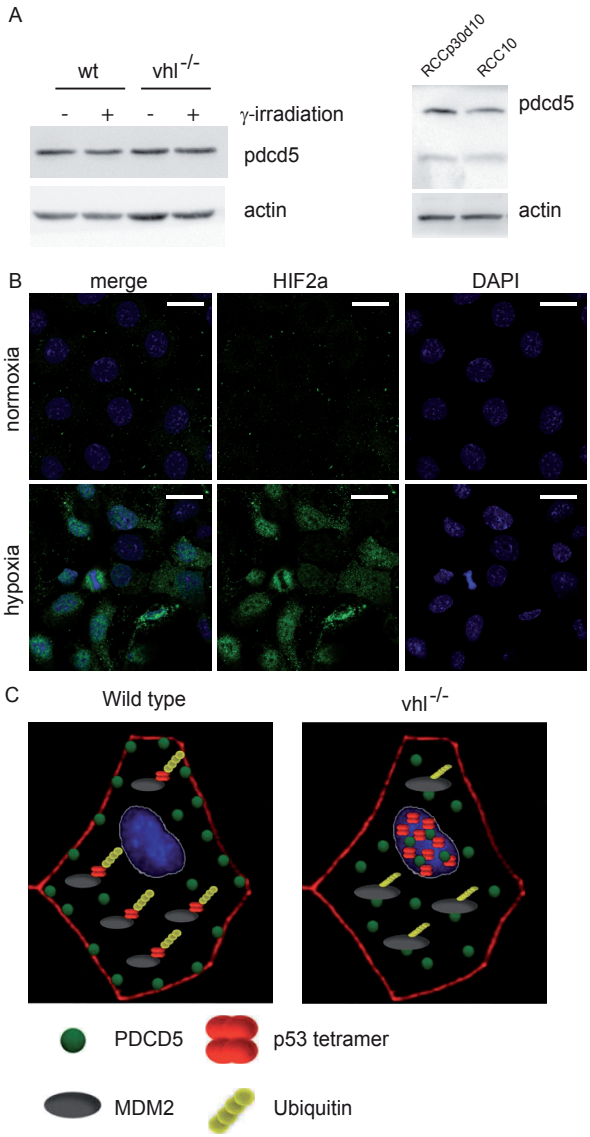

Figure S2. Loss of vhl has no effect on total PDCD5 levels. A, Western blot analysis of PDCD5 levels in 5dpf embryos, 6 hours after γ-irradiation. This experiment is representative of 3 experiments performed. B, Immunocytochemical analysis to confirm Hifα upregulation in the experiment described in Fig3E. C, model showing how loss of *vhl* leads to PDCD5 nuclear translocation and p53 stabilization

levels were significantly reduced as well in *vhl-/-* zebrafish embryos (Fig 3g). Altogether these data suggest the stabilization of p53 in the absence of pVHL or presence of hypoxia is due to the degradation of Mdm2 upon relocalization of PDCD5 to the nucleus (model illustrated in Figure S2c).

Vhl is required for p53-mediated cell cycle arrest and apoptosis

To investigate whether loss of *vhl* affects p53-mediated cell cycle arrest and apoptosis in our zebrafish model, we first measured the number of dividing cells in embryos after irradiation at 5 dpf. The application of gamma-radiation normally leads to cell cycle arrest and a decrease of the number of cells undergoing mitosis [45], which can be detected by labeling cells with a phospho-specific Histone 3 (pH3) antibody. While gamma-radiation led to an approximate 3-fold decrease in the number of mitotic cells in wild type embryos, we observed a significantly greater number of mitotic cells in *vhl-/-* mutant embryos, indicating an impaired cell cycle arrest response to DNA damage (Fig 4a, b). To examine the apoptotic response of the *vhl-/-* embryonic cells subject to the same DNA damage, we performed measurements of activated caspase-3/7 and caspase-2 activity. Fig 4c demonstrates that the loss of *vhl* prevents the activation of either caspase 3/7 or caspase 2. Consistent with these results, Fig 4d and e illustrate that in vivo *vhl* loss prevents the normal accumulation of apoptotic cells upon DNA damage as detected by acridine orange staining, (Fig 4d, e). RCC10 cells were likewise resistant to UV-induced caspase activation, while RCCP30D10 cells reconstituted with VHL were not (Fig 4f). As it has been shown in RCC cells that the nuclear factor κB (NFκB) dependent anti-apoptotic pathway can prevent tumor necrosis factor α induced cytotoxicity [28], we measured levels of NFκB targets in the *vhl-/-* embryos. We found that expression levels of *birc5a,* the zebrafish homolog of survivin, are

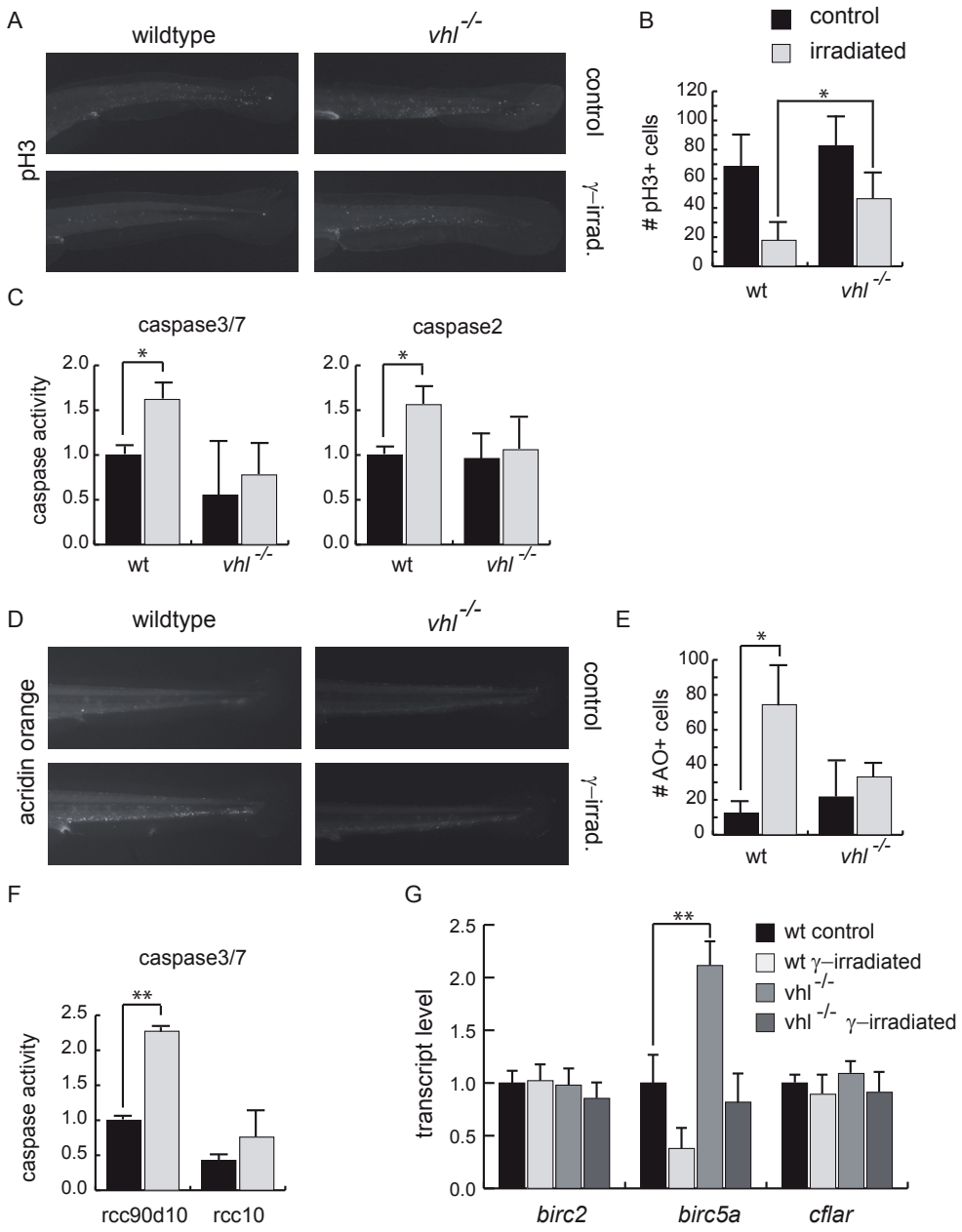

Figure 4. DNA damage fails to induce cell cycle arrest and apoptosis in vhl$^{-/-}$ embryos. A, immunohistochemical analysis of pH3 in the tails of 5dpf embryos after γ-irradiation. The tail of the embryo was used to enable quantification of positive cells. B, quantification of the number of pH3-positive cells in the tails of at least 4 embryos per condition. C, measurement of caspase activity in 5dpf embryos after γ-irradiation. D, measurement of caspase activity in RCC cell lines after UV-irradiation. E, acridin orange stain of apoptotic cells in the tails of 5dpf embryos after γ-irradiation. F, quantification of the number of acridin orange-positive cells in the tails of at least 9 embryos per condition. G, qPCR analysis of the transcript levels of several inhibitors of apoptosis in 5dpf embryos, 6 hours after γ-irradiation..* $p < 0.01$, ** $p < 0.00001$

substantially elevated in *vhl*$^{-/-}$ mutants (Fig 5a). Taken together, these data suggest that despite the hyperstabilization of p53 and transcription of target genes observed upon DNA damage in cells devoid of vhl as well as other compounding mutations expected in the human cancer cell lines, other factors such as increased *birc5a* expression prevent the activation of the apoptotic program.

Discussion

One advantage of studying *VHL* loss in the zebrafish model is the lack of other oncogenic mutations that are invariably present in the tumor suppressor pathways of immortalized cancer cell lines. This provided us with an opportunity to clearly gauge what amount of influence the p53 pathway has on the DNA damage response of cells in the absence of VHL. The hyperstabilization of p53 in the zebrafish mutants that we found coupled to the normal induction of p53 target genes may have been expected to produce a normal, or even augmented, DNA damage response. However, when the downstream effects of p53 activation were examined, it became clear that vhl is required farther downstream in the apoptotic pathway.

Initial murine studies of VHL-driven RCC tumorigensis were limited to heterozygous mice due to the embryonic lethality observed [46,47]. In these mice, liver vascular lesions were the only phenotype observed, and an increased incidence of RCC was not found [46], even when mice were treated with high doses of carcinogen [47]. When pVHL was conditionally knocked out in the renal proximal tubule, occasional renal cysts were observed, but not RCC [48]. Alternatively, mutating the hydroxylation sites in HIFα in mice results in a kidney histology that is similar to human RCC [49] with concomitant upregulation of proliferation markers and the presence of genomic instability in abnormal proximal tubule cells, but no RCC development is reported [49]. However, it should be pointed out that despite enormous efforts to date there are very few validated models of murine kidney cancer. RCC development in an animal model was recently reported for the first time, achieved through simultaneous deletion of *p53* and *Vhlh*. Although loss of p53 itself is a very rare event in RCC, these findings support the idea that loss of p53 downstream signaling pathways is important for malignant transformation of *VHL*$^{-/-}$ cells. In recent years it has become clear that pVHL is not only involved in HIFα regulation, but functions as an adaptor protein in many other processes [50], including stress response, survival, senescence, adhesion, invasion and primary cilium function. Using zebrafish embryos as a model system, the problem of embryonic lethality is bypassed without limiting studies to the role of pVHL in HIFα signaling.

We provide with this work a novel mechanism for the stabilization of p53 upon hypoxia, and show that despite the hyperstabilization of p53 upon DNA damage in vhl deficient cells there exists a powerful inhibition of apoptosis. However, given the multifunctional role of PDCD5 in driving apoptosis, it is possible that one of the more downstream functions, such as relocalizing Bax to the mitochondria and releasing cytochrome c, may be exploited clinically such that PDCD5 expression and/or activity is enhanced to overcome the apoptosis inhibition. Conversely, the inhibition of PDCD5 may be a promising treatment for conditions that arise from prolonged systemic hypoxia, such as neurodegeneration and Alzheimer's disease. Revealing the role of PDCD5 in the p53 pathway and in response to hypoxia thus presents an exciting new angle for the treatment of a wide-spanning range of diseases.

Acknowledgements

This research was supported by grants from the Netherlands Organization for Scientific Research to R.H.G. (NWO Vidi-917.66.354); the European Community's Seventh Framework Programme FP7/2009 under grant agreement no: 241955, SYSCILIA (R.H.G).

References

1. Gerlinger M, Rowan AJ, Horswell S, Larkin J, Endesfelder D, et al. (2012) Intratumor heterogeneity and branched evolution revealed by multiregion sequencing. N Engl J Med 366: 883-892.
2. Cohen HT, McGovern FJ (2005) Renal-cell carcinoma. N Engl J Med 353: 2477-2490.
3. Motzer RJ, Bander NH, Nanus DM (1996) Renal-cell carcinoma. N Engl J Med 335: 865-875.
4. Hsu T (2012) Complex cellular functions of the von Hippel-Lindau tumor suppressor gene: insights from model organisms. Oncogene 31: 2247-2257.
5. Semenza GL (2003) Targeting HIF-1 for cancer therapy. Nat Rev Cancer 3: 721-732.
6. Kondo K, Klco J, Nakamura E, Lechpammer M, Kaelin WG, Jr. (2002) Inhibition of HIF is necessary for tumor suppression by the von Hippel-Lindau protein. Cancer Cell 1: 237-246.
7. Mack FA, Rathmell WK, Arsham AM, Gnarra J, Keith B, et al. (2003) Loss of pVHL is sufficient to cause HIF dysregulation in primary cells but does not promote tumor growth. Cancer Cell 3: 75-88.
8. Maranchie JK, Vasselli JR, Riss J, Bonifacino JS, Linehan WM, et al. (2002) The contribution of VHL substrate binding and HIF1-alpha to the phenotype of VHL loss in renal cell carcinoma. Cancer Cell 1: 247-255.
9. Horn HF, Vousden KH (2007) Coping with stress: multiple ways to activate p53. Oncogene 26: 1306-1316.
10. Kubbutat MH, Jones SN, Vousden KH (1997) Regulation of p53 stability by Mdm2. Nature 387: 299-303.
11. Graeber TG, Peterson JF, Tsai M, Monica K, Fornace AJ, Jr., et al. (1994) Hypoxia induces accumulation of p53 protein, but activation of a G1-phase checkpoint by low-oxygen conditions is independent of p53 status. Molecular and cellular biology 14: 6264-6277.
12. Alarcon R, Koumenis C, Geyer RK, Maki CG, Giaccia AJ (1999) Hypoxia induces p53 accumulation through MDM2 down-regulation and inhibition of E6-mediated degradation. Cancer Res 59: 6046-6051.
13. Sermeus A, Michiels C (2011) Reciprocal influence of the p53 and the hypoxic pathways. Cell Death Dis 2: e164.
14. Chen LN, Wang Y, Ma DL, Chen YY (2006) Short interfering RNA against the PDCD5 attenuates cell apoptosis and caspase-3 activity induced by Bax overexpression. Apoptosis 11: 101-111.
15. Xu L, Chen Y, Song Q, Xu D, Wang Y, et al. (2009) PDCD5 interacts with Tip60 and functions as a cooperator in acetyltransferase activity and DNA damage-induced apoptosis. Neoplasia 11: 345-354.
16. Xu L, Hu J, Zhao Y, Hu J, Xiao J, et al. (2012) PDCD5 interacts with p53 and functions as a positive regulator in the p53 pathway. Apoptosis 17: 1235-1245.
17. Chen Y, Sun R, Han W, Zhang Y, Song Q, et al. (2001) Nuclear translocation of PDCD5 (TFAR19): an early signal for apoptosis? FEBS Lett 509: 191-196.
18. Zucchi I, Mento E, Kuznetsov VA, Scotti M, Valsecchi V, et al. (2004) Gene expression profiles of epithelial cells microscopically isolated from a breast-invasive ductal carcinoma and a nodal metastasis. Proceedings of the National Academy of Sciences of the United States of America 101: 18147-18152.
19. Yang YH, Zhao M, Li WM, Lu YY, Chen YY, et al. (2006) Expression of programmed cell death 5 gene involves in regulation of apoptosis in gastric tumor cells. Apoptosis 11: 993-1001.
20. Spinola M, Meyer P, Kammerer S, Falvella FS, Boettger MB, et al. (2006) Association of the PDCD5 locus with lung cancer risk and prognosis in smokers. J Clin Oncol 24: 1672-1678.
21. Xiong L, Tan WL, Yu ZC, Wu YD, Huang H, et al. (2006) [Expression of TFAR19(PDCD5) in normal human kidney, renal clear cell carcinoma, normal human bladder and bladder carcinoma]. Nan Fang Yi Ke Da Xue Xue Bao 26: 805-809.
22. Tan WL, Xiong L, Zheng SB, Yu ZC, Qi H, et al. (2006) [Relationship between programmed cell death 5 protein expression and prognosis of renal clear cell carcinoma]. Nan Fang Yi Ke Da Xue Xue Bao 26: 1316-1318.
23. Szymanska K, Moore LE, Rothman N, Chow WH, Waldman F, et al. (2010) TP53, EGFR, and KRAS mutations in relation to VHL inactivation and lifestyle risk factors in renal-cell carcinoma from central and eastern Europe. Cancer Lett 293: 92-98.
24. Albers J, Rajski M, Schonenberger D, Harlander S, Schraml P, et al. (2013) Combined mutation of Vhl and Trp53 causes renal cysts and tumours in mice. EMBO Mol Med.
25. Roe JS, Kim H, Lee SM, Kim ST, Cho EJ, et al. (2006) p53 stabilization and transactivation by a von Hippel-Lindau protein. Mol Cell 22: 395-405.
26. Dong Z, Nishiyama J, Yi X, Venkatachalam MA, Denton M, et al. (2002) Gene promoter of apoptosis inhibitory protein IAP2: identification of enhancer elements and activation by severe hypoxia. Biochem J 364: 413-421.

27. Dong Z, Wang JZ, Yu F, Venkatachalam MA (2003) Apoptosis-resistance of hypoxic cells: multiple factors involved and a role for IAP-2. Am J Pathol 163: 663-671.
28. Qi H, Ohh M (2003) The von Hippel-Lindau tumor suppressor protein sensitizes renal cell carcinoma cells to tumor necrosis factor-induced cytotoxicity by suppressing the nuclear factor-kappaB-dependent antiapoptotic pathway. Cancer Res 63: 7076-7080.
29. van Rooijen E, Voest EE, Logister I, Korving J, Schwerte T, et al. (2009) Zebrafish mutants in the von Hippel-Lindau tumor suppressor display a hypoxic response and recapitulate key aspects of Chuvash polycythemia. Blood 113: 6449-6460.
30. Westerfield M (2000) The zebrafish book. A guide for the laboratory use of zebrafish (Danio rerio). Eugene, OR: Univ. of Oregon Press.
31. van Rooijen E, Santhakumar K, Logister I, Voest E, Schulte-Merker S, et al. (2011) A zebrafish model for VHL and hypoxia signaling. Methods Cell Biol 105: 163-190.
32. Esteban MA, Tran MG, Harten SK, Hill P, Castellanos MC, et al. (2006) Regulation of E-cadherin expression by VHL and hypoxia-inducible factor. Cancer Res 66: 3567-3575.
33. Pereboom TC, van Weele LJ, Bondt A, MacInnes AW (2011) A zebrafish model of dyskeratosis congenita reveals hematopoietic stem cell formation failure resulting from ribosomal protein-mediated p53 stabilization. Blood 118: 5458-5465.
34. MacInnes AW, Amsterdam A, Whittaker CA, Hopkins N, Lees JA (2008) Loss of p53 synthesis in zebrafish tumors with ribosomal protein gene mutations. Proc Natl Acad Sci U S A 105: 10408-10413.
35. Kim EL, Wustenberg R, Rubsam A, Schmitz-Salue C, Warnecke G, et al. (2010) Chloroquine activates the p53 pathway and induces apoptosis in human glioma cells. Neuro Oncol 12: 389-400.
36. Coene KL, Mans DA, Boldt K, Gloeckner CJ, van Reeuwijk J, et al. (2011) The ciliopathy-associated protein homologs RPGRIP1 and RPGRIP1L are linked to cilium integrity through interaction with Nek4 serine/threonine kinase. Hum Mol Genet 20: 3592-3605.
37. Boldt K, Mans DA, Won J, van Reeuwijk J, Vogt A, et al. (2011) Disruption of intraflagellar protein transport in photoreceptor cilia causes Leber congenital amaurosis in humans and mice. J Clin Invest 121: 2169-2180.
38. Shepard JL, Stern HM, Pfaff KL, Amatruda JF (2004) Analysis of the cell cycle in zebrafish embryos. Methods Cell Biol 76: 109-125.
39. Kibel A, Iliopoulos O, DeCaprio JA, Kaelin WG, Jr. (1995) Binding of the von Hippel-Lindau tumor suppressor protein to Elongin B and C. Science 269: 1444-1446.
40. Pause A, Lee S, Worrell RA, Chen DY, Burgess WH, et al. (1997) The von Hippel-Lindau tumor-suppressor gene product forms a stable complex with human CUL-2, a member of the Cdc53 family of proteins. Proc Natl Acad Sci U S A 94: 2156-2161.
41. Kamura T, Koepp DM, Conrad MN, Skowyra D, Moreland RJ, et al. (1999) Rbx1, a component of the VHL tumor suppressor complex and SCF ubiquitin ligase. Science 284: 657-661.
42. Tsuchiya H, Iseda T, Hino O (1996) Identification of a novel protein (VBP-1) binding to the von Hippel-Lindau (VHL) tumor suppressor gene product. Cancer Res 56: 2881-2885.
43. Lai Y, Song M, Hakala K, Weintraub ST, Shiio Y (2011) Proteomic dissection of the von Hippel-Lindau (VHL) interactome. J Proteome Res 10: 5175-5182.
44. Xu L, Hu J, Zhao Y, Xiao J, Wang Y, et al. (2012) PDCD5 interacts with p53 and functions as a positive regulator in the p53 pathway. Apoptosis 17: 1235-1245.
45. Sansam CL, Cruz NM, Danielian PS, Amsterdam A, Lau ML, et al. (2010) A vertebrate gene, ticrr, is an essential checkpoint and replication regulator. Genes Dev 24: 183-194.
46. Haase VH, Glickman JN, Socolovsky M, Jaenisch R (2001) Vascular tumors in livers with targeted inactivation of the von Hippel-Lindau tumor suppressor. Proc Natl Acad Sci U S A 98: 1583-1588.
47. Kleymenova E, Everitt JI, Pluta L, Portis M, Gnarra JR, et al. (2004) Susceptibility to vascular neoplasms but no increased susceptibility to renal carcinogenesis in Vhl knockout mice. Carcinogenesis 25: 309-315.
48. Rankin EB, Tomaszewski JE, Haase VH (2006) Renal cyst development in mice with conditional inactivation of the von Hippel-Lindau tumor suppressor. Cancer Res 66: 2576-2583.
49. Fu L, Wang G, Shevchuk MM, Nanus DM, Gudas LJ (2011) Generation of a mouse model of Von Hippel-Lindau kidney disease leading to renal cancers by expression of a constitutively active mutant of HIF1alpha. Cancer Res 71: 6848-6856.
50. Frew IJ, Krek W (2008) pVHL: a multipurpose adaptor protein. Sci Signal 1: pe30.

Summarizing Discussion

Part 1: Ribosome biogenesis and translation

Ribosomes are the mediators of protein synthesis in the cell and therefore crucial to proper cell function. In addition, ribosomes are highly abundant, with ribosomal RNA making up 80% of the RNA in the cell [1]. A large amount of resources go into maintaining this pool of ribosomes, so ribosome biogenesis and translation are highly controlled mechanisms. In this thesis we explore both ribosome biogenesis defects and physiological control of ribosome numbers and translation efficiency.

Nucleostemin family members in ribosome biogenesis and neural differentiation

Guanine binding protein like 2 (*gnl2*), *nucleostemin* (*ns* or *gnl3)* and *gnl3-like* (*gnl3l)* are part of the family of YlqF Related GTPases. They are the only members of this family that localize to the nucleolus [2]. In a previous study in our lab, a *gnl2* loss of function mutant was found in a forward mutagenesis screen as having aberrant neuronal differentiation at 24hpf [3]. In addition, p53 was stabilized in these mutants. A *ns* loss of function mutant was found to have similar defects. Both *gnl2* and *ns* were shown to be required for correct timing of cell cycle exit and subsequent differentiation, independently of p53 signaling [3]. Multiple studies had already suggested that *ns* plays a role in stem cell maintenance and is likely to be required for proliferation. In line with their nucleolar localization, both *ns* [4,5] and *gnl3l [6]* were previously shown to function in ribosome biogenesis. In addition, loss of *ns* had been shown to induce p53 stabilization through ribosomal proteins released from the nucleolus as a result of defective ribosome biogenesis [7]. In chapter 2 of this thesis, we set out to determine what the role of each of the zebrafish *ns* family members is in ribosome biogenesis. In chapter 3 we explored what the relation is between their functions in ribosome biogenesis and neurogenesis.

Gnl2 *and* ns*, but not* gnl3l*, are required for ribosome biogenesis in zebrafish*

18S, 5.8S and 28S rRNA are transcribed in a single precursor transcript which subsequently cleaved in a series of processing steps to generate the mature rRNAs. Ns was shown to associate with factors involved in this processing, and loss of *Ns* resulted in impaired cleavage of 32S to 28S rRNA [4]. We observed reduced processing of the primary transcript in each *ns* family mutant. In addition, *gnl2* and *ns* showed more specific defects, both at set of cleavage steps resulting in the separation of 5.8S, ITS2 and 28S. This correlates well with the conclusions of Romanova et al. [4], although this study used a method with a lower resolution, which was unable to detect any processing intermediates or 5.8S rRNA. This study did also show the retention of the primary transcript, although the authors did not comment on these findings [4].

To assess these defects on a functional level, we performed polysome profiles and observed a loss of polysomes and the formation of halfmers in both the *gnl2* and *ns* mutants, with an additional decrease of 60S subunits in the ns mutant not observed in the *gnl2* mutant. The *gnl3* mutants only showed a mild decrease of monosomes and polysomes. These defects lead to a decrease in protein translation in *gnl2* and *ns*, but not in *gnl3l* mutants. We conclude that in zebrafish, *gnl2* and *ns*, but not *gnl3l*, are required for ribosome biogenesis. Combining these data with the previous finding that heterologous expression of human Gnl3l is able to rescue the ribosome biogenesis defects caused by the deletion of grn1 loss in yeast [6] suggests two possibilities: either *gnl3l* has a redundant function in ribosome biogenesis or zebrafish and human *gnl3l* function differently. The most likely gene with which *gnl3l* would be redundant is *ns*, so it would be interesting to see if simultaneous loss of *ns* and *gnl3l* uncovers any additional functions in ribosome biogenesis shared

between these two homologs.
Gnl3l mutants stabilize p53 to similar levels as the gnl2 and ns mutants, which was interesting given that in NS this phenomenon is ascribed to ribosomal proteins being released from an incorrectly processed pre-ribosomal subunit and binding MDM2 [7], known as ribosomal stress. Since ribosome biogenesis is mostly intact in *gnl3l* mutants, a mechanism unrelated to ribosomal stress must underlie the p53 stabilization. Although we did detect a large increase in the levels of an MDM2 cleavage product in the gnl2 and gnl3l mutant, this mechanism remains elusive.

Mutations in ribosome biogenesis genes result in defects in neural differentiation

In order to investigate to what extent these ribosome biogenesis defects are the underlying cause of the cell cycle exit and aberrant neuronal differentiation phenotypes observed in *gnl2* and *ns* mutants, we extended these studies to two unrelated ribosome biogenesis mutants, ribosomal protein S7 (*rps7*) and *nop10*. The screen in which the *gnl2* mutant was identified used overexpression of *zash1a* as a marker for neuronal differentiation [3]. *Zash1a* functions in the notch pathway [8], which, in the wildtype situation, ensures correct patterning of neural tissue through a process called lateral inhibition. A differentiating neural precursor, expressing the transcription factors *zash1a* and *ngn1*, ensures that its neighboring cells remain in a proliferative state by expressing notch ligands such as *deltaA*, inducing expression of the *her4* transcription factor which in turn downregulates *zash1a* and *ngn1* in the receiving cell [8]. In both the *rps4* and *nop10* mutants, overexpression of *zash1a* to a similar extent as in *gnl2* and *ns* could be observed. Likewise, both *ngn1* and *deltaA* were upregulated in each ribosome biogenesis mutant. In addition, *her4* levels were decreased and there was an overexpression of HuC/D, a marker for neurons that have undergone terminal differentiation. These findings indicate that, instead of select cells differentiating into neurons at this stage and their neighboring cells maintaining their pluripotency, most cells differentiated at an early timepoint. We propose that in the absence of a critical number of ribosomes, cells fail to maintain a proliferative state and instead differentiate.
As expected, this effect is not specific to neurogenesis or the notch pathway, as failure to expand progenitor cells in the developing tissue of other ribosome biogenesis mutants has been shown before, for instance in pancreas development [9]. Similarly, knockdown of nucleostemin 1 impairs cell growth, and midgut precursor cell maintenance in drosophila [10] and inhibiting translation by treatment with recombinant ribosome inactivating protein B-chain (rRBC) could induce osteoclast differentiation [11]. However, there is an increasing appreciation of variation in ribosome composition [12], consistent with the finding that knockdown of a variety of ribosomal proteins results in some cases in rp-gene specific phenotypic defects [13]. This indicates that loss of a specific rp does not necessarily have the same proliferation defects in each tissue, although our finding that three different classes of ribosome biogenesis mutants share the same defects in neural differentiation argues against such a mechanism being at work in *gnl2* and *ns* mutants with regard to neural differentiation.
In line with an increased requirement for ribosome biogenesis in proliferating cells, we also show the converse, that ribosome numbers decrease as terminal differentiation progresses. We demonstrate this by comparing ribosome levels in *her4* expressing cells to those in other cells and in K562 cells before and after differentiation into megakaryocytes. That ribosome levels decrease in differentiating tissue was already hinted at by the finding that nucleoli, the major sites for ribosome biogenesis, grow progressively smaller as drosophila eye differentiation progresses [14].

Concluding remarks

In this thesis, we provide evidence that *gnl2* and *ns*, but not *gnl3l*, are required for ribosome biogenesis. All three mutants stabilize p53, which in *ns* is believed to occur through ribosomal stress, but in *gnl3l* occurs through another, as of yet unidentified mechanism. The overexpression of neural progenitor genes in the *gnl2* and *ns* mutants is most likely a secondary effect of their ribosome biogenesis defects, since other ribosome biogenesis mutants display similar phenotypes.

Control of ribosome biogenesis and translation in aging

It has been known for a long time that the reduction of food intake (dietary restriction or DR) can extend the lifespan of a variety of organisms. The discovery that loss of the *daf-2* gene in the nematode *C. elegans* extends its lifespan more than two-fold was the first evidence that the rate of aging of any given organism is controlled through genetic and signaling pathways [15]. *Daf-2* is the *C. elegans* homolog of both the insulin and insulin growth factor (IGF) receptor, possibly linking lifespan extension in this mutant to nutrient sensing. However, lifespan extending effects of *eat-2* mutations, which cause difficulties in feeding and thus caloric restriction, are cumulative with those of *daf-2* mutations, suggesting they extend lifespan through separate pathways [16]. *Daf-2* mediated lifespan extension is dependent on several transcription factors, most notably *daf-16* [15]. The lifespan extension observed in DR was shown to be largely dependent on downregulation of the TOR pathway, which among other things results in inhibition of ribosome biogenesis and translation [17] independently of *daf-16* signaling [18]. This indicates that TOR either acts in parallel to or downstream of *daf-16* to extend lifespan. *Daf-16* was shown to inhibit the TOR pathway by repressing transcription of *daf-15*, the C elegans homolog of the TOR complex 1 component raptor [19]. Surprisingly, experiments aimed to measure protein synthesis in the *daf-2* mutant failed to show any change compared to normal *C.elegans*, while in contrast a reduction was observed in the *eat-2* mutant [17]. In addition, it was shown that knockdown of ribosomal proteins did not further increase *daf-2* lifespan, suggesting that these pathways do overlap [17].

Protein metabolism is highly reduced in daf-2 mutants

In chapter 4 we took an unbiased quantitative mass spectrometry approach to identify processes that are regulated by mutations in *daf-2.* This revealed a remarkable *daf-16* dependent decrease of proteins involved in the translational machinery and protein metabolism. We confirmed that translation was decreased by polysome profiling and found a drastic reduction of the number of polysomes in the *daf-2* mutant, as well as a reduction of total RNA content. Concurrently, the daf-2 mutants display lower amounts of 20S proteasome activity, thus maintaining total protein levels equal to that observed in wild types. In this final observation also lies the explanation as to why a reduction of protein synthesis was not observed in the earlier study, in which worms were fed bacteria containing radioactive proteins for 3 hours [17]. The amount of radioactive amino acids incorporated was taken as a measure of protein synthesis, but reduced protein degradation could have counterbalanced any reduction in protein synthesis, resulting in a similar level of radioactive proteins at the end of the incubation. Our findings now finally link reduced insulin/IGF signaling (IIS) to protein synthesis inhibition, showing that IIS- and DR mediated lifespan extension have more overlapping mechanisms than was previously appreciated.
In additions to proteins involved in global protein synthesis, total mRNA content was decreased and a number of RNA binding proteins, proteins involved in mRNA splicing and those involved in

transport were expressed at lower levels in *daf-2* mutants. Among these are snr-2, part of the mRNA splicing complex [20], vig-1, a component of the RNA induced silencing complex (RISC) [21], and car-1, a component of P-bodies [22]. Knockdown of the latter was able to extend lifespan in nematodes in our study. Reductions in mRNA splicing activity can affect translation efficiency, as freshly spliced mRNA contain marks, in the form of RNA binding protein complexes, that favor its translation, which are removed after the first round of translation [23]. It has been speculated that some of these RNA binding proteins are sequence specific, favoring translation of subsets of mRNAs [23].

Subsets of mRNA are translated with increased or decreased efficiency in daf-2 mutants

We noticed that several discrepancies existed between our proteomics data and previously published microarray data. High-throughput analyses in eukaryotes comparing mRNA and protein levels have indicated that there is no direct correlation between transcript levels and protein synthesis, suggesting a high degree of posttranscriptional regulation in eukaryote cells. There is however a strong correlation when the translation rate of mRNAs is taken into account [24]. We speculated that the reduction of the RNA binding proteins, proteins involved in mRNA splicing and transport and components of the translation machinery we observed could mediate not only global changes in translation, but could also result in preferential translation of specific transcripts. Regulation of translation rates between has been shown to occur in various processes, for instance adipocyte differentiation [25] and spermatogenesis [26]. Of particular interest is the finding that transcripts possessing short 5'UTRs were preferentially translated in dietary restricted drosophila. This resulted in increased translation of mitochondrial genes, which was shown to increase lifespan, posing a mechanism by which regulation of transcript translation can extend lifespan [27].

In chapter 5, we aimed to identify regulation of transcript translation in *daf-2* mutants. In polysome profiles from *daf*-2 mutants we had observed a striking decrease of polysomes, while the levels of monosomes seemed unaffected, suggesting that regulation takes place between these two. We isolated RNA from both the monosomal and polysomal fractions collected from the polysome profiles performed in chapter 4 and performed RNA-sequencing to identify the transcripts present in either fraction.

Gene ontology (GO) term analysis of the transcripts which are preferentially associated with the polysome in each worm line revealed that *daf*-2 mutants preferentially translate a specific subset of mRNAs. Transcripts associated with processes known to play a role in *daf-2* mediated lifespan extension were translated with increased efficiency (aging, cuticle formation, respiration) as or decreased efficiency (genetalia development, tRNA aminoacytilation, cell cycle components) compared to wildtypes. For many processes, this altered preference was *daf-16* dependent, but genes involved in larval and cuticle development, growth and metabolism were highly translated in the absence of *daf-16*, indicating that these must be under the control of another transcription factor.

Correlation between the abundance of RNAs in each fraction was very low, suggesting that there is a tight selection of RNAs that are to be translated with high efficiency. Interestingly, GO overrepresentation analysis of transcripts enriched in the polysomal fraction showed an overrepresentation of transcripts associated with many biological processes expected to be active. In contrast, such an analysis on transcripts enriched in the monosomal fractions showed no overrepresentation of specific biological processes. This suggests that after loading of an mRNA onto a preliminary ribosome, a decision is made based on the function of the transcript to load additional ribosomes and proceed with robust translation or to stall the process. There are a

number of mechanisms known that can stop a translating ribosome. Recognition of premature translation termination codons (PTC) and non-sense mediated decay (NMD) occur during the first, or pioneer, translation event [23]. When a translating ribosome encounters a stop codon upstream of an exon-junction complex (EJC), the EJC inhibits further translation initiation while the mRNA is degraded by NMD [23]. If a translating ribosome does not encounter a stop codon, it eventually stalls when it reaches the end of the transcript, after which it is removed and the mRNA is degraded by the exosome, a mechanisms known as non-stop decay (NSD) [28]. Binding of the RISC complex to miRNA target sites in the mRNA inhibits translation initiation, although multiple ribosomes can still be present on the mRNA when this occurs [29]. It is likely that many other mechanisms play a role in translation of specific mRNAs, including compartmentalization of mRNAs, regulation of polyA tail length and other, as of yet undiscovered mechanisms.

Non coding RNAs are involved in translation and lifespan extension

Most studies that have analysed RNA isolated from polysomes have used microarray analysis to detect the abundance of mRNAs [26,27]. Although this method has uncovered many interesting processes, only predefined transcripts can be detected. The advent of RNA sequencing technology has allowed us to look at ribosome bound RNAs with an unbiased approach. To our surprise, we found a high number of non-coding RNAs (ncRNAs) to be associated with both monosomes and polysomes. For rRNAs and tRNAs the reason for this is evident, but the presence of some other ncRNAs was more puzzling. Pseudogenes were mostly enriched in the monosome, where they are most probably undergoing a pioneer round of translation before undergoing either NMD or NSD. Also small nuclear, small nucleolar and other, longer, non-coding RNAs were detected, for most of which no function has been described as of yet. Their association with ribosomes suggests that at least some of these RNAs are involved in translational control, either by base pairing with the mRNA under translation, direct binding to the ribosome or possibly by being trans-spliced onto mRNAs, functioning as an alternative 5' or 3'UTR.

We focused on a 711bp long ncRNA that had been previously described to be induced during dauer formation in *C.elegans*, *transcribed telomere sequence 1* (*tts-1*) [30]. This ncRNA was also found to be induced by treatment with nitric oxide, which increases lifespan [31]. Furthermore, this induction was *daf-16* dependent [31]. In our study, *tts-1* was highly upregulated in both monosomes and polysomes in *daf-2* mutants in a *daf-16* dependent manner and was found to be most highly expressed in gut tissues. To determine whether *tts-1* plays a role in translation, we knocked it down using an siRNA approach and performed polysome profiling. We observed that loss of *tts-1* partially rescued the loss of polysomes in the *daf-2* mutants. Moreover, loss of *tts-1* also partially reversed the lifespan extension phenotype in these mutants, but does not decrease lifespan in *daf-2;daf-16* mutants. It will be interesting to see if overexpression of *tts-1* is sufficient to inhibit polysome formation and extend lifespan and if some of the other ncRNAs detected in our study also have specific functions in polysomes formation and lifespan extension.

Polysome profiling compared to ribosome profiling

Polysome profiling has been used to investigate ribosomes and translation since the early days of cellular biology [32]. The emergence of microarrays and next generation sequencing to measure transcript abundance has allowed genome wide detection of transcripts in active translation. Several years ago, a novel technique named ribosome profiling was developed, in which RNA not covered by ribosomes is degraded and so-called ribosome protected fragments are sequenced to determine the ribosome occupancy of mRNAs [33]. This technique detects only the coding regions of RNAs undergoing active translation, whereas fractions collected from polysome profiles can additionally contain RNA bound to the mRNA-ribosome complex in any way, including base pairing with the mRNA, interaction with the ribosome itself and with the nascent polypeptide chain. Combining the two techniques could be a powerful way to determine how the ncRNAs we

detected in our datasets are bound to the ribosomes.
Our data suggest that there is a biological distinction between monosomes and polysomes. Unfortunately, ribosome profiling cannot distinguish between monosome and polysome bound fragments. Conversely, ribosome profiling can detect translation of regulatory upstream open reading frames (uORF), which can have considerable effects on actual translation efficiency, while polysome profiling cannot distinguish between uORF and bona fide translation [34,35]. It was observed that ribosome density is higher at the 5' end of the mRNA and it was argued that this decrease in ribosome density along a transcript results from either increases in the rate of translation elongation and/or premature translation termination [33]. It would be interesting to determine where on the mRNA the ribosome is in the monosomal fractions, if there is enrichment of uORF translation and if translation of these mRNAs is prematurely stopped, possibly by a mechanism which also prevents loading of additional ribosomes, such as NMD.

Concluding remarks

Through an unbiased mass spectrometry approach, we identified a strong downregulation of protein metabolism in the *daf-2* mutant that was previously overlooked. This links the pathways of insulin/insulin growth factor signaling and dietary restriction mediated longevity more closely than was previously appreciated. In addition to a reduction in global translation, we also observed altered translation efficiency for several subsets of mRNAs. We identified a number of ribosome associated ncRNAs and provided evidence that one of these, *tts-1*, inhibits polysome formation and extends lifespan.

Effects of nitric oxide treatment during development

In chapter 6, we described that perinatal treatment of rats with the nitric oxide donor molsidomine reduces ribosome biogenesis in the kidney measured at 2 weeks after birth. At 9 to 10 months of age, ribosome biogenesis has returned to normal, but the treated rats still benefit from reduced blood pressure and have reduced chances of developing kidney failure [36]. We could not offer a satisfactory explanation of these effects at the time, but several studies that have been published more recently offer a possible explanation, related to the effect of NO on mitochondrial function. NO acts on the respiratory chain by binding to subunits of Complex I and Complex IV [37]. It inhibits oxidative phosphorylation through two chemical interactions, S-nitrosation and heme-metal binding [38]. Reduction in oxidative phosphorylation would result in increased levels of AMP, activating AMP activated protein kinase (AMPK). AMPK activation inhibits ATP consuming processes, partially by inhibiting the mTOR pathway through phosphorylation of TSC1 [39]. Inhibition of mTOR signaling then results in a decrease of ribosome biogenesis and translation (see chapter 1). This inhibition would be transient and indeed we observe the effect of perinatal NO treatment on ribosome biogenesis at 2 days after birth, while ribosome biogenesis has returned to normal after 2 weeks.
The reduction in blood pressure and kidney failure we observe in old age after perinatal treatment with molsidomine is reminiscent of how inhibition of mitochondrial genes extends lifespan in *C. elegans*. When mitochondrial gene expression was inhibited during development, the lifespan of worms was extended, even if this inhibition was removed after the worms had reached adulthood. Conversely, when mitochondrial genes were inhibited only during adulthood, there was no effect on lifespan [40]. A more recent study argues that inhibition of mitochondrial genes or nuclear encoded mitochondrial components results in a mito-nuclear imbalance and activates the mitochondrial unfolded protein response and that this response mediates the lifespan extension observed [41]. Besides mito-nuclear imbalance, several other processes can elicit the

mitochondrial unfolded protein response, including oxidative damage [42]. Treatment with NO has been shown to increase lifespan in *C.elegans* [31]. It is therefore a tantalizing possibility that perinatal NO treatment in our rats activated the mitochondrial unfolded protein response and resulted in an increased lifespan, the reduced blood pressure and incidence of kidney failure being a result of these rats being "physiologically younger" at the time of examination. Unfortunately, these rats were not allowed to die of natural causes, so more studies will have to be done to prove this hypothesis, including measuring the lifespan of rats after perinatal treatment with molsidomine and determining the age of onset of high blood pressure, kidney failure and other pathogeneses associated with old age.

Part 2: The relationship between the VHL and p53 tumor suppressors

Renal cell carcinoma is a malignancy that originates in the epithelium of the proximal convoluted tubule. It is the most prevalent type of kidney cancer and the 7th most prevalent type of cancer in general. The treatment is most commonly a partial or radical nephrectomy. However, when metastasis have already developed, as is the case for about 25-30% of patient when they enter the clinic, treatment options are very limited, since RCC is highly resistant to chemo and radiation therapy [43].

RCC is associated with mutations in the Von Hippel Lindau tumor suppressor, which occur in 40-70% of cases. In contrast, mutations in other tumor suppressors and oncgenes occur at much lower rates, 10% for TP53 (p53) and CDKN2A (p16 lnk4A) and 3% or less for all others [43]. The presence of both VHL and TP53 inactivating mutations is even lower, suggesting an interaction between the two [44]. A recent study compared multiple metastatic sites and multiple sites in the primary tumors within patients and found that there was a high heterogenity between mutations in all these, but an identical mutation in VHL was always shared between all tumor sites in the patient [45]. This indicates that mutations in VHL are driving RCC formation up to the point of metastasis.

The best described function of VHL is as a part of an SCF-type E3 ligase, where it binds to the hydroxylated form of hypoxia inducible factor a (HIFa) and targets it for proteasomal degradation. Consequently, loss of VHL leads to a continuous activation of hypoxic response pathways, including angiogenesis, erythropoiesis and increased glycolysis. Although these can clearly assist tumorigenesis, a number of studies have shown that activation of hypoxic response pathways is necessary [46] but not enough to induce tumor formation [47].

VHL controls p53 stabilization by regulating PDCD5 localization

Apart from this function in hypoxic signaling, a number of other functions of VHL have been described. Among others (see chapter 1), VHL has been described to complex with CARD9 and CK2 and inhibit NF-κB signalling, thereby inhibiting transcription of pro-survival genes. Also, VHL was described to bind to p53 and recruit it to ATM and p300. This binding was argued to be required for p53 stabilization and target gene transcription. However, these findings are based on in vitro overexpression studies. In chapter 7 of this thesis, we used a zebrafish model of loss of VHL [48] to confirm this interaction of VHL and p53 in vivo.

We induced DNA damage and found quite the opposite of what was expected from the aformentioned study. p53 was stabilized in response to DNA damage in the absence of VHL, at higher levels than in wildtypes. It was even stabilized in the absence of any DNA damage. This stabilization led to equal increases of target gene transcription in wildtype and vhl-/- embryos. These findings shed new light on the results of a previously performed mass spectrometry experiment, designed to identify new binding partners of VHL. Programmed cell death 5 (PDCD5)

was identified as a novel binding partner, a protein which had been described earlier to bind to p53. PDCD5 binding results loss of the interaction between MDM2 and p53 and leads to degradation of MDM2. This results in p53 stabilization and, depending on cofactor binding, cell cycle arrest or apoptosis [49]. We found that loss of VHL affected the localization of PDCD5. In the wildtype situation, PDCD5 was present on the cell membrane or in the cytoplasm, depending on the cell type. In the absence of VHL, PDCD5 translocated to the nucleus, where it would be expected to interact with p53. Exposing cells to hypoxia also resulted in nuclear translocation of PDCD5, indicating that this is at least partly HIFa mediated. In line with PDCD5 nuclear localization, MDM2 was found to be degraded in the absence of VHL. In conclusion, we show that VHL controls p53 stabilization by regulating the localization and therefore the activity of PDCD5.

VHL is required for the induction of cell cycle exit and apoptosis downstream of p53 activation

These findings did not make it clear how loss of VHL in RCC could lead to apoptosis resistance. The increase in p53 stabilization we observe, would be expected to result in high levels of apoptosis. However, we found that DNA damage failed to induce cell cycle exit, caspase activation and apoptosis in the absence of VHL. This indicates that VHL is required for apoptosis induction and operates downstream of p53 target gene transcription and upstream of caspase activation. This possibly explains why VHL and TP53 are rarely both mutated in RCC: since in the absence of vhl induction of apoptosis by p53 activation is blocked further downstream, loss of p53 does not confer any additional growth advantage.

A likely candidate for mediating this blockade is the activation of NF-κB. Involvement of NF-κB in apoptosis resistance in RCC has been recognized over the last couple of years [50]. NF-κB is a collective name for a series of transcription factors that heterodimerize in varying combinations. Among its target genes are the antiapoptotic genes c-FLIP, Survivin, c-IAP-1, and cIAP-2, which block the activities of caspases 8 and 3 [50]. NF-κB activity was first found to positively correlate with tumor progression in RCC in 2003 [51]. Moreover, VHL was shown to downregulate NF-κB expression and thus enable apoptosis in these cells [51]. Several studies have confirmed that levels of various NF-κB family members are increased in RCC [52,53]. In our study, we found increased expression of the NF-κB target gene birc5a/Survivin in vhl-/- embryos, although we have not determined whether this is truly the underlying cause for apoptosis resistance in these embryos. Determining which NF-κB family members and target genes are responsible for apoptosis resistance in the absence of VHL is a future challenge.

Concluding remarks

In contrast to earlier in vitro studies, we observed increased stabilization of p53 in the absence of vhl. We identified a novel interaction between VHL and PDCD5 and showed that loss of VHL results in nuclear translocation of PDCD5 and subsequent degradation of MDM2, leading to increased p53 stabilization and target gene transcription. However, vhl is required for caspase activation and apoptosis to occur in response to DNA damage. These findings possibly explain why VHL and p53 are rarely found both mutated in RCC, since loss of p53 would not confer any additional growth advantage to VHL negative cells.

References

1. Warner JR (1999) The economics of ribosome biosynthesis in yeast. Trends Biochem Sci 24: 437-440.
2. Kafienah W, Mistry S, Williams C, Hollander AP (2006) Nucleostemin is a marker of proliferating stromal stem cells in adult human bone marrow. Stem Cells 24: 1113-1120.
3. Paridaen JT, Janson E, Utami KH, Pereboom TC, Essers PB, et al. (2011) The nucleolar GTP-binding proteins Gnl2 and nucleostemin are required for retinal neurogenesis in developing zebrafish. Dev Biol 355: 286-301.
4. Romanova L, Grand A, Zhang L, Rayner S, Katoku-Kikyo N, et al. (2009) Critical role of nucleostemin in pre-rRNA processing. J Biol Chem 284: 4968-4977.
5. Kudron MM, Reinke V (2008) C. elegans nucleostemin is required for larval growth and germline stem cell division. PLoS Genet 4: e1000181.
6. Du X, Rao MR, Chen XQ, Wu W, Mahalingam S, et al. (2006) The homologous putative GTPases Grn1p from fission yeast and the human GNL3L are required for growth and play a role in processing of nucleolar pre-rRNA. Mol Biol Cell 17: 460-474.
7. Dai MS, Lu H (2004) Inhibition of MDM2-mediated p53 ubiquitination and degradation by ribosomal protein L5. J Biol Chem 279: 44475-44482.
8. Kageyama R, Ohtsuka T, Shimojo H, Imayoshi I (2009) Dynamic regulation of Notch signaling in neural progenitor cells. Curr Opin Cell Biol 21: 733-740.
9. Provost E, Weier CA, Leach SD (2013) Multiple ribosomal proteins are expressed at high levels in developing zebrafish endoderm and are required for normal exocrine pancreas development. Zebrafish 10: 161-169.
10. Rosby R, Cui Z, Rogers E, deLivron MA, Robinson VL, et al. (2009) Knockdown of the Drosophila GTPase nucleostemin 1 impairs large ribosomal subunit biogenesis, cell growth, and midgut precursor cell maintenance. Mol Biol Cell 20: 4424-4434.
11. Wang YM, Lu TL, Hsu PN, Tang CH, Chen JH, et al. (2011) Ribosome inactivating protein B-chain induces osteoclast differentiation from monocyte/macrophage lineage precursor cells. Bone 48: 1336-1345.
12. Gilbert WV (2011) Functional specialization of ribosomes? Trends Biochem Sci 36: 127-132.
13. Uechi T, Nakajima Y, Nakao A, Torihara H, Chakraborty A, et al. (2006) Ribosomal protein gene knockdown causes developmental defects in zebrafish. PLoS One 1: e37.
14. Baker NE (2013) Developmental regulation of nucleolus size during Drosophila eye differentiation. PLoS One 8: e58266.
15. Kenyon C, Chang J, Gensch E, Rudner A, Tabtiang R (1993) A C. elegans mutant that lives twice as long as wild type. Nature 366: 461-464.
16. Lakowski B, Hekimi S (1998) The genetics of caloric restriction in Caenorhabditis elegans. Proc Natl Acad Sci U S A 95: 13091-13096.
17. Hansen M, Taubert S, Crawford D, Libina N, Lee SJ, et al. (2007) Lifespan extension by conditions that inhibit translation in Caenorhabditis elegans. Aging Cell 6: 95-110.
18. Vellai T, Takacs-Vellai K, Zhang Y, Kovacs AL, Orosz L, et al. (2003) Genetics: influence of TOR kinase on lifespan in C. elegans. Nature 426: 620.
19. Jia K, Chen D, Riddle DL (2004) The TOR pathway interacts with the insulin signaling pathway to regulate C. elegans larval development, metabolism and life span. Development 131: 3897-3906.
20. Barbee SA, Lublin AL, Evans TC (2002) A novel function for the Sm proteins in germ granule localization during C. elegans embryogenesis. Curr Biol 12: 1502-1506.
21. Caudy AA, Ketting RF, Hammond SM, Denli AM, Bathoorn AM, et al. (2003) A micrococcal nuclease homologue in RNAi effector complexes. Nature 425: 411-414.
22. Dunn EF, Hammell CM, Hodge CA, Cole CN (2005) Yeast poly(A)-binding protein, Pab1, and PAN, a poly(A) nuclease complex recruited by Pab1, connect mRNA biogenesis to export. Genes Dev 19: 90-103.
23. Le Hir H, Seraphin B (2008) EJCs at the heart of translational control. Cell 133: 213-216.
24. Wang T, Cui Y, Jin J, Guo J, Wang G, et al. (2013) Translating mRNAs strongly correlate to proteins in a multivariate manner and their translation ratios are phenotype specific. Nucleic Acids Res 41: 4743-4754.
25. Spangenberg L, Shigunov P, Abud AP, Cofre AR, Stimamiglio MA, et al. (2013) Polysome profiling shows extensive posttranscriptional regulation during human adipocyte stem cell differentiation into adipocytes. Stem Cell Res 11: 902-912.
26. Iguchi N, Tobias JW, Hecht NB (2006) Expression profiling reveals meiotic male germ cell mRNAs that are translationally up- and down-regulated. Proc Natl Acad Sci U S A 103: 7712-7717.
27. Zid BM, Rogers AN, Katewa SD, Vargas MA, Kolipinski MC, et al. (2009) 4E-BP extends lifespan upon dietary restriction by enhancing mitochondrial activity in Drosophila. Cell 139: 149-160.

28. Vasudevan S, Peltz SW, Wilusz CJ (2002) Non-stop decay--a new mRNA surveillance pathway. Bioessays 24: 785-788.
29. Bazzini AA, Lee MT, Giraldez AJ (2012) Ribosome profiling shows that miR-430 reduces translation before causing mRNA decay in zebrafish. Science 336: 233-237.
30. Jones SJ, Riddle DL, Pouzyrev AT, Velculescu VE, Hillier L, et al. (2001) Changes in gene expression associated with developmental arrest and longevity in Caenorhabditis elegans. Genome Res 11: 1346-1352.
31. Gusarov I, Gautier L, Smolentseva O, Shamovsky I, Eremina S, et al. (2013) Bacterial nitric oxide extends the lifespan of C. elegans. Cell 152: 818-830.
32. Warner JR, Knopf PM, Rich A (1963) A multiple ribosomal structure in protein synthesis. Proc Natl Acad Sci U S A 49: 122-129.
33. Ingolia NT, Ghaemmaghami S, Newman JR, Weissman JS (2009) Genome-wide analysis in vivo of translation with nucleotide resolution using ribosome profiling. Science 324: 218-223.
34. Gerashchenko MV, Lobanov AV, Gladyshev VN (2012) Genome-wide ribosome profiling reveals complex translational regulation in response to oxidative stress. Proc Natl Acad Sci U S A 109: 17394-17399.
35. Michel AM, Baranov PV (2013) Ribosome profiling: a Hi-Def monitor for protein synthesis at the genome-wide scale. Wiley Interdiscip Rev RNA.
36. Koeners MP, Braam B, van der Giezen DM, Goldschmeding R, Joles JA (2008) A perinatal nitric oxide donor increases renal vascular resistance and ameliorates hypertension and glomerular injury in adult fawn-hooded hypertensive rats. Am J Physiol Regul Integr Comp Physiol 294: R1847-1855.
37. Erusalimsky JD, Moncada S (2007) Nitric oxide and mitochondrial signaling: from physiology to pathophysiology. Arterioscler Thromb Vasc Biol 27: 2524-2531.
38. Brown GC (2007) Nitric oxide and mitochondria. Front Biosci 12: 1024-1033.
39. Piantadosi CA, Suliman HB (2012) Redox regulation of mitochondrial biogenesis. Free Radic Biol Med 53: 2043-2053.
40. Dillin A, Hsu AL, Arantes-Oliveira N, Lehrer-Graiwer J, Hsin H, et al. (2002) Rates of behavior and aging specified by mitochondrial function during development. Science 298: 2398-2401.
41. Houtkooper RH, Mouchiroud L, Ryu D, Moullan N, Katsyuba E, et al. (2013) Mitonuclear protein imbalance as a conserved longevity mechanism. Nature 497: 451-457.
42. Haynes CM, Fiorese CJ, Lin YF (2013) Evaluating and responding to mitochondrial dysfunction: the mitochondrial unfolded-protein response and beyond. Trends Cell Biol 23: 311-318.
43. Jonasch E, Futreal PA, Davis IJ, Bailey ST, Kim WY, et al. (2012) State of the science: an update on renal cell carcinoma. Mol Cancer Res 10: 859-880.
44. Szymanska K, Moore LE, Rothman N, Chow WH, Waldman F, et al. (2010) TP53, EGFR, and KRAS mutations in relation to VHL inactivation and lifestyle risk factors in renal-cell carcinoma from central and eastern Europe. Cancer Lett 293: 92-98.
45. Gerlinger M, Rowan AJ, Horswell S, Larkin J, Endesfelder D, et al. (2012) Intratumor heterogeneity and branched evolution revealed by multiregion sequencing. N Engl J Med 366: 883-892.
46. Kondo K, Klco J, Nakamura E, Lechpammer M, Kaelin WG, Jr. (2002) Inhibition of HIF is necessary for tumor suppression by the von Hippel-Lindau protein. Cancer Cell 1: 237-246.
47. Fu L, Wang G, Shevchuk MM, Nanus DM, Gudas LJ (2011) Generation of a mouse model of Von Hippel-Lindau kidney disease leading to renal cancers by expression of a constitutively active mutant of HIF1alpha. Cancer Res 71: 6848-6856.
48. van Rooijen E, Santhakumar K, Logister I, Voest E, Schulte-Merker S, et al. (2011) A zebrafish model for VHL and hypoxia signaling. Methods Cell Biol 105: 163-190.
49. Xu L, Hu J, Zhao Y, Xiao J, Wang Y, et al. (2012) PDCD5 interacts with p53 and functions as a positive regulator in the p53 pathway. Apoptosis 17: 1235-1245.
50. Morais C, Gobe G, Johnson DW, Healy H (2011) The emerging role of nuclear factor kappa B in renal cell carcinoma. Int J Biochem Cell Biol 43: 1537-1549.
51. Dong Z, Wang JZ, Yu F, Venkatachalam MA (2003) Apoptosis-resistance of hypoxic cells: multiple factors involved and a role for IAP-2. Am J Pathol 163: 663-671.
52. Djordjevic G, Matusan-Ilijas K, Sinozic E, Damante G, Fabbro D, et al. (2008) Relationship between vascular endothelial growth factor and nuclear factor-kappaB in renal cell tumors. Croat Med J 49: 608-617.
53. Meteoglu I, Erdogdu IH, Meydan N, Erkus M, Barutca S (2008) NF-KappaB expression correlates with apoptosis and angiogenesis in clear cell renal cell carcinoma tissues. J Exp Clin Cancer Res 27: 53.

Appendix

Nederlandse Samenvatting

About the Author

List of Publications

Dankwoord

Nederlandse Samenvatting

Het lichaam bestaat uit miljarden cellen, die elk een specifieke functie hebben, bijvoorbeeld zenuwcellen, spiercellen en bloedcellen. De functie van een cel wordt voor een groot deel bepaald door de eiwitten waaruit deze bestaat. Eiwitten zijn misschien wel de belangrijkste componenten van de cel. Ze zijn verantwoordelijk voor het grootste deel van de processen die in het lichaam plaatsvinden, zoals communicatie tussen en binnen cellen, spiersamentrekking en zuurstoftransport.
Elke cel bevat alle erfelijke informatie die nodig is om een organisme vanaf de bevruchting te laten ontwikkelen tot een individu. Deze informatie is opgeslagen in de celkern in de vorm van DNA. DNA laat zich het best beschrijven als een lang lint met een code. Een belangrijk deel van de erfelijke informatie bestaat uit instructies over wanneer, waar en hoe elk eiwit gemaakt moet worden. Als de productie van een eiwit nodig is, wordt dat deel van het DNA waar de betreffende instructies staan opgeslagen gekopieerd naar een korter lint. Dit is het messenger (boodschapper) RNA, afgekort tot mRNA.
De instructies op dit mRNA worden gebruikt door zogenaamde ribosomen om de eiwitten te maken. Ze binden aan het begin van het mRNA en lopen vervolgens stapje voor stapje het lint af. Elke 'woord' code die ze daarbij tegenkomen, staat voor een onderdeel waaruit het eiwit bestaat. Dit onderdeel wordt toegevoegd aan het groeiende eiwit en het ribosoom schuift naar het volgende woord, om het volgende onderdeel toe te voegen. Dit gaat net zo lang door tot het ribosoom het woord "stop" tegenkomt en het eiwit af is.
Ribosomen zijn dus verantwoordelijk voor het maken van eiwitten in de cel en daarom van vitaal belang. Een cel bevat zeer grote aantallen ribosomen, waardoor de aanmaak van ribosomen een groot deel van het energieverbruik van een cel beslaat. Daarom is het cruciaal dat deze aanmaak goed geregeld is. In dit proefschrift bekijken we zowel fouten die kunnen ontstaan in de aanmaak van ribosomen als de mechanismen die bepalen hoeveel ribosomen er gemaakt worden.

De rol van de gnl familie van genen in de aanmaak van ribosomen.

Een ribosoom bestaat uit 4 stukken ribosomaal RNA (niet te verwarren met boodschapper mRNA) en 80 kleine eiwitten. Daarbij zijn er nog zo'n 200 andere eiwitten betrokken bij het maken van ribosomen. Deze zijn onder andere verantwoordelijk voor het knippen en vouwen van het ribosomaal RNA in de benodigde vorm. In het eerste deel van dit proefschrift (Hoofdstuk 2) onderzochten we eiwitten waren we vermoeden dat deze betrokken zijn bij de aanmaak van ribosomen.
Deze eiwitten zijn "nucleostemin" (ook wel bekend als "gnl3") en twee nauw gerelateerde eiwitten, "gnl2" en "gnl3-like". Hiervoor gebruikten we zebravis embryos waarin het DNA zo veranderd is dat deze eiwitten niet langer gemaakt kunnen worden, zogenaamde knock out mutanten.
Door de aanmaak van een ribosoom te volgen in onze knock out mutanten, konden we laten zien dat gnl2 en nucleostemin wel, maar gnl3-like niet, nodig zijn om ribosomen te maken. Bovendien laten we zo zien op welk punten van het aanmaakproces elk van deze twee genen nodig is.
De knock out mutanten van gnl2 en nucleostemin trokken oorspronkelijk de aandacht omdat ze een defect hebben in de ontwikkeling van hun hersenen en ogen. Door zebravis embryos zonder nucleostemin of gnl2 te vergelijken met embryos waarin andere genen die nodig zijn om ribosomen te maken ontbreken (Hoofdstuk 3), laten we zien dat de deze ontwikkelingsproblemen deels toe te schrijven zijn aan het gebrek aan ribosomen.
We laten in dit deel van het proefschrift dus zien nucleostemin en gnl2 van belang zijn voor de aanmaak van ribosomen en dat een verlaagde aanmaak van ribosomen het ontwikkelingsproces kan beinvloeden.

Verlaagde ribosoom productie in lang levende wormen.

Caenorhabditis Elegans is een minuscule worm die vanwege zijn korte levensloop en het gemak waarmee hij kan worden gekweekt regelmatig in laboratoria wordt gebruikt. In de vroege jaren '90 leverde de zoektocht naar mutaties die het leven van deze worm kunnen verlengen een variant op die wel drie keer zo lang leefde als normaal. In deze wormen bleek het eiwit dat verantwoordelijk is voor de ontvangst van insuline signalen, het zogenoemde daf-2, te zijn uitgeschakeld.

In het tweede deel van dit proefschrift laten we zien dat er in daf-2 knock out wormen een sterke vermindering optreedt van het aantal ribosomen en de eiwit productie (Hoofdstuk 4). Dit betekent dat de daf-2 mutant meer gemeen heeft dan gedacht met een andere bekende manier om het leven te verlengen, het beperken van de voedselinname. Hiervan was al langer bekend dat dit de productie van eiwitten verlaagt.

Behalve naar het totale niveau van eiwitproductie in de daf-2 knock out worm, hebben we ook gekeken welke specifieke eiwitten gemaakt werden (Hoofdstuk 5). Dit deden we door de ribosomen op te vangen en te kijken welk mRNA ze op dat moment aan het aflezen waren. Hieruit bleek dat van sommige mRNAs meer eiwitten worden gemaakt dan van andere en dat deze voorkeur veranderd is in de daf-2 knock out worm.

Wat we niet hadden verwacht, is dat we naast messenger RNA ook niet coderend RNA (ncRNA) zouden vinden. Zoals de naam doet vermoeden, bevatten deze RNAs geen instructies voor het maken van eiwitten, maar hebben ze een andere functie. Wat deze functie is, is voor een groot deel van de ncRNAs nog niet bekend. Dit is ook het geval bij tts-1, het meest opvallende ncRNA dat wij vonden in de daf-2 ribosomen. We ontdekten dat tts-1 nodig is om het aantal ribosomen in daf-2 knock out wormen te verminderen en het leven van deze wormen te verlengen. Om te ontdekken hoe tts-1 dit precies doet, is verder onderzoek nodig.

In hoofdstuk 6 van dit proefschrift laten we zien dat ratten waarvan de moeders tijdens de zwangerschap werden behandeld met molsidomine, een medicijn dat de bloedvaten verwijdt, langere tijd na de geboorte verminderde hoeveelheden ribosomen hebben. Dezelfde ratten hebben op latere leeftijd ook veel minder last van hoge bloeddruk en nierfalen, typische ouderdomsverschijnselen. We kunnen niet aantonen dat dit het gevolg is van de verlaagde hoeveelheid ribosomen, maar het is verleidelijk het verband te leggen tussen het levensverlengende effect van verlaagde hoeveelheden ribosomen en het uitblijven van deze ouderdomsverschijnselen. In dit deel van het proefschrift tonen we een verband aan tussen verlaging van de hoeveelheid ribosomen en vertraging van het verouderingsproces. Mogelijk kunnen deze bevindingen in de toekomst helpen om het verouderingsproces te vertragen en ouderdomsziekten te verkomen bij mensen.

De relatie tussen VHL en p53 in nierkanker

Het laatste deel van dit proefschrift heeft niks te maken met ribosomen, maar gaat over nierkanker. Kanker is in feite een ongeremde celgroei. Een cel heeft verschillende veiligheidsmechanismen om deze ongeremde groei te voorkomen. Pas als deze mechanismen uitgeschakeld worden kan er kanker ontstaan. Veruit het belangrijkste onderdeel van deze veiligheidsmechanismen is p53. Bij de meeste vormen van kanker is p53 dan ook uitgeschakeld.

In nierkanker is p53 maar zelden uitgeschakeld. Daar staat tegenover dat een ander gen, Von-Hippel Lindau (VHL, vernoemd naar de ontdekkers), in bijna alle gevallen uitgeschakeld is. Daarom vermoedden we dat VHL belangrijk is voor het functioneren van p53.

In tegenstelling tot de verwachting, vonden we dat p53 juist extra actief is als VHL is uitgeschakeld, zoals vaak het geval is bij nierkanker (Hoofdstuk 7). We ontdekten dat dit veroorzaakt wordt door de interactie van zowel VHL als p53 met een derde factor: PDCD5. Activatie van p53 heeft normaal

tot gevolg dat de (kanker)cel stopt met zich te vermenigvuldigen en zichzelf vernietigt. In de afwezigheid van VHL bleek de activatie van p53 echter geen van deze gevolgen te hebben. Dit kan verklaren waarom de inactivatie van VHL genoeg is om nierkanker te kunnen veroorzaken, zonder dat p53 uitgeschakeld hoeft te zijn.
Dit onderzoek is werpt dus nieuw licht op het ontstaan van nierkanker. Hopelijk leidt dit in de toekomst tot een verbetering van de behandeling van deze dodelijke ziekte.

About the Author.

Paul Essers was born in Maastricht on March 18th in 1983. In 2001 he received his VWO gymnasium diploma from the "Jeanne D'Arc College" in Maastricht. After a year at the Technical University in Eindhoven, where he studied Electrical Engineering, he decided to shift his attention to biology. He returned to Maastricht to study Molecular Life Sciences at Maastricht University. He obtained his bachelors' degree in 2005 and continued with a masters' program in Clinical Molecular Science, from which he graduated in 2007.

He did his final internship under the supervision of Dr Adriaan Duijvestijn, in the department of Immunology of the Maastricht University and Medical Centre, where he studied the pathogenic role of anti-endothelial cell antibodies in systemic lupus erythematosus. After graduation, he worked as a research assistant in the lab of Dr Gommert van Koeveringe, at the department of Urology at the Maastricht University and Medical Centre, where he investigated signal transduction in the urinary bladder. In September 2009, he moved to the lab of Dr Alyson MacInnes, at the Hubrecht Institute in Utrecht, to start his PhD project. The results of this project are described in this thesis.

List of Publications

Essers PB, Pereboom TC, Goos YG, Paridaen J, MacInnes AW, *A comparative study of Nucleostemin family members in zebrafish reveals specific roles in ribosome biogenesis*, Dev Biol. 2013 in press

Stout GJ*, Stigter EC*, **Essers PB***, Mulder KW, Kolkman A, Snijders DS, van den Broek NJ, Betist MC, Korswagen HC, Macinnes AW, Brenkman AB, *Insulin/IGF-1-mediated longevity is marked by reduced protein metabolism,* Mol Syst Biol. 2013 Jul 2;9:679.

Wesseling S*, **Essers PB***, Koeners MP, Pereboom TC, Braam B, van Faassen EE, Macinnes AW, Joles JA, *Perinatal exogenous nitric oxide in fawn-hooded hypertensive rats reduces renal ribosomal biogenesis in early life,* Front Genet. 2011;2:52.

Paridaen JT, Janson E, Utami KH, Pereboom TC, **Essers PB**, van Rooijen C, Zivkovic D, MacInnes AW, *The nucleolar GTP-binding proteins Gnl2 and nucleostemin are required for retinal neurogenesis in developing zebrafish,* Dev Biol. 2011 Jul 15;355(2):286-301.

Rahnama'i MS, van Koeveringe GA, **Essers PB**, de Wachter SG, de Vente J, van Kerrebroeck PE, Gillespie JI, *Prostaglandin receptor EP1 and EP2 site in guinea pig bladder urothelium and lamina propria,* J Urol. 2010 Mar;183(3):1241-7.

Grol S, **Essers PB**, van Koeveringe GA, Martinez-Martinez P, de Vente J, Gillespie JI, *M(3) muscarinic receptor expression on suburothelial interstitial cells,* BJU Int. 2009 Aug;104(3):398-405.

Grol S, **Essers PB**, van Koeveringe GA, de Vente J, Gillespie JI, *Ubiquitin hydrolase (protein gene product 9.5) in the obstructed bladder: evidence for tissue remodelling involving a subset of interstitial cells*, BJU Int. 2009 Sep;104(5):698-706.

*These authors contributed equally to this work

List of Oral Presentations

Essers PB, Klasson TA, Pereboom TC, Mans DA, Boldt K, Giles RH, MacInnes AW, *The Von Hippel Lindau tumor suppressor regulates Programmed Cell Death 5-mediated degradation of Mdm2,* The 8th European Zebrafish Meeting 2013 Jul 12

Dankwoord

Zo, mijn proefschrift is eindelijk af. Toen ik vier jaar geleden Maastricht voor Utrecht verruilde wist ik dat dit moment zou komen, maar het blijft een raar gevoel. Natuurlijk heb ik het niet allemaal alleen gedaan, dus er zijn een hoop mensen die ik moet bedanken, voor zowel concrete wetenschappelijke bijdragen als de broodnodige ontspanning.

First of all, Alyson, thank you for having me in your lab. Although my attitude can probably be best described as "mañana", while you prefer things to be done "ayer", I feel we worked together pretty well. Both your good ideas and your ability to start up cooperations everywhere have resulted in a large diversity of projects over the last couple of years, many of which are now (almost) successfully completed.

Tamara, lange tijd was jij mijn enige echte directe collega en ik had het niet beter kunnen treffen! Door jou voelde ik me meteen thuis op het Hubrecht en dat is altijd zo gebleven. Bedankt voor al je gezelligheid op het lab, alle borrels en feesten, je steun als het allemaal niet zo lekker liep en niet in het minst voor al je bijdragen aan mijn projecten. Viel Spaβ in der Schweiz und Ich Hoffe Sie nog oft zu sehen!
Linda, ook al ben je al een hele tijd niet meer in het land, voor mij hoor je er nog altijd bij. Ik kijk met veel plezier terug op de tijd dat we met zijn drieën in het lab stonden en radio 100% NL of Bingo FM door het lab schalde.

Dina, Britt en Marjon, bedankt voor jullie enthousiasme en inzet tijdens jullie stage, ik heb er veel aan gehad, zowel wat betreft jullie werk op het lab als de ervaring als begeleider, hopelijk was het voor jullie net zo nuttig. Yvonne en Julie, het was kort maar gezellig deze afgelopen maanden. Het blijft een beetje raar dat jullie nu aan wat ooit mijn project was werken, hopelijk komt er een mooie paper uit. Alle andere mensen die op het een of ander moment voor kortere of langere tijd in de onderzoeksgroep groep zaten, ook jullie bedankt.

De helft van de experimentele hoofdstukken in dit boekje zijn samenwerkingen met andere groepen, zonder wie dit boekje een stuk dunner was geweest. Rachel and Tim, I enjoyed our cooperation and working on VHL. I hope that our paper will be accepted by the time you read this. Gerdien, Edwin en Arjan, bedankt voor een prettige samenwerking en bedankt dat jullie mij in een erg interessant onderzoeksveld hebben geïntroduceerd. Sebastiaan, Paula en Prof. Joles, ook jullie bedankt voor een efficiënte en vruchtbare samenwerking.

Sjoerd en Flore, jullie gingen mij net in alles voor en zonder jullie praktische tips was de datum van mijn verdediging vast wel een keer uitgesteld, omdat ik het een of ander formulier vergeten zou zijn. Niki, dankjewel voor een lange avond tekstvakken verschuiven, regelafstanden aanpassen, figuren zwart-wit maken en port drinken (terwijl ik dit schrijf, gaat ook de rest van de fles leeg).

PV 2010: Frans-Paul, Alex, Jeroen, Laila en Yuva, bedankt voor een geweldig jaar, vol met onvergetelijke borrels (Zoals de beruchte St Patrick's day borrel en de Corrie Konings Verjaardags-Camping Disco) en allerlei andere activiteiten. Jeroen, ook onze ochtenden in het vislab met goa trance, psytrance, hardcore en breakcore ga ik missen, alsmede de nachten die we samen in mijn bed doorbrachten. FP, het was me een genoegen je huisgenoot te zijn. Er zal nooit meer een betere Sausage Fest editie zijn dan 2011. Ook alle PV-leden van andere jaren wil ik bedanken voor die onvergetelijke PV-weekendjes. Aan alle andere mensen van het Hubrecht waarmee ik regelmatig gelunched, geborreld en gefeest heb: ik ga jullie missen!

Ik heb natuurlijk niet alleen gedronken op het Hubrecht. Anoek en Leon, met jullie heb ik nog wel het meest gesport de afgelopen jaren. Het was me een eer samen met jullie kikkersprongen te maken, belachelijke afstanden te rennen door de ardennen en spaanse ruiters te beklimmen en tot aan mijn oksels in een sloot te staan in de achterhoek. Inmiddels sta ik ingeschreven voor Beltrum 2014, mijn leercurve wat pijn betreft is niet al te steil. Roel, het valt me een beetje tegen dat je niet meegaat dit jaar. Ook Sjoerd, Maaike, Bart, Rene en vele anderen: Bedankt voor alle gezellige hardloop, trailrun en survival evenementen.

Gelukkig heb ik ook nog buiten het Hubrecht mijn leven enigszins weten te behouden. Mensen van DDA, ik was de eerste die Maastricht verliet en zich vestigde in Utrecht. Toen heb ik jullie erg gemist, maar inmiddels wonen we weer allemaal bij elkaar in de buurt, al is het maar voor heel even. Bedankt voor alle slechte grappen, gezellige etentjes en weekendjes weg. Erg relaxed dat jullie nooit precies wisten wat mijn werk inhield, daar hoefden we het dan ook niet al te uitgebreid over te hebben, een verademing.

Heren van de RGV, tot voor kort was ik de enige die Maastricht had verlaten. Maar het voelde altijd als een vakantie als ik weer terug was voor een weekend gezelligheid en gastvrij werd ontvangen in de Abtstraat of de Rechtstraat. Dit werd zeer gewaardeerd, ook al verblijf ik heden ten dagen exclusief op het Keizer Karelplein als ik in Maastricht ben.

Ook mijn pap en mam bedankt, zonder jullie steun had ik uberhaubt nooit zo lang door kunnen studeren, meer afgestudeerd dan dit wordt het niet meer. Ook bedankt voor een onvergetelijke reis dwars door Siberië en Mongolië tot in Peking, dat had ik nooit willen missen.

En tot slotte, lieve Pauline, jij bent het beste dat me is overkomen het afgelopen jaar. En dat nog wel minder dan 2 uur nadat het jaar begonnen was. Je bent zowel een enorme steun als een erg plezierige afleiding geweest tijdens het laatste jaar van mijn promotie. De fysieke afstand tussen ons valt wel wat zwaar, dus ik hoop dat we binnenkort (iets dichter) bij elkaar kunnen gaan wonen. Ik kijk er naar uit om nog veel meer tijd met je door te brengen!